UNIVERSITY OF BATH

PHD

The Separation of Phytosterols from Orange Juice Using Synthetic Membrane Filtration
(Alternative Format Thesis)

Abd Razak, Nurul Hainiza

Award date:
2021

Awarding institution:
University of Bath

[Link to publication](#)

Alternative formats

If you require this document in an alternative format, please contact:
openaccess@bath.ac.uk

PHD

The Separation of Phytosterols from Orange Juice Using Synthetic Membrane Filtration
(Alternate Format Thesis)

Abd Razak, Nurul Hainiza

Award date:
2021

Awarding institution:
University of Bath

Link to publication

The Separation of Phytosterols from Orange Juice Using Synthetic Membrane Filtration

Nurul Hainiza Abd Razak

A thesis submitted for the degree of Doctor of Philosophy

University of Bath

Department of Chemical Engineering

February 2021

Abstract

The aim of this study is to develop the ultrafiltration process for the separation of phytosterols and proteins from orange juice using synthetic membranes made from regenerated cellulose acetate, polyethersulfone and fluoropolymer. This project was derived from the issues found in utilisation of by-products of rubber processing waste called natural rubber serum (NRS) that contains phytosterols compounds. Owing to the difficulty of securing supplies of NRS, a cheap and readily available alternative was sought. Orange juice was found to have similar total phytosterols content ($0.2 - 0.3$ mg ml^{-1}) to those present in NRS. A cross-flow filtration rig with a total filtration area of 336 cm^2 was operated at transmembrane pressure (TMP) of 1 bar and the process was optimised at 10 to 40 ºC. The ultrafiltration performance has been determined in terms of flux, resistances and rejection ratio towards phytosterols and proteins. The membrane surface modification due to fouling and cleaning has been investigated in terms of membrane hydrophobicity, surface roughness, charge and porosity. A desirable membrane separation rejects proteins whilst transmitting phytosterols. The best separation of phytosterols from orange juice (43 ± 2 mg L^{-1}) with the lowest rejection of phytosterols ($32 \pm 4\%$) and the highest rejection of proteins ($96 \pm 1\%$) with a selectivity factor of 17, was achieved using RCA 10 kDa membrane at 20 °C using 3 L orange juice. Ultrafiltration at low temperature was found to be more effective in separating phytosterols in orange juice to reduce membrane fouling. Membrane surface roughness and surface charge varied as a function of molecular weight cut-off (MWCO) such that RCA30 kDa > RCA100 kDa > RCA10 kDa. Membranes with rougher surfaces exhibited a higher fouling than those with smoother surfaces. Fouling increased the membrane porosity and decreased the membrane hydrophobicity. It can be concluded that membranes properties were more important than MWCO in determining the performance of ultrafiltration membranes in this system. The fluid dynamic gauging (FDG) obtained 80 - 95% surface removal at shear stress values of 3.9 Pa, corresponding to a water velocity of 1.3 m s^{-1}. By applying the FDG, the fouling layer on RCA membranes can be removed without affecting the membrane surface modification caused by chemical cleaning.

Acknowledgements

Table of Contents

Nomenclature

Symbols

A	absorbance	nm
C_p	solute concentration in the permeate	mg ml^{-1}
C_r	solute concentration in retentate	mg ml^{-1}
ΔP	transmembrane pressure	bar or Pa
d	tube inner diameter	m
d_t	nozzle inner diameter	m
h	distance between the gauge and fouling layer	m
h_0	distance between the gauge and membrane	m
J	flux	L m^{-2} h^{-1}
m	gauging mass flow rate	kg s^{-1}
n	blocking index	-
P	pressure	bar or Pa
R	rejection ratio	%
R_{cp}	concentration polarisation resistance	m^{-1}
R_f	fouling resistance	m^{-1}
R_{ir}	irreversible fouling resistance	m^{-1}
R_m	membrane resistance	m^{-1}
R_r	reversible fouling resistance	m^{-1}
R_{tot}	total resistance	m^{-1}
T	temperature	°C
t	time	sec or min or hr

Greek symbols

ξ	zeta potential	mV
θ	contact angle	°
ρ	fluid density	kg m^{-3}
τ	fluid shear stress	Pa
τ_{wall}	wall shear stress	Pa
μ	dynamic viscosity of fluid	Pa s
μ_m	mean pipe flow velocity	m s^{-1}

List of Abbreviation

AFM	Atomic force microscopy
BET	Brunauer-Emmet-Teller
BHT	Butylated hydroxytoluene
BSA	Bovine serum albumin
CIP	Clean-in-place
CFV	Cross flow velocity (m s^{-1})
DPPH	1, 1-diphenyl-2-picryl-hydrazyl
FDA	Food and Drug Administration
FDG	Fluid dynamic gauging
FP	Fluoropolymer
FTIR	Fourier Transform Infrared
GC-FID	Gas chromatography-flame ionization detection
LB	Liebermann-Buchard
MRB	Malaysian Rubber Board
MWCO	Molecular weight cut-off
NF	Nanofiltration
NFC	Not from concentrate
NRS	Natural rubber serum
PES	Polyethersulfone
PME	Pectin methylesterase
PP	Polypropylene
PTFE	Polytetrafluoroethylene
PWF	Pure water flux
RCA	Regenerated cellulose acetate
RO	Reverse osmosis
SEM	Scanning electron microscopy
TMP	Transmembrane pressure
TPC	Total phytosterol content
TSS	Total suspended solid
UF	Ultrafiltration
UV	Ultraviolet

List of Table

List of Figures

Chapter 1: Introduction

1.1 Background

The natural rubber industry in Malaysia plays an important role in the country's economic development. In 2020, the rubber industry contributed 5.8% (MYR 52 billion, USD 13 billion) to Malaysia's export earnings (Malaysian-Rubber-Board, 2018). Malaysia is renowned for the high-quality rubber products such as medical gloves, automotive components, hoses and structural bearings. An aqueous solution of natural rubber serum (NRS) is obtained when natural rubber latex from *Hevea Brasiliensis* tree is coagulated and processed during the production of rubber products. NRS is a by-product of rubber processing and discharged as effluent from rubber processing factories. The effluent consists of sulphuric acid contaminated serum with a high biological oxygen demand (Devaraj *et al.*, 2006). The effluent needs to be treated before discharge to effluent ponds, which incurs additional operating costs. The effluent also needs to be treated in order to comply with the regulatory standards established by the Malaysian Department of the Environment.

A clean rubber processing technology should be designed to minimise effluent discharge, to recover value-added products from the waste and to maximise revenue by the integration of NRS and latex processing factories. NRS consists of 3 - 5 wt % of non-rubber compounds such as phytosterols, tocotrienols, lipids, carotenoid, proteins and carbohydrates (Zairossani *et al.*, 2005). The Malaysian Rubber Board (MRB) has developed an ultrafiltration process to separate the protein fractions (Aimi Izyana and Zairossani, 2011) and sugar fractions (Devaraj and Zairossani, 2006) from NRS (Figure 1.1). NRS could potentially be used to produce other minor high value-added compounds such as phytosterols. Although the phytosterols composition is low in NRS, the nutritional benefits of phytosterols could be their most valuable advantage. Furthermore, new classes of natural products that could be of great value should be exploited from agro-industrial by-products (Almanasrah *et al.*, 2015; Cypriano *et al.*, 2018; Okino Delgado and Fleuri, 2016).
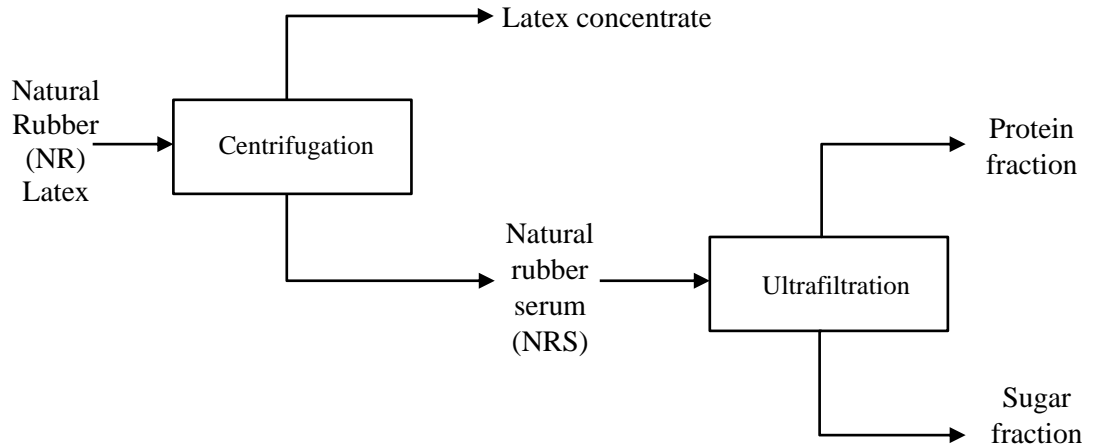
Figure 1.1: Process flow diagram of valuable product recovery from natural rubber (Devaraj and Zairossani, 2006).

Nowadays, natural products are being used in food (Shahidi and Ambigaipalan, 2015), nutraceutical (Sundram *et al.*, 2003), and pharmaceutical (Aiello *et al.*, 2019) industries. Studies are needed to recover and test new classes of high value added bioactive compounds such as sterols from plants. Plant sterols, generally known as phytosterols are cholesterol-like compounds that are found in vegetable oils, nuts and fruits (Wang *et al.*, 2018). Commercial phytosterols were isolated mostly from soybean oil. Phytosterols are one of the most widely used groups of food additives in food products such as margarine, milk and yogurt drinks (Tolve *et al.*, 2018). By 2025, the global market size of phytosterols will increase to USD 1,100 million from USD 590 million in 2018 (Market-Insights-Reports, 2019). Phytosterols possess many outstanding properties such as anti-oxidative (Wang *et al.*, 2002), anticancer properties (Shahzad *et al.*, 2017) and cholesterol lowering effects (Brufau *et al.*, 2008). Studies have shown that phytosterols can lower blood cholesterol levels and thus decrease risk of coronary heart diseases (Meng *et al.*, 2019; Ogbe *et al.*, 2015). Steroids from *Cynanchum* plant possess a variety of structures and pharmacological activities such as anticancer, antidepressant and antifungal (Woyengo *et al.*, 2009; Xu *et al.*, 2016).

A major limitation is the lack of economical techniques that can be used for the extraction and separation of nutraceutical compounds such as phytosterols. Conventional techniques such as solvent extraction, chromatography and microwave extraction consume large amounts of energy and produce considerable amount of

waste making them costly and unsustainable (Conidi *et al.*, 2017). Alternative extraction methods such as supercritical fluid extraction techniques have been used to isolate phytosterols from melon seeds at high pressure and high temperature (Nyam *et al.*, 2011). This excludes them from being considered suitable for nutraceutical manufacturing in improving the environmental impact and minimising operating costs.

Membrane technology such as ultrafiltration offer great potential, due to their ability to separate bioactive compounds from plants and by-products of agro-industrial applications at low temperature (Almanasrah *et al.*, 2015; Basu and Balakrishnan, 2017; Conidi *et al.*, 2017). Ultrafiltration is a pressure-driven process that separate particles in the size range 1-100 nm (Echavarría *et al.*, 2011). Ultrafiltration is commonly used in pharmaceutical fractionation, water treatment and biochemical processing. Membrane fouling and cleaning have been of great interest since both steps potentially shortens membrane life. Fouling depends on physical properties of the membrane such as MWCO, pore size and membrane material (Jeon *et al.*, 2016), and also membrane surface chemistry such as surface charge hydrophobicity, roughness and chemical bonding interactions (Argyle *et al.*, 2015; Evans *et al.*, 2009).

Among fruit juices, orange juice has been recognised as one of the important food due to high levels of soluble sugars, pectin, proteins, hemicelluloses and cellulose fibers (Awan *et al.*, 2013). The presence of proteins (Lerma-García *et al.*, 2016) and sugars (Jesus *et al.*, 2007) in orange juice has been reported previously. Jiménez-Escrig *et al.* (2006) and Piironen *et al.*, (2003) demonstrated that orange juice is a promising potential source of phytosterols, such as β-sitosterol, stigmasterol, campesterol and other minor sterols.

1.2   Scope of research

This thesis reports the use of membrane filtration techniques in fruit juice processing. This research adds to the field by reporting the separation of phytosterols from orange juice via ultrafiltration technology. There is currently no existing publicly available literature that describes the use of ultrafiltration processes for the separation of phytosterols from fruit juices especially orange juice. A model solution with similar bioactive compounds to rubber serum is used in this study. Orange juice was selected as a representative feedstock, a proxy for natural rubber serum, due to the similar phytosterols profile. This research is performed using commercial ultrafiltration membranes made from regenerated cellulose acetate (RCA), polyethersulphone (PES) and fluoropolymer (FP). The hypothesis is that membrane with larger MWCO may be used to transmit compounds of lower molecular weight passing through the membrane. RCA membrane with different MWCO is therefore tested to transmit more sterols into the permeate. This study elucidates the mechanisms of fouling and flux loss, whilst optimising the ultrafiltration process to separate the targeted sterol compounds. This study also investigates the surface science of membrane fouling and cleaning processes. The performance of the separation is evaluated in terms of flux, rejection, membrane resistance and cleaning efficiency. Samples were analysed for total phytosterol content, protein and sugar. Contact angle measurement, atomic force microscopy (AFM), Fourier transform infrared (FTIR) spectroscopy, scanning electron microscopy (SEM), surface charge and porosity analysis were carried out to investigate the membrane surface modification occurring as a result of fouling and cleaning during the ultrafiltration.

1.3   General purpose

A model solution that has similar bioactive compound with natural rubber serum will be used in this study. Bioactive compound such as phytosterols can be isolated from the model solution using membrane separation technology. Thus, the general purpose of this study is to investigate the feasibility of using ultrafiltration technology to separate phytosterols from orange juice. The same concept is thought to be applicable and transferable to natural rubber industry.

1.4   Disseminations

The research work presented in this PhD thesis is in the form of peer-reviewed journal articles, which are either published or submitted. The research work has been disseminated in 3 peer reviewed journal articles, 1 submitted manuscript and 5 international conferences.

Peer Reviewed Journal Articles

Nurul Hainiza Abd-Razak, Y. M. John Chew, Michael R. Bird (2019). Membrane fouling during the fractionation of phytosterols isolated from orange juice. *Food and Bioproducts Processing*, 113, 10–21. https://doi.org/10.1016/j.fbp.2018.09.005. This publication is presented as Chapter 3.

Nurul Hainiza Abd-Razak, Zairossani Mohd Nor, Y.M. John Chew, Michael R. Bird (2020). Fouling Analysis and the Recovery of Phytosterols from Orange Juice Using Regenerated Cellulose Ultrafiltration Membranes. *Food and Bioprocess Technology*, 13, 2012–2028. https://doi.org/10.1007/s11947-020-02541-7. This publication is presented as Chapter 4.

Nurul Hainiza Abd-Razak, Arto Pihlajamäki, Tiina Virtanen, Y.M. John Chew, Michael R. Bird (2021). The influence of membrane charge and porosity upon fouling and cleaning during the ultrafiltration of orange juice. *Food and Bioproducts Processing* 126, 184-194. https://doi.org/10.1016/j.fbp.2021.01.009. This publication is presented as Chapter 5.

Manuscript in Process

Nurul Hainiza Abd-Razak, Y. M. John Chew, Michael R. Bird (2021). The application of Fluid Dynamic Gauging to determine the properties of regenerated cellulose membranes used for orange juice ultrafiltration. This manuscript has been submitted to *International Journal of Food Engineering* and this manuscript is presented as Chapter 6.

Conferences/ Symposiums

<u>Nurul Hainiza Abd-Razak</u>, Y. M. John Chew, Michael R. Bird (2018). The Fouling of Ultrafiltration Membranes during the Isolation of Phytosterols from Orange Juice. 10th International Conference on Fouling and Cleaning in Food Processing (FCFP 2018), Lund, Sweden. 17th – 20th April 2018. An oral presentation. The extended abstract has been published in the conference proceeding.

<u>Nurul Hainiza Abd-Razak</u>, Y. M. John Chew, Michael R. Bird (2018). The Isolation of Phytosterols from Orange Juice using Ultrafiltration. 7th International Conference on Biotechnology for the Wellness Industry (ICBWI 2018), Kuala Lumpur, Malaysia. 27th – 28th November 2018. An oral presentation. The full paper has been published in the conference proceeding. Organised by Universiti Teknologi Malaysia.

<u>Nurul Hainiza Abd-Razak</u>, Y. M. John Chew, Michael R. Bird (2019). Investigation of Regenerated Cellulose Membrane Cleaning Using Fluid Dynamic Gauging: Preliminary Study. Fluid Dynamic Gauging (FDG) Fest 2019, University of Bath, UK. 10th December 2019. An oral presentation.

<u>Nurul Hainiza Abd-Razak</u>, Y. M. John Chew, Michael R. Bird (2019). Comparison of Regenerated Cellulose Membrane Cleaning Using Chemical Cleaning and Fluid Dynamic Gauging. Fluid Dynamic Gauging (FDG) Fest 2020, Technische Universität Braunschweig, Germany. 3rd December 2020. An oral presentation.

<u>Nurul Hainiza Abd-Razak</u>, Y. M. John Chew, Michael R. Bird (2020). Investigation of Regenerated Cellulose Membrane Cleaning Using Fluid Dynamic Gauging. International Congress on Membranes & Membrane Processes 2020 (ICOM 2020), London, UK. 6th - 11th December 2020. A poster presentation. Organised by Elsevier.

Chapter 2: Literature review

2.1 Phytosterols

Natural product such as phytosterols are increasingly being used in the food (Cantrill, 2008) and nutraceutical (Santini and Novellino, 2017) industries. Phytosterols are a group of steroids that occur naturally in plants.

2.1.1 Plant sterols

There are more than 100 phytosterol compounds known to exist in plants (Fernandes and Cabral, 2007). The term phytosterols also refer to plant sterols which are cholesterol-like compounds that are found mostly in vegetable oils, nuts and fruits (Wang *et al.*, 2018). They are structurally related to cholesterol but differ from cholesterol in the structure of the side chain. They consist of a steroid skeleton with a hydroxyl group attached to the C-3 atom of the A-ring and an aliphatic side chain attached to the C-17 atom of the D-ring. Sterols have a double bond between C-5 and C-6 of the sterol moiety as depicted in Figure 2.1. The most common phytosterols are stigmasterol and β-sitosterol. Commercial phytosterols are recovered mostly from soybean oil via saponification using ethanol, methyl esterification using sulphuric acid, and crystallisation process (Yan *et al.*, 2012). Phytosterols are also extracted from sugarcane using solvent extraction with diethyl ether (Feng *et al.*, 2015). Stigmasterol has a molecular weight of 412 g mol^{-1} with elemental formula $C_{29}H_{48}O$. For β-sitosterol, the elemental formula is $C_{29}H_{50}O$ with molecular weight of 414 g mol^{-1} (Kongduang *et al.*, 2012; McDonald *et al.*, 2012). Phytosterols are well known for their cholesterol lowering effect and thus decrease risk of coronary heart diseases (Brufau *et al.*, 2008; Ogbe *et al.*, 2015; Stinco *et al.*, 2012). Phytosterols also possess outstanding properties such as anti-oxidative properties (Wang *et al.*, 2002; Woyengo *et al.*, 2009) and anti-cancer properties (Shahzad *et al.*, 2017; Suttiarporn *et al.*, 2015).
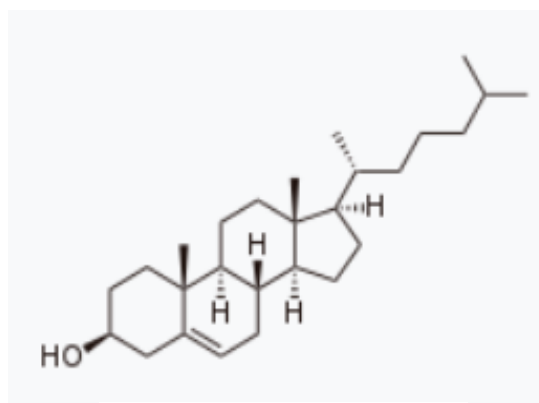
(a) MW = 386.65 g mol^{-1}
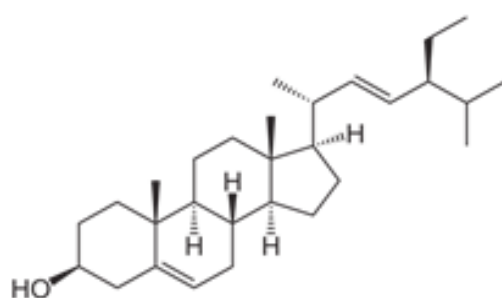
(b) MW = 414.71 g mol^{-1}
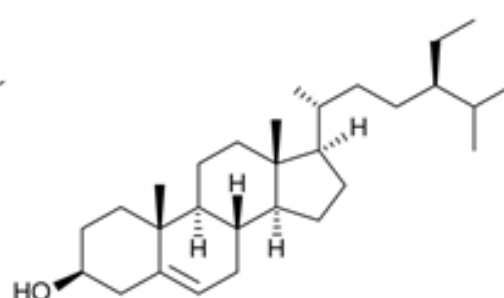
(c) MW = 412.7 g mol^{-1}

Figure 2.1: Molecular structures of (a) cholesterol, (b) stigmasterol and (c) β-sitosterol (Fernandes and Cabral, 2007).

2.1.2 Phytosterols in *Hevea* latex

Table 2.1 shows the composition of natural rubber latex and natural rubber serum (NRS). Natural rubber derived from *Hevea* latex contains 4 - 5% non-rubber substances and are comprised of proteins, lipids, amines and carbohydrates. The total lipids constituted about 1.6% of the latex, comprised of carotenoids pigments, free and esterified phytosterols and free and esterified tocotrienols (Hasma and Subramaniam, 1986). The presence of lipids such as tocotrienols, phytosterols and carotenoids in *Hevea* latex was confirmed using liquid-liquid extraction method (Ho. *et al.*, 1975). Hasma and Subramaniam (1986) reported that latex phytosterols was comparable to the amount of tocotrienols in rubber serum. The amount of tocotrienols in rubber serum is around 0.3 mg ml^{-1} (Sajari *et al.*, 2014). Since NRS is discharged as waste from the rubber processing (Devaraj and Zairossani, 2006), the NRS has a great potential to be used as an alternative source for nutraceutical and

8

pharmaceutical compounds such as proteins, sugars and steroids. The Malaysian Rubber Board (MRB) has successfully separated the protein fractions (Aimi Izyana and Zairossani, 2011) and sugar fractions (Devaraj and Zairossani, 2006) from NRS using an ultrafiltration process.

Potentially, NRS could also be used to produce other minor compounds of high added value such as phytosterols. Although the composition of phytosterols is low in NRS, most valuable advantage could be the nutritional beneficial effect of phytosterols. The utilisation of by-product from rubber processing (mainly non-rubber component) for the production of high-value added compounds is very important in order to sustain the growth of the rubber industry. The exploitation of NRS benefits the rubber industry by enhance raw rubber factories via integration of latex and NRS processing, and improve competitiveness by generating value added products from rubber processing waste. Furthermore, this mid-stream process is geared towards a cleaner technology and improving the effluent treatment system.

Table 2.1: Composition of natural rubber latex and natural rubber serum.

Components	Natural rubber latex (Archer et al., 1969; Hasma and Subramaniam, 1986) % (w/w)	Natural rubber serum (Zairossani et al., 2005) % (w/w)
Water	58.6	94.6
Rubber hydrocarbons	36.0	-
Protein, amino acid & nitrogenous compounds	1.7	1.1
Sugar and carbohydrate	1.6	2.7
Lipids (Phytosterols)	1.6 (0.03)	1.6 (0.03)
Ash	0.5	-

2.1.3 Phytosterols in orange juice

Due to the difficulties in transporting NRS from MRB in Malaysia, a model solution with similar bioactive compounds to rubber serum will be used in this study. An extensive literature review has been performed in order to find a model solution which is a plant based solution that can replace NRS as the feed solution for this project. Orange juice contains phytosterols (Balme and Gulacar, 2012; Jiménez-Escrig *et al.*, 2006; Piironen *et al.*, 2003), and also other compounds such as sugars (Jesus *et al.*, 2007) and protein (Lerma-García *et al.*, 2016) (Table 2.2). Previous studies confirmed that both orange juice and kiwi juice contain phytosterols as shown in Table 2.3. However, kiwi juice showed low amount of total phytosterols compared to orange juice. Orange juice has been chosen as a model feed solution for this project, as the type and amount of phytosterols present are similar to those present in NRS as tabulated in Table 2.3.

In industrial processing, fruit juice is commonly marketed in three different packaging which are frozen concentrate, fruit juice from concentrate and fruit juice not from concentrate (NFC) (Stinco *et al.*, 2012). In this study, orange juice NFC was chosen as orange juice NFC can retain as much of the features of the raw fruit in which no water is added or removed. The components of the fruit that are removed in the production process are the pulp, skin and seeds. In general, the processing begins with the washing process and then the fruit is placed in an extractor to separate the juice from the pulp and skin. Next steps are centrifugation to push the juice out and finally pasteurisation step to reduce microbiological loading whilst maintaining as much of the colour, flavour and aroma of the fruit.

Table 2.2: Composition of orange juice

Components	Amount
Phytosterols (Jiménez-Escrig *et al.*, 2006; Piironen *et al.*, 2003)	$0.2 - 0.3$ mg ml^{-1}
Sugar (Cobell, 2016)	$\geq 10°$ Brix
Protein (Cobell, 2016)	0.7 mg ml^{-1}

Table 2.3: Comparison of phytosterols in natural rubber serum (NRS), orange juice and kiwi juice

Plant	Stigmasterol (mg ml^{-1})	Sitosterol (mg ml^{-1})	Fucosterol (mg ml^{-1})	Campesterol (mg ml^{-1})	Avenasterol (mg ml^{-1})	Stanol (mg ml^{-1})	Other sterol (mg ml^{-1})	Total phytosterols (mg ml^{-1})
Natural Rubber Serum (Hasma and Subramaniam, 1986)	0.034	0.127	0.079	-	-	-	-	0.240
Orange (Piironen *et al.*, 2003)	0.009	0.170	-	0.034	0.004	-	0.012	0.229
Orange (Jiménez-Escrig *et al.*, 2006)	0.012	0.220	-	0.038	-	0.004	0.032	0.306
Kiwi (Piironen *et al.*, 2003)	0.023	0.137	-	0.005	-	0.004	0.012	0.181
Kiwi (Jiménez-Escrig *et al.*, 2006)	0.007	0.049	-	0.002	-	-	0.012	0.070

2.1.4 Phytosterols in the nutraceutical industry

Plant sterols or phytosterols in free or esterified form have been added to foods due to their properties to reduce absorption of cholesterol in the gut and thereby lower blood cholesterol levels (Clement *et al.*, 2010; Lagarda *et al.*, 2006). Phytosterols may be beneficial as food additives because they can lower the absorption of cholesterol in intestines by 10% to 15% (Brufau *et al.*, 2008; Ostlund *et al.*, 2003). The U.S Food and Drug Administration has stated that a moderate intake of phytosterols in the daily diet can decrease the risk of coronary heart disease (Food-And-Drug-Administration, 2019). Phytosterols were used as an ingredient in a variety of foods, beverages and supplements that produced by food or nutraceutical companies such as Danone, Nestle and Unilever (Cantrill, 2008). Phytosterols were one of the food additive categories most commonly used in food products such as margarine, butter, and yoghurt drinks (Tolve *et al.*, 2018). Figure 2.2 illustrates the absorption of cholesterol and phytosterols inside the small intestine. Phytosterols are structurally related to cholesterol but differ in their side chain. Even though both phytosterols and cholesterol are structurally similar, their metabolism differs in some parts. Cholesterol is produced in the human body by the liver and also from the daily food intake. In the human intestine, cholesterol is grouped as micelles and is easily absorbed into the blood stream. Phytosterols cannot be synthesized by human body and derive from the daily diet. Phytosterols are poorly adsorbed in the intestine (0.4 – 3.5 %) (Calpe Berdiel *et al.*, 2010). By consuming phytosterols, they can compete with cholesterol in micelle formation and reduced the absorption of cholesterol into the blood stream because mixed cholesterol-phytosterols micelle will be excreted from the body. Low absorption of cholesterol into the blood stream resulted in reduced blood cholesterol level, thereby reducing the risk of cardiovascular disease (Brufau *et al.*, 2008).
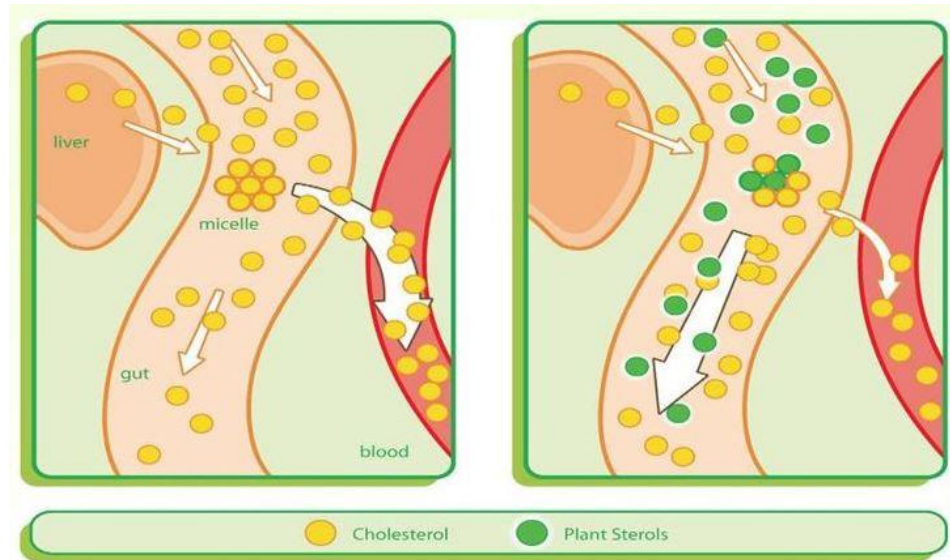
Figure 2.2: The absorption of cholesterol and phytosterols inside the small intestine, (left) without phytosterols and (right) with phytosterols (Unilever, 2018)

2.2 Membrane separation

2.2.1 Membrane applications in fruit juice processing

Membrane separation techniques such as ultrafiltration have been widely used in fruit juice processing (Ilame and V. Singh, 2015; Mohammad *et al.*, 2012). Membrane technology offers the possibility of simultaneously isolating and concentrating high value added natural products from fruit juice. A research was carried out for the recovery of bioactive compounds such as folic acid, citric acid, total phenolics and proteins from kiwi juice using cellulose acetate membrane at 30 kDa MWCO (Cassano *et al.*, 2008). The rejection of total phenolics was 13.5% and the rejection of protein was 61%. Sugar and phenolics compounds including anthocyanin, flavonoids and tannins were separated from pomegranate juice by using polyethersulfone and fluoropolymer membranes with MWCO ranging from 1 to 4 kDa (Conidi *et al.*, 2017). Ultrafiltration of black currant juices was carried out using 100 kDa polyethersulfone membrane at a transmembrane pressure of 2 bars and the temperature of 25 °C. 50% of total anthocyanins and 54% of the total flavonol content were recovered after the ultrafiltration (Pap *et al.*, 2012). Cassano *et al.*, (2007) reported the ultrafiltration of orange juice in separating anthocyanin, naritunin and hesperidin using 15 kDa PVDF membrane. The ultrafiltration was carried out at

three different temperatures (15, 21 and 25 °C). The ultrafiltration process at 21 °C gave the best separation performance. No literature is available on the performance of ultrafiltration processes for the separation of phytosterols from proteins in fruit juices.

2.2.2 Membrane system design

A membrane is a selective barrier between two phases and controls the transport of various components from one phase to another. In general, two system designs are available such as frontal filtration and cross flow filtration. Cross flow filtration is a filtration process in which feed solution flows tangentially across the membrane surface (Mulder, 1996) as illustrated in Figure 2.3 (a). This filtration mode works by introducing feed stream over the membrane surface, instead of directly onto the membrane. Components smaller than the membrane pore size will pass through the membrane during filtration and collected as permeate. While larger components remain in the retentate stream and recycled back to the feed tank for further processing. A cross flow filtration is preferred for industrial application due to the lower fouling tendency. In contrast to cross flow filtration, all the feed solution in dead end filtration passes perpendicularly through the membrane, forced by pressure (Figure 2.3 (b)). This indicates that the quality of the permeate decrease with time as a result of the increase in the concentration of rejected compounds in the feed (Mulder, 1996). The formation of a cake layer on the membrane surface will cause the permeate flux to decline (Echavarría *et al.*, 2011).

Membrane science was first reported in the eighteenth century (Mulder, 1996; Nollet, 1995; Strathmann, 2011). In 1866, Graham performed the first dialysis experiments using synthetic membrane (Graham, 1866). Recently, separations by the use of membrane are becoming increasingly important in industrial applications. The membrane acts as a semipermeable barrier that separates various molecules between two phases. Membrane processes include microfiltration, ultrafiltration, nanofiltration, reverse osmosis, electrodialysis and pervaporation. There are many pressure-driven membrane processes available to fractionate a broad range of chemical and biochemical compounds based on particle size and molecular weight cut-off (MWCO). Figure 2.4 describes the application range of various membrane processes.
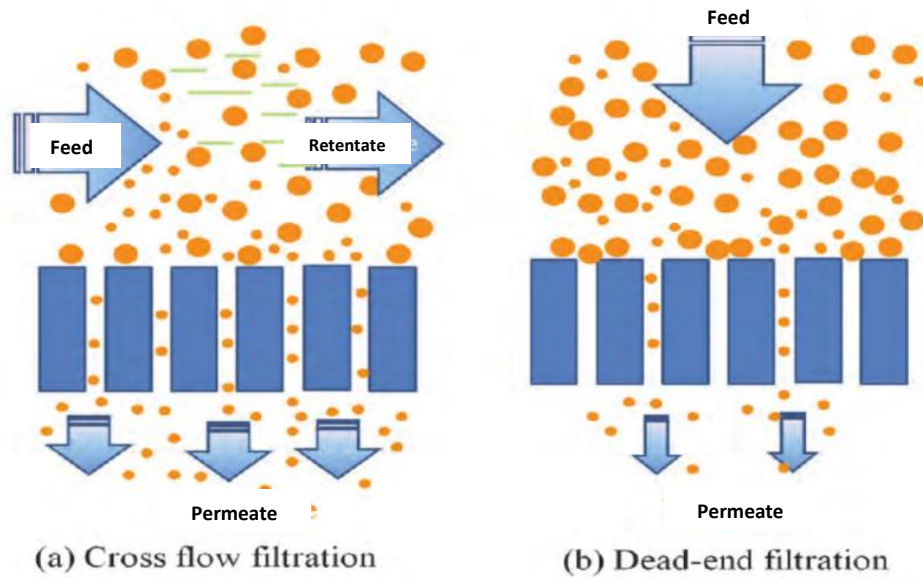
Figure 2.3: Two basic membrane filtration designs; (a) cross flow filtration (b) dead end filtration (modified from Strathmann (2011) (Strathmann, 2011)).
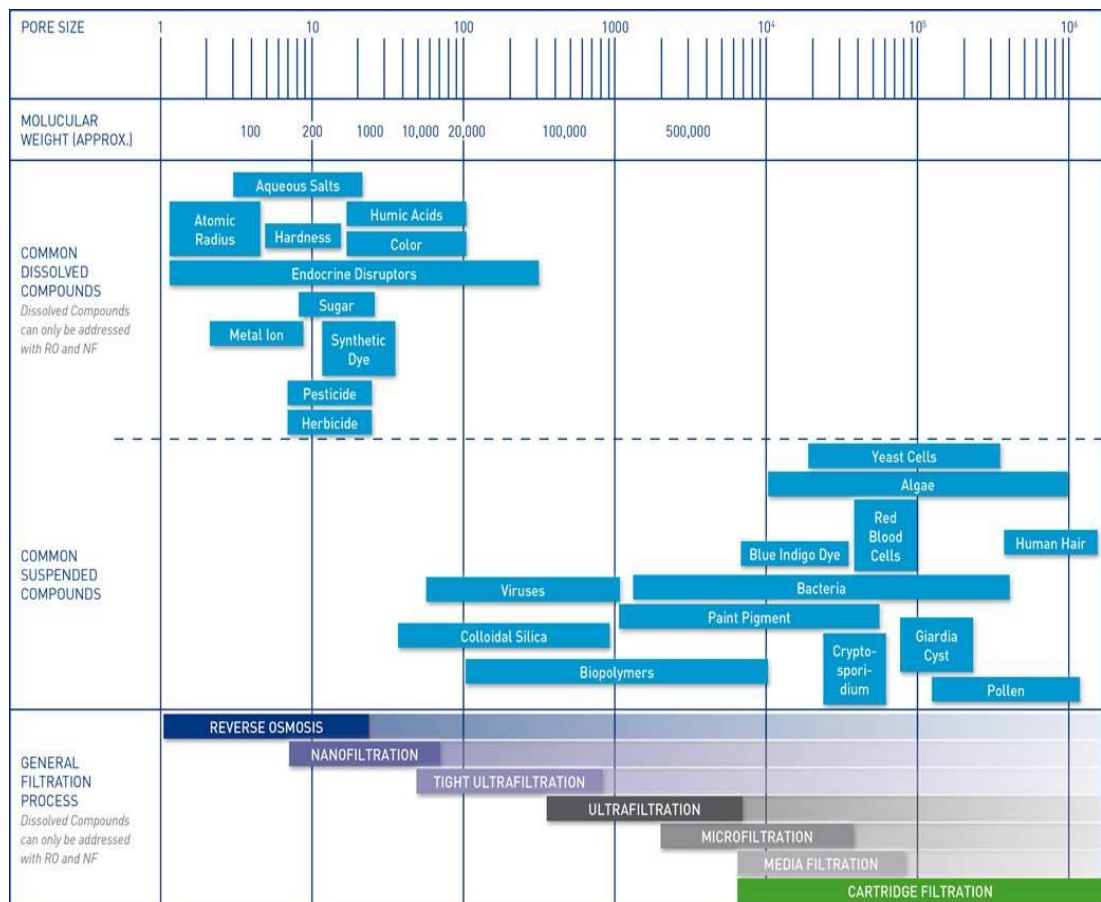
Figure 2.4: Application range of various membrane processes (Pentair, 2017).

2.2.3   Permeate flux, selectivity and resistances

Membrane process is usually characterised by flux and selectivity properties that provide functional transport across the barrier. The effectiveness of any membrane process is described in terms of permeation rate (or permeate flux) and the selectivity. The permeation rate or flux is defined as the volumetric flow rate of the fluid through the membrane. The permeate flux through a membrane can be calculated as the following equation (Mulder, 1996):

$$J = \frac{\Delta P}{\mu R_{tot}} \qquad\qquad (2.1)$$

where J is the flux through the membrane (L m^{-2} h^{-1}), ΔP (Pa) is the transmembrane pressure (TMP), μ is the dynamic viscosity (Pa s) and R_{tot} represents the total resistance (m^{-1}). The flux decline can be calculated using Equation (2.2):

$$Flux\ decline = \frac{J_0 - J_{ss}}{J_0} \qquad\qquad (2.2)$$

where J_0 is the initial permeate flux and J_{ss} is the steady-state permeate flux. In constant TMP experiment, flux decreases as R increases (Miller *et al.*, 2014). Therefore, the change in resistance during filtration process offers an indicator for comparing the constant flux in order to study the fouling and cleaning effects. Table 2.4 shows the typical values of TMP, flux and pore size for different membrane process.

Table 2.4: TMP, flux range and pore size in pressure driven membrane process (Mulder, 1996).

Membrane process	TMP (bar)	Flux (L m^{-2} h^{-1})	Pore size (nm)
Microfiltration	0.1 – 2.0	> 50	> 100
Ultrafiltration	1.0 – 5.0	10 – 50	10 – 100
Nanofiltration	5.0 – 20	1.4 – 12	< 10
Reverse osmosis	10 - 100	0.05 – 1.4	< 1

Meanwhile, selectivity is the degree to which one component preferentially permeates the membrane and thus determines the degree of enrichment achieved. Selectivity is expressed as the rejection ratio (R) and calculated using Equation (2.3) (Argyle *et al.*, 2015; Wu and Bird, 2007):

$$R = (1 - \frac{C_p}{C_r})$$
(2.3)

where C_p is the solute concentration in the permeate and C_r is the solute concentration in the retentate (Mulder, 1996). Membrane performance often changes over time and this performance is measured based on the permeate flux. The flux will be declined under a steady state transmembrane pressure which means the flux decline can be observed when the TMP is kept constant. There are two factors affecting the flux such as membrane fouling and concentration polarisation as shown in Figure 2.5.
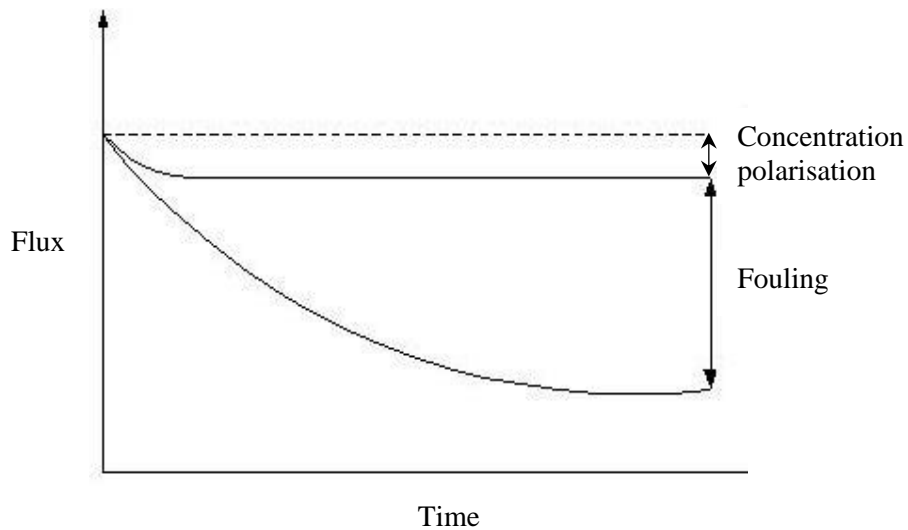
Figure 2.5: Flux as function of time (adapted from (Mulder, 1996)).

In pressure driven process such as ultrafiltration, fouling can be represented in the resistance in series model as shown in Equations (2.4) and (2.5) (Jiraratananon and Chanachai, 1996):

$$J = \frac{\Delta P}{\mu R_{tot}} = \frac{\Delta P}{\mu \ (R_m + R_f + R_{cp})}$$
(2.4)

$$R_f = R_{ir} + R_r \qquad\qquad\qquad (2.5)$$

where R_m is the resistance of conditioned virgin membrane, R_f is the total fouling resistance, R_{ir} is the irreversible fouling resistance, R_r is the reversible fouling resistance and R_{cp} is the resistance due to concentration polarisation. R_m is determined by measuring the flux of RO water through the conditioned membrane. Irreversible fouling is defined as any foulant not being removed by rinsing. Reversible fouling is defined as any foulant is removed from the membrane pores and surfaces by rinsing.

The declining in flux is due to several factors such as pore blocking or fouling, absorption, cake layer formation and concentration polarisation (Mulder, 1996) (Figure 2.6). Since the membrane retains the solutes, there will be an accumulation of molecules near the membrane surface. As time increased, highly concentrated layer of molecules on the surface can be formed and this will cause a resistance called concentration polarisation (R_{cp}). Meanwhile, fouling resistance (R_f) caused by cake layer formation and pore blocking resistance when the solutes penetrate into the membrane and block into it. Finally, there is also a resistance that related to the membrane itself known as membrane resistance, R_m.
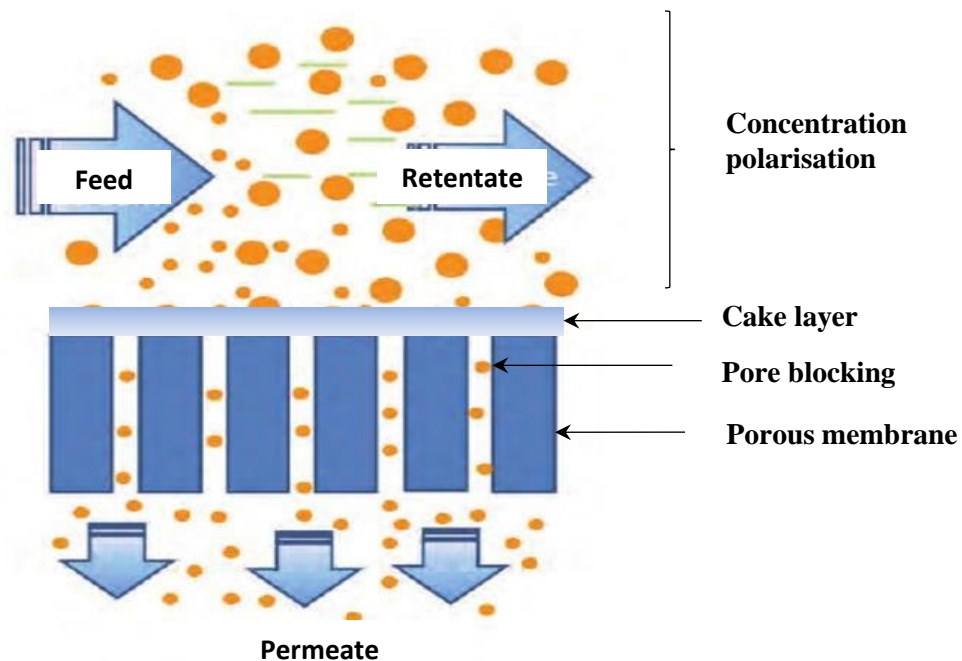
Figure 2.6: Various type of resistance in cross flow filtration (Strathmann, 2011).

2.2.4   Membrane fouling

For a fixed TMP, membrane fouling is the major reason for the declining in permeates flux. This fouling phenomenon is dependent on physical and chemical properties of the membrane, solute and feed solution such as concentration, pH, ionic strength and chemical bonding interactions (Mulder, 1996). The foulants will produce a cake layer on the membrane surface and clog the membrane pores as well. The fouling of a membrane is also dependent on the parameters such as transmembrane pressure, surface charge, hydrophobicity and membrane pore size (Jeon *et al.*, 2016; Weber *et al.*, 2004). In order to reduce fouling, a few steps can be taken out such as pre-treatment of feed solution, changing the membrane properties, changing the module design or by membrane cleaning. Practically, all membrane application needs to have a proper cleaning method. The fouling index was evaluated by comparing the pure water permeability before and after the ultrafiltration (Conidi *et al.*, 2017).

Hermia divided fouling into four mechanisms namely cake filtration, standard blocking, intermediate pore blocking and complete pore blocking (Hermia, 1982). The Hermia law allows a prediction of the blocking type that caused the fouling during the filtration. Figure 2.7 described the pore blocking model. In the complete blocking (Figure 2.7 (a)), it is assumed that the particle diameter is larger than the pore size and the pores are completely blocked by particles arriving at the membrane surface. Thus, no further particles can pass through the pores. For the standard blocking (Figure 2.7 (b)), the particle diameter is considerably smaller than the pore size. Therefore, the particles can pass through the membrane pores and attached to the inner surface of membrane pores. This leads to the reduction of pore volumes and eventually blocked the membrane. Figure 2.7 (c) shows the intermediate pore blocking which is the transition between complete blocking and cake filtration. In this mechanism, some arriving particles are attached to the particles that already deposited on the membrane surface. The molecules are trapped inside the pore due to the steric effect. The steric effect forms a diffusive barrier and creates an interaction between the pore walls and the molecules; which leading to pore blocking (Han *et al.*, 2008). The cake filtration (Figure 2.7 (d)) described the growth of particles on top of the membrane surface due to the accumulation and agglomeration of particles (Iritani and Katagiri, 2016).

An analytical model was produced by Field *et. al.* (1995) based on Hermia's pore blocking laws (Field *et al.*, 1995):

$$-\frac{dJ}{dt} J^{n-2} = k (J - J^*)$$

(2.6)

where *J* is flux, *J** is limiting flux, *t* is time, *n* and *k* are constants specific to the type of fouling. The different fouling laws concerned are cake filtration, intermediate, standard and complete blocking where *n* values are 0, 1, 1.5 and 2 respectively (Figure 2.7). This model suggests that the fouling mechanism take place sequentially (not simultaneously) from intermediate blocking and finally cake filtration (Lewis *et al.*, 2017). According to Equation (2.7), a function of flux can be described as:

$$f(J) = -\frac{dJ}{dt} J^{n-2}$$

(2.7)

where a linear relationship between *f (J)* and *J* is observed (Field *et al.*, 1995). Experimental flux data was analysed to evaluate the type of membrane fouling using a MATLAB script (Lewis *et al.*, 2017).
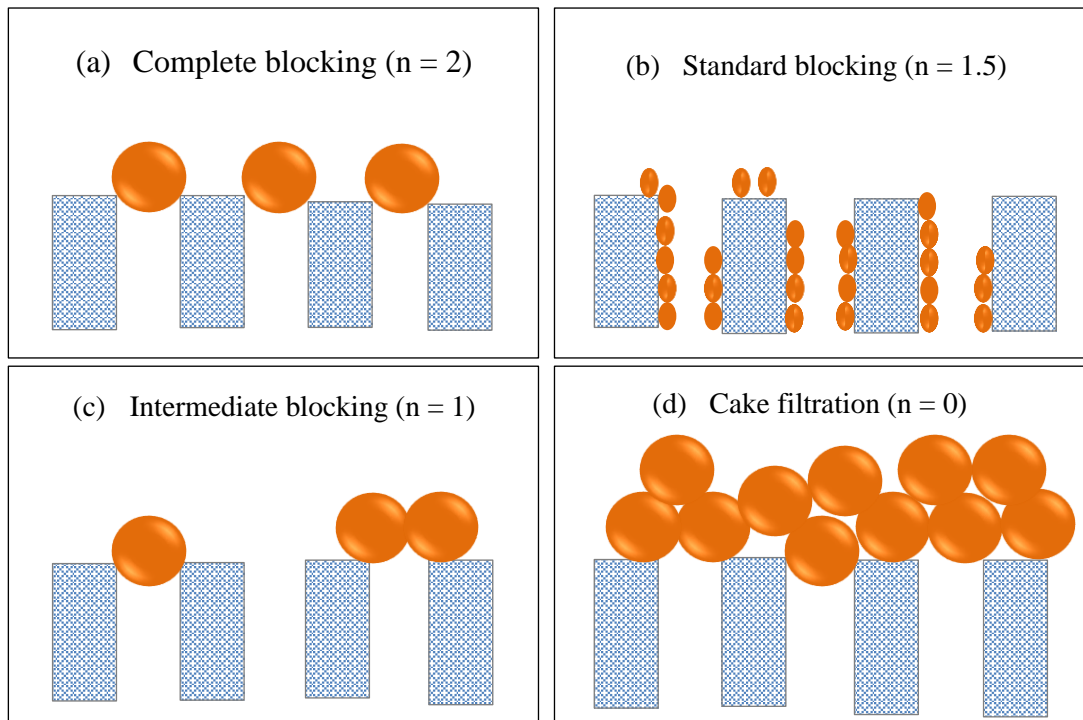
Figure 2.7: Mechanism of different fouling in Hermia pore blocking model.

2.2.5 Factors affecting permeate flux and fouling

2.2.5.1 *Transmembrane pressure (TMP)*

The influence of transmembrane pressure has been observed by many researchers and reported that the permeate flux is increased by increasing the operating pressure (Echavarría *et al.*, 2011; Miller *et al.*, 2014). However, after a certain period of time, the permeate flux will level off at a constant TMP owing to the cake formation on the membrane surface. At a certain higher pressure, the flux becomes independent of the pressure where further increases in TMP do not increase the flux as a result of limiting flux due to the concentration polarisation (Sablani *et al.*, 2001). The process was then controlled by mass transfer as illustrated in Figure 2.8.
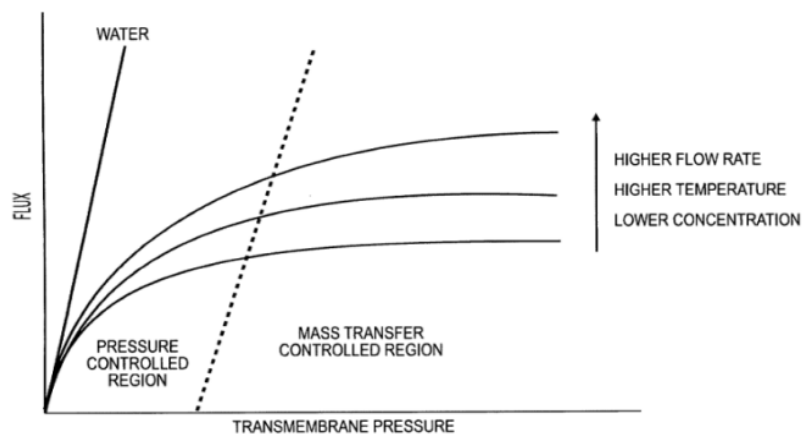
Figure 2.8: Relationship between flux and TMP at two different controlled regions (Ng *et al.*, 2017).

2.2.5.2 *Molecular weight cut off*

Fouling depends on physical properties of the membrane such as MWCO and membrane pore size (Jeon *et al.*, 2016). In the case of ultrafiltration and microfiltration processes, the separation is largely depending on the relative sizes of the particles and the membrane pores. For ultrafiltration membranes with lower pore size, the concept of MWCO has been adopted as a reference to the molar mass of retained macromolecules. The molar mass of macromolecules is proportional to its molecular size (Zeman and Zydney, 1996). Ultrafiltration cannot be used to separate

molecules of similar size. The ultrafiltration membrane retains larger particles including proteins, lipids and colloids (Ilame and V. Singh, 2015). Meanwhile small particles such as vitamins (Cassano *et al.*, 2008) and sugar (Conidi *et al.*, 2017) flow pass through the membrane. A larger MWCO membrane is assumed to transmit lower molecular weight compounds passing through the membrane.

2.2.5.3   Membrane hydrophobicity

Membrane hydrophobicity has been measured in order to investigate the relationship between membrane material and the development of membrane fouling (Jeon *et al.*, 2016). Synthetic polymeric membranes can be separated into two categories such as hydrophilic or hydrophobic membrane. A drop of distilled water is placed on the membrane surface and the angle (α) is measured between the water droplet and the membrane surface. The angle indicates whether the membrane surface is hydrophilic or hydrophobic (Arahman *et al.*, 2015) as displayed in Figure 2.9. The angle with $\alpha >$ 90° shows a hydrophobic surface. Meanwhile hydrophilic surface will have angle $\alpha <$ 90° (Yuan and Lee, 2013). The higher the angle ($\alpha > $ 90°) indicates a hydrophobic surface of the membrane. In order to define the performance of the membrane, the membrane hydrophobicity will be determined by measuring the contact angle (Arahman *et al.*, 2015; Evans *et al.*, 2008; Yuan and Lee, 2013). Membranes with more hydrophobic surface had higher fouling capacity than the ones with hydrophilic surface (Gulec *et al.*, 2017).
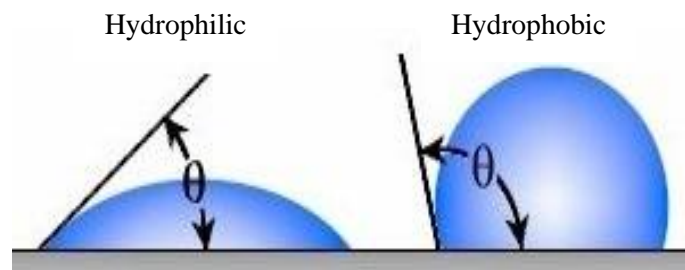
Figure 2.9: Illustration of contact angles formed by water droplet on membrane surface.

2.2.5.4   Surface charge

Besides the TMP and hydrophobicity, membrane surface charge also affects the membrane performance. Figure 2.10 illustrates the potential difference at different distance from the particle charged surface. The presence of a surface charge on the material surface leads to the attraction of ions in the solution of an opposite charge towards the surface. This leads to a greater concentration of counter ions close to the surface rather than in the solution. Thus, a bound layer of counter ions at the surface called Stern layer and a diffusive layer at greater distance from the surface will be formed. Zeta potential is defined as the charge at a boundary within the diffuse layer (Taqvi and Bassioni, 2019). Zeta potential can be measured via the streaming potential method (Pihlajamaki and Nyström, 1995). The influence of surface charge upon ultrafiltration of black tea (Evans *et al.*, 2008) and sulphite liquor (Weis *et al.*, 2005) using regenerated cellulose membrane has been reported by other researchers. Surface charge may affect the membrane tendency to foul and its subsequent cleanability. Fouling caused the regenerated cellulose membranes to have a greater negative charge and cleaning returned the surface charge to a pristine state (Evans *et al.*, 2008; Weis *et al.*, 2005). Membranes subjected to fouling and cleaning were found to have surface charge modification (Argyle et al., 2015; Breite et al., 2016). The determination of zeta potential by streaming potential or current is applied in various fields such as semiconductors, textiles, polymers and mineral processing (Anton-Paar, 2012). *SurPASS* Electrokinetic Analyzer is used to measure the surface charge at different pH. For each pH, the zeta potential (ξ) was calculated according to the Helmholtz-Smoluchowski equation (Equation 2.8):

$$\xi = \frac{\Delta E}{\Delta P} \frac{\mu R}{\varepsilon_0 \ \varepsilon_r} \hspace{3cm} (2.8)$$

where *ΔE* is the streaming potential, *ΔP* is the transmembrane pressure drop, μ is the dynamic viscosity of the electrolyte solution, k is the conductivity of the electrolyte solution, ε_0 is the vacuum permittivity and ε_r is the dielectric constant of pure water.
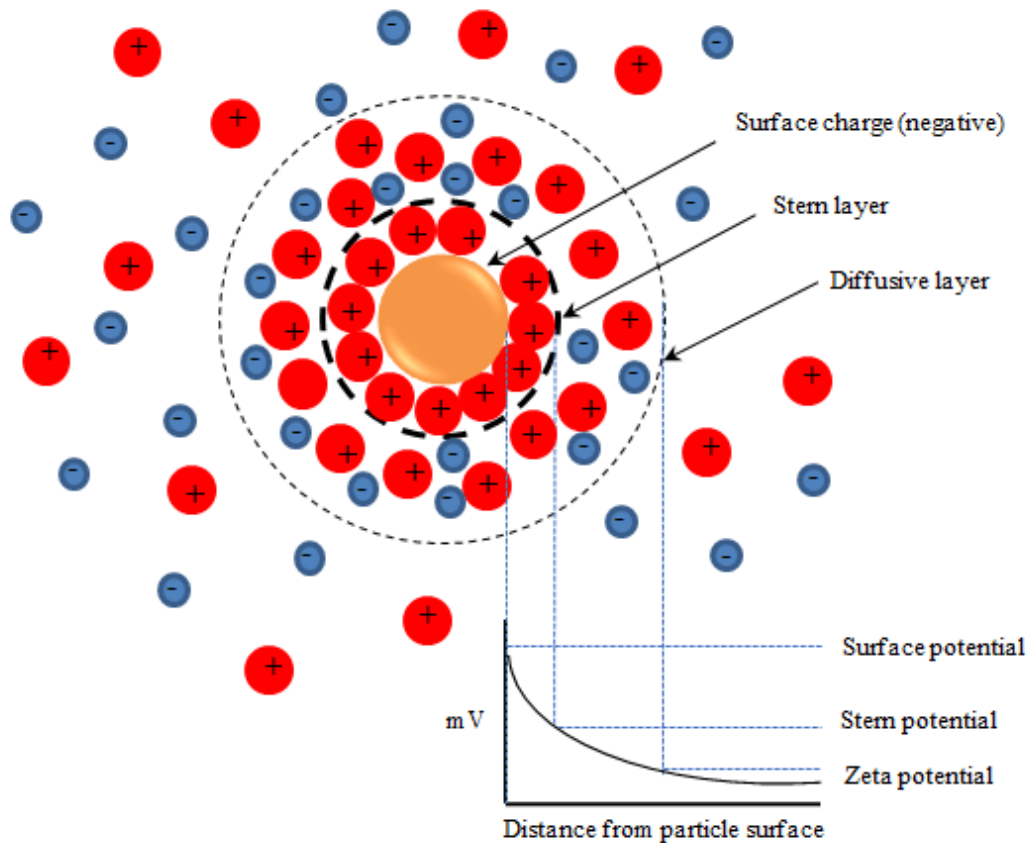
Figure 2.10: Illustration of surface zeta potential formed on membrane surface.

2.2.5.5   *Surface roughness*

Other membrane surface parameters such as surface roughness also contributed to the understanding of the nature of fouling and cleaning (Evans *et al.*, 2008). The surface roughness of the membranes has been investigated by atomic force microscopy (AFM) (Jones *et al.*, 2011). Membranes with rougher surfaces displayed a higher fouling capacity than those with smoother surfaces (Gulec *et al.*, 2017). The foulant appears to be more highly entrapped by rougher surfaces.

2.2.5.6   *Surface area and pore volume*

Changes in membrane surface area can be characterised by Brunauer-Emmett-Teller (BET) technique which has been used to analyse the effect of membrane fouling caused by wood originated compounds. The formation of a fouling layer was observed in the meso-pores region and resulted in an increase in accumulated pore

volumes and pore areas (Virtanen *et al.*, 2020). The Barrett-Joyner-Halenda (BJH) calculation can be used to determine the pore diameter, pore volume and pore distribution (Bardestani *et al.*, 2019).

2.2.5.7   *Temperature*

Temperature can affect the permeate flow rate because the viscosity of the solution can be controlled by the temperature (Evans and Bird, 2010). It has been reported that an increase in temperature leads to a decrease in fluid viscosity and increase the diffusivity of fluid (Ilame and V. Singh, 2015). In the ultrafiltration of black tea, the total fouling resistance was increased at low feed temperature due to viscosity changes in the feed solution (Evans and Bird, 2010).

2.2.6   Polymeric membranes

Membranes can be divided into two groups which are biological and synthetic membranes. Every living cell is surrounded by biological membranes that have very complex structures in order to accomplish specific functions. On the other hand, synthetic membranes are produced from two classes of materials; polymer consisting of organic material such as cellulose acetate (CA), polyethersulfone (PES), fluoropolymer (FP) and inorganic materials such as metals and ceramic (Cuperus and Nijhuis, 1993). The aim of this study is to generate sets of data with three different polymer membranes of different hydrophobicity which are cellulose acetate (hydrophilic), polyethersulfone (less hydrophobic) and fluoropolymer (hydrophobic).

2.2.6.1   *Cellulose acetate*

Cellulose acetate (CA) was one of the first polymeric membrane material to be used for aqueous base separations, and was the material used by Sidney *et al.* (1964) in producing the first reverse osmosis membrane (Sidney and Srinivasa, 1964). CA membranes are formed from blends of cellulose diacetate and cellulose triacetate by phase inversion method. The advantage of this membrane is that CA membrane is relatively cheap and hydrophilic whereby gives a good resistance to fouling (Bai *et*

al., 2012). On the other hand, this membrane tends to hydrolysis at pH below 3 and temperature higher than 30 °C. CA membrane also used for only certain application since this membrane is not capable to withstand cleaning conditions that consist of higher temperatures. The chemical structure of cellulose acetate is shown in Figure 2.11.
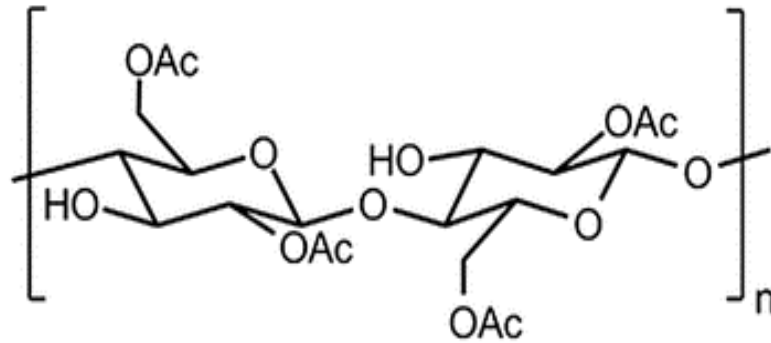
Figure 2.11: Chemical structure of cellulose acetate (Lee *et al.*, 2016).

2.2.6.2   *Polyethersulfone*

Polyethersulfone (PES) membranes have good chemical stability and can tolerate pH values from 1 – 13. They are stable up to an operating temperature of 80 °C, which is often is very useful for cleaning steps. The hydrophobicity of PES is in between that of CA and FP membranes. However, PES is more expensive than CA. Figure 2.12 shows the chemical structure of polyethersulfone.
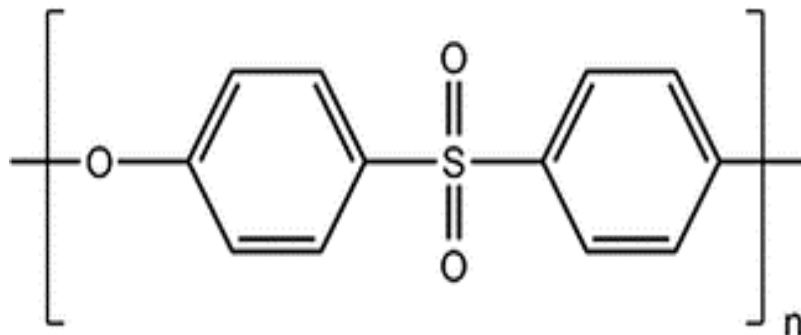
Figure 2.12: Chemical structure of polyethersulfone (Lee *et al.*, 2016).

2.2.6.3   Fluoropolymer

These fluoropolymer (FP) membranes are made of polytetrafluoroethylene (PTFE) as an active layer with based on a unique construction of polypropylene (PP) support material (Fang *et al.*, 2014). FP membrane can be categorised as hydrophobic membrane based on their contact angle as measured by Nguyen *et al.* (2015) (Nguyen *et al.*, 2015). The chemical structure of FP–PTFE is shown in Figure 2.13.
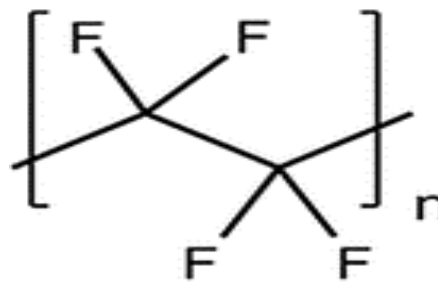
Figure 2.13: Chemical structure of fluoropolymer (Lee *et al.*, 2016).

2.2.7   Membrane cleaning methods

The membrane can be clogged due to deposition of solutes on the membrane surface (Ilame and Satyavir, 2015). Therefore, membrane cleaning is needed after every filtration process to prolong the lifespan of the membrane and maintain the membrane performance. The choice of cleaning method depends on the module design, the type of membrane, the type of foulant and the severity of fouling (Echavarría *et al.*, 2011; Mulder, 1996). There are various methods of membrane cleaning as discussed below.

2.2.7.1   Chemical cleaning

Chemical cleaning is the most commonly used method of reducing fouling in membrane separations. This cleaning method depends upon the deposit to be removed and the surface of the membrane. Cleaning is an interaction between the fouled layer, the detergent and the membrane surface. Chemical cleaning involves alkali treatment using sodium hydroxide, acid flush using nitric acid, enzymatic hydrolysis and surfactant flush or in combination of them (Ilame and V. Singh,

2015). Commercial cleaning agent containing surfactant such as *Ultrasil 11* has the functions of wetting, emulsifying, dispersing and cleaning. *Ultrasil 11* was proved to be more effective in regenerated the membrane after fouling and cleaning (Wu and Bird, 2007). The membrane was undergone surface modification due to the adsorption of *Ultrasil 11* surfactant to the membrane surface (Weis *et al.*, 2003). Chemical cleaning is usually carried out as "clean in place" (CIP) techniques by filling the retentate channels of the membrane module with cleaning solution for a period of time at low pressure and high velocity at temperatures between 40 °C to 60 °C. This method can combined with other cleaning methods.

2.2.7.2   *Mechanical cleaning*

Mechanical cleaning can be applied to tubular membrane module using sponge balls (Mulder, 1996). The use of mechanical cleaning in membrane bioreactor by using scouring agents was developed as a new approach to control membrane fouling (Aslam *et al.*, 2017).

2.2.7.3   *Electric cleaning*

The electric field is applied across the membrane in this cleaning method. The particles or molecules that contain positive or negative charged will migrate following the electric field direction (Mulder, 1996). The disadvantage of this method is, electric cleaning requires a special system design with electrodes and electric conducting membrane need to be used.

2.2.7.4   *Hydraulic cleaning*

Back-flushing is a common technique in hydraulic cleaning method. When back-flushing is applied, the filtration process is in reversed mode where the flow direction is changed (Echavarría *et al.*, 2011). The feed pressure is released after a certain period of time. Then, a small volume of permeate is flushed back through the membrane and removes foulants that clogged on the membrane surface or in the pores.

2.3   Fluid dynamic gauging (FDG)

Fluid dynamic gauging (FDG) is a technique used to measure the thickness and strength of cake layers that cause fouling on solid surfaces immersed in a liquid (Chew *et al.*, 2004). FDG was applied to monitor the removal of cake layers in membrane cleaning through thickness measurement with controlled application of fluid shear to the surface of the cake layer (Lewis et al., 2012). Removal of stains in fabric cleaning caused by suction flow in FDG was studied by Thongpiam *et al.* (2016) (Thongpiam *et al.*, 2016). The advantages of applying this FDG technique are (Tuladhar *et al.*, 2000):

(i)   Thickness is determined by measuring the discharge flow rate of fluid

(ii)   Easy installation and operation

(iii)   Simple equipment and cheap to construct

FDG measurements can be performed in two modes of operations such as mass flow mode and pressure mode. Tuladhar *et al.* (2000) developed the FDG using mass flow mode wherein the differential pressure is maintained constant and the gauging mass flow rate is measured. Pressure mode FDG was used by Lister *et al.* (2011) (Lister *et al.*, 2011) to study the deposition of ballotini suspension in cross-flow microfiltration system. In pressure mode, gauging mass flow rate is controlled at a set level and the pressure drop across the nozzle is measured. The pressure mode is the best option for studies of fouling and cleaning in flowing environment because by controlling the gauging flows, it allows experiments at higher pressure (Jones *et al.*, 2010) and the shear stress applied on the fouling layers can be controlled more accurately (Lewis *et al.*, 2012).

Figure 2.14 shows the schematic of a FDG nozzle. This technique works by inducing a constant flow rate of fluid into the FDG nozzle. The suction flow into the gauge imposes a fluid shear stress (τ) on the fouling layers, to remove the foulant from the membrane surface. The fluid shear stress can be estimated by using Equation (2.9) that represents the radial flow between two parallel discs (Middleman, 1997):

$$\tau = \frac{3\mu m}{\rho \pi h^2 r} \tag{2.9}$$

where μ is the dynamic viscosity of fluid, m is the gauging mass flow rate, ρ is the fluid density, h is the gap between the gauge and fouling sample and r is the inner radius of the FDG nozzle. The shear stress on the surface due to gauging flow depends on the dimensionless value of h/d_t and flow conditions. The dimensionless value of h/d_t is the ratio of nozzle clearance distance to the nozzle inner diameter. The gauging mass flow rate (m) through the nozzle is sensitive to the clearance between the nozzle and the surface when h/dt is <0.25. The shear stress imposed by the gauging flow is related to the mean pipe flow velocity (u_{min}) (Peck et $al.$, 2015) as shown in Equation (2.10):

$$u_{min} = \sqrt{\frac{2\,\tau_{wall}}{\rho\,C_f}} \qquad\qquad (2.10)$$

where τ_{wall} is the wall shear stress, C_f is the Fanning friction factor, and ρ is the fluid density. Therefore, the fluid velocity can be calculated from the shear stress value. Removal of stains in fabric cleaning caused by suction flow in FDG was analysed using $ImageJ$ analysis (Thongpiam et $al.$, 2016). Thus, $ImageJ$ analysis can be applied to analyse the removal of foulants in membrane cleaning.
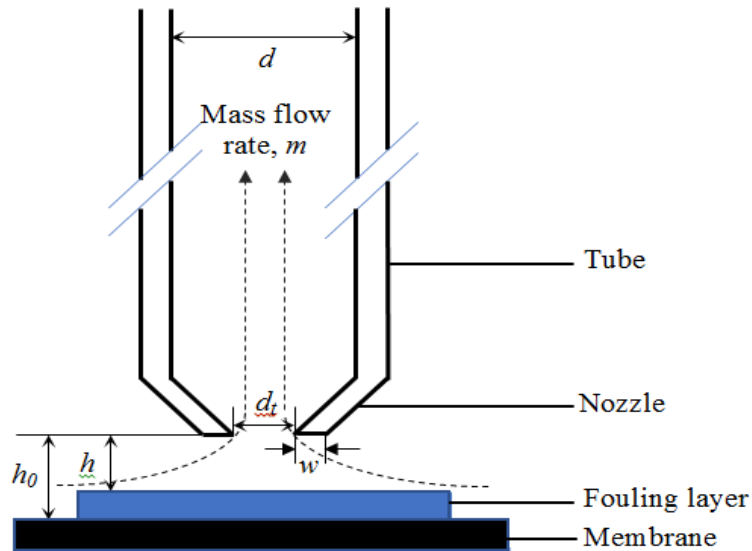
Figure 2.14: Schematic of a FDG nozzle showing dimensions, where the nozzle inner diameter, d_t = 5 mm, tube inner diameter, d = 25 mm and nozzle thickness, w = 2mm; (dashed line shows the fluid flow into the nozzle).

2.4　Gap analysis

A literature review has been performed in order to find a model solution that can replace NRS as the raw material for this project. Natural rubber serum is difficult to obtain in sufficient quantities in a suitable form for experimentation. The phytosterols content in orange juice varies from 0.229 mg ml^{-1} to 0.306 mg ml^{-1} (Jiménez-Escrig *et al.*, 2006; Piironen *et al.*, 2003). In addition, the pH of orange juice (pH 3.45) is very similar to that of NRS (pH 3.56) (Muhammad, 2018). Based on literature review, orange juice can be used as a model solution as the type and amount of phytosterols present are similar to those present in NRS. Orange juice also contains other bioactive compounds such as sugar and protein fractions.

Ultrafiltration can be applied in separating natural compounds from agro-industrial by-products. Membrane separation techniques have been widely applied previously in fruit juices processing (Echavarría *et al.*, 2011; Ilame and V. Singh, 2015). However, there is no available literature that reports the application of ultrafiltration for the separation of phytosterols from orange juice. Therefore, UF will be selected as the main process in separating phytosterols from orange juice in this study. Ultrafiltration process using different membrane materials at different MWCO, different pressure and temperature resulted in different amount of targeted bioactive compounds, due to the fouling effect. Fouling phenomena depend upon the physical properties of the membrane such as molecular weight cut off (MWCO), pore size distribution and membrane material (Jeon *et al.*, 2016), and also membrane surface chemistry such as surface charge, hydrophobicity, roughness and chemical bonding interactions (Argyle *et al.*, 2015; Evans *et al.*, 2009). Fouling is also dependent on operating conditions such as transmembrane pressure, feed component concentrations and pH (Mulder, 1996). Thus, the performance of the orange juice ultrafiltration will be studied in terms of permeate flux, rejection, fouling and cleaning efficiency.

Chemical cleaning is the most commonly used method of reducing fouling in membrane separations especially in practical operations, where industrially relevant feeds are filtered. Chemical cleaning was found to cause surface modification such as hydrophobicity, roughness and surface charge (Jones *et al.*, 2011). Fluid dynamic gauging (FDG) was applied to monitor the removal of fouling layers of yeast

suspension on microfiltration membrane through thickness measurement with controlled application of fluid shear (Lewis *et al.*, 2012). Therefore, the novelty of this work is the application of FDG to remove the fruit juice foulants formed on UF membranes via mechanical cleaning.

2.5   Aim and Objectives

Based on the literature review, these aim and objectives were proposed. The aim of this study is to develop the ultrafiltration process for the separation of phytosterols and proteins from orange juice using synthetic membranes made from regenerated cellulose acetate, polyethersulfone and fluoropolymer. The same concept is thought to be applicable to natural rubber serum that potentially be used to produce other minor high value-added compounds such as phytosterols. With this scope in mind, the specific research objectives are as follows:

Objective 1: To identify a suitable model feedstock with similar bioactive compounds to natural rubber serum (NRS).

Objective 2: To characterise the NRS and the model feedstock (orange juice) used in this study in term of amount of total phytosterols, proteins, pH and viscosity.

Objective 3: To develop appropriate ultrafiltration process using different membrane types and different operating conditions in order to recover high amount of phytosterols from orange juice.

Objective 4: To investigate the effects of fouling and cleaning during the ultrafiltration that affected the membrane performances by determining the membranes characteristics such as hydrophobicity, surface roughness and charge.

Objective 5: To apply the fluid dynamic gauging (FDG) technique to assess the mechanical cleaning performance compared to the chemical cleaning in this system.

References

Aiello, P., Sharghi, M., Mansourkhani, S.M., Ardekan, A.P., Jouybari, L., Daraei, N., Peiro, K., Mohamadian, S., Rezaei, M., Heidari, M., Peluso, I., Ghorat, F., Bishayee, A., Kooti, W., 2019. Medicinal Plants in the Prevention and Treatment of Colon Cancer. *Oxidative medicine and cellular longevity* 2019, 2075614.

Aimi Izyana, I., Zairossani, M.N., 2011. Effect of Spray Drying on Protein Content of Natural Rubber Serum. *IIUM Engineering Journal* 12, 61-65.

Almanasrah, M., Brazinha, C., Kallioinen, M., Duarte, L.C., Roseiro, L.B., Bogel-Lukasik, R., Carvalheiro, F., Mänttäri, M., Crespo, J.G., 2015. Nanofiltration and reverse osmosis as a platform for production of natural botanic extracts: The case study of carob by-products. *Separation and Purification Technology* 149, 389-397.

Arahman, N., Nursidik, Mukramah, Maulidayanti, S., Putri, A.O., 2015. The Stability of Poly(ether sulfone) Membranes Treated in Hot Water and Hypochlorite Solution. *Procedia Chemistry* 16, 709-715.

Archer, B.L., Audley, B.G., McSweeney, G.P., Tan, C.H., 1969. Studies on Composition of Latex Serum and 'Bottom Fraction Particles. *Journal of Rubber Research* 21(4), 560-569

Argyle, I.S., Pihlajamäki, A., Bird, M.R., 2015. Black tea liquor ultrafiltration: Effect of ethanol pre-treatment upon fouling and cleaning characteristics. *Food and Bioproducts Processing* 93, 289-297.

Aslam, M., Charfi, A., Lesage, G., Heran, M., Kim, J., 2017. Membrane bioreactors for wastewater treatment: A review of mechanical cleaning by scouring agents to control membrane fouling. *Chemical Engineering Journal* 307, 897-913.

Awan, A.T., Tsukamoto, J., Tasic, L., 2013. Orange waste as a biomass for 2G-ethanol production using low cost enzymes and co-culture fermentation. *RSC Advances* 3, 25071-25078.

Bai, H., Zhou, Y., Wang, X., Zhang, L., 2012. The Permeability and Mechanical Properties of Cellulose Acetate Membranes Blended with Polyethylene glycol 600 for Treatment of Municipal Sewage. *Procedia Environmental Sciences* 16, 346-351.

Balme, S., Gulacar, F.O., 2012. Rapid screening of phytosterols in orange juice by solid-phase microextraction on polyacrylate fibre derivatisation and gas chromatographic-mass spectrometric. *Food Chem* 132, 613-618.

Bardestani, R., Patience, G.S., Kaliaguine, S., 2019. Experimental methods in chemical engineering: specific surface area and pore size distribution measurements—BET, BJH, and DFT. *The Canadian Journal of Chemical Engineering* 97, 2781-2791.

Basu, S., Balakrishnan, M., 2017. Polyamide thin film composite membranes containing ZIF-8 for the separation of pharmaceutical compounds from aqueous streams. *Separation and Purification Technology* 179, 118-125.

Brufau, G., Canela, M.A., Rafecas, M., 2008. Phytosterols: physiologic and metabolic aspects related to cholesterol-lowering properties. *Nutrition research (New York, N.Y.)* 28, 217-225.

Calpe Berdiel, L., Mendez-Gonzalez, J., Llaverias, G., Escolà-Gil, J., Blanco-Vaca, F., 2010. Plant sterols, cholesterol metabolism and related disorders, pp. 223-242.

Cantrill, R., 2008. Phytosterols, Phytostanols and Their Esters, in: Kawamura, Y. (Ed.), Chemical and Technical Assessment for the 69th JECFA.

Cassano, A., Donato, L., Conidi, C., Drioli, E., 2008. Recovery of bioactive compounds in kiwifruit juice by ultrafiltration. *Innovative Food Science & Emerging Technologies* 9, 556-562.

Cassano, A., Marchio, M., Drioli, E., 2007. Clarification of blood orange juice by ultrafiltration: analyses of operating parameters, membrane fouling and juice quality. *Desalination* 212, 15-27.

Chew, J.Y.M., Paterson, W.R., Wilson, D.I., 2004. Fluid dynamic gauging for measuring the strength of soft deposits. *Journal of Food Engineering* 65, 175-187.

Clement, L.M., Hansen, S.L., Costin, C.D., Perri, G.L., 2010. Quantitation of Sterols and Steryl Esters in Fortified Foods and Beverages by GC/FID. *Journal of the American Oil Chemists' Society* 87, 973-980.

Cobell, 2016. Orange Juice Not From Concentrate (NFC). Cobell, Exeter, United Kingdom.

Conidi, C., Cassano, A., Caiazzo, F., Drioli, E., 2017. Separation and purification of phenolic compounds from pomegranate juice by ultrafiltration and nanofiltration membranes. *Journal of Food Engineering* 195, 1-13.

Cuperus, F.P., Nijhuis, H.H., 1993. Applications of membrane technology to food processing. *Trends in Food Science & Technology* 4, 277-282.

Cypriano, D.Z., da Silva, L.L., Tasic, L., 2018. High value-added products from the orange juice industry waste. *Waste Management* 79, 71-78.

Devaraj, V., Zairossani, M.N., 2006. Zero Discharge and Value Added Products from NR Skim Latex Processing Malaysian Rubber Technology Developments. Malaysian Rubber Board, Kuala Lumpur, pp. 19-21.

Devaraj, V., Zairossani, M.N., Pretibaa, S., 2006. Membrane Separation as a Cleaner Processing Technology for Natural Raw Rubber Processing. *J. Applied Membrane Science & Technology* 4, 13 - 22.

Echavarría, A.P., Torras, C., Pagán, J., Ibarz, A., 2011. Fruit Juice Processing and Membrane Technology Application. *Food Engineering Reviews* 3, 136-158.

Evans, P.J., Bird, M.R., 2010. The role of black tea feed conditions upon ultrafiltration performance during membrane fouling and cleaning. *Journal of Food Process Engineering* 33, 309 - 332.

Evans, P.J., Bird, M.R., Pihlajamäki, A., Nyström, M., 2008. The influence of hydrophobicity, roughness and charge upon ultrafiltration membranes for black tea liquor clarification. *Journal of Membrane Science* 313, 250-262.

Evans, P.J., Bird, M.R., Rogers, D., Wright, C.J., 2009. Measurement of polyphenol–membrane interaction forces during the ultrafiltration of black tea liquor. *Colloids and Surfaces A: Physicochemical and Engineering Aspects* 335, 148-153.

Fang, Y., Bian, L., Bi, Q., Li, Q., Wang, X., 2014. Evaluation of the pore size distribution of a forward osmosis membrane in three different ways. *Journal of Membrane Science* 454, 390-397.

Feng, S., Liu, S., Luo, Z., Tang, K., 2015. Direct saponification preparation and analysis of free and conjugated phytosterols in sugarcane (Saccharum officinarum L.) by reversed-phase high-performance liquid chromatography. *Food Chem* 181, 9-14.

Fernandes, P., Cabral, J.M.S., 2007. Phytosterols: Applications and recovery methods. *Bioresource Technology* 98, 2335-2350.

Field, R.W., Wu, D., Howell, J.A., Gupta, B.B., 1995. Critical flux concept for microfiltration fouling. *Journal of Membrane Science* 100, 259-272.

Food-And-Drug-Administration, 2019. CFR - Code of Federal Regulations Title 21. U.S. Food And Drug Administration.

Graham, T., 1866. On the Absorption and Dialytic Separation of Gases by Colloid Septa. *Philosophical Transactions of the Royal Society of London* 156, 399-439.

Gulec, H.A., Bagci, P.O., Bagci, U., 2017. Clarification of Apple Juice Using Polymeric Ultrafiltration Membranes: a Comparative Evaluation of Membrane Fouling and Juice Quality. *Food and Bioprocess Technology* 10, 875-885.

Han, J., Fu, J., Schoch, R.B., 2008. Molecular sieving using nanofilters: past, present and future. *Lab Chip* 8, 23-33.

Hasma, H., Subramaniam, A., 1986. Composition of Lipids in Latex of Hevea Brasiliensis Clone RRIM 501. *Journal of Natural Rubber Research* 1, 30-40.

Hermia, J., 1982. Constant pressure blocking filtration laws–application to power law non-Newtonian fluids. *Trans IChemE* 60, 183-187.

Ho., C.C., Subramaniam, A., Yong, W.M., 1975. Lipids Associated with the Particles in Hevea Latex, International Rubber Conference, Kuala Lumpur, pp. 441-456.

Ilame, S.A., Satyavir, V.S., 2015. Application of membrane separation in fruit and vegetable juice processing: a review. *Crit Rev Food Sci Nutr* 55, 964-987.

Ilame, S.A., V. Singh, S., 2015. Application of Membrane Separation in Fruit and Vegetable Juice Processing: A Review. *Critical Reviews in Food Science and Nutrition* 55, 964-987.

Iritani, E., Katagiri, N., 2016. Developments of Blocking Filtration Model in Membrane Filtration. *KONA Powder and Particle Journal* 33, 179-202.

Jeon, S., Rajabzadeh, S., Okamura, R., Ishigami, T., Hasegawa, S., Kato, N., Matsuyama, H., 2016. The Effect of Membrane Material and Surface Pore Size on the Fouling Properties of Submerged Membranes. *Water* 8, 602.

Jesus, D.F., Leite, M.F., Silva, L.F.M., Modesta, R.D., Matta, V.M., Cabral, L.M.C., 2007. Orange (Citrus sinensis) juice concentration by reverse osmosis. *Journal of Food Engineering* 81, 287-291.

Jiménez-Escrig, A., Santos-Hidalgo, A.B., Saura-Calixto, F., 2006. Common Sources and Estimated Intake of Plant Sterols in the Spanish Diet. *Journal of Agricultural and Food Chemistry* 54, 3462-3471.

Jiraratananon, R., Chanachai, A., 1996. A study of fouling in the ultrafiltration of passion fruit juice. *Journal of Membrane Science* 111, 39-48.

Jones, S.A., Bird, M.R., Pihlajamäki, A., 2011. An experimental investigation into the pre-treatment of synthetic membranes using sodium hydroxide solutions. *Journal of Food Engineering* 105, 128-137.

Jones, S.A., Chew, Y.M.J., Bird, M.R., Wilson, D.I., 2010. The application of fluid dynamic gauging in the investigation of synthetic membrane fouling phenomena. *Food and Bioproducts Processing* 88, 409-418.

Kongduang, D., Wungsintaweekul, J., De-Eknamkul, W., 2012. Established GC-FID for simultaneous determination of diterpenes and phytosterols in Plaunoi (Croton stellatopilosus Ohba).

Lagarda, M.J., García-Llatas, G., Farré, R., 2006. Analysis of phytosterols in foods. *Journal of Pharmaceutical and Biomedical Analysis* 41, 1486-1496.

Lee, A., Elam, J.W., Darling, S.B., 2016. Membrane materials for water purification: design, development, and application. *Environmental Science: Water Research & Technology* 2, 17-42.

Lerma-García, M.J., D'Amato, A., Simó-Alfonso, E.F., Righetti, P.G., Fasoli, E., 2016. Orange proteomic fingerprinting: From fruit to commercial juices. *Food Chemistry* 196, 739-749.

Lewis, W.J.T., Chew, Y.M.J., Bird, M.R., 2012. The application of fluid dynamic gauging in characterising cake deposition during the cross-flow microfiltration of a yeast suspension. *Journal of Membrane Science* 405-406, 113-122.

Lewis, W.J.T., Mattsson, T., Chew, Y.M.J., Bird, M.R., 2017. Investigation of cake fouling and pore blocking phenomena using fluid dynamic gauging and critical flux models. *Journal of Membrane Science* 533, 38-47.

Lister, V.Y., Lucas, C., Gordon, P.W., Chew, Y.M.J., Wilson, D.I., 2011. Pressure mode fluid dynamic gauging for studying cake build-up in cross-flow microfiltration. *Journal of Membrane Science* 366, 304-313.

Malaysian-Rubber-Board, 2018. UKKP Information Sheet 4th Quarter 2018. Malaysian Rubber Board, Kuala Lumpur.

Market-Insights-Reports, 2019. Global Phytosterols Market Insights, Forecast To 2025. QY Research, USA.

McDonald, J.G., Smith, D.D., Stiles, A.R., Russell, D.W., 2012. A comprehensive method for extraction and quantitative analysis of sterols and secosteroids from human plasma. *Journal of lipid research* 53, 1399-1409.

Meng, S., Zhang, M., Yao, M., Qiu, Z., Hong, Y., Lan, W., Xia, H., Jin, X., 2019. Membrane Fouling and Performance of Flat Ceramic Membranes in the Application of Drinking Water Purification. *Water* 11, 2606.

Middleman, S., 1997. An Introduction to Fluid Dynamics: Principles of Analysis and Design. Wiley, New York.

Miller, D.J., Kasemset, S., Paul, D.R., Freeman, B.D., 2014. Comparison of membrane fouling at constant flux and constant transmembrane pressure conditions. *Journal of Membrane Science* 454, 505-515.

Mohammad, A.W., Ng, C.Y., Lim, Y.P., Ng, G.H., 2012. Ultrafiltration in Food Processing Industry: Review on Application, Membrane Fouling, and Fouling Control. *Food and Bioprocess Technology* 5, 1143-1156.

Muhammad, A.K., 2018. Personal Correspondance. Malaysian Rubber Board, Kuala Lumpur, Malaysia.

Mulder, M., 1996. Basic Principles of Membrane Technology, Second ed. Kluwer Academic Publishers, The Netherlands.

Ng, K.S.Y., Haribabu, M., Harvie, D.J.E., Dunstan, D.E., Martin, G.J.O., 2017. Mechanisms of flux decline in skim milk ultrafiltration: A review. *Journal of Membrane Science* 523, 144-162.

Nguyen, L.A.T., Schwarze, M., Schomäcker, R., 2015. Adsorption of non-ionic surfactant from aqueous solution onto various ultrafiltration membranes. *Journal of Membrane Science* 493, 120-133.

Nollet, J.A., 1995. Investigations on the causes for the ebullition of liquids. *Journal of Membrane Science* 100, 1-3.

Nyam, K.L., Tan, C.P., Lai, O.M., Long, K., Che Man, Y.B., 2011. Optimization of supercritical CO2 extraction of phytosterol-enriched oil from Kalahari melon seeds. *Food and Bioprocess Technology* 4, 1432-1441.

Ogbe, R.J., O.Ochalefu, D., Mafulul, S.G., Olaniru, O.B., 2015. A review on dietary phytosterols: Their occurance, metabolism and health benefits. *Asian Journal of Plant Science and Research* 5(4), 10-21.

Okino Delgado, C.H., Fleuri, L.F., 2016. Orange and mango by-products: Agro-industrial waste as source of bioactive compounds and botanical versus commercial description—A review. *Food Reviews International* 32, 1-14.

Ostlund, R.E., Jr., Racette, S.B., Stenson, W.F., 2003. Inhibition of cholesterol absorption by phytosterol-replete wheat germ compared with phytosterol-depleted wheat germ. *The American journal of clinical nutrition* 77, 1385-1389.

Pap, N., Mahosenaho, M., Pongrácz, E., Mikkonen, H., Jaakkola, M., Virtanen, V., Myllykoski, L., Horváth-Hovorka, Z., Hodúr, C., Vatai, G., Keiski, R.L., 2012. Effect of Ultrafiltration on Anthocyanin and Flavonol Content of Black Currant Juice (Ribes nigrum L.). *Food and Bioprocess Technology* 5, 921-928.

Peck, O.P.W., John Chew, Y.M., Bird, M.R., Bolhuis, A., 2015. Application of Fluid Dynamic Gauging in the Characterization and Removal of Biofouling Deposits. *Heat Transfer Engineering* 36, 685-694.

Pentair, 2017. Filtration spectrum, The Netherlands.

Pihlajamaki, A., Nyström, M., 1995. Streaming potential methods in characterization of membranes, in: Bowen, W.R., Field, R.W., Howell, J.A. (Eds.), Proceedings of EuroMembrane 95. European Membrane Society, Bath, UK, pp. 521-524.

Piironen, V., Toivo, J., Puupponen-Pimiä, R., Lampi, A.-M., 2003. Plant sterols in vegetables, fruits and berries. *Journal of the Science of Food and Agriculture* 83, 330-337.

Sablani, S.S., Goosen, M.F.A., Al-Belushi, R., Wilf, M., 2001. Concentration polarization in ultrafiltration and reverse osmosis: a critical review. *Desalination* 141, 269-289.

Sajari, R., Abd-Razak, N.H., Yusof, F., Arif, S.A.M., Perkins, M., Yeang, H.Y., 2014. Improved Efficiency of Tocotrienol Extraction from Fresh and Processed Latex. *Journal of Rubber Research* 17, 245-260.

Santini, A., Novellino, E., 2017. Nutraceuticals in hypercholesterolaemia: an overview. *Br J Pharmacol* 174, 1450-1463.

Shahidi, F., Ambigaipalan, P., 2015. Phenolics and polyphenolics in foods, beverages and spices: Antioxidant activity and health effects – A review. *Journal of Functional Foods* 18, 820-897.

Shahzad, N., Khan, W., Md, S., Ali, A., Saluja, S.S., Sharma, S., Al-Allaf, F.A., Abduljaleel, Z., Ibrahim, I.A.A., Abdel-Wahab, A.F., Afify, M.A., Al-Ghamdi, S.S., 2017. Phytosterols as a natural anticancer agent: Current status and future perspective. *Biomedicine & Pharmacotherapy* 88, 786-794.

Sidney, L., Srinivasa, S., 1964. High flow porous membranes for separating water from saline solutions. Google Patents.

Stinco, C.M., Fernández-Vázquez, R., Escudero-Gilete, M.L., Heredia, F.J., Meléndez-Martínez, A.J., Vicario, I.M., 2012. Effect of Orange Juice's Processing on the Color, Particle Size, and Bioaccessibility of Carotenoids. *Journal of Agricultural and Food Chemistry* 60, 1447-1455.

Strathmann, H., 2011. Introduction to Membrane Science and Technology. Wiley-VCH, Germany.

Sundram, K., Sambanthamurthi, R., Tan, Y.A., 2003. Palm fruit chemistry and nutrition. *Asia Pacific journal of clinical nutrition* 12, 355-362.

Suttiarporn, P., Chumpolsri, W., Mahatheeranont, S., Luangkamin, S., Teepsawang, S., Leardkamolkarn, V., 2015. Structures of Phytosterols and Triterpenoids with Potential Anti-Cancer Activity in Bran of Black Non-Glutinous Rice. *Nutrients* 7, 1672-1687.

Taqvi, S., Bassioni, G., 2019. Understanding Wettability through Zeta Potential Measurements, in: Khanna, R. (Ed.), Wettability and Interfacial Phenomena-Implications for Material Processing. IntechOpen Limited, UK.

Thongpiam, M., Lertruamporn, S., Saikhwan, P., John Chew, Y.M., 2016. Investigation of Fabric Cleaning Using Fluid Dynamic Gauging: Effects of Fine Bubbles, 2nd Annual InterPore UK Chapter conference. Royal Society of Chemistry, Loughborough, UK.

Tolve, R., Condelli, N., Can, A., Tchuenbou-Magaia, F.L., 2018. Development and Characterization of Phytosterol-Enriched Oil Microcapsules for Foodstuff Application. *Food and Bioprocess Technology* 11, 152-163.

Tuladhar, T.R., Paterson, W.R., Macleod, N., Wilson, D.I., 2000. Development of a novel non-contact proximity gauge for thickness measurement of soft deposits and its application in fouling studies. *The Canadian Journal of Chemical Engineering* 78, 935-947.

Unilever, 2018. What are plant sterols?

Virtanen, T., Rudolph, G., Lopatina, A., Al-Rudainy, B., Schagerlöf, H., Puro, L., Kallioinen, M., Lipnizki, F., 2020. Analysis of membrane fouling by Brunauer-Emmet-Teller nitrogen adsorption/desorption technique. *Scientific Reports* 10, 3427.

Wang, M., Huang, W., Hu, Y., Zhang, L., Shao, Y., Wang, M., Zhang, F., Zhao, Z., Mei, X., Li, T., Wang, D., Liang, Y., Li, J., Huang, Y., Zhang, L., Xu, T., Song, H., Zhong, Y., Lu, B., 2018. Phytosterol Profiles of Common Foods and
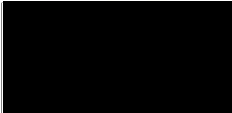
Estimated Natural Intake of Different Structures and Forms in China. *Journal of Agricultural and Food Chemistry* 66, 2669-2676.

Wang, T., Hicks, K.B., Moreau, R., 2002. Antioxidant activity of phytosterols, oryzanol, and other phytosterol conjugates. *Journal of the American Oil Chemists' Society* 79, 1201-1206.

Weber, S., Gallenkemper, M., Melin, T., Dott, W., Hollender, J., 2004. Efficiency of nanofiltration for the elimination of steroids from water. *Water Science and Technology* 50, 9-14.

Weis, A., Bird, M.R., Nyström, M., 2003. The chemical cleaning of polymeric UF membranes fouled with spent sulphite liquor over multiple operational cycles. *Journal of Membrane Science* 216, 67-79.

Weis, A., Bird, M.R., Nyström, M., Wright, C., 2005. The influence of morphology, hydrophobicity and charge upon the long-term performance of ultrafiltration membranes fouled with spent sulphite liquor. *Desalination* 175, 73-85.

Woyengo, T.A., Ramprasath, V.R., Jones, P.J.H., 2009. Anticancer effects of phytosterols, European Journal of Clinical Nutrition, pp. 813-820.

Wu, D., Bird, M.R., 2007. The Fouling and Cleaning of Ultrafiltration Membranes During The Filtration of Model Tea Component Solutions. *Journal of Food Process Engineering* 30, 293-323.

Xu, L.-Q., Liu, Y.-J., Yao, K., Liu, H.-H., Tao, X.-Y., Wang, F.-Q., Wei, D.-Z., 2016. Unraveling and engineering the production of 23,24-bisnorcholenic steroids in sterol metabolism, Scientific Reports. Nature Publishing Group, p. 21928.

Yan, F., Yang, H., Li, J., Wang, H., 2012. Optimization of Phytosterols Recovery from Soybean Oil Deodorizer Distillate. *Journal of the American Oil Chemists' Society* 89, 1363-1370.

Yuan, Y., Lee, T.R., 2013. Contact Angle and Wetting Properties, in: Bracco, G., Holst, B. (Eds.), Surface Science Techniques. Springer Berlin Heidelberg, Berlin, Heidelberg, pp. 3-34.

Zairossani, M.N., Devaraj, V., Zin, A.K.M., Zaid, I., 2005. Modern approaches towards effective effluent treatment, Rubber Planters Conference 2005. Malaysian Rubber Board, Kuala Lumpur, Malaysia.

Zeman, L.J., Zydney, A.L., 1996. Microfiltration and Ultrafiltration - Principles and Applications. Marcel Dekker, Inc., New York, USA.

Chapter 3: Membrane fouling during the fractionation of phytosterols isolated from orange juice

Introductory text

This project was derived from the issues found in utilisation of by-products of rubber processing mainly non-rubber components for the production of high value-added compounds. Based on the literature review (Chapter 2), rubber serum contains phytosterols compounds. Model feedstock that has similar bioactive compounds with rubber serum has been used in this work. This chapter presents the novel use of ultrafiltration method in separating phytosterols from orange juice by using synthetic membranes comprised of different polymeric composition made from regenerated cellulose acetate, polyethersulfone and fluoropolymer. The phytosterols separation was performed at different transmembrane pressure (TMP) of 0.5 - 2 bar, and a cross-flow velocity (CFV) of 0.5 - 1.5 m s^{-1}. The ultrafiltration performances of the tested membranes were determined in terms of flux, rejection ratio and total resistances. Membrane rejection towards total phytosterols, proteins, sugars, antioxidant activity and suspended solid were determined in order to study the separation of phytosterols and to investigate the effect of membrane fouling. In order to define the performance of the membrane after fouling and cleaning, the membrane hydrophobicity, Fourier transform infrared (FTIR) and scanning electron microscopy (SEM) analysis were carried out. The ultrafiltration protocol for separating phytosterols from orange juice followed by compounds and membranes characterisation studies have been reported in this paper.

Statement of Authorship

This declaration concerns the article entitled:
Membrane fouling during the fractionation of phytosterols isolated from orange juice

Publication status (tick one)									
Draft manuscript	☐	**Submitted**	☐	**In review**	☐	**Accepted**	☐	**Published**	✓

Publication details (reference)	Abd-Razak, N. H., Chew, Y. M. J., & Bird, M. R. (2019). Membrane fouling during the fractionation of phytosterols isolated from orange juice. *Food and Bioproducts Processing*, 113, 10–21.https://doi.org/10.1016/j.fbp.2018.09.005
Candidate's contribution to the paper (provide details, and also indicate as a percentage)	**Formulation of ideas (60%):** I proposed ideas for separation of phytosterols from a model solution with similar properties to natural rubber serum. Mike Bird and John Chew suggested the application of ultrafiltration process using M10 filtration rig and three different types of commercial polymeric membranes. **Design of methodology (70%):** The analytical tests for compounds and membranes characterisations were suggested by Mike Bird. I further built on the design of the experiments presented in this paper. **Experimental work (90%):** I performed all the ultrafiltration experiments, analysis of compounds and characterisation of membranes. SEM analysis of the samples was carried out by the technical staff. I carried out the data interpretation after discussions with my co-authors. **Presentation of data in journal format (80%):** I prepared the manuscript for the journal including the outlines, graphics in the journal format and incorporated feedback from co-authors. The co-authors contributed in revising the draft manuscript.
Statement from Candidate	This paper reports on original research I conducted during the period of my Higher Degree by Research candidature.
Signed	███████	**Date**	25 Feb 2021

Membrane fouling during the fractionation of phytosterols isolated from orange juice

Nurul Hainiza Abd-Razak[a,b], Y.M. John Chew[a], Michael R. Bird[a*],

[a]*Department of Chemical Engineering, University of Bath, Bath BA2 7AY, UK*

[b]*Malaysian Rubber Board, 50450 Kuala Lumpur, Malaysia*

Abstract

The aim of this study is to isolate phytosterol compounds from orange juice using ultrafiltration (UF) flat sheet membranes (supplied by Alfa Laval) with molecular weight cut-off (MWCO) values of 10 kDa fabricated from regenerated cellulose, polyethersulphone and fluoropolymer. A cross-flow filtration rig operated at a transmembrane pressure (TMP) of 0.5 - 2 bar, and a cross-flow velocity (CFV) of 0.5 - 1.5 m s⁻¹. Membrane rejection towards total phytosterols, proteins, sugars were determined along with antioxidant activity. The regenerated cellulose membrane displayed the highest permeate flux (a pseudo steady-state value of 22 L m⁻² h⁻¹), with a higher fouling index (75%) and a good separation efficiency of phytosterols (32% rejection towards phytosterols) from orange juice. Although the yield of phytosterols was relatively low (40 mg/L), there is a great potential to optimise the filtration process to produce commercially relevant amount of phytosterols. All membranes investigated displayed cleaning efficiencies of > 95%.

Keywords: Ultrafiltration; Phytosterols; Orange juice; Fouling; Membrane separation

*Corresponding author. *Email address:* M.R.Bird@bath.ac.uk

1.   Introduction

Plants produce diverse and complex molecules. Many of them are of high value due to their bioactivity such as phytosterols that possess cholesterol lowering (Brufau *et al.*, 2008) and anti-oxidative properties (Wang *et al.*, 2002). Phytosterols are also known for their anticancer effects due to their potential to inhibit cancer cell cycle progression (Shahzad *et al.*, 2017). Increasingly, natural products are being used in many nutraceutical, pharmaceutical and food industries. Better routes for their isolation are becoming core drivers in minimising both environmental impact and operating costs. Studies are needed to recover new classes of natural products that could be of great value from agro-industrial by-products (Almanasrah *et al.*, 2015; Conidi *et al.*, 2017). Global market size of phytosterols was over USD 500 million in 2015 and would expand at 9% up to 2024 (Global-Market-Insight, 2016).

In 2015, the natural rubber industry in Malaysia contributed RM20 billion to the country's export earnings. This arises from the export of technically specified and speciality rubbers, latex concentrates, latex dipped goods, rubber based and rubber-wood products (MITI, 2016). The rubber tree or *Hevea brasiliensis* is key ingredient for many industrial applications related to rubber products such as tyres, gloves and automotive devices (Kadir, 1994). The concentrated latex can be obtained by increasing the dry rubber content of *Hevea brasiliensis* field latex from *ca.* 30% to *ca.* 60% via centrifugation method (Devaraj and Zairossani, 2006). Centrifugation produces natural rubber serum (NRS) as a by-product that consists of primarily water and variety of non-rubber substances together with sulphuric acid with high biological oxygen demand (BOD). The by-product or waste effluent is discharged into the effluent ponds. Factories without proper maintenance of the effluent ponds face environmental problems such as air pollution and land constraints. Biological treatment system also require high operating costs to comply with the stringent environmental regulatory requirement standards set by the Malaysian Department of Environment (DOE), since water is used extensively in the rubber processing. Thus, an alternative processes for an effective rubber effluent treatment was developed using membrane separation technology to minimise waste and recover value added products from waste (Zairossani *et al.*, 2005).

Hevea brasiliensis latex tapped from rubber tree contains rubber and non-rubber particles that dispersed in an aqueous serum phase (Hasma and Subramaniam,

1986; Ho. *et al.*, 1975; Hwee, 2013). Previous studies at the Malaysian Rubber Board (MRB) showed that both the sugar fraction (Devaraj and Zairossani, 2006; Mun, 1996) and the protein fraction (Aimi Izyana and Zairossani, 2011) can be successfully separated from NRS using ultrafiltration (Fig. 1). NRS contains 1–5% non-rubbers such as phytosterols, tocotrienols, lipids, carotenoid, proteins and carbohydrates (Hasma and Subramaniam, 1986; Sajari *et al.*, 2014) as presented in Table 1. The viscosity of NRS at 20 °C is 3.5 mPa s (Muhammad, 2018). Since NRS is discharged as a waste stream from rubber processing, the NRS has a great potential to be used as an alternative source for nutraceutical compounds such as phytosterols. This project arose from the issues found in utilising the by-products of rubber processing for the recovery of high value added small non-rubber compounds from the waste. The exploitation of NRS benefits the rubber industry as it enhances raw rubber factories via integration of latex and NRS processing, and it improve competitiveness by generating value added products from rubber processing waste. Furthermore, both waste minimisation and effluent utilisation approaches are important in developing a sustainable and competitive rubber processing industry.
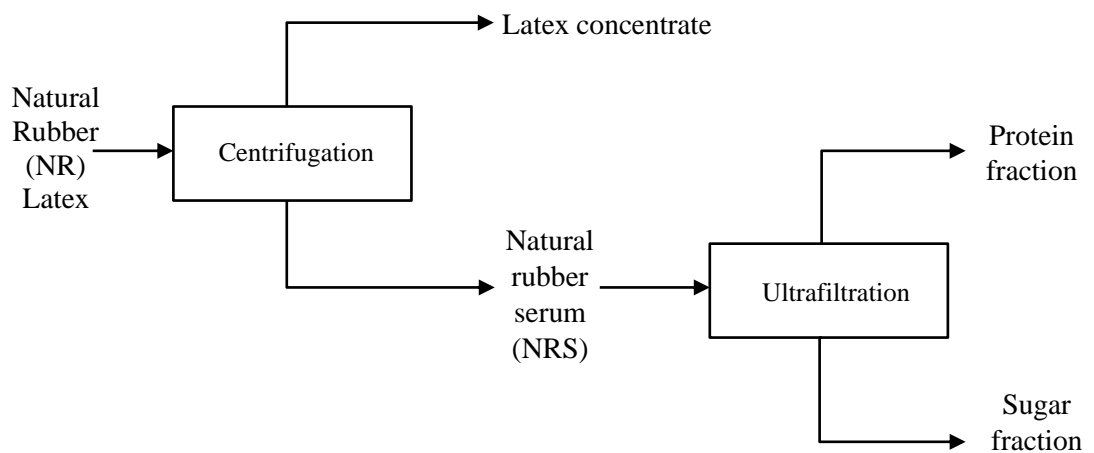
Fig. 1 - Process flow diagram of valuable product recovery from natural rubber (Devaraj and Zairossani, 2006)

Table 1 - Major components of natural rubber latex

Components	% (*w/w*)
Water	58.6
Rubber hydrocarbons	36.0
Protein, amino acid & nitrogenous compounds	1.7
Sugar and carbohydrate	1.6
Lipids (Phytosterols)	1.6 (0.03)
Ash	0.5

Nevertheless, many high value-added bioactive compounds that are available have currently not been recovered and tested. A major limitation is the lack of techniques that can be used for the economical extraction and separation of these compounds. Conventional techniques such as solvent extraction, chromatography and microwave extraction consume large amounts of energy and produce considerable waste, making them costly and unsustainable (Conidi *et al.*, 2017). This excludes them from being considered suitable for nutraceutical manufacturing. Membrane technologies such as ultrafiltration (UF) and nanofiltration (NF) offer great potential, due to their ability to separate bioactive compounds from plants and by-products of agro-industrial applications (Almanasrah *et al.*, 2015). Ultrafiltration is a pressure-driven process that separate particles in the size range 1-100 nm (Echavarría *et al.*, 2011). Nanofiltration is a separation process between ultrafiltration and reverse osmosis in flux and selectivity which offers relatively high permeation fluxes, high retention of molecules in the size range 100-1000 g mol^{-1} and a much lower operational pressure than reverse osmosis (Basu and Balakrishnan, 2017). UF and NF are commonly used in pharmaceutical fractionation, water treatment and biochemical processing. The efficacy of ultrafiltration and nanofiltration in isolating steroids from wastewater (Bodzek and Dudziak, 2006; Jin *et al.*, 2010; Nghiem *et al.*, 2004), anthocyanin from pomegranate juice (Conidi *et al.*, 2017), phenolic compounds from carob by-products (Almanasrah *et al.*, 2015) and acetaminophen from pharmaceutical by-product (Basu and Balakrishnan, 2017) has been clearly demonstrated.

A model solution with similar bioactive compounds to rubber serum will be used in this study. NRS is difficult to obtain in sufficient quantities in a suitable form

for experimentation due to the difficulties in transporting NRS from MRB in Malaysia to the UK. Phytosterols will be isolated from the model solution by the use of ultrafiltration technology. The same concept is thought to be applicable to natural rubber industry, potentially leading to new nutraceutical products. An extensive literature review has been performed in order to find a model solution that can replace NRS as the raw material for this project. Phytosterols or plant sterols are mostly found in vegetable oils, fruits and nuts (Jiménez-Escrig *et al.*, 2006; Piironen *et al.*, 2003; Plumb *et al.*, 2011). Consequently, orange juice has been chosen as a model solution, as the type and amount of phytosterols present are similar to those present in NRS (Jiménez-Escrig *et al.*, 2006; Piironen *et al.*, 2003) as tabulated in Table 2. Orange juice also contains sugars (Jesus *et al.*, 2007) and protein (Okino Delgado and Fleuri, 2016) (Table 3). In the industrial processing, fruit juice is commonly marketed in three different packaging which are frozen concentrate, fruit juice from concentrate and fruit juice not from concentrate (NFC) (Stinco *et al.*, 2012). In this study, orange juice NFC was chosen as not from concentrate (NFC) juice can retain as much of the character of the raw fruit in which no water is added or removed. Furthermore, the pH of orange juice (pH 3.45) was found to be almost similar with pH of NRS (pH 3.56) (Muhammad, 2018).

Table 3 - Composition of orange juice

Components	Amount
Phytosterols (Jiménez-Escrig *et al.*, 2006; Piironen *et al.*, 2003)	0.2 – 0.3 mg/ml
Sugar (Cobell, 2016)	$\geq 10°$ Brix
Protein (Cobell, 2016)	0.7 mg/ml

Membrane separation techniques have been widely applied previously in fruit juices processing (Echavarría *et al.*, 2011; Ilame and V. Singh, 2015). However, the literature does not report the use of ultrafiltration or nanofiltration processes for the separation of phytosterols from fruit juices. Therefore, this work will be focused on the isolation of phytosterols from orange juice via ultrafiltration technology. The performances of the selected membranes are quantified in terms of flux, rejection ratio, fouling and cleaning efficiency.

Table 2 - Comparison of phytosterols in natural rubber serum, orange juice and kiwi juice

Plant	Stigmasterol (mg/kg)	Sitosterol (mg/kg)	Fucosterol (mg/kg)	Campesterol (mg/kg)	Avenasterol (mg/kg)	Stanol (mg/kg)	Other sterol (mg/kg)	Total phytosterols (mg/kg)
Natural Rubber Serum (Hasma and Subramaniam, 1986; Sajari *et al.*, 2014)	34	127	79	-	-	-	-	240
Orange (Piironen *et al.*, 2003)	9	170	-	34	4	-	12	229
Orange (Jiménez-Escrig *et al.*, 2006)	12	220	-	38	-	4	32	306
Kiwi (Piironen *et al.*, 2003)	23	137	-	5	-	4	12	181
Kiwi (Jiménez-Escrig *et al.*, 2006)	7	49	-	2	-	-	12	70

2.   Materials and methods

2.1.   Materials

Chloroform, acetic anhydride, sulphuric acid and methanol were sourced from *Merck*, UK. Stigmasterol and butylated hydroxytoluene (BHT) acquired from *Sigma Aldrich*, UK were used as standard. A protein assay kit was purchased from *Bio-Rad*, UK. The cleaning agent *P3-Ultrasil 11* was purchased from *Ecolab*, UK. Orange juice Not From Concentrate was purchased from *Cobell*, Exeter, UK, and then stored in a cold room at 4 °C. The viscosity of orange juice (10 °Brix) at 20 °C is 9.24 ± 0.03 mPa s. Orange juice was pre-filtered by using *Amicon* (Danvers, USA) pressurized feed vessel that consist of stainless steel 25 μm cartridge filter (*Memtech*, Swansea, UK) prior to ultrafiltration to remove the pulp. Three commercial flat-sheet membranes manufactured by *Alfa Laval*, Denmark, from regenerated cellulose (RC – product code RC70PP), polyethersulphone (PES – product code GR80PP) and fluoropolymer (FP – product code ETNA10PP) respectively, were tested. Their characteristics are described in Table 4 based on the manufacturer's data sheet.

Table 4 - Characteristics of the selected membranes

Membrane	RC70PP	GR80PP	ETNA10PP
Manufacturer	*Alfa Laval*	*Alfa Laval*	*Alfa Laval*
Membrane material	Regenerated cellulose acetate (RC)	Polyethersulphone (PES)	Composite fluoropolymer (FP)
MWCO (kDa)	10	10	10
pH operating range	1-10	1-13	1-11
pH cleaning	1-11.5	1-13	1-11.5
Operating pressure (bar)	1-10	1-10	1-10
Operating temperature (°C)	5-60	5-75	5-60
Permeability (L m^{-2} h^{-1} bar^{-1}) (at 1.0 bar)	21	18	19

2.2. Cross-flow filtration setup

2.2.1 Cross-flow filtration system

The M10 module was connected to a pump (*ECO Gearchem*, NY, USA), shell and tube heat exchanger (*Alfa Laval*, Nakskov, Denmark), 10 L conical borosilicate glass feed tank (*Soham Scientific,* Soham, UK) and weighing balance (*Mettler Toledo*, Switzerland). A schematic design of the M10 filtration system used is shown in Fig. 2. The orange juice sample (4 L) was placed in the feed tank and around 1 L sample was drained to the sink before the filtration to ensure that water from pure water flow has been fully removed from the system. The system had a computerized instrumentation and process control loop. Permeate mass was recorded from a weighing balance. The cross-flow velocity (CFV) was measured from the flow rate reading that was monitored by a rotameter. The pressures at the feed and retentate sides of the system were recorded by transducers in order to calculate the transmembrane pressure (TMP). A thermocouple was used to measure the temperature of the feed prior to entry into the module. All data from the balance, rotameter, transducers and thermocouple were collected by data acquisition module (model ADAM-4012, *Advantech*, Milpitas, USA) and then processed by *Labview* software (*National Instruments*, Austin, USA).
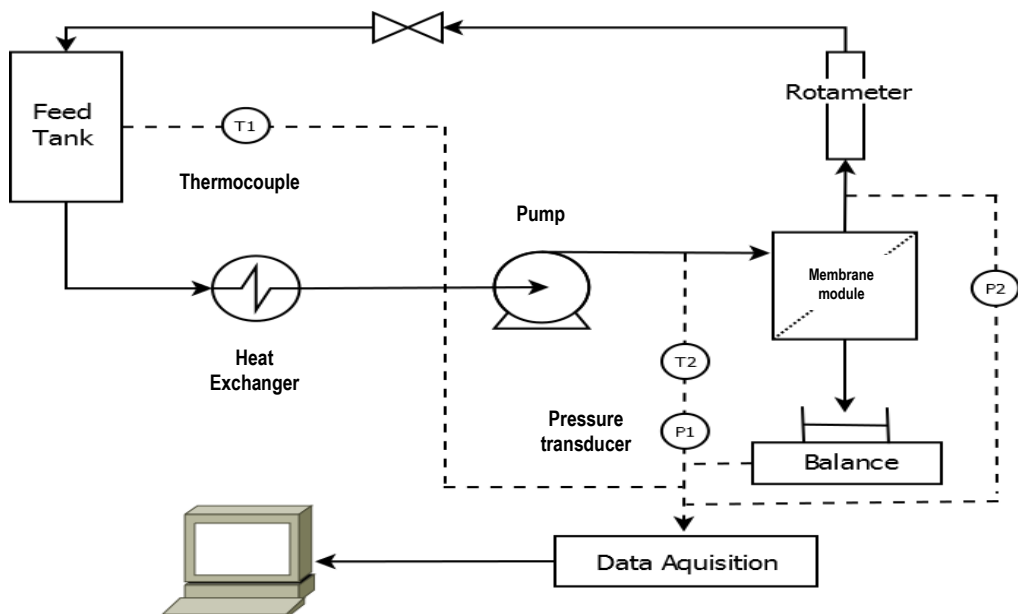
Fig. 2 - A schematic design of the M10 filtration system

2.2.2   Membrane module

Ultrafiltration experiments were performed by using a cross-flow membrane filtration bench unit *LabStak M10* manufactured by *DSS* (now *Alfa Laval*), Denmark. This apparatus consists of four flat sheet membranes in a module with a total filtration area of 336 cm^2. The plate-and-frame module consists of four stacked polysulfone support plates, which arranged in pairs and clamped together by two stainless steel frame. Fig. 3 illustrates the M10 module plate used in this work.
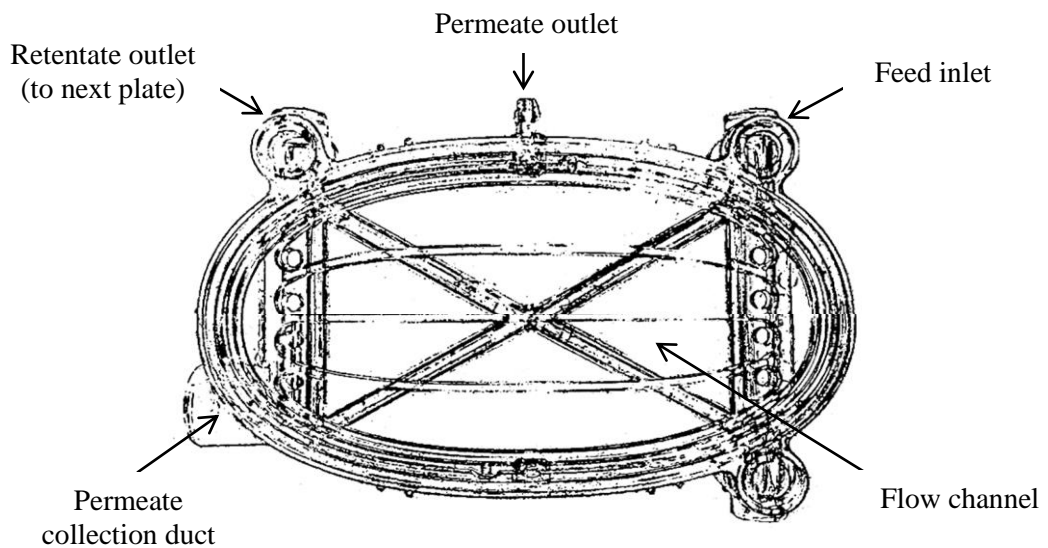
Fig. 3 - M10 module plate (Argyle *et al.*, 2015a)

2.2.3   Cross-flow operating protocol

The cross-flow filtration cycle protocol including membrane conditioning, pure water flux (PWF) measurement, filtration, rinsing and cleaning at different time, TMP and CFV conditions (Argyle *et al.*, 2015b) is illustrated in Table 5. The temperature of the feedstock was maintained at 20 ^{o}C, and a TMP value in the range 0.5 - 2.0 bar was used. The CFV was in the range 0.5 - 1.5 m s^{-1}. Cleaning was carried out using 0.5 wt% *Ultrasil 11* (pH 10) from *Henkel Ecolab*, US. All membranes were coated with glycerol by the manufacturer to extend the shelf life of the membrane during storage. Therefore, new membranes were washed with water at 60 °C for 90 min with 1.0 bar TMP and 1.0 ms^{-1} CFV, before filtration. This conditioning technique was established by Weis *et al.* (2003) to remove glycerol coating from the membrane surface. The PWF of the membrane was determined

using reverse osmosis (RO) water at three different times; before filtration, after rinsing and after cleaning. The filtration time was limited to 60 min.

Table 5 – Cross-flow filtration cycle conditions

Operation stage	Duration (min)	TMP (bar)	CFV (m s^{-1})	Temp (°C)	Resistance calculated
Membrane conditioning	90	1.0	1.0	60	-
PWF 1	10	1.0	1.0	20	R_m
Filtration	60	0.5-2.0	0.5-1.5	20	R_{tot}
Rinse	5	1.0	1.0	20	-
PWF 2	10	1.0	1.0	20	R_m
Cleaning	10	1.0	1.0	60	-
Rinse	5	1.0	1.0	20	-
PWF 3	10	1.0	1.0	20	R_m

2.3.   Characterisation of membranes

2.3.1. Contact angle measurements

Water contact angle measurements of membranes were measured via the sessile drop technique using contact angle measuring instrument (*DataPhysics Instrument*, Filderstadt, Germany). This measurement represents the surface wetting characteristic of the membrane which provided information on the hydrophobicity of the membrane based on contact angle data. This procedure was repeated six times at different points on the membrane surface, taken from both sides of the drop, which were then averaged. Deionized water was used as the probe liquid.

2.3.2   Attenuated total reflectance-Fourier transform infrared (ATR-FTIR) analysis

ATR-FTIR analysis was carried out to study the surface of membrane samples. Three membrane samples were prepared; conditioned membrane, fouled membrane and cleaned membrane. The membrane samples were dried for 24 hours at room temperature prior to analysis (Pihlajamäki *et al.*, 1998). The FTIR spectra were

recorded from the membrane surface using a *FTIR Spectrum 100* spectrometer (*Perkin Elmer*, USA). Acquisition software used was *Perkin Elmer Spectrum* version 10.4.00.

2.3.3 Scanning electron microscope and elemental analysis

Scanning electron microscope (SEM) was used to observe the state of membrane surface at different conditions; conditioned membrane, fouled membrane and cleaned membrane. Air and vacuum-dried membranes were stuck to SEM stubs using conductive paste, followed by coating with a thin layer of gold. Then, the gold coated samples were viewed with a *JEOL SEM* model *JSM 6480LV* from Japan. The presence of elemental composition on the membrane surfaces was evaluated by energy dispersive X-ray (EDX) coupled with the SEM.

2.4. Characterisation of compounds

Feed, permeate and retentate samples from ultrafiltration experiments were collected and stored at -18 °C prior to analysis. Samples were analysed for total phytosterol content, antioxidant activity, total suspended solid content, sugar and protein. These analyses were used in the calculation of rejection ratio (*R*) that is described in next section.

2.4.1 Total phytosterol quantification

Total phytosterol analysis was carried out using a Liebermann-Buchard (LB) based method (Mbaebie *et al.*, 2012; Sathishkumar and Baskar, 2014) via a spectrometry assay using an Ultraviolet-visible (UV-Vis) Spectrophotometer (Cary 100, *Agilent,* USA). Absorbance was measured at 420 nm. Formation of a green colour indicated the presence of phytosterol. A calibration curve was constructed by dilution of standards of stigmasterol. The concentration of standard was performed in series dilution from 0.0625 to 1.0 mg ml^{-1}. Chloroform was used as the blank. 5 ml chloroform was added to 1 ml sample in a test tube. The mixture was vortex mixed for 1 minute for nine samples. A portion of 2 ml extract was taken from that solution and mixed with 2 ml LB reagent. The LB reagent was prepared by dissolving 5 ml sulphuric acid in 50 ml acetic anhydride. The tubes were incubated for 15 minutes

under dark condition. The total phytosterol content (TPC) was calculated using the standard photometric formula (Araújo *et al.*, 2013; Kim and Goldberg, 1969):

$$\text{TPC} = C_s \times \frac{A_u}{A_s} \tag{1}$$

where C_s = standard concentration, A_u = Absorbance of the sample, A_s = Absorbance of the standard. All measurements were done in triplicate.

2.4.2 Antioxidant activity determination

Antioxidant activity of the samples were determined by detecting the scavenging radical of 1,1-diphenyl-2-picrylhydrazyl (DPPH) (Iqbal *et al.*, 2015; Mbaebie *et al.*, 2012). The assay is based on the colour change caused by reduction of DPPH radical which was determined by measuring absorbance at 517 nm (Cary 100, UV-Vis Spectrophotometer, *Agilent*, USA). This assay was carried out as described by Iqbal *et al.* (2015) with some modifications. A methanolic solution of DPPH radical was freshly prepared at concentration of 0.1 mM. BHT was prepared at concentration of 0.03 – 0.25 mg/mL in methanol as reference. Both extract (1 ml) and BHT solution (1 ml) were mixed with 1 ml methanolic solution of DPPH. The solution was mixed vigorously and let to stand at room temperature in the dark for 30 min. Methanol was used as a control instead of extract. Absorbance at 517 nm was measured after 30 min using methanol as a blank. Antioxidant activity was expressed as percentage inhibition of the DPPH radical and was calculated according to the following equation (Mbaebie *et al.*, 2012):

$$\text{Antioxidant activity} = \frac{(A_0 - A)}{A_0} \times 100\% \tag{2}$$

where A_0 is the absorbance of the control at t = 0 min and A is the absorbance of the sample at t = 30 min. All measurements were done in triplicate.

2.4.3 Total suspended solid quantification

Suspended solids were quantified after centrifuging 20 ml samples at 2000 rpm for 20 min using a Heraeus, *Thermo Scientific* centrifuge (Loughborough, UK) according to a method performed by Cassano *et al.* (2008). The supernatant was

removed and the settled solids were dried in the oven (*Townson & Mercer*, Manchester, UK) at 40 °C for 48 hours to ensure all water was removed. The final weight of the samples was weighed using semi-micro balance (*Precisa*, Newport Pagnell, UK). All measurements were done in triplicate.

2.4.4   Sugar quantification

Sugar content concentration expressed in °Brix was determined using a digital hand held refractometer (*Reichert*, New York, USA). Distilled water at 0° Brix was used as a control. Samples were pipetted on the glass surface of the refractometer and Brix analysis was carried out in triplicate.

2.4.5   Protein concentration measurement

Protein concentration was determined using the Bradford assay method (Cassano *et al.*, 2008; Kruger, 1994). The protein assay is a simple colorimetric assay for measuring total protein concentration based on the binding of the acidic dye solution Coomassie Brilliant Blue G-250 to protein at maximum absorbance from 465 to 595 nm (Bradford, 1976). The dye reagent was prepared by diluting one part of protein assay dye reagent concentrate (*Bio-Rad Laboratories*, Hercules, USA) with 4 parts deionized water. Bovine serum albumin (BSA) was used as standard protein and prepared at different concentration ranging from 0.2 to 1.0 mg/ml. 100 µl of standard and sample solution were pipetted into a tube and 5 ml diluted dye reagent was added. The mixed solutions were vortexed and incubated at room temperature for at least 5 minutes. Absorbance for the protein concentration was measured at 595 nm using UV-Vis Spectrophotometer (*Cary 100, Agilent*, USA). The standard calibration curve was plotted for absorbance vs. protein concentration. All measurements were done in triplicate.

2.5. Evaluation of permeate flux, selectivity, fouling index and cleaning efficiency

The effectiveness of any membrane process is described in terms of permeation rate (or permeate flux) and the selectivity. The permeate flux through a membrane can be calculated as the following equation (Mulder, 1996):

$$J = \frac{\Delta P}{\mu R} \qquad (3)$$

where J indicates the flux through the membrane (L m^{-2} h^{-1}), ΔP (bar) is the applied transmembrane pressure (TMP), μ is the viscosity and R represents the total resistance (all resistances are in m^{-1}). Selectivity is expressed as the rejection ratio (R) and calculated using this equation (Mulder, 1996):

$$R = (1 - \frac{C_p}{C_r}) \times 100\% \qquad (4)$$

where C_p is the solute concentration in the permeate and C_r is the solute concentration in the retentate.

The fouling index (FI) was evaluated by comparing the pure water permeability before and after the ultrafiltration using this equation (Conidi *et al.*, 2017):

$$FI = (\frac{WP_1}{WP_0}) \times 100\% \qquad (5)$$

where WP_0 is the pure water permeability of the virgin membrane and WP_1 is the pure water permeability after the ultrafiltration. The cleaning efficiency (CE) was measured according to this equation (Conidi *et al.*, 2017):

$$CE = (\frac{WP_2}{WP_0}) \times 100\% \qquad (6)$$

where WP_2 is the pure water permeability after the cleaning.

3. Results and discussion

3.1. Contact angle measurements

Contact angle measurements were conducted to evaluate the hydrophobicity of the membranes tested (Table 6). The conditioned RC membrane displayed a contact angle of *ca.* 11°, corresponding to a highly hydrophilic surface. The contact angles of the conditioned PES and FP membranes were 60° and 65° respectively. These two types of membranes tested were both considered to be moderately hydrophilic, as the contact angles measured were less than 90°. The FP membrane surface was relatively hydrophobic, which is in agreement with findings by other researcher (Nguyen *et al.*, 2015).

Table 6 also shows the contact angles of fouled membranes. The contact angles of fouled RC, PES and FP membranes were $10 \pm 2°$, $40 \pm 2°$ and $46 \pm 2°$ respectively. These values are much lower than those for the conditioned membranes, indicating that the membranes became more hydrophilic after fouling. The contact angle measurements of fouled membranes showed the modifications of membranes hydrophobicity owing that the membrane surface is modified by surface fouling with protein-based foulants or other hydrophilic submicelles (Argyle *et al.*, 2015b; Wu and Bird, 2007). After cleaning, contact angles of the cleaned surfaces increased for all three membranes. Surfaces were not returned to their original state; but instead contact angles were slightly lower than those recorded for the conditioned membranes. However, within experimental error, no difference was detected between the contact angles of the conditioned and the cleaned membranes.

Table 6 - Membrane surface angles of RC, PES and FP membranes

Membrane	Contact angle (°)		
	Conditioned	Fouled	Cleaned
RC70PP	11 ± 2	10 ± 2	8 ± 2
GR80PP	60 ± 2	40 ± 2	58 ± 2
ETNA10PP	65 ± 2	46 ± 2	63 ± 2

3.2. Permeate flux analysis

Fig. 4 shows the time course of permeate flux for orange juice ultrafiltration at four different TMPs for all membranes. The viscosity of the permeates obtained were 6.41 ± 0.09 mPa s, 6.50 ± 0.08 mPa s and 6.43 ± 0.08 mPa s for the regenerated cellulose, polyethersulphone and fluoropolymer membranes respectively. Fig. 4(a) shows the initial permeate flux varied for RC membranes varied between 25 and 33 L m^{-2} h^{-1}, and decreased gradually with filtration time. The highest initial flux was obtained at a TMP value of 1.5 bar. However, the highest steady-state flux of *ca.* 22 L m^{-2} h^{-1} was obtained at a TMP of 1.0 bar. For the PES membrane, the highest initial permeate flux of 30 L m^{-2} h^{-1} was seen at a TMP value of 2.0 bar (Fig. 4(b)). The flux also reduced with time. A steady-state flux value of 17 L m^{-2} h^{-1} was obtained at a TMP value of 1.0 bar. There was no change to the permeate flux observed at TMP 0.5 bar for this membrane. It can be seen from Fig. 4(c), that the trend in permeate flux for the FP membrane was similar to that recorded for the RC and PES membranes. The initial flux of the FP membrane (25 L m^{-2} h^{-1}) decreased gradually over time. The permeate flux then reached a steady-state value of 14 to 19 L m^{-2} h^{-1}. Both PES and FP membranes showed lower filtration fluxes than those seen for RC. The permeate flux declined gradually with time until it reached a pseudo steady-state value. The decrease of permeate flux can be explained by the effect of fouling (Cassano *et al.*, 2007; Conidi *et al.*, 2017). From the values tested, a TMP of 1.0 bar was the optimal value based on the filtration performance. The highest pseudo steady-state permeate flux for all membranes were achieved at TMP of 1.0 bar. Thus, operation at a TMP of 1.0 bar has been selected for further filtration analyses.

Fig. 5 summarises the effect of increasing the TMP from 0.5 bar to 2.0 bar upon the steady-state permeate flux at 20 °C. The three membranes tested showed a similar trend and the optimal TMP for the UF of orange juice from the range tested was 1 bar. The RC membrane exhibited the highest permeate flux value of *ca.* 22 L m^{-2} h^{-1}. However, when permeability (L m^{-2} h^{-1} bar^{-1}) is examined (Table 7), results show a different trend. The FP membrane at TMP 0.5 bar displayed the highest permeability value. These results suggest that the permeate flux and permeability are affected not only by TMP but also by membrane material as well as by interactions between membranes and solutes. When moving above 0.5 bar, it is clear that the

linear dependency of flux upon pressure is lost for the regenerated cellulose and fluoropolymer membranes. However, the polyethersulphone membrane is operating in the pressure dependant region when moving from 0.5 to 1.0 bar. Once 1.5 bar is achieved, pressure or flux linearity is lost.
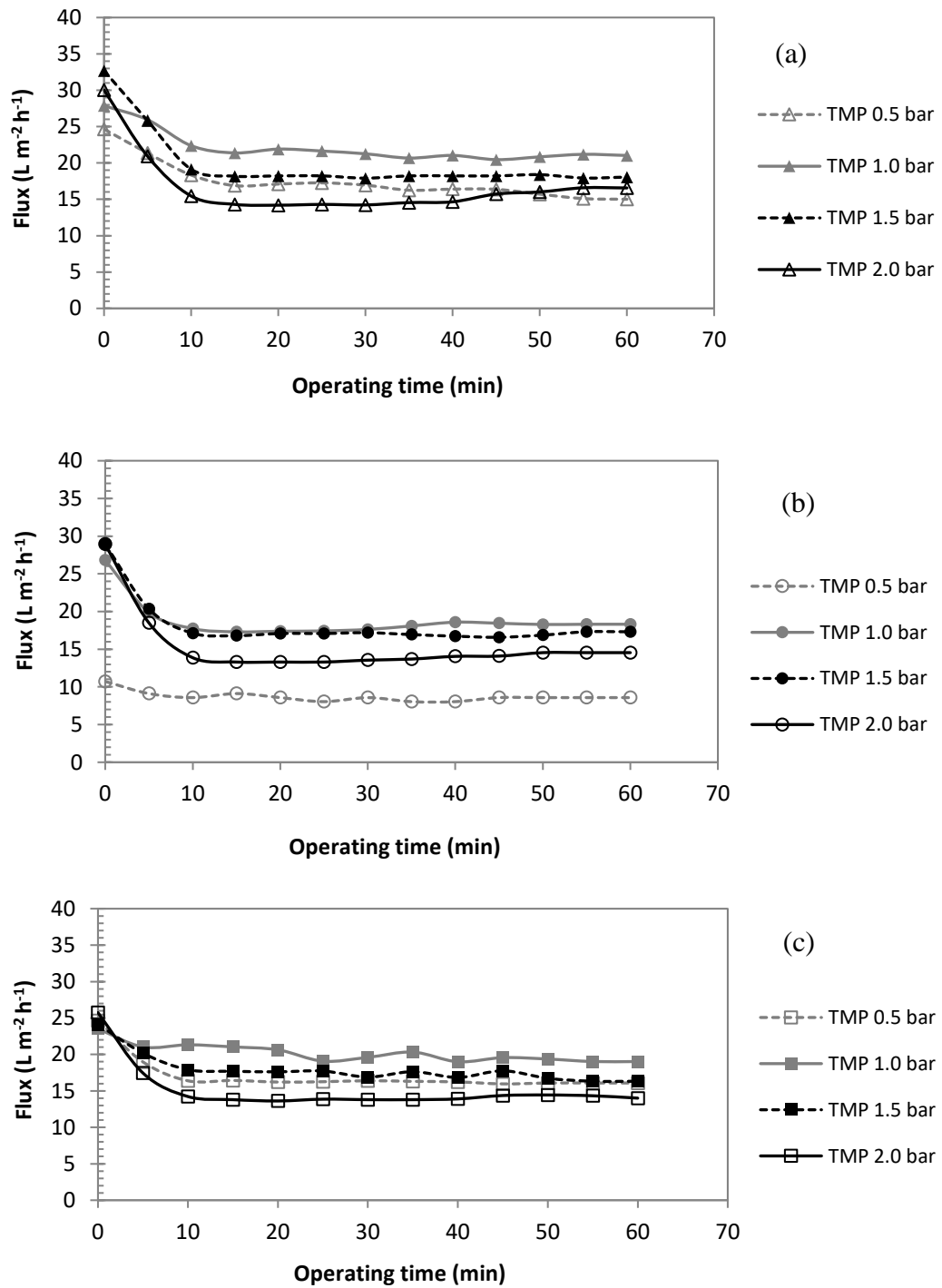
Fig. 4 - Time course of permeate flux for orange juice ultrafiltration at different pressures for a 10 kDa membrane; (a) RC (b) PES and (c) FP
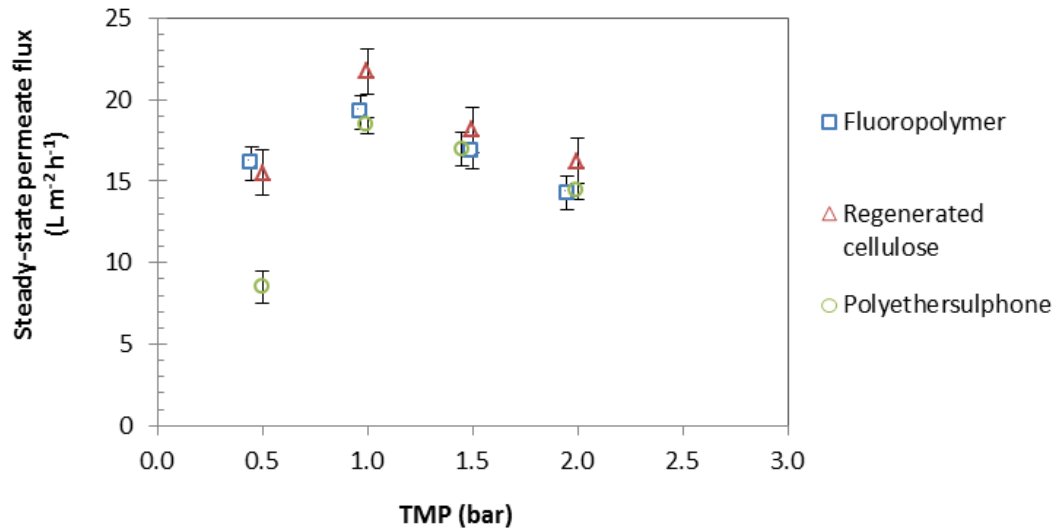
Fig. 5 - Effect of TMP upon steady-state permeate flux for orange juice UF with different membrane materials (all 10 kDa MWCO)

Table 7 - Permeability of RC, PES and FP membranes

Membrane	Permeability ($L\ m^{-2}\ h^{-1}\ bar^{-1}$)			
	0.5 bar	1.0 bar	1.5 bar	2.0 bar
RC70PP	31 ± 1	21 ± 2	12 ± 1	8 ± 1
GR80PP	17 ± 1	18 ± 1	11 ± 1	7 ± 1
ETNA10PP	32 ± 1	19 ± 1	11 ± 1	7 ± 1

3.3.   Rejection of key compounds

The rejection of key compounds such as total phytosterols, sugars, proteins, total suspended solids and also the antioxidant activity was analysed for all three membranes in order to study the fractionation of phytosterols and to study the effect of membrane fouling (Fig. 6). Phytosterol compounds are hydrophobic in nature (Ostlund, 2007). Theoretically, the more hydrophobic molecules in the feed solution have a tendency to be attracted to a membrane with more hydrophobic surface (Evans *et al.*, 2008). The RC membrane (which is highly hydrophilic) gave 32% rejection towards phytosterols (Fig. 6(a)). Nevertheless, PES (Fig. 6(b)) and FP (Fig.

6(c)) membranes exhibited higher rejections towards phytosterol compounds; with rejections of 76% and 75% respectively. This observation suggests that membrane hydrophobicity is not the key factor in determining phytosterol rejection in orange juice filtration. It is also possible that the hydrophobic membrane surface is trapping more foulant than the hydrophilic membrane. Therefore, other important characteristics for rejection such as surface charge, surface roughness and membrane-foulant interaction should be explored. The antioxidant activity was expected to be directly correlated with the total phytosterol content, since phytosterols were found to have antioxidant properties (Wang *et al.*, 2002). However, no correlation was observed between antioxidant activity and total phytosterols (Fig. 6). The rejection of antioxidant activity was in the range 10% - 23% for all selected membranes. It is possible that the antioxidant activity detected can be attributed to other chemical compounds present in orange juice, such as phenolic compounds (Stinco *et al.*, 2012).
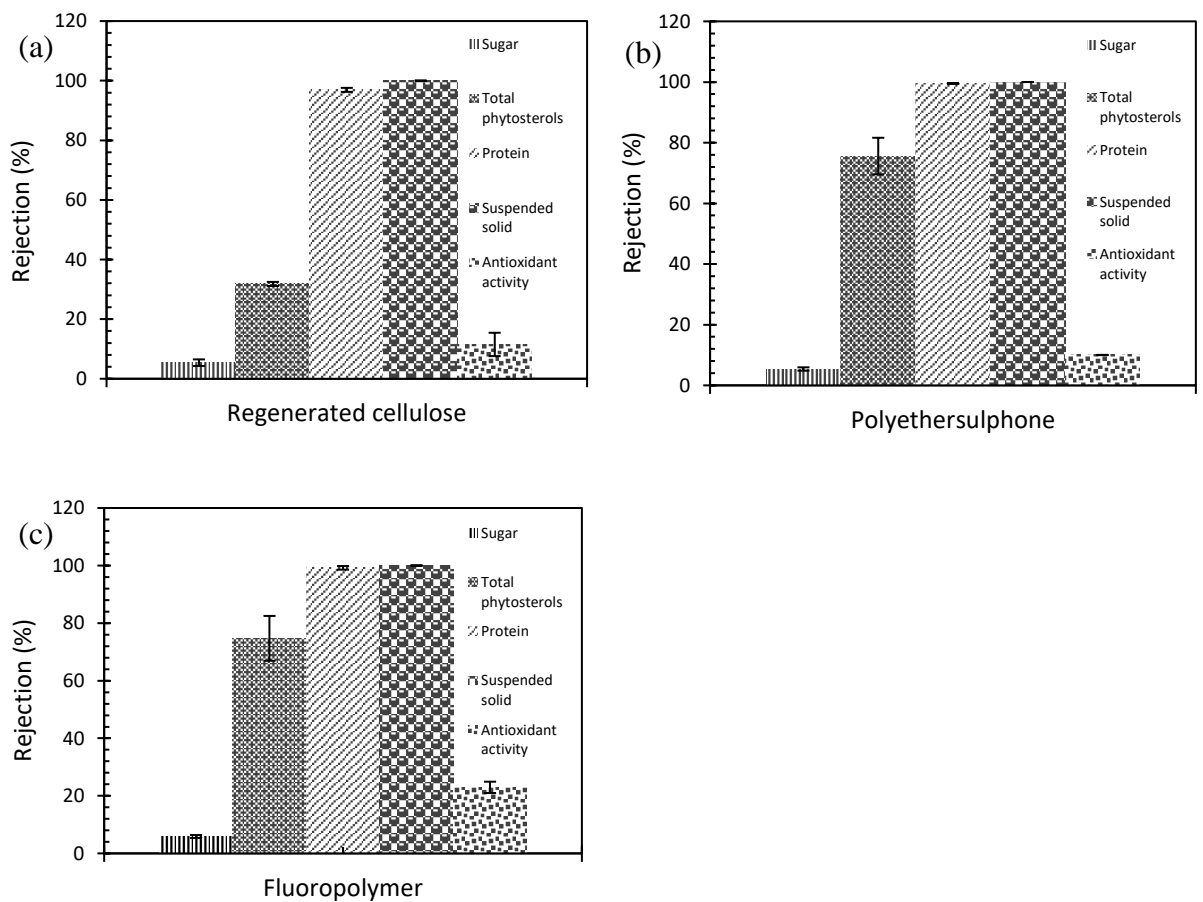
Fig. 6 - Rejection of key compounds by the three different membranes tested; (a) RC, (b) PES and (c) FP

For protein, the rejection recorded for all membranes tested was found to be 96% - 100%. Protein was especially highly rejected by the 10 kDa MWCO ultrafiltration membrane. The molecular weights of the proteins in orange juice were from 12 kDa to 71 kDa (Sass-Kiss and Sass, 2000). Thus, it would also be expected that the cake layer formed on the membrane surface would consist of a highly proteinaceous nature (Evans *et al.*, 2008). Total suspended solids were totally removed from the orange juice, and collected as retentate in all membranes tested (100% rejection) (Fig. 6). Unsurprisingly, all of the membranes examined showed a low rejection towards sugars (5% - 6%).

Table 8 shows a mass balance for the total phytosterols and proteins following RC membrane filtration. The initial volume of the orange juice for the ultrafiltration was 3000 ml. Total phytosterols in feed solution were *ca.* 780 to 800 mg. The highest recovery of phytosterols in the permeate stream was achieved by using a RC membrane (albeit the amount was relatively low at 40 mg/L). In addition, the 10% loss of phytosterols in the system for RC membrane, 17% loss for PES and 16% loss for FP membranes were presumably due to the fouling effect during filtration (Cassano *et al.*, 2008). The higher rejections seen with PES and FP in Fig. 6 are linked to a greater loss of sterols from the feed into the foulants. This is perhaps not surprising, as the surface concentrations are presumably higher, leading to an increase in the mass transfer into the foulants. The proteins detected in the retentate for all the membranes tested were found to be between 74% and 97% (Table 8). Most proteins were rejected by the 10 kDa MWCO UF membrane, since the molecular weights of protein were 12 kDa to 71 kDa. It would also be expected that the higher molecular weight compounds were rejected by smaller pore size membrane, and this increased the degree of membrane fouling (Evans *et al.*, 2008).

Table 8 - Mass balance for total phytosterols and protein by UF process of orange juice with different membranes; (a) RC (b) PES and (c) FP

(a) RC	Feed	Total permeate		Final retentate		Total (%)
Volume (ml)	3000	850	28%	2150	72%	100
Total phytosterols (mg)	781	121	15%	584	75%	90
Protein (mg)	2883	29	1%	2371	82%	83

(b) PES	Feed	Total permeate		Final retentate		Total (%)
Volume (ml)	3000	650	22%	2350	78%	100
Total phytosterols (mg)	777	34	4%	615	79%	83
Protein (mg)	3121	7	0.2%	3036	97%	97

(c) FP	Feed	Total permeate		Final retentate		Total (%)
Volume (ml)	3000	850	28%	2150	72%	100
Total phytosterols (mg)	809	54	7%	622	77%	84
Protein (mg)	1499	3	0.2%	1110	74%	74

3.4. Pure water flux analysis

Fig. 7 presents the pure water fluxes of selected membranes at a TMP of 1.0 bar and at 20 °C. PWF values were measured for membranes under the following conditions (i) before fouling, (ii) after fouling and (iii) after cleaning. The PES membranes displayed the lowest water flux of 69 - 105 $L\ m^{-2}\ h^{-1}$, and the FP membrane gave the highest water flux of 153 - 191 $L\ m^{-2}\ h^{-1}$. The highest PWF of all membranes before fouling was achieved by using FP membranes (174 - 189 $L\ m^{-2}\ h^{-1}$) and the lowest PWF was shown by PES membranes (84 - 105 $L\ m^{-2}\ h^{-1}$). The PWF had declined

after fouling for both PES and FP membranes, although flux declines were small, at *ca.* 10%. The RC membrane flux after fouling was broadly similar to that seen for the membrane before fouling. There were no significant changes in PWF through RC membranes during first and third cycle. The PWF declined for PES and FP membranes during the three fouling cycles examined (Table 9). These results indicate that the ultrafiltration process was affected by the membrane fouling phenomena. Therefore, a proper cleaning technique is needed to regenerate the membrane. In this study a commercial cleaning agent, *Ultrasil 11* (*Henkel Ecolab*), was used as suggested by Wu and Bird (2007).
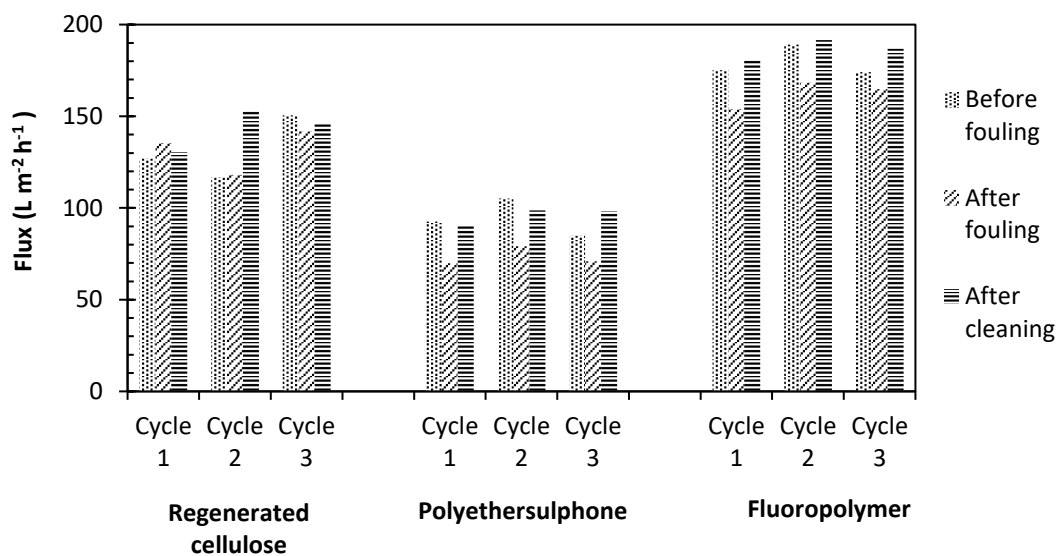
Fig. 7 - Pure water fluxes of three membranes tested; RC, PES and FP

Table 9 - Reduction in pure water fluxes of PES and FP membranes

Cycle	Flux (L m^{-2} h^{-1})	
	PES	FP
1	92 to 69	175 to 153
2	105 to 79	189 to 168
3	84 to 70	174 to 164

For both PES and FP membranes, the PWF passing through the membrane after cleaning was higher than that seen after fouling. In most cases, the PWF after cleaning seen was approximately the same as that seen for the virgin membrane (Fig. 7). It is postulated that this is due to the adsorption of *Ultrasil 11* surfactant to the membrane surface (Weis *et al.*, 2003). Given that cleaning is achieving PWF regeneration to values comparable to that virgin membrane, it can be concluded that the cleaning method using 0.5 % (*w/w)* of *Ultrasil 11* is effective in regenerating the membrane. Fig. 8 shows the membrane resistances of the three membranes tested, under the same pressure and temperature conditions for three foul-clean cycles. It can be seen that the membrane resistances before filtration and after cleaning were similar for all three membranes (except for sample of PES membrane cycle 1, where differences were not large). The membrane resistances before filtration for RC, PES and FP membranes were 2.5 x 10^{12} m^{-1}, 3.3 x 10^{12} m^{-1} and 2.0 x 10^{12} m^{-1} respectively. After filtration, these values increased to 2.7 x 10^{12} m^{-1}, 5.3 x 10^{12} m^{-1} and 2.3 x 10^{12} m^{-1} for the RC, PES and FP membranes respectively. Following cleaning, resistances had reduced in all cases similar values to those for clean membranes.
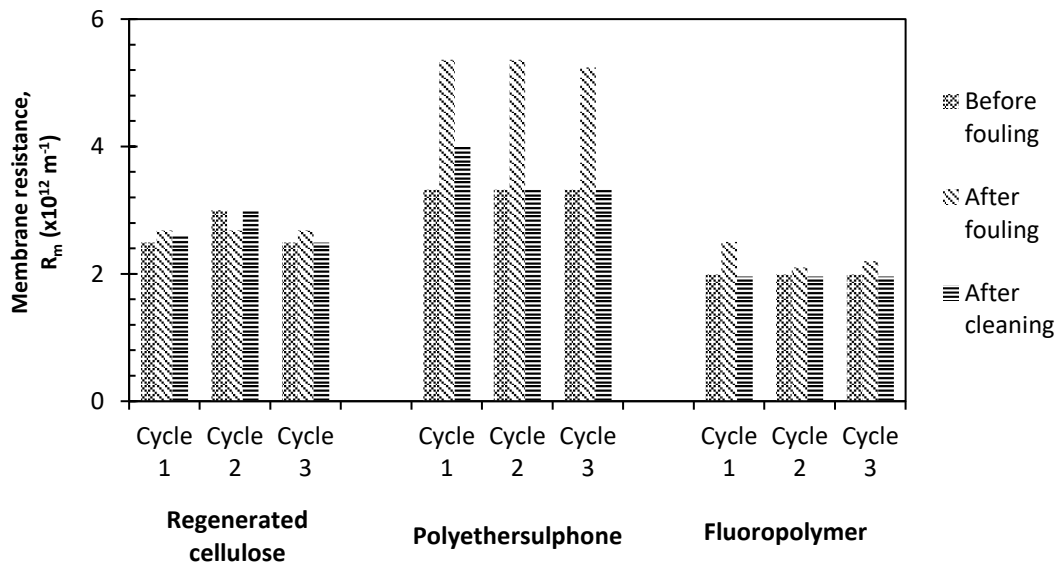
Fig. 8 - Variation in membrane resistance for selected membranes

Fig. 9 displays the fouling index and cleaning efficiency measured for all membranes tested. All measurements were carried out in triplicate. The three membranes generally displayed the almost similar fouling index. The lowest fouling index value was measured for the PES membrane (71%) followed by RC membrane

(75%) and the highest fouling index was measured for FP membrane (77%). These results indicate that the ultrafiltration process was affected by the membrane fouling phenomena. In addition, all those three tested membranes (RC, PES and FP) displayed almost similar cleaning efficiencies which were 98%, 99% and 96% respectively.
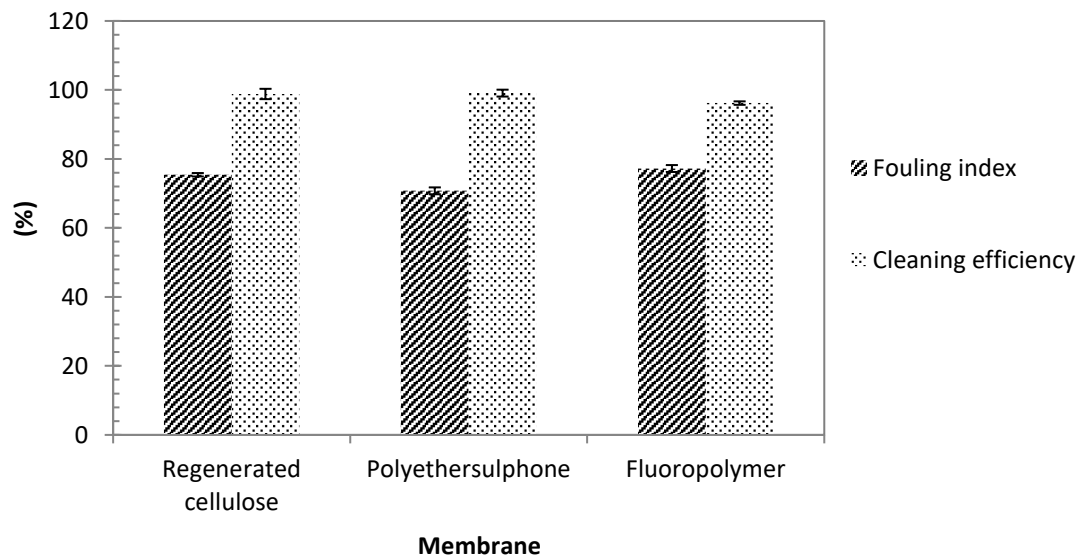
Fig. 9 - Fouling index and cleaning efficiency for RC, PES and FP membranes

3.5   Spectral analysis of membranes

FTIR spectra were collected to identify any changes in the composition of material on the membrane surfaces occurring due to fouling and cleaning processes. The intensity of IR absorption bands can be used to quantify the amount of targeted compounds deposited on the membrane (Wu and Bird, 2007). However, the foulant layers on the membrane surface were found to be too thin to generate quantitative data in this study. Thus, the FTIR spectra in the range of $4000 - 515$ cm^{-1} were used to analyse the membrane surfaces at different conditions. Fig. 10 displays the overlay results of FTIR spectra of membrane at three conditions; conditioned, fouled and cleaned condition. It was observed that all samples showed identical FTIR spectra with slightly shifted absorption bands. The RC membrane showed a higher intensity in absorbance compared to either of the PES and FP membranes. The higher intensity recorded demonstrated that more foulant was deposited on the membrane

surface (Evans *et al.*, 2008). When a membrane was fouled, the FTIR peaks of the cleaned membrane were changed in absorbance intensity. In each of the figures, fouled membranes offered higher intensity values compared to either the conditioned or cleaned membrane samples. For cleaned membranes, the intensity was reduced to values very similar intensity to those recorded for conditioned membrane. This indicates that foulant deposits present on the membrane surface were removed after cleaning.

Fig. 10 (a) shows the FTIR spectrum for the RC membrane. A strong and broad band observed around $3500 - 3000$ cm^{-1} corresponds to O-H stretching vibration of hydroxyl group in the RC membrane (Madaeni and Heidary, 2011). The band at 2900 cm^{-1} is assigned to –CH stretching vibration. The highest peak at 1020 cm^{-1} attribute to C-O stretching (Azuwa *et al.*, 2015). The H-O-H bending was characterised at 1640 cm^{-1} and the band at 895 cm^{-1} is due to the C-O-C stretching (Yang *et al.*, 2017). Fig.10 (b) illustrates the FTIR spectrum of the PES membrane. A broad peak at 3400 cm^{-1} is associated with the OH stretching. Two bands located at 2925 cm^{-1} and 2852 cm^{-1} are assigned to CH2 asymmetric stretching band (Belfer *et al.*, 2000). The absorption bands corresponding to the PES also observed at 1670 cm^{-1} (C=O), 1580 cm^{-1} (benzene ring C=C) and 1485 cm^{-1} (C-C bond stretching) (Zhu *et al.*, 2015). The aromatic ether band was strongly observed at around 1240 cm^{-1}. Fig. 10 (c) shows the FTIR spectrum for the FP membrane. The main characteristic of FP membrane is assigned by bands in the region of $1000 - 1300$ cm^{-1} (Evans *et al.*, 2008). The absorption band at 1200 is due to stretching vibrations of CF_2 (Mihaly *et al.*, 2006).
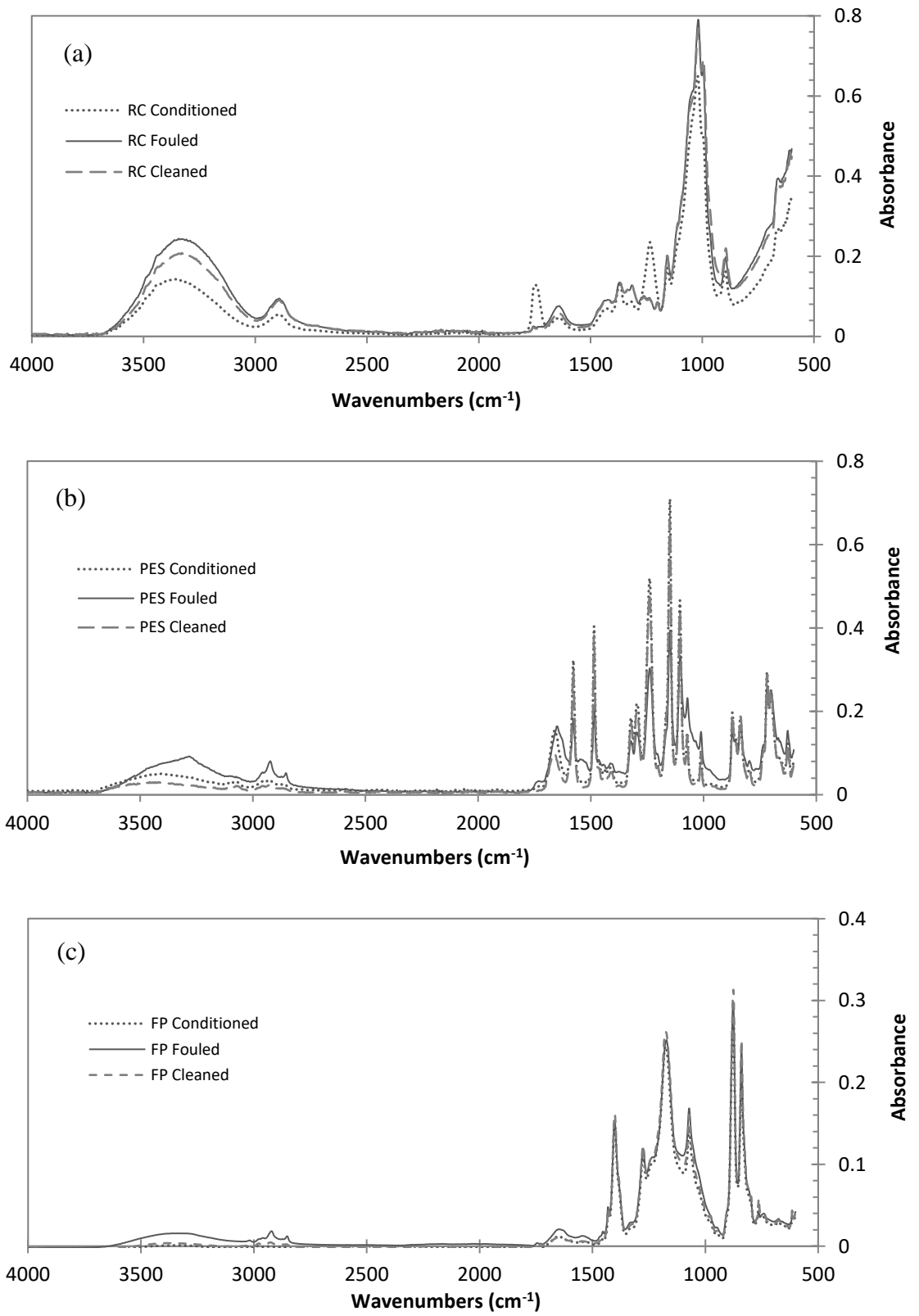
Fig. 10 – FTIR spectra of three membranes tested; (a) RC, (b) PES and (c) FP for conditioned, fouled and cleaned membranes

3.6.   SEM analysis of membranes

The morphology of fouled deposits on membrane surfaces was evaluated scanning electron microscope (SEM). SEM was applied to monitor the differences of membrane before and after fouling and subsequent cleaning. Fig. 11 shows SEM images of 10 kDa membrane surfaces of all three membranes tested for conditioned, fouled and cleaned membrane conditions. Figs. 11(a) to 11(c) show the surfaces of RC membranes. The surface morphology of PES and FP membranes is shown in Fig. 11(d) - (f) and Fig. 11(g) - (i) respectively. Conditioned membrane of all three membranes appeared to have clean membrane surfaces. The deposits could be seen very clearly on the fouled membrane surfaces. The fouled membrane was completely covered with a fouling layer (Fig. 11(b), (e) and (h)). This may suggest that a cake layer may dominate the filtration properties of the membrane and this is in agreement with the flux data and rejection results. The deposits could be the rejected protein and other compounds such as phytosterols that retain on the membrane surface. After the cleaning steps, cleaned membranes demonstrate that the cleaning process was able to remove most of the fouled deposits and regenerate the membrane. This observation indicates that the membranes are effectively cleaned after the 0.5% *Ultrasil 11* protocol was applied.

The elemental examinations were carried out by EDX analysis that coupled with the SEM. The EDX results confirm the presence of Ca and Fe on the membrane surfaces after fouling. According to the literature (Navarro *et al.*, 2011; Schmutzer *et al.*, 2016), orange juice contains elements such as Ca and Fe. The EDX analyses on the surface of conditioned and cleaned membranes were also carried out. The RC membranes showed the presence of C and O elements. These results are not surprising, given that the membranes were fabricated from cellulose (Li *et al.*, 2014). Three elements (C, O and S) were observed on the PES membranes, consistent with membranes made of polyethersulphone (Basri *et al.*, 2011). FP membranes showed the existence of C and F elements. It can be seen that the elements exist in conditioned membranes were similar to the elements in cleaned membranes. This result correlates well with the SEM analysis that suggests the membranes were regenerated effectively after the cleaning protocol was applied.
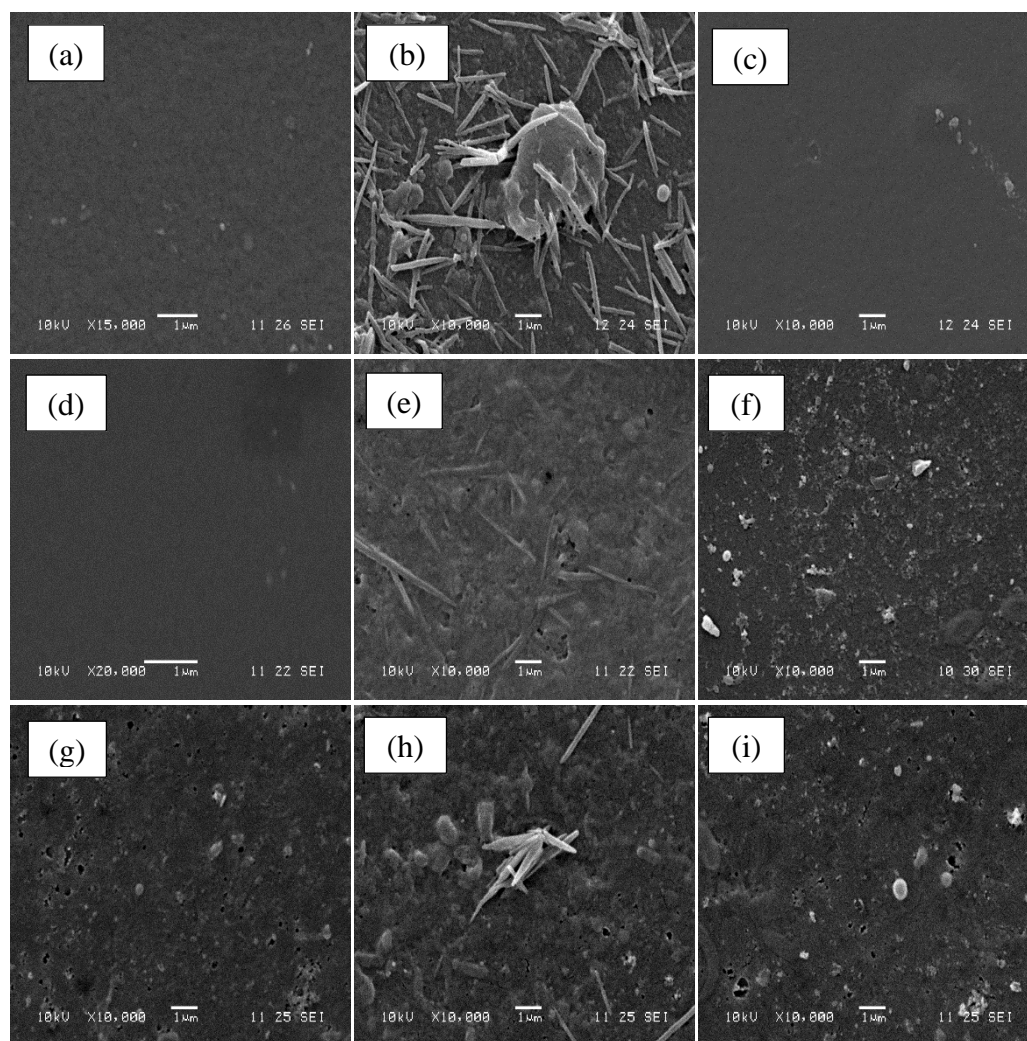
Fig. 11 – Scanning electron microscope images of 10 kD ultrafiltration membrane surfaces (a) RC conditioned membrane, (b) RC fouled membrane, (c) RC cleaned membrane, (d) PES conditioned membrane, (e) PES fouled membrane, (f) PES cleaned membrane, (g) FP conditioned membrane, (h) FP fouled membrane and (i) FP cleaned membrane

3.7. Process development

Now that the effectiveness of membranes as a technology for phytosterol concentration has been established, future work on process development will look to build on this foundation by maximising rejection of sterols and minimising fouling. Since the yield of total phytosterols compounds that are fractionated by using 10 kDa ultrafiltration membrane was relatively low, there is the potential for process optimisation. From the three membrane types tested, hydrophilic RC membranes gave the best rejection ratio of phytosterol (32%). Thus, an experimental programme

will be developed to introduce hybrid membrane filtration using the regenerated cellulose membrane. Membranes with larger MWCO will be tested in order to remove the proteins and transmit the sterols. Then, a second membrane step with a small MWCO can reject the sterols and transmit the sugars. Diafiltration may also be applied in concentrating the targeted compounds.

4. Conclusions

The isolation of phytosterols from orange juice has been investigated using three types of 10 kDa molecular weight cut-off (MWCO) ultrafiltration (UF) membranes made from regenerated cellulose (RC), polyethersulphone (PES) and fluoropolymer (FP). For the PES and FP membranes, there was a significant concentration of sterols in the retentate, with sterol rejections of *ca.* 80%. However, feed volumes used were small (3 litres) and *ca.* 20% of the sterols originally present in the feed formed part of the fouling layer on the membrane surface. Permeate fluxes decreased gradually with operating time until they reached steady-state values. The optimum TMP condition tested was found to be 1 bar based on the highest pseudo steady-state permeate flux for all membranes that were achieved at TMP of 1.0 bar. The RC membrane exhibited the highest permeate flux seen, which was *ca.* 22 L m^{-2} h^{-1}. Hydrophilic RC gave a 32% phytosterol rejection ratio. PES and FP (more hydrophobic membranes) demonstrated higher rejections towards phytosterol compounds (76% and 75% respectively). This could be due to the fact that the membrane hydrophobicity was not the decisive factor for phytosterols rejection in orange juice. There was no correlation observed between antioxidant activity and total phytosterol content. Proteins were 100% rejected by the 10 kDa membrane, and sugar has been readily recovered in the permeate (although diafiltration was not applied). Fouling lead to a 10% reduction of phytosterols in the system recorded for RC membrane filtration, and a *ca.* 20% reduction was recorded for the PES and FP membranes. Permeate water fluxes after cleaning increased to levels similar to those seen for membranes before fouling. Of the membranes tested, the RC membrane displayed the highest permeate flux, the highest transmission of phytosterols from orange juice, and the highest fouling index and cleaning efficiency, when compared to the PES and FP membranes. *Ultrasil 11* (0.5 wt%) was found to be effective in regenerating all membranes tested.

Acknowledgements

References

Aimi Izyana, I., Zairossani, M.N., 2011. Effect of Spray Drying on Protein Content of Natural Rubber Serum. *IIUM Engineering Journal* 12, 61-65.

Almanasrah, M., Brazinha, C., Kallioinen, M., Duarte, L.C., Roseiro, L.B., Bogel-Lukasik, R., Carvalheiro, F., Mänttäri, M., Crespo, J.G., 2015. Nanofiltration and reverse osmosis as a platform for production of natural botanic extracts: The case study of carob by-products. *Separation and Purification Technology* 149, 389-397.

Araújo, L.B.D.C., Silva, S.L., Galvão, M.A.M., Ferreira, M.R.A., Araújo, E.L., Randau, K.P., Soares, L.A.L., 2013. Total phytosterol content in drug materials and extracts from roots of Acanthospermum hispidum by UV-VIS spectrophotometry. *Revista Brasileira de Farmacognosia* 23, 736-742.

Argyle, I.S., Pihlajamaki, A., Bird, M.R., 2015a. Ultrafiltration of black tea using diafiltration to recover valuable components. *Desalination and Water Treatment* 53, 1532-1546.

Argyle, I.S., Pihlajamäki, A., Bird, M.R., 2015b. Black tea liquor ultrafiltration: Effect of ethanol pre-treatment upon fouling and cleaning characteristics. *Food and Bioproducts Processing* 93, 289-297.

Azuwa, M.M., W., S.W.N., Juhana, J., F., I.A., Muhazri, A.M., Munira, J.S., 2015. Feasibility of recycled newspaper as cellulose source for regenerated cellulose membrane fabrication. *Journal of Applied Polymer Science* 132.

Basri, H., Ismail, A.F., Aziz, M., 2011. Polyethersulfone (PES)–silver composite UF membrane: Effect of silver loading and PVP molecular weight on membrane morphology and antibacterial activity. *Desalination* 273, 72-80.

Basu, S., Balakrishnan, M., 2017. Polyamide thin film composite membranes containing ZIF-8 for the separation of pharmaceutical compounds from aqueous streams. *Separation and Purification Technology* 179, 118-125.

Belfer, S., Fainchtain, R., Purinson, Y., Kedem, O., 2000. Surface characterization by FTIR-ATR spectroscopy of polyethersulfone membranes-unmodified, modified and protein fouled. *Journal of Membrane Science* 172, 113-124.

Bodzek, M., Dudziak, M., 2006. Elimination of steroidal sex hormones by conventional water treatment and membrane processes. *Desalination* 198, 24-32.

Bradford, M.M., 1976. A rapid and sensitive method for the quantitation of microgram quantities of protein utilizing the principle of protein-dye binding. *Anal Biochem* 72, 248-254.

Brufau, G., Canela, M.A., Rafecas, M., 2008. Phytosterols: physiologic and metabolic aspects related to cholesterol-lowering properties. *Nutrition research (New York, N.Y.)* 28, 217-225.

Cassano, A., Donato, L., Conidi, C., Drioli, E., 2008. Recovery of bioactive compounds in kiwifruit juice by ultrafiltration. *Innovative Food Science & Emerging Technologies* 9, 556-562.

Cassano, A., Marchio, M., Drioli, E., 2007. Clarification of blood orange juice by ultrafiltration: analyses of operating parameters, membrane fouling and juice quality. *Desalination* 212, 15-27.

Cobell, 2016. Orange Juice Not From Concentrate (NFC). Cobell, Exeter, United Kingdom.

Conidi, C., Cassano, A., Caiazzo, F., Drioli, E., 2017. Separation and purification of phenolic compounds from pomegranate juice by ultrafiltration and nanofiltration membranes. *Journal of Food Engineering* 195, 1-13.

Devaraj, V., Zairossani, M.N., 2006. Zero Discharge and Value Added Products from NR Skim Latex Processing Malaysian Rubber Technology Developments. Malaysian Rubber Board, Kuala Lumpur, pp. 19-21.

Echavarría, A.P., Torras, C., Pagán, J., Ibarz, A., 2011. Fruit Juice Processing and Membrane Technology Application. *Food Engineering Reviews* 3, 136-158.

Evans, P.J., Bird, M.R., Pihlajamäki, A., Nyström, M., 2008. The influence of hydrophobicity, roughness and charge upon ultrafiltration membranes for black tea liquor clarification. *Journal of Membrane Science* 313, 250-262.

Global-Market-Insight, 2016. Phytosterols Market Size By Product (Beta-Sitosterol, Campesterol, Stigmasterol), By Application (Pharmaceuticals, Food ingredients, Cosmetics), Regional Outlook (U.S., Canada, Mexico, Germany, UK, France, Italy, Russia, Poland, China, India, Japan, Indonesia, Malaysia, Thailand, Australia, Brazil, South Africa, Saudi Arabia, UAE), Growth Potential, Price Trend, Competitive Market Share & Forecast, 2016 – 2024. Global Market Insights, Inc., Delaware USA.

Hasma, H., Subramaniam, A., 1986. Composition of Lipids in Latex of Hevea Brasiliensis Clone RRIM 501. *Journal of Natural Rubber Research* 1, 30-40.

Ho., C.C., Subramaniam, A., Yong, W.M., 1975. Lipids Associated with the Particles in Hevea Latex, International Rubber Conference, Kuala Lumpur, pp. 441-456.

Hwee, E.A., 2013. Non Rubbers and Abnormal Groups in Natural Rubber, in: Thomas, S., Chan, C.H., Pothen, L.A., Rajisha, K.R., Maria, H.J. (Eds.), Natural Rubber Materials. The Royal Society of Chemistry, United Kingdom, pp. 53-72.

Ilame, S.A., V. Singh, S., 2015. Application of Membrane Separation in Fruit and Vegetable Juice Processing: A Review. *Critical Reviews in Food Science and Nutrition* 55, 964-987.

Iqbal, E., Salim, K.A., Lim, L.B.L., 2015. Phytochemical screening, total phenolics and antioxidant activities of bark and leaf extracts of Goniothalamus velutinus (Airy Shaw) from Brunei Darussalam. *Journal of King Saud University - Science* 27, 224-232.

Jesus, D.F., Leite, M.F., Silva, L.F.M., Modesta, R.D., Matta, V.M., Cabral, L.M.C., 2007. Orange (Citrus sinensis) juice concentration by reverse osmosis. *Journal of Food Engineering* 81, 287-291.

Jiménez-Escrig, A., Santos-Hidalgo, A.B., Saura-Calixto, F., 2006. Common Sources and Estimated Intake of Plant Sterols in the Spanish Diet. *Journal of Agricultural and Food Chemistry* 54, 3462-3471.

Jin, X., Hu, J., Ong, S.L., 2010. Removal of natural hormone estrone from secondary effluents using nanofiltration and reverse osmosis. *Water Research* 44, 638-648.

Kadir, A.A.S.A., 1994. Advances in Natural Rubber Production. *Rubber Chemistry and Technology* 67, 537-548.

Kim, E., Goldberg, M., 1969. Serum cholesterol assay using a stable Liebermann-Burchard reagent. *Clinical chemistry* 15, 1171-1179.

Kruger, N.J., 1994. The Bradford method for protein quantitation. *Methods in molecular biology (Clifton, N.J.)* 32, 9-15.

Li, R., Liu, L., Yang, F., 2014. Removal of aqueous Hg(II) and Cr(VI) using phytic acid doped polyaniline/cellulose acetate composite membrane. *Journal of Hazardous Materials* 280, 20-30.

Madaeni, S.S., Heidary, F., 2011. Improving separation capability of regenerated cellulose ultrafiltration membrane by surface modification. *Applied Surface Science* 257, 4870-4876.

Mbaebie, B.O., Edeoga, H.O., Afolayan, A.J., 2012. Phytochemical analysis and antioxidants activities of aqueous stem bark extract of Schotia latifolia Jacq. *Asian Pacific Journal of Tropical Biomedicine* 2, 118-124.

Mihaly, J., Sterkel, S., M. Ortner, H., Kocsis, L., Hajba, L., Furdyga, É., Minka, J., 2006. FTIR and FT-Raman Spectroscopic Study on Polymer Based High Pressure Digestion Vessels. *Croatica Chemica Acta* 79, 497-501.

MITI, 2016. Ministry of International Trade and Industry (MITI) Report 2015. Ministry of International Trade and Industry, Kuala Lumpur, Malaysia.

Muhammad, A.K., 2018. Personal Correspondance. Malaysian Rubber Board, Kuala Lumpur, Malaysia.

Mulder, M., 1996. Basic Principles of Membrane Technology, Second ed. Kluwer Academic Publishers, The Netherlands.

Mun, L.C., 1996. QUEBRACHITOL - A Carbohydrate Extract from Hevea Latex. Rubber Research Institute of Malaysia, Kuala Lumpur.

Navarro, P., Perez-Lopez, A.J., Mercader, M.T., Carbonell-Barrachina, A.A., Gabaldon, J.A., 2011. Antioxidant activity, color, carotenoids composition, minerals, vitamin C and sensory quality of organic and conventional mandarin juice, cv. Orogrande. *Food science and technology international = Ciencia y tecnologia de los alimentos internacional* 17, 241-248.

Nghiem, L.D., Schäfer, A.I., Elimelech, M., 2004. Removal of Natural Hormones by Nanofiltration Membranes: Measurement, Modeling, and Mechanisms. *Environmental Science & Technology* 38, 1888-1896.

Nguyen, L.A.T., Schwarze, M., Schomäcker, R., 2015. Adsorption of non-ionic surfactant from aqueous solution onto various ultrafiltration membranes. *Journal of Membrane Science* 493, 120-133.

Okino Delgado, C.H., Fleuri, L.F., 2016. Orange and mango by-products: Agro-industrial waste as source of bioactive compounds and botanical versus commercial description—A review. *Food Reviews International* 32, 1-14.

Ostlund, R.E., Jr., 2007. Phytosterols, cholesterol absorption and healthy diets. *Lipids* 42, 41-45.

Pihlajamäki, A., Väisänen, P., Nyström, M., 1998. Characterization of clean and fouled polymeric ultrafiltration membranes by Fourier transform IR spectroscopy–attenuated total reflection. *Colloids and surfaces. A, Physicochemical and engineering aspects* 138, 323-333.

Piironen, V., Toivo, J., Puupponen-Pimiä, R., Lampi, A.-M., 2003. Plant sterols in vegetables, fruits and berries. *Journal of the Science of Food and Agriculture* 83, 330-337.

Plumb, J.A., Rhodes, M.J.C., Lampi, A.M., Buchgraber, M., Kroon, P.A., 2011. Phytosterols in plant foods: Exploring contents, data distribution and aggregated values using an online bioactives database. *Journal of Food Composition and Analysis* 24, 1024-1031.

Sajari, R., Abd-Razak, N.H., Yusof, F., Arif, S.A.M., Perkins, M., Yeang, H.Y., 2014. Improved Efficiency of Tocotrienol Extraction from Fresh and Processed Latex. *Journal of Rubber Research* 17, 245-260.

Sass-Kiss, A., Sass, M., 2000. Immunoanalytical method for quality control of orange juice products. *J Agric Food Chem* 48, 4027-4031.

Sathishkumar, T., Baskar, R., 2014. Screening and quantification of phytochemicals in the leaves and flowers in the leaves and flowers of Tabernaemontana heyneana Wall. *Indian Journal of Natural Products and Resources* 5, 237-243.

Schmutzer, G.R., Dehelean, A., Magdas, D.A., Cristea, G., Voica, C., 2016. Determination of Stable Isotopes, Minerals, and Volatile Organic Compounds in Romanian Orange Juice. *Analytical Letters* 49, 2644-2658.

Shahzad, N., Khan, W., Md, S., Ali, A., Saluja, S.S., Sharma, S., Al-Allaf, F.A., Abduljaleel, Z., Ibrahim, I.A.A., Abdel-Wahab, A.F., Afify, M.A., Al-Ghamdi, S.S., 2017. Phytosterols as a natural anticancer agent: Current status and future perspective. *Biomedicine & Pharmacotherapy* 88, 786-794.

Stinco, C.M., Fernández-Vázquez, R., Escudero-Gilete, M.L., Heredia, F.J., Meléndez-Martínez, A.J., Vicario, I.M., 2012. Effect of Orange Juice's Processing

on the Color, Particle Size, and Bioaccessibility of Carotenoids. *Journal of Agricultural and Food Chemistry* 60, 1447-1455.

Wang, T., Hicks, K.B., Moreau, R., 2002. Antioxidant activity of phytosterols, oryzanol, and other phytosterol conjugates. *Journal of the American Oil Chemists' Society* 79, 1201-1206.

Weis, A., Bird, M.R., Nyström, M., 2003. The chemical cleaning of polymeric UF membranes fouled with spent sulphite liquor over multiple operational cycles. *Journal of Membrane Science* 216, 67-79.

Wu, D., Bird, M.R., 2007. The Fouling and Cleaning of Ultrafiltration Membranes During The Filtration of Model Tea Component Solutions. *Journal of Food Process Engineering* 30, 293-323.

Yang, E., Zakaria, S., Chia, C.H., Rosenau, T., 2017. Bifunctional Regenerated Cellulose Membrane Containing TiO_2 Nanoparticles for Absorption and Photocatalytic Decomposition. *Sains Malaysiana* 46, 637-644.

Zairossani, M.N., Devaraj, V., Zin, A.K.M., Zaid, I., 2005. Modern approaches towards effective effluent treatment, Rubber Planters Conference 2005. Malaysian Rubber Board, Kuala Lumpur, Malaysia.

Zhu, S., Shi, M., Zhao, S., Wang, Z., Wang, J., Wang, S., 2015. Preparation and characterization of a polyethersulfone/polyaniline nanocomposite membrane for ultrafiltration and as a substrate for a gas separation membrane. *RSC Advances* 5, 27211-27223.

Chapter 4: Fouling Analysis and the Recovery of Phytosterols from Orange Juice Using Regenerated Cellulose Ultrafiltration Membranes

Introductory text

In the previous chapter (Chapter 3), ultrafiltration was shown to be successful in the separation of phytosterols from orange juice at transmembrane pressure (TMP) of 1 bar. The 10 kDa regenerated cellulose acetate (RCA) membrane displayed the highest concentration of phytosterols in the permeate. However, the phytosterols compounds obtained by using 10 kDa RCA membrane was relatively low. In this study, RCA membranes with larger MWCO have been tested in order to remove the proteins and transmit more sterols. The separation performance is evaluated in terms of flux, rejection, membrane resistance and cleaning efficiency. Contact angle measurement, atomic force microscopy (AFM), Fourier transform infrared (FTIR) spectroscopy and scanning electron microscopy (SEM) were conducted to study the membrane surface modification as a result of ultrafiltration due to fouling and cleaning. This chapter describes the isolation of phytosterols from orange juice via an ultrafiltration process using RCA membrane at different MWCO values. This chapter also provides the study on surface science of membrane fouling and cleaning processes, whilst optimising the ultrafiltration process to separate the phytosterol compounds from proteins in orange juice. The ultrafiltration process using different MWCO of RCA membranes in separating phytosterols from proteins in orange juice has been reported in this paper.

Statement of Authorship

This declaration concerns the article entitled:	
Fouling Analysis and the Recovery of Phytosterols from Orange Juice Using Regenerated Cellulose Ultrafiltration Membranes	

Publication status (tick one)

Draft manuscript	☐	Submitted	☐	In review	☐	Accepted	☐	Published	✓

Publication details (reference)	Abd-Razak, N.H., Zairossani, M.N., Chew, Y.M.J., Bird, M.R., 2020. Fouling Analysis and the Recovery of Phytosterols from Orange Juice Using Regenerated Cellulose Ultrafiltration Membranes. *Food and Bioprocess Technology*, 13, 2012–2028. https://doi.org/10.1007/s11947-020-02541-7
Candidate's contribution to the paper (provide details, and also indicate as a percentage)	**Formulation of ideas (90%):** I presented the main ideas of this work and discussed with my co-authors, in order to improve the separation process. Mike Bird suggested the application of membranes with larger MWCO to transmit more phytosterols and to remove the proteins. **Design of methodology (80%):** I planned the characterisation studies based on the data and results in previous paper and also from this work. John Chew suggested the GPC analysis to study the polymer composition of three different RCA membranes. The AFM analysis was suggested by Mike Bird. **Experimental work (85%):** I performed the ultrafiltration experiments, analysis of compounds and most of the membranes characterisation. SEM and GPC analysis of the samples were conducted by the technical staff. I carried out the data interpretation after discussions with my co-authors. **Presentation of data in journal format (90%):** I prepared the manuscript for the journal including the outlines, graphics in the journal format and incorporated feedback from co-authors and reviewers. The co-authors contributed in revising the draft manuscript.
Statement from Candidate	This paper reports on original research I conducted during the period of my Higher Degree by Research candidature.
Signed	██████ **Date** 25 Feb 2021

Fouling Analysis and the Recovery of Phytosterols from Orange Juice Using Regenerated Cellulose Ultrafiltration Membranes

Nurul Hainiza Abd-Razak[1,2], M. N. Zairossani[2], Y.M. John Chew[1], Michael R. Bird[1*]

[1]Centre of Advanced Separations Engineering, Department of Chemical Engineering, University of Bath, Bath BA2 7AY, UK

[2]Rubber Research Institute of Malaysia, Malaysian Rubber Board, PO Box 10150, 50908 Kuala Lumpur, Malaysia

*Corresponding author. Email address: M.R.Bird@bath.ac.uk

Abstract

This study describes the use of regenerated cellulose (RCA) membranes with molecular weight cut-off (MWCO) values of 10, 30 and 100 kDa respectively, to separate phytosterols from orange juice for possible nutraceutical production. A desirable membrane separation rejects protein whilst transmitting phytosterols and other low molecular mass compounds such as sugars. The ultrafiltration was performed in a cross-flow membrane system with a total filtration area of 336 cm^2. Total phytosterols analysis was carried out by using a Liebermann-Buchard based method. Protein concentration was quantified by the Bradford method. The effects of three different membranes upon the rejection of total phytosterols content, proteins, sugar and antioxidant activity were studied. Of the membranes tested, the 10 kDa membrane displayed the highest concentration of phytosterols in the permeate. 30 kDa and 100 kDa membranes gave comparatively higher phytosterols rejection. The membrane surface roughness and corresponding pure water flux values varied as a function of MWCO such that RCA30 > RCA100 > RCA10. Membranes with rougher surfaces displayed a higher fouling than those with smoother surfaces. Hydrophobicity and surface roughness both influenced filtration performance, by controlling the development of the protein-based foulant which modified membrane selectivity.

Keywords: Fouling; Membrane selectivity; Water flux; Surface roughness; Hydrophobicity

Introduction

Plant sterols, generally known as phytosterols, are cholesterol-like compounds that are found mostly in vegetable oils, nuts and fruits (Wang et al. 2018). The structure is related to cholesterol but differs in the structure of the side chain. Phytosterols consists of a steroid skeleton with a hydroxyl group attached to the C-3 atom of the A-ring. The most common phytosterols are stigmasterol and β-sitosterol. Commercial phytosterols were isolated mostly from soybean oil. Stigmasterol has a molecular weight of 412 g mol^{-1} with elemental formula $C_{29}H_{48}O$. For β-sitosterol, the elemental formula is $C_{29}H_{50}O$ with molecular weight of 414 g mol^{-1} (Kongduang et al. 2012; McDonald et al. 2012). Phytosterols are widely used as food additives due to their ability to lower human cholesterol levels (Marangoni and Poli 2010). Phytosterols are also known for their anticancer properties by inhibiting the progression of cancer cell cycle (Shahzad et al. 2017). The global market size of phytosterols is expected to increase to USD 1,100 million by 2025, from USD 590 million in 2018 (Market-Insights-Reports 2019).

The main limitations concern the lack of techniques that can be used for the economical extraction and separation of phytosterols compounds from various plants. Conventional techniques such as Soxhlet extraction has been used to extract phytosterols from melon seeds (Nyam et al. 2011). Phytosterols from rapeseed was extracted using microwave extraction technique (Yang et al. 2013). Alternative extraction methods such as supercritical fluid extraction have been used to isolate phytosterols from melon seeds (Nyam et al. 2011). There are some drawbacks associated with these techniques. The use of toxic organic solvents and the use of supercritical fluid that involves high pressures and high temperatures; consume large amounts of energy and produce considerable waste, making them costly and unsustainable (Conidi et al. 2017). Membrane separation techniques such as ultrafiltration have been widely used in fruit juice processing (A. W. Mohammad et al. 2012; Ilame and V. Singh 2015). The effectiveness of ultrafiltration in separating anthocyanin and flavonols from black currant juice (Pap et al. 2012), phenolic compounds from pomegranate juice (Conidi et al. 2017), bioactive compounds from kiwifruit juice (Cassano et al. 2008), polyphenols from banana juice (Sagu et al. 2014) and phenolics from broccoli juice (Yilmaz and Bagci 2019) has been clearly demonstrated. Gulec *et al.* (2017) analysed membrane fouling during the

ultrafiltration of apple juice. Although works on many fruit juices have been reported, there is no report on the separation of phytosterols from orange juice by ultrafiltration.

Orange juice contains bioactive compounds such as phytosterols (Piironen et al. 2003; Jiménez-Escrig et al. 2006; Balme and Gulacar 2012), sugars (Jesus et al. 2007) and protein (Okino Delgado and Fleuri 2016). The composition of orange juice is shown in Table 1. Orange juice contains a polydisperse distribution of particle sizes from pulp trashes to small particles less than 2 μm in diameter (Corredig et al. 2001; Stinco et al. 2012). In addition, the molecular weight of proteins in orange juice was 12 to 71 kDa (Sass-Kiss and Sass 2000). No literature is available on the performance of ultrafiltration processes for the separation of phytosterols from proteins in fruit juices. Our previous study was performed using three types of 10 kDa molecular weight cut-off (MWCO) ultrafiltration (UF) membranes made from regenerated cellulose (RC), polyethersulfone (PES) and fluoropolymer (FP). The 10 kDa regenerated cellulose membrane displayed the best rejection ratio of phytosterols (32%) from proteins in orange juice (Abd-Razak et al. 2019). Thus, a process optimisation is important since the phytosterols yield was relatively low. It is hypothesised that membrane with larger MWCO can be used to transmit lower molecular weight compounds passing through the membrane.

This paper investigates the surface science of membrane fouling and cleaning processes, and builds upon our previous study (Abd-Razak et al. 2019) which demonstrated the principle of using ultrafiltration to separate phytosterols from proteins in orange juice. This paper describes the isolation of phytosterols from orange juice for nutraceutical fabrication via an ultrafiltration process using regenerated cellulose membrane at different MWCO values. This study elucidates the mechanisms of fouling and flux loss, whilst optimising the ultrafiltration process to fractionate the targeted sterol compounds. The performance of the separation is evaluated in terms of flux, rejection, membrane resistance and cleaning efficiency. Contact angle measurement, atomic force microscopy (AFM), Fourier transform infrared (FTIR) spectroscopy and scanning electron microscopy (SEM) were carried out to investigate the membrane surface modification occurring as a result of ultrafiltration.

Table 1   Composition of orange juice in term of phytosterols, protein and sugar contents.

Components	Amount	
	This study	Literature
Phytosterols	0.2 – 0.3 mg/ml	0.2 – 0.3 mg/ml (Piironen et al. 2003; Jiménez-Escrig et al. 2006)
Protein	0.8 – 1.0 mg/ml	0.7 – 0.9 mg/ml (Cobell 2016)
Sugar	10 – 11 °Brix	≥ 10 °Brix (Cobell 2016)

Materials and Methods

Materials

Chemicals and standards used in this work are listed in Table 2. All solvents and reagents were purchased from *Merck* (UK). Butylated hydroxytoluene and stigmasterol were sourced from *Sigma Aldrich* (UK) were used as characterisation standards. Protein assay kit was acquired from *Bio-Rad* (UK). Cleaning of membranes was carried out using 0.5 wt%. *P3-Ultrasil 11* (*Henkel Ecolab*, USA) which contains sodium hydroxide, tetrasodium salt of EDTA, anionic surfactant and non-ionic surfactant (Weis et al. 2005).

Table 2   Chemicals and standards used

Chemical	Function	Analysis
Chloroform	Solvent	Total phytosterol content
Acetic anhydride	Reagent	Total phytosterol content
Sulfuric acid	Reagent	Total phytosterol content
Stigmasterol	Standard	Total phytosterol content
Methanol	Solvent	Antioxidant assay
1,1-diphenyl-1-picrylhydrazyl (DPPH)	Reagent	Antioxidant assay
Butylated hydroxytoluene (BHT)	Standard	Antioxidant assay
Protein assay kit (Dye reagent)	Reagent	Protein assay
Bovine serum albumin (BSA)	Standard	Protein assay

Membranes

Three flat-sheet regenerated cellulose acetate (RCA) membranes with 10 kDa, 30 kDa and 100 kDa MWCO values, were supplied by *Alfa Laval* (Denmark). RCA 10 kDa is a commercial membrane with *Alfa Laval* code RC70PP. RCA 30 and 100 kDa are prototype membranes. The characteristics of membrane are summarised in Table 3 (Alfa-Laval 2017). Membranes were cut to size with a membrane area of 336 cm^2 and placed in the membrane module. Prior to filtration, new membranes were conditioned by passing reverse osmosis (RO) water through the membrane at 60 °C and at TMP of 1 bar for 120 minutes. This conditioning technique was established to remove glycerol coating from the membrane surface applied by the manufacturer (Weis et al. 2003).

Table 3 Characteristics of the RCA membranes. (From *Alfa Laval* (Alfa-Laval 2017))

Membrane	RCA 10	RCA 30	RCA 100
Manufacturer	*Alfa Laval*		
Material for selective layer	Regenerated cellulose acetate (RCA)		
Material for support layer	Polypropylene (PP)	Polyethylene terephthalate (PET)	
MWCO (kDa)	10	30	100
pH operating range	1 - 10		
pH cleaning	1 – 11.5		
Operating pressure (bar)	1 - 10		
Operating temperature (°C)	5 - 60		
Pure water permeance (L m^{-2} h^{-1} bar^{-1}) at 1.0 bar	100 ± 5	240 ± 5	210 ± 5

Pre-filtration of Orange Juice

Processed orange juice (not from concentrate) was sourced from *Cobell* (UK). At the factory, the processing begins with the washing process and then the fruit was placed in an extractor to separate the juice from the pulp and skin. It was then centrifuged to

push the juice out and finally pasteurised to reduce microbiological loading whilst maintaining as much of the colour, flavour and aroma of the fruit (Cobell 2016). Processed orange juice was received in a bulk (100 L/ batch) and then stored in a cold room at 4 °C up to 2 months. The juice was first pre-filtered through a stainless steel 25 μm cartridge filter (*Memtech*, UK) that attached to *Amicon* (Danvers, USA) pressurized feed vessel, to remove pulp prior to ultrafiltration. The pre-filtration was carried out at 1.5 bar at room temperature.

Ultrafiltration Experimental Setup

Three RCA membranes of each MWCO (10 kDa, 30 kDa and 100 kDa) were used in the experiments. Each membrane samples were run at three different cycles. The standard deviation was calculated based on three membrane samples for each MWCO. The ultrafiltration experiments were carried out by using a cross flow membrane filtration system *LabStak M10* containing four polymeric flat sheet membranes in series, manufactured by *DSS* (now *Alfa Laval*) (Denmark) with a total filtration area of 336 cm^2. The ultrafiltration was performed using 3 L orange juice for each run. Additional details concerning the ultrafiltration apparatus and the schematic design of the system can be found in Abd-Razak *et al.* (2019). The ultrafiltration fouling and cleaning cycle consists of membrane conditioning, pure water flux (PWF), filtration, rinsing and cleaning steps (Abd-Razak et al. 2019). Permeate flux was measured during the ultrafiltration of orange juice. Pure water flux (PWF) values were measured for membranes using RO water under these conditions (i) before fouling, (ii) after fouling and (iii) after cleaning at three different cycles. The cross-flow filtration cycle protocol is including PWF before fouling (10 minutes), filtration using orange juice (60 minutes), rinsing (5 minutes), PWF after fouling (10 minutes), cleaning (10 minutes), rinsing (5 minutes) and PWF after cleaning (10 minutes). The temperature of the feedstock was maintained at 20 ± 1 °C. A TMP value of 1.0 bar was used and the cross flow velocity (CFV) was in the range 1.4 - 1.5 m s^{-1}. The PWF of the membrane was determined using RO water at three different times; before filtration, after first rinsing and after cleaning. The filtration time was limited to 60 min; as this is sufficient to obtain a pseudo steady-state permeate flux.

Evaluation of Membrane Performance and Fouling Process

The membrane performance was evaluated in terms of permeate flux, resistances, rejection ratio and fouling index (Mulder 1996). The permeate flux is defined as the volumetric flow rate of the fluid through the membrane. The permeate flux through a membrane can be calculated using Equation (1):

$$J = \frac{\Delta P}{\mu R_{tot}} \tag{1}$$

where J is the flux through the membrane (L m^{-2} h^{-1}), ΔP (Pa) is the transmembrane pressure (TMP), μ is the dynamic viscosity (Pa s) and R_{tot} represents the total resistance (m^{-1}). The flux decline can be calculated using Equation (2):

$$Flux\ decline = \frac{J_0 - J_{ss}}{J_0} \tag{2}$$

where J_0 is the initial permeate flux and J_{ss} is the steady-state permeate flux. In pressure driven process such as ultrafiltration, fouling can be represented in the resistance in series model as shown in Equations (3) and (4) (Jiraratananon and Chanachai 1996):

$$J = \frac{\Delta P}{\mu\ (R_m + R_f + R_{cp})} \tag{3}$$

$$R_f = R_{ir} + R_r \tag{4}$$

where R_m is the resistance of conditioned virgin membrane, R_f is the total fouling resistance, R_{ir} is the irreversible fouling resistance, R_r is the reversible fouling resistance and R_{cp} is the resistance due to concentration polarisation. R_m is determined by measuring the flux of RO water through the conditioned membrane. Irreversible fouling is defined as any foulant not being removed by rinsing. Reversible fouling is defined as any foulant is removed from the membrane pores and surfaces by rinsing.

The cleaning efficiency was determined by comparing the pure water permeability before and after cleaning (Conidi et al. 2017). Selectivity is the degree to which one component preferentially permeates the membrane and thus determines the degree of enrichment achieved. Selectivity is expressed as the rejection ratio (R) and can be calculated by using Equation (5); where C_p is the solute concentration in the permeate and C_r is the solute concentration in the retentate (Mulder 1996).

$$R = (1 - \frac{C_p}{C_r}) \tag{5}$$

Hermia divided fouling into four mechanisms namely cake filtration, standard blocking, intermediate pore blocking and complete pore blocking (Hermia 1982). An analytical model was produced by Field et al. (1995) based on Hermia's pore blocking laws:

$$-\frac{dJ}{dt} J^{n-2} = k (J - J^*) \tag{6}$$

where J is flux, J^* is limiting flux, t is time, n and k are constants specific to the type of fouling. The different fouling laws concerned are cake filtration, intermediate and complete blocking where n values are 0, 1 and 2 respectively. This model suggests that the fouling mechanism take place sequentially (not simultaneously) from intermediate pore blocking and then cake filtration (Lewis et al. 2017). According to Equation (6), a function of flux can be described as:

$$f(J) = -\frac{dJ}{dt} J^{n-2} \tag{7}$$

where a linear relationship between $f(J)$ and J is observed (Field et al. 1995). Experimental flux data was analysed to evaluate the type of membrane fouling using a MATLAB script (Lewis et al. 2017). Flux data shows $f(J)$ as described by Equation (7) where $n = 0$ for cake filtration and $n = 1$ for intermediate pore blocking. The calculated data from MATLAB was re-plotted in the Excel to determine the correlation coefficient of the graph using a linear regression type. The Hermia model is more reasonable when results fit a straight line (Nguyen et al. 2015).

Characterisation Techniques

Feed, permeate and retentate samples from ultrafiltration experiments were collected and kept frozen at -18 °C until analysed. After thawing, the samples were vortex-mixed for 3 minutes at room temperature to homogenise the samples. Samples were analysed for total phytosterols, proteins, sugars and antioxidant activity. All measurements were done in triplicate and the results were averaged. These analyses were used in the calculation of rejection ratio.

The total phytosterol content was determined calorimetrically using a modified Liebermann-Buchard (LB) based method (Mbaebie et al. 2012; Sathishkumar and Baskar 2014; Tolve et al. 2018). Formation of a green colour indicated the presence of phytosterols at absorbance 420 nm using an ultraviolet-visible (UV-Vis) spectrophotometer (Cary 100, *Agilent,* USA). Standard solutions of stigmasterol were used for the calibration. Protein concentration was quantified by the Bradford method (Cassano et al. 2008; Kruger 1994). The assay is based on the binding of the acidic dye solution Coomassie Brilliant Blue G-250 to protein at absorbance 595 nm (Bradford 1976). Bovine serum albumin (BSA) was used as a standard solution.

The sugar content expressed as °Brix was determined using a digital hand-held refractometer (*Reichert*, New York, USA). The refractometer measures the refractive index which indicates the degree to which the light changes direction when it passes through the fruit juice. The antioxidant activity was measured by detecting the scavenging of 1, 1-diphenyl-2-picrylhydrazyl (DPPH) radical (Iqbal et al. 2015) at absorbance 517 nm using an ultraviolet-visible (UV-Vis) spectrophotometer (Cary 100, *Agilent,* USA). Butylated hydroxytoulene was prepared in methanol as reference.

Membranes Characterisation

Contact angle

Contact angle measurements were conducted to evaluate the hydrophobicity of the membranes via sessile drop technique using *DataPhysics Optical Contact Angle System OCA 25* (Filderstadt, Germany) equipped with image processing software *DataPhysics Instruments SCA 22*. Membranes were dried at room temperature for 30

minutes. A deionized water droplet of 5 μL at the end of syringe needle was deposited onto the membrane surface. The contact angle values were determined as the averaged values during measurement periods of 300 – 500 frames in 10 – 15 seconds (Baek et al. 2012). The procedure was repeated five times at different points on the same membrane sample. All measurements were done in triplicates.

Atomic Force Microscopy (AFM)

The surface roughness values of the membrane surfaces were determined by atomic force microscopy (AFM). The flexible cantilever and the AFM tip gently touch the surface and record the small force between the tip and the surface (De Oliveira et al. 2012). This measurement was performed using a Multimode AFM (*Veeco Metrology*, USA) with a *Nanoscope Analysis 1.7* software. The cantilever was used in contact mode with silicon soft tapping mode tips (*Tap150AI-G, Budget Sensors*, Bulgaria). Images were scanned at 1 μm × 1 μm scan size at a rate of 1 Hz for conditioned membranes, fouled membranes and cleaned membranes. Samples were analysed in three replicates for the AFM analysis.

Fourier transform infrared (FTIR) spectroscopy

Attenuated Total Reflection-Fourier Transform Infrared (ATR-FTIR) (*Frontier FT-IR*, *PIKE Technologies Inc.*, USA) was used to examine the foulant on the membrane surfaces due to fouling. Three fouled membrane samples were prepared for each molecular weight cut off. The membrane samples were dried at room temperature for 24 hours prior to analysis (Pihlajamäki et al. 1998). The FTIR apparatus was used to record the IR-spectra at Mid Infra Red (MID) region. The scan speed was 0.2 cm^{-1} and a spectral resolution of 4 cm^{-1} using a KBr beam splitter was used in this study.

Scanning electron microscope (SEM) and energy dispersive X-ray (EDX)

Air and vacuum-dried membranes were mounted on aluminium stubs with conductive paste and gold sputter coated on a Sputter coater model *E150B* (*Edwards*, UK) under an argon gas. Then, the samples were viewed with a *JEOL SEM* model *JSM 6480LV* (Japan). The elemental composition of a material on the membrane surface was examined by energy dispersive X-ray (EDX) that attached to the SEM. High sensitivity Oxford INCA X-Act SDD x-ray detector (*Oxford Instruments*, UK) was used for EDX analysis.

Gel permeation chromatography (GPC)

GPC analysis was carried out to study the polymer composition of three different RCA membranes by determining the distribution of molecular mass of polymer repeating unit in the membranes. Conditioned membranes were dissolved in tetrahydrofuran (THF) to give a concentration of 2 mg ml^{-1}. The solutions were left overnight at 4 °C prior to the GPC analysis. The molecular weight (MW) of the samples were determined using a 1260 GPC/SEC system (*Agilent Technologies*, USA) attached to a 2× PLgel 5 μm *MIXED-D* (7.5 x 300 mm) column and refractive index detector. The data was generated using *Agilent GPC/SEC* software. THF was used as the mobile phase.

Matrix-Assisted Laser Desorption Ionisation (MALDI)

Bruker AutoFlex Matrix-Assisted Laser Desorption Ionisation (MALDI) mass spectrometer was used for polymer analysis of three different RCA membranes. Conditioned membranes were dissolved in two different solvents (THF and dichloromethane). Solvents were prepared at concentration of 1 mg/ml. THF was used as the eluent. Dithranol and dihydroxybenzoic acid were used as the matrix.

Results and Discussion

Flux Analysis

Permeate flux

At the beginning of the experiment, 5 kDa membrane was also tested. The membrane showed low permeate flux (10 L m^{-2}) at a TMP of 1.0 bar. Therefore, the experiment was continued with 10 kDa membrane. Figure 1 presents the time course of permeate flux for orange juice ultrafiltration using RCA membranes for the three different MWCO values tested. It can be seen in Figure 1, the trend for permeate flux for UF by using all membranes were similar. The initial permeate flux decreased gradually with filtration time until it reached a steady-state value. At the beginning of the ultrafiltration, the permeate fluxes for RCA 10, RCA 30 and RCA 100 were 29 L m^{-2} h^{-1}, 39 L m^{-2} h^{-1} and 42 L m^{-2} h^{-1} respectively. After approximately 2 min, permeate fluxes continued to decline gradually until the filtration was stopped at 60 min. All

membranes displayed steady-state permeate flux at *ca.* 22 L m^{-2} h^{-1}. In the previous studies (Abd-Razak et al. 2019), the steady-state flux of *ca.* 22 L m^{-2} h^{-1} was obtained at a TMP of 1.0 bar using RCA 10 kDa membrane. A steady-state flux value of 17 L m^{-2} h^{-1} was obtained for PES 10 kDa membrane. Fluoropolymer 10 kDa membrane reached a steady-state value at 14 L m^{-2} h^{-1}. It can be concluded that the highest steady-state flux was achieved using RCA membrane. Higher flux resulted in less total resistances. Thus, filtration using RCA membrane has been selected in this study. The permeate flux of RCA 10, RCA 30 and RCA 100 dropped to 22 L m^{-2} h^{-1}, indicating a flux decline of 24%, 44% and 48% respectively. It is notable that the steady-state permeate flux value is the same for all three membranes tested, irrespective of the MWCO value. The decrease of permeate flux can be explained by the effect of fouling (Conidi et al. 2017).
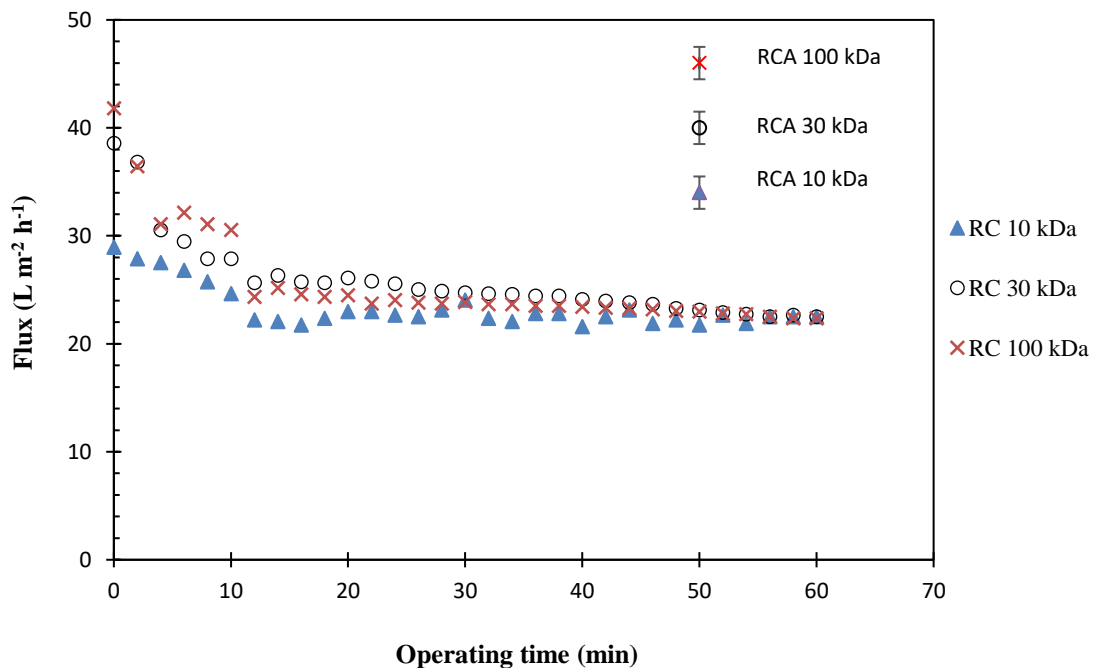
Fig. 1   Time course of permeate flux decline for RCA membranes tested. The largest error for this set of data is ± 1.2 L m^{-2} h^{-1}. Data are shown as averages of 3 replicates of each membrane; with error bars represent the standard deviation.

Pure water flux

Figure 2 shows the PWF of the membranes tested at TMP of 1.0 bar and at 20 °C. In general, the RCA 10 kDa and RCA 100 kDa membranes showed lower pure water fluxes than the RCA 30 kDa membrane. The PWF decreased in the following order,

RCA30 > RCA100 > RCA10 which was not correlated with the MWCO of the membranes. The RCA 30 membrane with the intermediate MWCO (30 kDa) gave the highest water flux of 226 - 289 L m^{-2} h^{-1}. Meanwhile RCA 100 with the highest MWCO (100 kDa) gave the PWF of 170 - 219 L m^{-2} h^{-1} and the RCA 10 membrane displayed the lowest water flux of 77 - 132 L m^{-2} h^{-1}. This may suggest that PWF was a poor indicator of permeate flux in this system as the higher MWCO membrane showed lower fluxes. The PWF (PWF2) reduced after fouling for all membranes in all cycles. These results indicate that the ultrafiltration process was affected by the membrane fouling. Thus, a good cleaning method is required to regenerate the membrane.

The commercial cleaning formulation, *Ultrasil 11* was used – this product finds wide application for membrane cleaning in laboratory situations (Wu and Bird 2007). Figure 2 demonstrates that the pure water permeate flux of the membrane after cleaning was higher than that seen after fouling (*eg:* PWF 3 III > PWF 2 III). It is possible that surface modification is occurring due to the adsorption of *Ultrasil 11* surfactant to the membrane surface (Weis et al. 2003). It can be concluded that the cleaning technique is effective in regenerating the membrane. However, the membranes behave differently for the first cycle of RCA 10 and RCA 30 filtration, during which the fluxes after cleaning were higher than those recorded for the membrane before fouling (*eg:* PWF 3 I > PWF 1 I). Hydrophobicity, charge and roughness all affect the filtration process, and it is usual for these factors to dominate species / pore size considerations when examining small pore UF membranes. The results presented in Figure 2 also demonstrate that the PWF for all membranes did not vary following three fouling/ cleaning cycles.
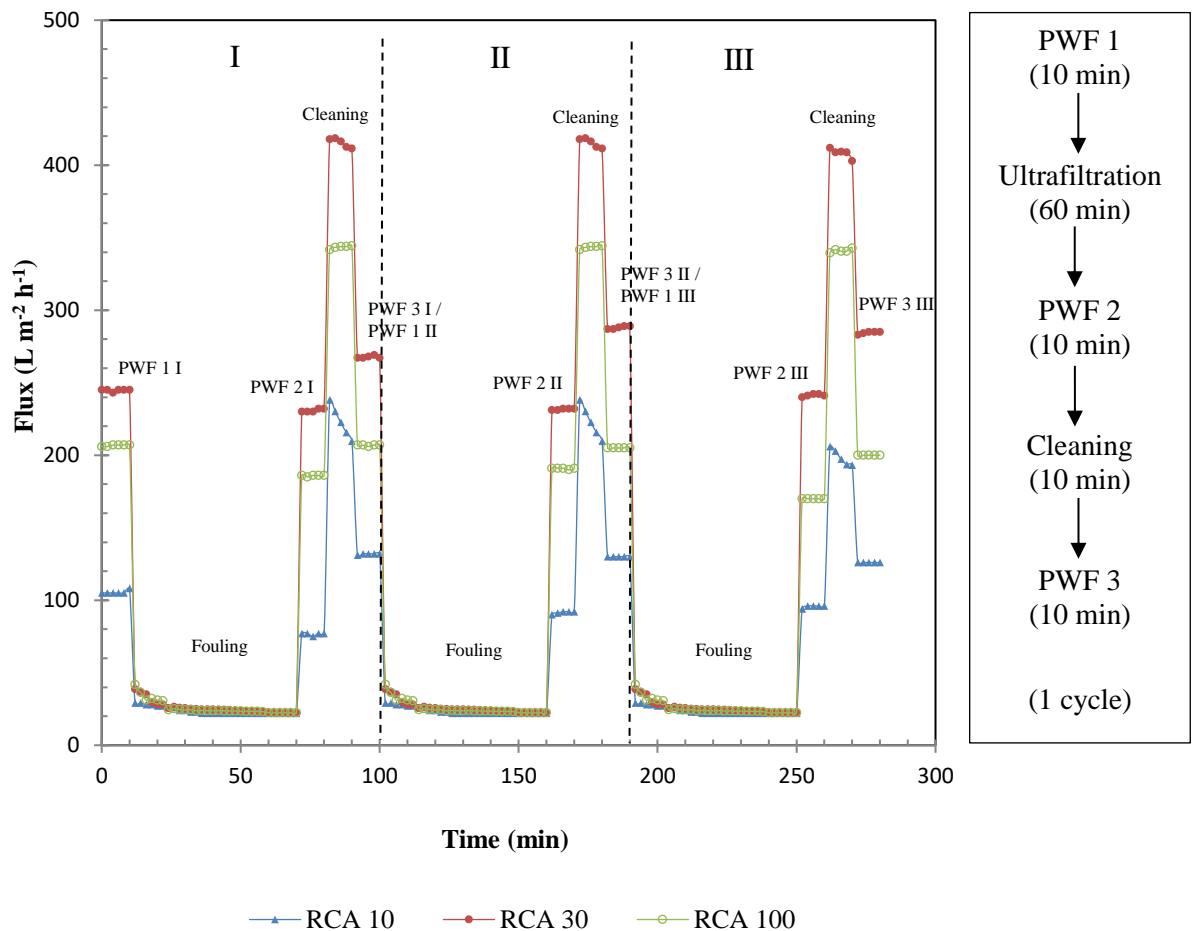
Fig. 2 Pure water fluxes of three membranes tested; RCA 10, RCA 30 and RCA 100 during three filtration cycles (1 h of fouling, 10 min of pure water flow, 10 min of cleaning) operated at TMP = 1 bar. Regions identified by roman numerals represent the three filtration cycles. Average uncertainty of the pure water flux is ± 2 L m^{-2} h^{-1}. The error represents the standard deviation.

The membranes were also compared in terms of cleaning efficiency. The cleaning efficiency was evaluated by comparing the pure water permeability values before fouling and after cleaning (Conidi et al. 2017). The pure water permeabilities were taken from each cycle, which were then averaged. Table 4 displays the cleaning efficiency measured for all membranes tested. All three membranes (RCA 10, RCA 30, and RCA 100) displayed high cleaning efficiencies of greater than 97%. From this observation, it can be concluded that the chemical cleaning method using 0.5 wt% *Ultrasil 11* was effective in regenerating all of the membranes tested [39].

Table 4   Cleaning efficiency for RCA 10, RCA 30 and RCA 100 membranes.

Membrane	Cleaning Efficiency (%)
RCA 10 kDa	98 ± 1
RCA 30 kDa	98 ± 1
RCA 100 kDa	97 ± 1

Resistances

Flux measurements were used to calculate the total resistances, including those due to the membrane, concentration polarisation, reversible fouling and irreversible fouling (Equation 2). The rejection of components at the membrane surface will lead to an increase in the viscosity of the retentate close to the membrane surface. However, the flux is primarily a function of the viscosity of the permeate through the pores. The viscosity of the feed is important in forming resistances such as by gelation, and concentration polarisation (CP). A diagnostic test for CP was carried out whereby the feed pump was turned off, and 60 seconds later turned on again. No jump in flux was seen, and accordingly it is concluded that concentration polarisation is not an important fouling related resistance in this system.

Figure 3 shows the total resistances including membrane, reversible fouling and irreversible fouling for the membranes tested. The conditioned virgin membrane resistances before fouling for RCA 10, RCA 30 and RCA 100 were 3.0×10^{12} m^{-1}, 1.7×10^{12} m^{-1} and 1.5×10^{12} m^{-1} respectively. After fouling, the total resistances increased to 4.7×10^{12} m^{-1}, 3.0×10^{12} m^{-1} and 2.6×10^{12} m^{-1} respectively, which were 1.6, 1.8 and 1.7 times more than those seen before fouling. These results indicate that the membranes became fouled during filtration. The RCA 10 membrane displayed the highest total membrane resistance, most probably due to the fact that this membrane had the lowest MWCO value of 10 kDa. This is also reflected in the lowest pure water flux for RCA 10 in Fig. 2. The increase in the total resistance recorded after fouling was mainly due to reversible rather than irreversible fouling (Fig. 3). Table 5 shows the percentages of total resistances including membrane resistance, reversible fouling and irreversible fouling. The conditioned virgin membrane resistances for RCA 10, RCA 30 and RCA 100 were 64%, 55% and 59% respectively. The 10 kDa RCA membrane showed total fouling resistances of 36%. The 30 kDa and 100 kDa membranes displayed a higher percentage of total fouling

resistances of 45% and 41% respectively. Reversible fouling showed higher percentage compared to irreversible fouling as shown in Table 5. Thus, reversible fouling was found to play an important role in the flux decline in this system. Hydrophilic membranes were subject to more reversible fouling than irreversible fouling, which is in agreement with the findings of Metsamuuronen in ultrafiltration of proteins using regenerated cellulose membrane (Metsamuuronen 2003).
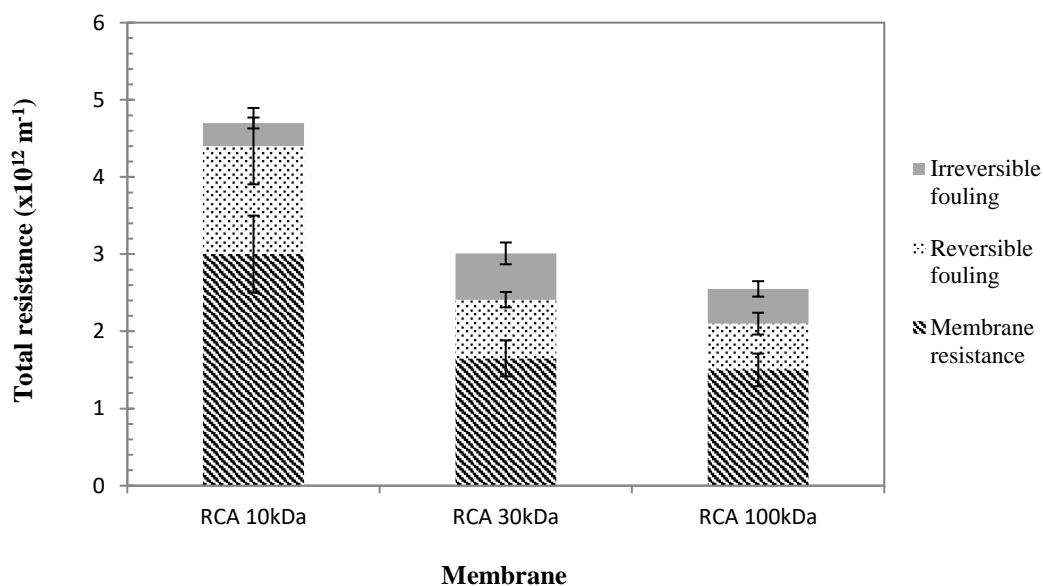
Fig. 3 Breakdown of total resistances during the ultrafiltration of phytosterols from orange juice using RCA 10, RCA 30 and RCA 100 membranes. Total resistances were divided into membrane resistance, irreversible fouling and reversible fouling. Data are shown as averages of 3 replicates of each membrane; with error bars represent the standard deviation.

Table 5   Percentages of the breakdown of total resistances

	RCA 10kDa	RCA 30kDa	RCA 100kDa
Membrane resistance (%)	64	55	59
Reversible fouling (%)	30	25	23
Irreversible fouling (%)	6	20	18
Total Resistances (%)	100	100	100

Rejection of Key Compounds

Samples from the feed, retentate and permeate streams were collected and characterised for total phytosterols, protein, sugar contents and antioxidant activity. The separation efficiency and the effect of membrane fouling were characterised by measuring the rejection of key compounds such as phytosterols, protein, sugar and antioxidant activity (Figure 4). A desirable separation outcome is that a membrane shows a high rejection to protein and a low rejection to sterols. As reported previously (Abd-Razak et al. 2019) the 10 kDa RCA membrane displayed good separation efficiency with $32 \pm 4\%$ rejection of phytosterols. The 30 kDa and 100 kDa membranes displayed a higher rejection of phytosterols of $74 \pm 6\%$ and $58 \pm 4\%$ respectively. Protein was highly rejected ($96 \pm 1\%$ rejection) by 10 kDa membrane. The 30 kDa and 100 kDa membranes gave lower rejection of protein of $69 \pm 3\%$ and $67 \pm 2\%$, respectively. It is possible that the larger pore membranes enabled protein-based foulants to enter the structure more deeply, and whilst this led to a lower rejection of proteins, it also led to a higher rejection of sterols due to species interaction inside the pore. It is postulated that the molecules are trapped inside the pore due to the steric effect (Han et al. 2008). The steric effect forms a diffusive barrier and creates an interaction between the pore walls and the molecules; which leading to pore blocking. The 10 kDa membrane was likely to be fouled with a cake of proteins, which enabled sterols to pass into the permeate. It can be noted that most proteins were rejected by the 10 kDa MWCO membrane, since the molecular weight of proteins in orange juice was 12 to 71 kDa (Sass-Kiss and Sass 2000). The higher molecular weight compounds were rejected by smaller pore size membrane and this increased the fouling layer (Evans et al. 2008). This may suggest that the membrane was fouled by protein-based compounds that alter the selectivity of the membrane. This is supported by the modification of membrane hydrophobicity (Table 7) and surface roughness (Table 8) and also in agreement with the FTIR data (Fig. 6).

All membranes showed lower rejection of sugar (4% to 6%) in comparison to phytosterols and proteins. For antioxidant activity, the rejection was in the range 12% to 30% inhibition. No correlation was observed between antioxidant activity and phytosterols content. It is possible that the antioxidant activity detected can be attributed to other chemical compounds present in orange juice, such as phenolic compounds (Stinco et al. 2012). According to these results, the RCA 10 kDa

displayed the best separation with the highest transmission of phytosterols (32%) and the highest rejection (97%) of proteins from orange juice. Thus, it can be concluded that RCA 10 kDa membrane is the best membrane in rejecting the protein from the sterols stream in orange juice.
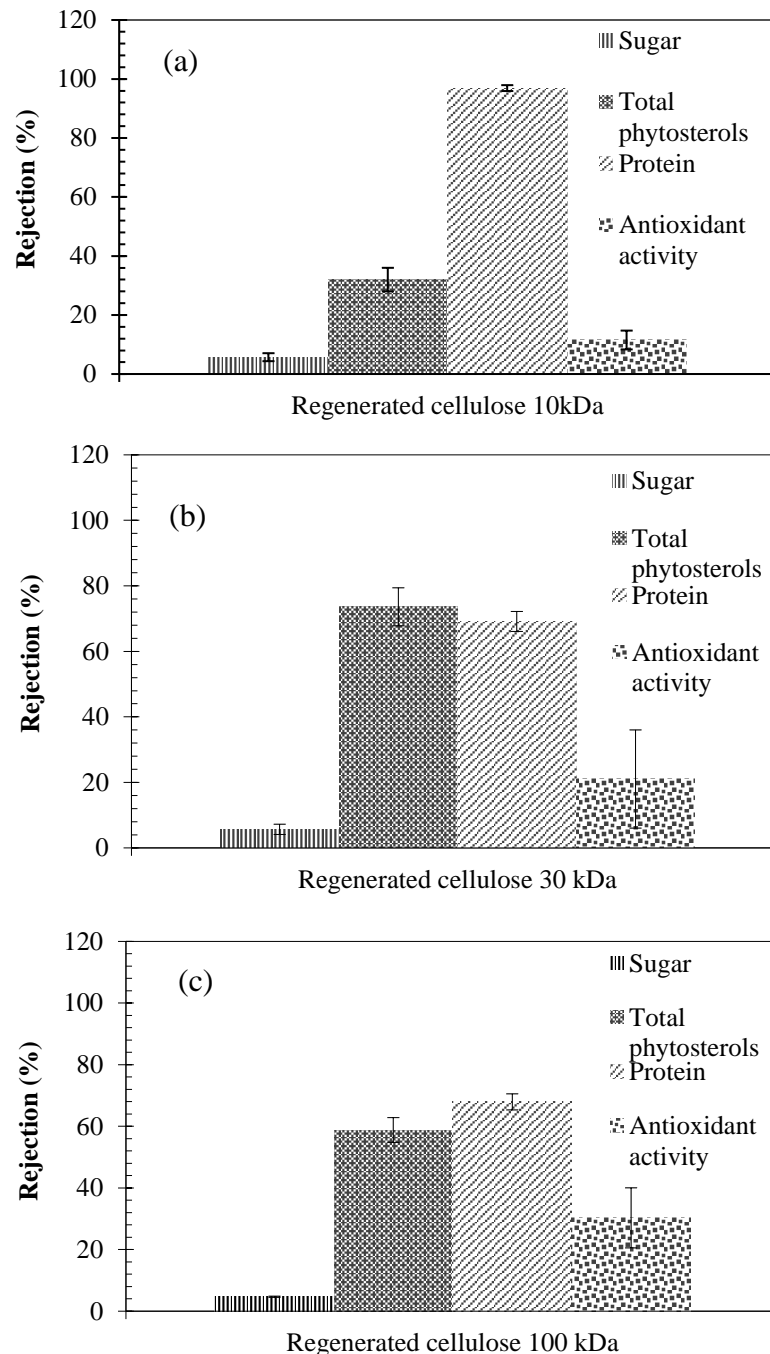

Fig. 4 Rejection of compounds by RCA membranes in term of total phytosterols content, protein, sugar and antioxidant activity at (a) 10 kDa, (b) 30 kDa, (c) 100 kDa membranes. Data are shown as averages of 3 replicates of each membrane; with error bars represent the standard deviation.

Hermia's blocking model was applied to all the filtration experiments. Hermia divided fouling into four mechanisms namely cake filtration, standard blocking, intermediate pore blocking and complete pore blocking (Hermia 1982). According to Nguyen et al. (2015), the Hermia model is more reasonable when results fit a straight line. The fouling mechanism change at a flux transition point, J_T (Lewis et al. 2017; Iritani and Katagiri 2016). It should be noted that the flux in Fig. 5 is plotted on the x-axis with the filtration time would move in the direction from right to left. Figure 5 (a) and (b) show the Hermia's blocking model applied to RCA 10 kDa membrane. A linear line was seen from the beginning of the flux curve until the end of the filtration. A linear regression was applied in determining the correlation coefficient of the graph. The linear fit was limited to linear region as shown in Fig. 5. The linear region for RCA 10 kDa was between 22 L m^{-2} h^{-1} and 25 L m^{-2} h^{-1}. The correlation coefficient for RCA 10 kDa at $n = 0$ and $n = 1$ were 0.9795 and 0.9796 respectively (Fig. 5 (a) and (b)). Neither model showed a close fit to flux decline curves for the RCA 10 kDa membranes tested. However, it is postulated that the 10 kDa membrane was fouled with a cake of proteins, as proteins were highly rejected by the 10 kDa membrane as shown in Fig. 4.

The linear region for RCA 30 kDa was between 25 L m^{-2} h^{-1} and 30 L m^{-2} h^{-1}. The correlation coefficient for RCA 30 kDa at $n = 0$ and $n = 1$ were 0.966 and 0.9891 respectively (Fig. 5 (c) and (d)). The linear region for RCA 100 kDa was between 24 L m^{-2} h^{-1} and 30 L m^{-2} h^{-1}. The correlation coefficient for RCA 100 kDa at $n = 0$ and $n = 1$ were 0.9431 and 0.9756 respectively (Fig. 5 (e) and (f)). It can be seen in Fig. 5 (c) to (f) that Hermia's model indicates that the curve of $f (J)$ versus flux, J was more linear for $n = 1$ compared to $n = 0$, for RCA 30 kDa and RCA 100 kDa membranes, confirming that intermediate pore blocking was the dominant mechanism in both systems, particularly at high fluxes (i.e. initially during the filtration process). It could be that larger pore membranes enabled protein-based foulants to enter the structure more deeply. Transition points were observed for RCA 30 kDa and RCA 100 kDa membranes at J = 25 L m^{-2} h^{-1} and J = 24 L m^{-2} h^{-1} respectively. This suggests that a transition from intermediate pore blocking to cake fouling has occurred in both RCA 30 kDa and RCA 100 kDa membranes. In the intermediate blocking mechanism, some arriving particles are attached to the particles that already deposited on the membrane surface. The cake filtration described the growth of particles on top of the membrane surface due to the

accumulation and agglomeration of particles (Iritani and Katagiri 2016). Hermia's blocking model demonstrates the difference in fouling mechanism for all three membranes based on flux data. This may suggest that the membranes fouled by protein-based compounds change their selectivity. Fouled membranes also become rougher (Table 8) and more hydrophilic (Table 7).

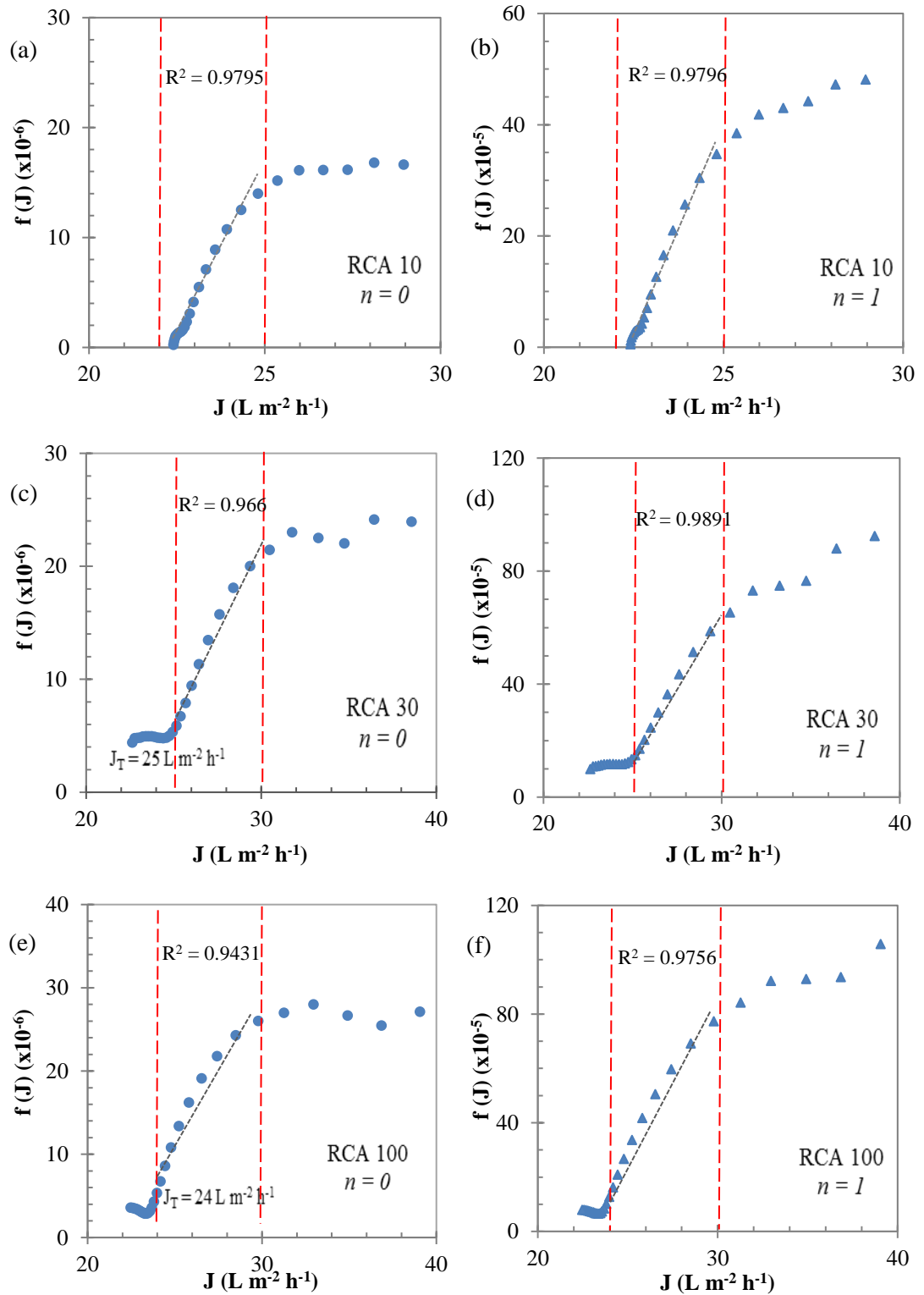**Fig. 5** Hermia's blocking model applied to the data obtained from the ultrafiltration of orange juice using different MWCO membranes (a) and (b) RCA 10 kDa, (c) and (d) RCA 30 kDa and (e) and (f) RCA 100 kDa. Data shows $f(J)$ as described by Eq. (7) where $n = 0$ for (a), (c), (e) and $n = 1$ for (b), (d), (f). The linear trendline is shown in grey line. Red lines indicate the linear region.

Table 6 presents a mass balance for the ultrafiltration of total phytosterols and protein using three different RCA membranes. The initial volume of the orange juice for the ultrafiltration was 3000 ml. The total phytosterols present in feed solution were 780 ± 30 mg. The yields of total phytosterols in the permeate streams for RCA 10, 30 and 100 kDa were 135 mg, 34 mg and 65 mg respectively. It can be seen in Table 6 that the mass concentration ratio of sterol to protein reduced from 0.27 in the feed to 0.16 in the permeate for the ultrafiltration using RCA 30 kDa. The mass concentration ratio of sterol to protein changed from 0.27 in the feed to 0.31 in the permeate for the RCA 100 kDa membrane. The permeate from the RCA 10 kDa membrane showed the highest ratio of sterols to protein than the feed. The ratio of the mass of phytosterols to protein for the RCA 10 membrane in the feed was 0.27 and in the permeate was 5.0. This result as it represented an increased in the ratio of sterol to protein of 18.5 when the permeate was compared to the feed. The 21% loss of phytosterols in the system for RCA 10 membrane, 50% loss for RCA 30 and 28% loss for RCA 100 membranes were most probably due to the fouling effect during the filtration (Cassano et al. 2008). The higher rejections seen in Table 6 for RCA 30 and RCA 100 membranes are linked to a greater loss of phytosterols into the foulants. This may suggest that the sterols were trapped by the fouling layer and not passed through the membrane, and also incorporated into the fouling.

In addition, protein in the feed solution was *ca.* 2850 ± 60 mg. The fraction of the original feed proteins still presents in the retentate after filtration for the RCA 10, 30 and 100 kDa membranes were 83%, 68% and 71% respectively. The 16%, 24% and 21% losses of the feed proteins for RCA 10, 30 and 100 membranes respectively were presumably due to the solute-membrane interaction and consequent adsorption of solute inside the membrane pores or on the membrane surface (Cassano et al. 2008). It can be noted that the highest recovery of phytosterols in the permeate was achieved by using RCA 10 membrane (43 ± 2 mg/L). Even though the sterols concentration in the permeate of RCA 10 kDa was lower than in the feed, the permeate stream was relatively high in sterols and low in protein. This important result demonstrates that protein can be removed from the sterols stream by using RCA 10 membrane. This theory is also supported by the rejection data.

Table 6 Mass balance for total phytosterols and protein by UF process of orange juice with different membranes; (a) RCA 10, (b) RCA 30 and (c) RCA 100.

(a) RCA 10	Feed	Retentate		Permeate		Total (%)
Volume (ml)	3000	2150	72%	850	28%	100
Phytosterols (mg)	810	504	62%	135	17%	79
Protein (mg)	2910	2408	83%	26	1%	84
Mass concentration ratio (sterols to protein)	0.27			5.00		

(b) RCA 30	Feed	Retentate		Permeate		Total (%)
Volume (ml)	3000	2200	73%	800	27%	100
Phytosterols (mg)	773	359	46%	34	4%	50
Protein (mg)	2880	1958	68%	216	8%	76
Mass concentration ratio (sterols to protein)	0.27			0.16		

(c) RCA 100	Feed	Retentate		Permeate		Total (%)
Volume (ml)	3000	2240	75%	760	25%	100
Phytosterols (mg)	747	467	63%	65	9%	72
Protein (mg)	2790	1971	71%	213	8%	79
Mass concentration ratio (sterols to protein)	0.27			0.31		

Contact Angle Measurements

Membrane hydrophobicity was characterised by using contact angle data. All membranes tested were considered to be highly hydrophilic, as the contact angles measured were much less than 90° (Table 7). The contact angles of conditioned RCA 10, RCA 30 and RCA 100 membranes were 11 ± 2°, 13 ± 2° and 18 ± 2° respectively. The hydrophobicity of conditioned and fouled RCA membranes varied with MWCO such that RCA100 > RCA30 > RCA10. The hydrophobicity of conditioned RCA membranes were in agreement with findings by other researchers (Amy 2001; Nguyen et al. 2015; A. Mohammad et al. 2011). Membranes with more hydrophobic surface had higher fouling capacity than the ones with hydrophilic surface (Gulec et al. 2017). Table 7 also shows the contact angles of fouled membranes. All fouled membranes displayed contact angle of 10 ± 2°. It can be seen that the membranes became more hydrophilic after fouling. The contact angle measurements of fouled membranes showed the modification of membranes hydrophobicity due to protein-based foulants or other hydrophilic sub micelles (Wu and Bird 2007; Argyle et al. 2015). This data supported the flux declining results, the membrane has been fouled during the filtration and it was modified after fouling. Cleaned membrane surfaces had contact angles between that of conditioned and fouled surfaces, implying that the membranes were not returned to their original state. However, within statistical error, no difference was detected between the contact angles of the conditioned and the cleaned membranes.

Table 7   Contact angles of water drops on RCA membranes.

Membrane	Contact Angle (°)			
	Conditioned		Fouled	Cleaned
RCA 10 kDa	11 ± 2	5[a], 10.2[b]	10 ± 2	8 ± 2
RCA 30 kDa	13 ± 2	12[c]	10 ± 2	12 ± 2
RCA 100 kDa	18 ± 2	18[a]	10 ± 2	15 ± 2

[a]From Amy (Amy 2001)

[b]From Nguyen (Nguyen et al. 2015)

[c]From Mohammad (A. Mohammad et al. 2011)

Surface Roughness by AFM

Atomic force microscopy (AFM) is an effective tool for the study of surface morphology and texture, including roughness, waviness, lay and flaws (Kumar and Subba Rao 2012). In this study, the surface roughness of the RCA membranes has been investigated using AFM. The roughness of RCA membranes varied with MWCO such that RCA30 > RCA100 > RCA10 (Table 8). This result is in agreement with the flux analysis, FTIR spectra and membrane surfaces analysis by SEM. The roughness value for the virgin conditioned RCA 10 membrane was similar to that reported in the literature (Evans et al. 2008). After fouling, all membranes displayed increased roughness values, indicating that relatively rough surface deposits were present (Jones et al. 2011). Membranes with rougher surfaces displayed a higher fouling capacity than those with smoother surfaces (Gulec et al. 2017). The foulant appears to be more highly entrapped by rougher surfaces. The surface roughness values reduced after cleaning but did not return to the initial roughness values. This may suggest that the surfaces have not been returned to a pristine condition.

Table 8   Surface roughness values as measured by AFM.

Membrane	Surface Roughness (nm)		
	Conditioned	Fouled	Cleaned
RCA 10 kDa	3 ± 1	31 ± 2	10 ± 2
RCA 30 kDa	17 ± 1	42 ± 3	20 ± 2
RCA 100 kDa	10 ± 2	39 ± 2	15 ± 1

Spectral Chemistry Determination Using FTIR

FTIR analyses allowed the identification of the functional groups present on polymeric membranes. The intensity of IR absorption bands was used qualitatively to identify changes in the composition of material present on membrane surfaces due to fouling and cleaning processes (Wu and Bird 2007). The FTIR spectra in the range of $4000 - 650$ cm^{-1} were used to analyse the membrane surfaces at different conditions. Figure 6 displays the overlay results of FTIR spectra of fouled membranes for all RCA membranes. It was observed that all samples showed identical FTIR spectra with slightly shifted absorption bands. The intensity of RCA membrane deposits

varied with MWCO such that RCA30 > RCA100 > RCA10. This also corresponds to the order of the increased surface roughness and pure water fluxes declining results. The higher intensity recorded demonstrated that more foulant was deposited on the membrane surface. Rougher membranes would potentially trap more foulants on the membrane surfaces (Evans et al. 2008). This demonstrated that more foulant was deposited on the RCA 30 kDa membrane. This result correlates well with the surface roughness and SEM analyses. The fouled membranes might be due to protein-based foulants or other hydrophilic sub micelles (Wu and Bird 2007; Argyle et al. 2015). The area $1400 - 1800$ cm^{-1} was studied for the presence of protein foulant on the membrane surface. The protein peaks can be identified in this area with two peaks called amide I peak at 1540 cm^{-1} and amide II peak near 1650 cm^{-1}. Amide I peak at 1540 cm^{-1} corresponds to C=O groups stretching vibration. Meanwhile amide II due to the combination of –NH deformation and C-N stretching vibration (Metsamuuronen 2003). The amide peaks in the spectra of RCA 10 membrane are much lower than those presented in RCA 30 and RCA 100 membranes. C-H stretching vibration peaks at 2850 and 2900 cm^{-1} that were observed in RCA 10 kDa membrane are characteristic for polypropylene as it was used as the support layer.
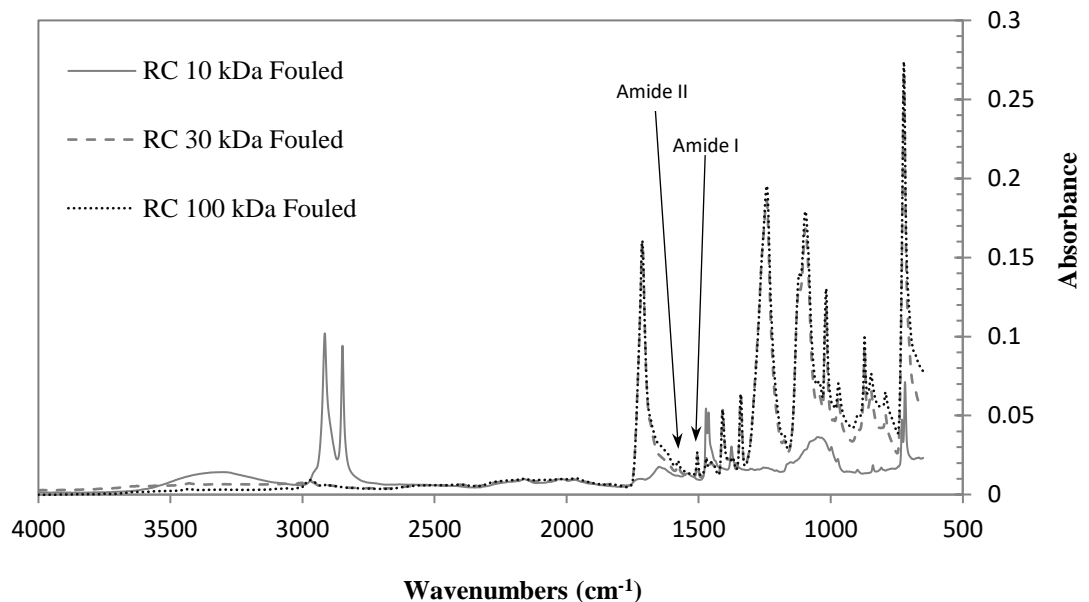

Fig. 6 Infrared spectra of protein foulants (which represented by Amide I and Amide II) deposited on the different membranes tested.

Membrane Morphology by SEM

The morphology of the membranes was examined via scanning electron microscopy (SEM). SEM was used to visualise the differences of membranes before and after fouling and subsequent cleaning. Membrane surface images of RCA membranes tested are presented in Figure 7. The surface structures of conditioned membranes in Fig. 7 (a, d, g) were changed from a rather smooth surface to a rough surface on fouled membranes in Fig. 7 (b, e, h). Fouling is clearly seen on the fouled membrane surfaces which are agreement with the contact angle, surface roughness and flux results. The inspection on cleaned membrane surfaces in Fig. 7 (c, f, i) show that the cleaning method used is effective in removing the foulants. The presence of crystalline structures on fouled membrane surfaces was further evaluated by energy dispersive X-ray (EDX) analysis. The difference in surface morphology for the membrane is a function of the membrane formation process, which is related to the composition of the formulation. Although all membrane active layers were comprised of regenerated cellulose acetate, the RCA 30 kDa membrane contains one amphiphilic polymer. A particular pattern was formed on top of the membrane surface due to self-assembly of this polymer. This created distinctive membrane surface properties (Guo 2018).
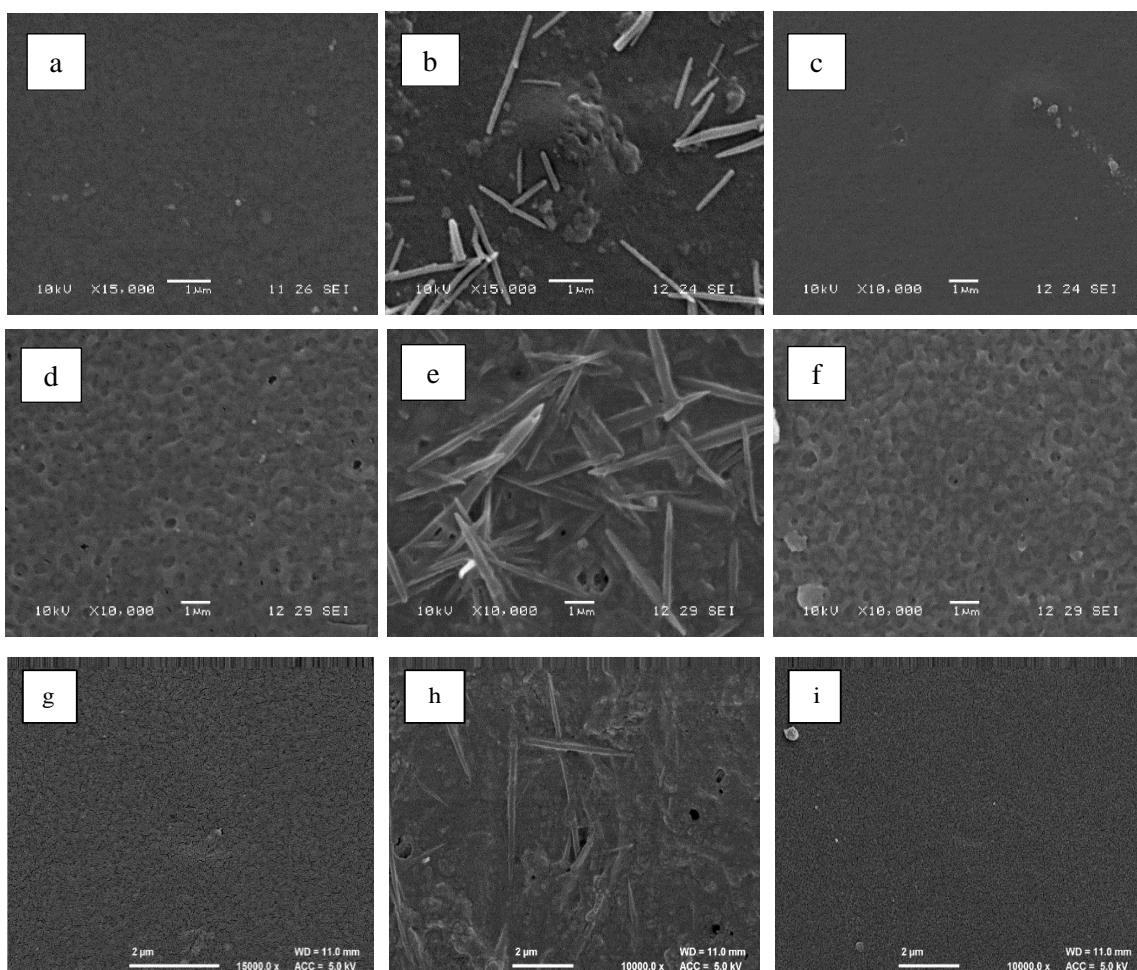
Fig. 7 Scanning electron microscope (SEM) images of RCA membranes taken at 10,000 or 15,000 x magnification (a) RCA 10 kDa conditioned, (b) RCA 10 kDa fouled, (c) RCA 10 kDa cleaned, (d) RCA 30 kDa conditioned, (e) RCA 30 kDa fouled, (f) RCA 30 kDa cleaned, (g) RCA 100 kDa conditioned, (h) RCA 100 kDa fouled and (i) RCA 100 kDa cleaned.

Studies on the membrane polymer composition have been carried out by using gel permeation chromatography (GPC) to determine polymer molecular weight distribution (Engel et al. 2012). Figure 8 shows the chromatogram of GPC analyses for RCA 10 kDa membrane. All samples were dissolved in THF for 24 hours in order to remove the coating layer of the polymeric membranes. It can be seen in Fig. 8, there was a peak found indicating the presence of oligomers in RCA 10 as highlighted in the chromatogram. However, there was no peak detected for either the RCA 30 or the RCA 100 membranes. This may suggest that the polymer coatings

were not dissolved in THF for either of the samples tested. Further investigation on the RCA 10 membrane was performed using Matrix-Assisted Laser Desorption Ionisation (MALDI). Based on the chromatogram in Figure 9, the mass region of ion peaks was observed with a peak-to-peak mass difference of *ca.* 300 gmol^{-1}. Thus, it can be concluded that RCA 10 contains polymer repeating units at a molar mass of *ca.*300 gmol^{-1}. It can also be concluded that the polymer compositions of RCA 30 and 100 are different to those present for the RCA 10 membrane.
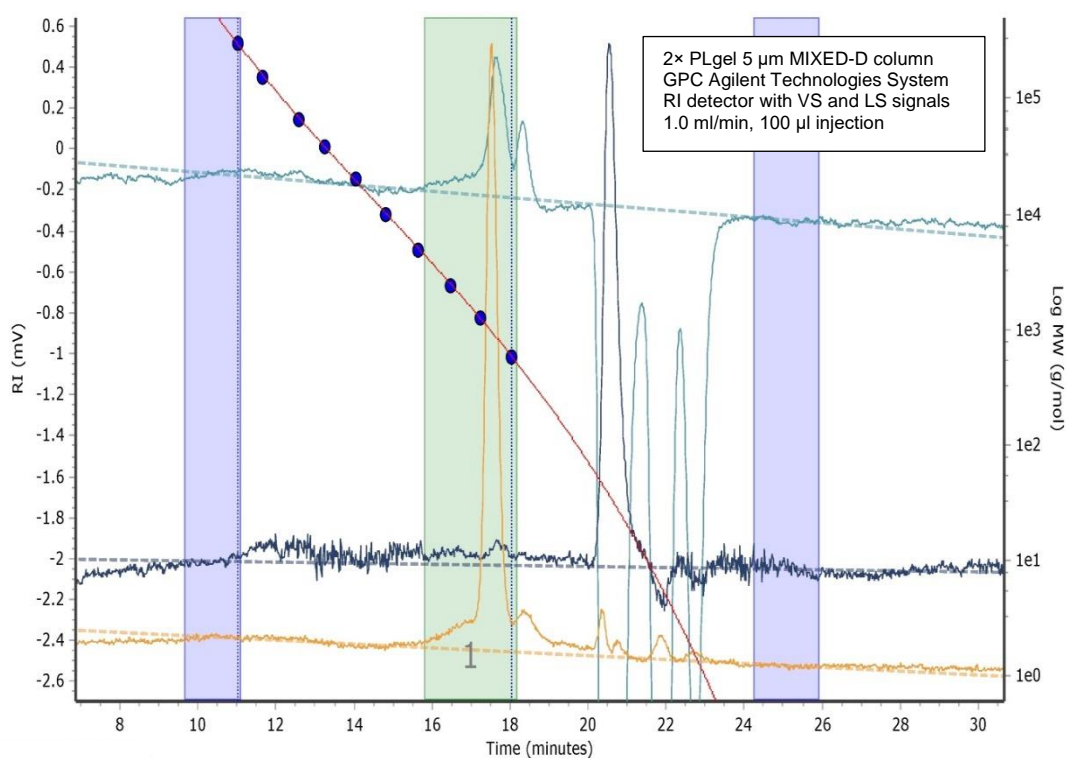

Fig. 8 The chromatogram shows the GPC analysis of RCA 10 kDa membrane. In the chromatogram, the refractive index (RI) detector signal is shown in light blue, the viscometer (VS) signal is shown in dark blue and the light scattering (LS) signal is shown in yellow. A calibration curve is shown in red line with blue dots. Blue columns indicate the beginning and end of the baseline. Peaks indicating the presence of oligomers in RCA 10 were highlighted in region 1 at ~17.5 min.
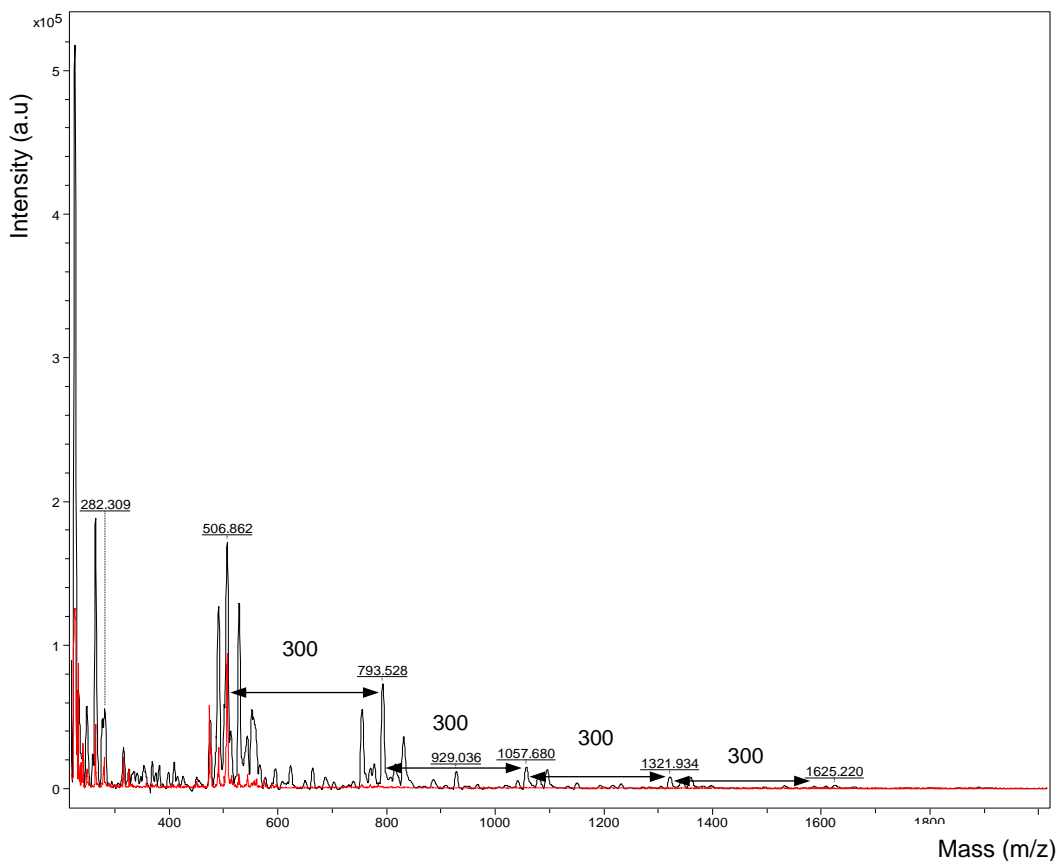
Fig. 9 MALDI mass spectra of RCA 10 kDa membrane analysed in positive ion mode by using dithranol and dihydroxybenzoic acid as matrices. The mass difference of *ca.* 300 gmol^{-1} between neighbouring peaks is observed. The chromatogram shows polymer repeating units at a molar mass of *ca.* 300 gmol^{-1} between *m*/*z* 400 and 1700.

Elemental Analysis by EDX

The elemental examinations were carried out by energy dispersive X-ray (EDX) analysis that coupled with the SEM, to investigate the elemental composition on the membrane surfaces. As displayed in Figure 10, RCA membrane consists of carbon (C) and oxygen (O) elements. These results are not surprising, given that the membranes were fabricated from cellulose (Li et al. 2014). It can be seen that the element present in conditioned membranes were similar to the elements in cleaned membranes. This result correlates well with the FTIR and SEM analyses that suggest the membranes were regenerated effectively after the cleaning protocol was applied. Aluminium (Al) was found on certain membrane samples due to the aluminium stub

used in the analysis. The EDX analyses for fouled membranes were focused on the crystalline structures. The fouled membranes were coated with gold prior to the EDX analysis at higher magnification. The crystalline structures could not be observed at low magnification. Therefore, gold (Au) was also observed on the fouled membranes.

The result in Fig. 10 confirming that potassium (K) elements exist on the membrane surfaces after fouling. According to the literature (Navarro et al. 2011; Schmutzer et al. 2016), potassium is present in orange juice in relatively high concentrations. Potassium in orange juice is commonly associated with citrate (Odvina 2006). Thus, it can be concluded that the crystalline structure on fouled membranes might be potassium salt which is potassium citrate. The potassium citrate was relatively hydrophilic which an analysis is in agreement with findings in contact angle and FTIR, which foulants might be due to hydrophilic sub micelles (Argyle et al. 2015). In addition, the absorption band corresponding to potassium citrate was observed at 1650 cm^{-1} (stretching symmetric and asymmetric vibrations of COO groups) (Naidenko et al. 2012). However, this band was overlapping with the protein absorption band.
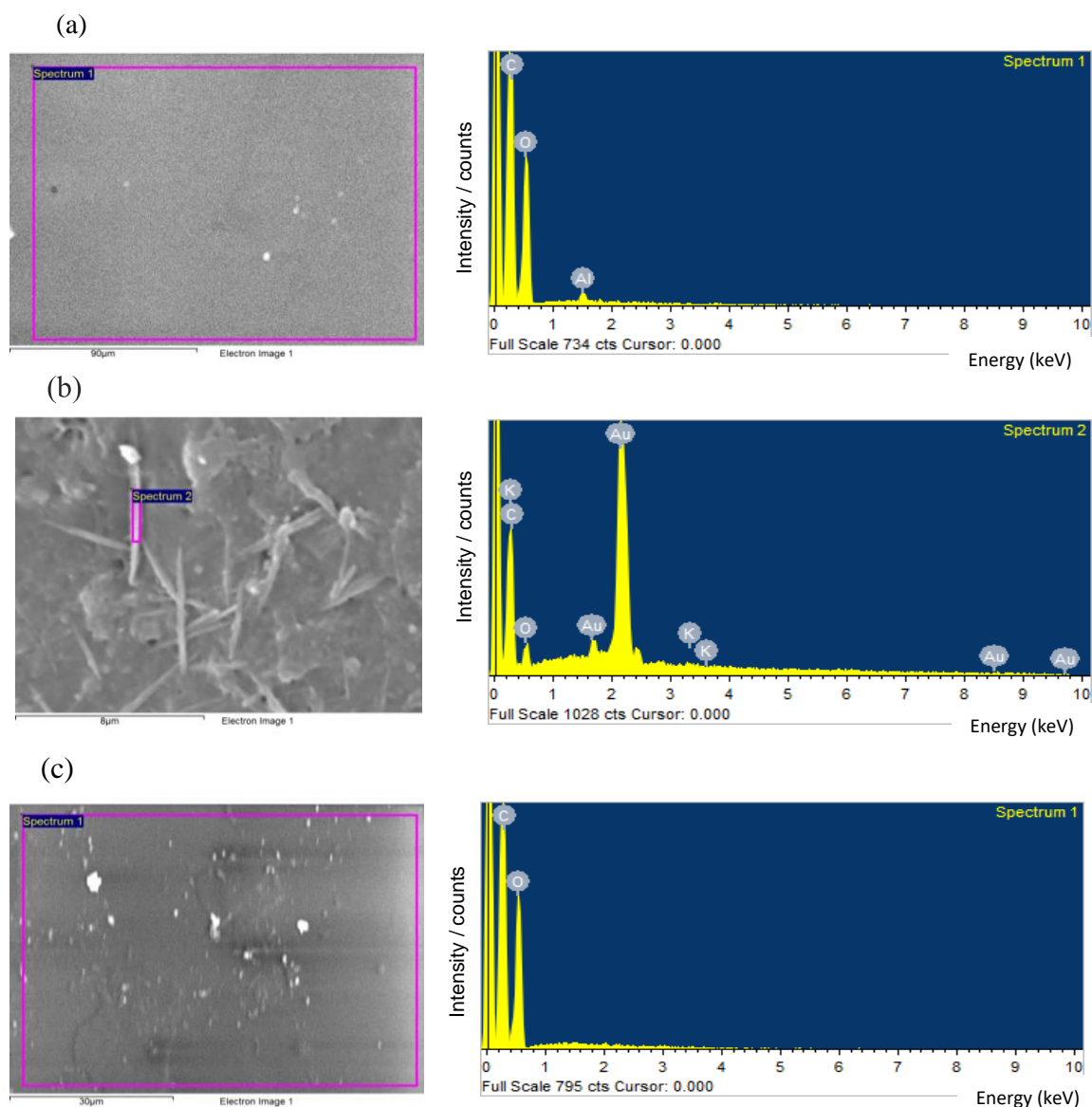
(a)

(b)

(c)

Fig. 10 SEM images with EDX analysis. SEM-EDX analysis was performed on RCA 10 kDa membrane surfaces at (a) conditioned, (b) fouled, and (c) cleaned membranes. The EDX spectra are dominated by carbon (C) and oxygen (O) elements. Aluminium (Al) was found on the conditioned membrane (a). The fouled membrane (b) shows the presence of gold (Au) element.

Conclusions

The effectiveness of regenerated cellulose acetate (RCA) based ultrafiltration membranes as a technology for isolating phytosterol from orange juice has been established. The isolation of phytosterols from orange juice has been studied by

using RCA membranes with 10 kDa, 30 kDa and 100 kDa MWCO. From the permeate flux analysis, product fluxes declined gradually to similar steady-state values. This indicates that the PWF was a poor indicator of product flux in this system, as fouling is key. Fouling layers change the membrane selectivity. All membranes exhibited steady-state permeate flux values of 22 L m^{-2} h^{-1}. Counter-intuitively, the smallest MWCO membrane tested (10 kDa RCA) gave the lowest rejection of phytosterols, and hence the best performance. The RCA 10 membranes also gave the highest rejection of proteins, at 96% - a desirable result. However, fouling led to a reduction in the total amount of phytosterol presented in the system, leading to a reduction in the concentration of sterols in both the retentate and the permeate, when compared to the feed. The mass concentration ratio of sterol to protein changed from 0.27 in the feed to 5.0 in the permeate for the ultrafiltration using RCA 10 kDa.

Reversible fouling was found to play an important role in the flux decline. However, irreversible fouling for RCA 30 and RCA 100 membranes was higher than that seen for the RCA 10 membrane. It is postulated that proteins were trapped in the RCA 30 and RCA 100 membrane pores - this is supported by the Hermia flux decline analysis. It is possible that membranes with bigger pores trapped more protein-based foulants, or other hydrophilic compounds such as potassium citrate, than the small MWCO membrane. This leads to a change in membrane selectivity and an increased rejection of the smaller phytosterol molecules. Membranes after fouling and cleaning were found to have undergone surface modification including changes in hydrophobicity and roughness. The surface roughness and pure water flux decline of RCA membranes varied with MWCO, such that RCA 30 > RCA 100 > RCA 10. The RCA 10 membranes displayed the greatest hydrophilicity and the smoothest surface of the three membranes examined. Moreover, the fouling deposits presented on the RCA 10 membrane were the smoothest of the three fouled membranes tested. These results confirmed that hydrophobicity and roughness were more important than molecular weight cut off in determining the performance of UF membranes for the fractionation of sterols from proteins in orange juice filtration.

This result has important implications for the industrial application of this technology to process orange juice, and possibly other sterol-rich feeds. Based on this study, for 15 m^2 RCA membrane with 2 years shelf life, the ultrafiltration using *M10* filtration system costs are estimated to be £23,500. Assuming that the total

volume of orange juice filtered in 2 years is 21 tonnes, the profit is estimated to be £5,000 after 2 years. Therefore, this paper presents some evidence which suggests that with this operating procedure, phytosterols and proteins can be separated from orange juice with the possibility of scaling up the process. Since the yield of phytosterols compounds separated by 10 kDa RCA membrane was relatively low, there is the potential for process optimisation. Thus, the ultrafiltration will be carried out at different process temperatures. In future studies, the loss of sterols to the foulant layers will be addressed by increasing the total volume of feed filtered, whilst maintaining the membrane area at the same value, thereby increasing the total amount of sterol present in the system. Diafiltration may also be applied in concentrating the targeted compounds.

Acknowledgements

Conflict of Interest

The authors declare that they have no conflicts of interest.

References

Abd-Razak, N. H., Chew, Y. M. J., & Bird, M. R. (2019). Membrane fouling during the fractionation of phytosterols isolated from orange juice. *Food and Bioproducts Processing, 113*, 10-21, doi:https://doi.org/10.1016/j.fbp.2018.09.005.

Alfa-Laval (2017). Alfa Laval - UF flat sheet membrane. https://www.alfalaval.co.uk/products/separation/membranes/flat-sheet-membranes/uf-flat-sheet/. Accessed 11 July 2019.

Amy, G. L. (2001). NOM Rejection By, and Fouling Of, NF and UF Membranes. American Water Works Association.

Argyle, I. S., Pihlajamäki, A., & Bird, M. R. (2015). Black tea liquor ultrafiltration: Effect of ethanol pre-treatment upon fouling and cleaning characteristics. *Food and Bioproducts Processing, 93*(Supplement C), 289-297, doi:https://doi.org/10.1016/j.fbp.2014.10.010.

Baek, Y., Kang, J., Theato, P., & Yoon, J. (2012). Measuring hydrophilicity of RO membranes by contact angles via sessile drop and captive bubble method: A comparative study. *Desalination, 303*, 23-28, doi:https://doi.org/10.1016/j.desal.2012.07.006.

Balme, S., & Gulacar, F. O. (2012). Rapid screening of phytosterols in orange juice by solid-phase microextraction on polyacrylate fibre derivatisation and gas chromatographic-mass spectrometric. *Food Chem, 132*(1), 613-618, doi:10.1016/j.foodchem.2011.10.097.

Bradford, M. M. (1976). A rapid and sensitive method for the quantitation of microgram quantities of protein utilizing the principle of protein-dye binding. *Analytical Biochemistry, 72*(1), 248-254, doi:https://doi.org/10.1016/0003-2697(76)90527-3.

Cassano, A., Donato, L., Conidi, C., & Drioli, E. (2008). Recovery of bioactive compounds in kiwifruit juice by ultrafiltration. *Innovative Food Science & Emerging Technologies, 9*(4), 556-562, doi:https://doi.org/10.1016/j.ifset.2008.03.004.

Cobell (2016). Orange Juice Not From Concentrate (NFC). Exeter, United Kingdom: Cobell.

Conidi, C., Cassano, A., Caiazzo, F., & Drioli, E. (2017). Separation and purification of phenolic compounds from pomegranate juice by ultrafiltration and nanofiltration membranes. *Journal of Food Engineering, 195*, 1-13, doi:http://dx.doi.org/10.1016/j.jfoodeng.2016.09.017.

Corredig, M., Kerr, W., & Wicker, L. (2001). Particle size distribution of orange juice cloud after addition of sensitized pectin. *J Agric Food Chem, 49*(5), 2523-2526.

De Oliveira, R. R. L., Albuquerque, D. A. C., Cruz, T. G. S., Yamaji, F. M., & Leite, F. L. (2012). Measurement of the Nanoscale Roughness by Atomic Force Microscopy: Basic Principles and Applications, Atomic Force Microscopy - Imaging, Measuring and Manipulating Surfaces at the Atomic Scale, Victor Bellitto, IntechOpen.

Engel, P., Hein, L., & Spiess, A. C. (2012). Derivatization-free gel permeation chromatography elucidates enzymatic cellulose hydrolysis. *Biotechnology for biofuels, 5*(1), 77-77, doi:10.1186/1754-6834-5-77.

Evans, P. J., Bird, M. R., Pihlajamäki, A., & Nyström, M. (2008). The influence of hydrophobicity, roughness and charge upon ultrafiltration membranes for black tea liquor clarification. *Journal of Membrane Science, 313*(1), 250-262, doi:https://doi.org/10.1016/j.memsci.2008.01.010.

Field, R. W., Wu, D., Howell, J. A., & Gupta, B. B. (1995). Critical flux concept for microfiltration fouling. *Journal of Membrane Science, 100*(3), 259-272, doi:https://doi.org/10.1016/0376-7388(94)00265-Z.

Gulec, H. A., Bagci, P. O., & Bagci, U. (2017). Clarification of Apple Juice Using Polymeric Ultrafiltration Membranes: a Comparative Evaluation of Membrane Fouling and Juice Quality. *Food and Bioprocess Technology, 10*(5), 875-885, doi:10.1007/s11947-017-1871-x.

Guo, H. (2018). Personal Correspondance. Denmark: Alfa Laval.

Han, J., Fu, J., & Schoch, R. B. (2008). Molecular sieving using nanofilters: past, present and future. *Lab on a chip, 8*(1), 23-33, doi:10.1039/b714128a.

Hermia, J. (1982). Constant pressure blocking filtration laws–application to power law non-Newtonian fluids. *Trans IChemE, 60*, 183-187.

Ilame, S. A., & V. Singh, S. (2015). Application of Membrane Separation in Fruit and Vegetable Juice Processing: A Review. *Critical Reviews in Food Science and Nutrition, 55*(7), 964-987, doi:10.1080/10408398.2012.679979.

Iqbal, E., Salim, K. A., & Lim, L. B. L. (2015). Phytochemical screening, total phenolics and antioxidant activities of bark and leaf extracts of Goniothalamus velutinus (Airy Shaw) from Brunei Darussalam. *Journal of King Saud University - Science, 27*(3), 224-232, doi:http://dx.doi.org/10.1016/j.jksus.2015.02.003.

Iritani, E., & Katagiri, N. (2016). Developments of Blocking Filtration Model in Membrane Filtration. *KONA Powder and Particle Journal, 33*, 179-202, doi:10.14356/kona.2016024.

Jesus, D. F., Leite, M. F., Silva, L. F. M., Modesta, R. D., Matta, V. M., & Cabral, L. M. C. (2007). Orange (Citrus sinensis) juice concentration by reverse osmosis. *Journal of Food Engineering, 81*(2), 287-291, doi:http://dx.doi.org/10.1016/j.jfoodeng.2006.06.014.

Jiménez-Escrig, A., Santos-Hidalgo, A. B., & Saura-Calixto, F. (2006). Common Sources and Estimated Intake of Plant Sterols in the Spanish Diet. *Journal of Agricultural and Food Chemistry, 54*(9), 3462-3471, doi:10.1021/jf053188k.

Jiraratananon, R., & Chanachai, A. (1996). A study of fouling in the ultrafiltration of passion fruit juice. *Journal of Membrane Science, 111*(1), 39-48, doi:https://doi.org/10.1016/0376-7388(95)00270-7.

Jones, S. A., Bird, M. R., & Pihlajamäki, A. (2011). An experimental investigation into the pre-treatment of synthetic membranes using sodium hydroxide solutions. *Journal of Food Engineering, 105*(1), 128-137, doi:https://doi.org/10.1016/j.jfoodeng.2011.02.015.

Kongduang, D., Wungsintaweekul, J., & De-Eknamkul, W. (2012). Established GC-FID for simultaneous determination of diterpenes and phytosterols in Plaunoi (Croton stellatopilosus Ohba). *Songklanakarin J. Sci. Technol., 34*, 623-628.

Kruger, N. J. (1994). The Bradford method for protein quantitation. *Methods Mol Biol, 32*, 9-15, doi:10.1385/0-89603-268-x:9.

Kumar, B., & Subba Rao, T. (2012). AFM studies on surface morphology, topography and texture of nanostructured zinc aluminum oxide thin films. *Digest Journal of Nanomaterials and Biostructures, 7*, 1881-1889.

Lewis, W. J. T., Mattsson, T., Chew, Y. M. J., & Bird, M. R. (2017). Investigation of cake fouling and pore blocking phenomena using fluid dynamic gauging and critical flux models. *Journal of Membrane Science, 533*, 38-47, doi:http://dx.doi.org/10.1016/j.memsci.2017.03.020.

Li, R., Liu, L., & Yang, F. (2014). Removal of aqueous Hg(II) and Cr(VI) using phytic acid doped polyaniline/cellulose acetate composite membrane. *Journal of Hazardous Materials, 280*, 20-30, doi:https://doi.org/10.1016/j.jhazmat.2014.07.052.

Marangoni, F., & Poli, A. (2010). Phytosterols and cardiovascular health. *Pharmacological Research, 61*(3), 193-199, doi:https://doi.org/10.1016/j.phrs.2010.01.001.

Market-Insights-Reports (2019). Global Phytosterols Market Insights, Forecast To 2025. https://www.marketinsightsreports.com/reports/02011075734/global-phytosterols-market-insights-forecast-to-2025?source=nevadagreentimes&Mode=19. Accessed 16 April 2019 2019.

Mbaebie, B. O., Edeoga, H. O., & Afolayan, A. J. (2012). Phytochemical analysis and antioxidants activities of aqueous stem bark extract of Schotia latifolia Jacq. *Asian Pacific Journal of Tropical Biomedicine, 2*(2), 118-124, doi:10.1016/S2221-1691(11)60204-9.

McDonald, J. G., Smith, D. D., Stiles, A. R., & Russell, D. W. (2012). A comprehensive method for extraction and quantitative analysis of sterols and secosteroids from human plasma. *J Lipid Res, 53*(7), 1399-1409, doi:10.1194/jlr.D022285.

Metsamuuronen, S. (2003). *Critical flux and fouling in ultrafiltration of proteins*. Lappeenrannan: Lappeenrannan : Lappeenrannan teknillinen yliopisto.

Mohammad, A., Hilal, N., Ying Pei, L., Nurul Hasyimah Mohd Amin, I., & Raslan, R. (2011). Atomic Force Microscopy as a Tool for Asymmetric Polymeric Membrane Characterization. *Sains Malaysiana, 40*(3), 237-244.

Mohammad, A. W., Ng, C. Y., Lim, Y. P., & Ng, G. H. (2012). Ultrafiltration in Food Processing Industry: Review on Application, Membrane Fouling, and Fouling Control. *Food and Bioprocess Technology, 5*(4), 1143-1156, doi:10.1007/s11947-012-0806-9.

Mulder, M. (1996). *Basic Principles of Membrane Technology* (Second ed.). The Netherlands: Kluwer Academic Publishers.

Naidenko, E. S., Yukhin, Y. M., Afonina, L. I., & Gerasimov, K. B. (2012). Obtaining Bismuth-Potassium Citrate. *Chemistry for Sustainable Development, 20*, 523-528.

Navarro, P., Perez-Lopez, A. J., Mercader, M. T., Carbonell-Barrachina, A. A., & Gabaldon, J. A. (2011). Antioxidant activity, color, carotenoids composition, minerals, vitamin C and sensory quality of organic and conventional mandarin juice cv. Orogrande. *Food science and technology international, 17*(3), 241-248, doi:10.1177/1082013210382334.

Nguyen, L. A. T., Schwarze, M., & Schomäcker, R. (2015). Adsorption of non-ionic surfactant from aqueous solution onto various ultrafiltration membranes. *Journal of Membrane Science, 493*(Supplement C), 120-133, doi:https://doi.org/10.1016/j.memsci.2015.06.026.

Nyam, K. L., Tan, C. P., Lai, O. M., Long, K., & Che Man, Y. B. (2011). Optimization of supercritical CO_2 extraction of phytosterol-enriched oil from Kalahari melon seeds. *Food and Bioprocess Technology, 4*(8), 1432-1441, doi:10.1007/s11947-009-0253-4.

Odvina, C. V. (2006). Comparative Value of Orange Juice versus Lemonade in Reducing Stone-Forming Risk. *Clinical Journal of the American Society of Nephrology, 1*(6), 1269, doi:10.2215/CJN.00800306.

Okino Delgado, C. H., & Fleuri, L. F. (2016). Orange and mango by-products: Agro-industrial waste as source of bioactive compounds and botanical versus commercial description—A review. *Food Reviews International, 32*(1), 1-14, doi:10.1080/87559129.2015.1041183.

Pap, N., Mahosenaho, M., Pongrácz, E., Mikkonen, H., Jaakkola, M., Virtanen, V., et al. (2012). Effect of Ultrafiltration on Anthocyanin and Flavonol Content of Black Currant Juice (Ribes nigrum L.). *Food and Bioprocess Technology, 5*(3), 921-928, doi:10.1007/s11947-010-0371-z.

Pihlajamäki, A., Väisänen, P., & Nyström, M. (1998). Characterization of clean and fouled polymeric ultrafiltration membranes by Fourier transform IR spectroscopy–attenuated total reflection. *Colloids and surfaces. A, Physicochemical and engineering aspects, 138*(2), 323-333, doi:10.1016/S0927-7757(96)03883-6.

Piironen, V., Toivo, J., Puupponen-Pimiä, R., & Lampi, A.-M. (2003). Plant sterols in vegetables, fruits and berries. *Journal of the Science of Food and Agriculture, 83*(4), 330-337, doi:10.1002/jsfa.1316.

Sagu, S. T., Karmakar, S., Nso, E. J., Kapseu, C., & De, S. (2014). Ultrafiltration of Banana (Musa acuminata) Juice Using Hollow Fibers for Enhanced Shelf Life. *Food and Bioprocess Technology, 7*(9), 2711-2722, doi:10.1007/s11947-014-1309-7.

Sass-Kiss, A., & Sass, M. (2000). Immunoanalytical method for quality control of orange juice products. *J Agric Food Chem, 48*(9), 4027-4031.

Sathishkumar, T., & Baskar, R. (2014). Screening and quantification of phytochemicals in the leaves and flowers in the leaves and flowers of Tabernaemontana heyneana Wall. *Indian Journal of natural Products and Resources, 5*(3), 237-243.

Schmutzer, G. R., Dehelean, A., Magdas, D. A., Cristea, G., & Voica, C. (2016). Determination of Stable Isotopes, Minerals, and Volatile Organic Compounds in Romanian Orange Juice. *Analytical Letters, 49*(16), 2644-2658, doi:10.1080/00032719.2015.1130713.

Shahzad, N., Khan, W., Md, S., Ali, A., Saluja, S. S., Sharma, S., et al. (2017). Phytosterols as a natural anticancer agent: Current status and future perspective. *Biomedicine & Pharmacotherapy, 88*(Supplement C), 786-794, doi:https://doi.org/10.1016/j.biopha.2017.01.068.

Stinco, C. M., Fernández-Vázquez, R., Escudero-Gilete, M. L., Heredia, F. J., Meléndez-Martínez, A. J., & Vicario, I. M. (2012). Effect of Orange Juice's Processing on the Color, Particle Size, and Bioaccessibility of Carotenoids. *Journal of Agricultural and Food Chemistry, 60*(6), 1447-1455, doi:10.1021/jf2043949.

Tolve, R., Condelli, N., Can, A., & Tchuenbou-Magaia, F. L. (2018). Development and Characterization of Phytosterol-Enriched Oil Microcapsules for Foodstuff Application. *Food and Bioprocess Technology, 11*(1), 152-163, doi:10.1007/s11947-017-1990-4.

Wang, M., Huang, W., Hu, Y., Zhang, L., Shao, Y., Wang, M., et al. (2018). Phytosterol Profiles of Common Foods and Estimated Natural Intake of Different Structures and Forms in China. *Journal of Agricultural and Food Chemistry, 66*(11), 2669-2676, doi:10.1021/acs.jafc.7b05009.

Weis, A., Bird, M. R., & Nyström, M. (2003). The chemical cleaning of polymeric UF membranes fouled with spent sulphite liquor over multiple operational cycles. *Journal of Membrane Science, 216*(1), 67-79, doi:https://doi.org/10.1016/S0376-7388(03)00047-4.

Weis, A., Bird, M. R., Nyström, M., & Wright, C. (2005). The influence of morphology, hydrophobicity and charge upon the long-term performance of ultrafiltration membranes fouled with spent sulphite liquor. *Desalination, 175*(1), 73-85, doi:https://doi.org/10.1016/j.desal.2004.09.024.

Wu, D., & Bird, M. R. (2007). The Fouling and Cleaning of Ultrafiltration Membranes During The Filtration of Model Tea Component Solutions. *Journal of Food Process Engineering, 30*(3), 293-323, doi:doi:10.1111/j.1745-4530.2007.00115.x.

Yang, M., Huang, F., Liu, C., Zheng, C., Zhou, Q., & Wang, H. (2013). Influence of Microwave Treatment of Rapeseed on Minor Components Content and Oxidative Stability of Oil. *Food and Bioprocess Technology, 6*(11), 3206-3216, doi:10.1007/s11947-012-0987-2.

Yilmaz, E., & Bagci, P. O. (2019). Ultrafiltration of Broccoli Juice Using Polyethersulfone Membrane: Fouling Analysis and Evaluation of the Juice Quality. *Food and Bioprocess Technology, 12*(8), 1273-1283, doi:10.1007/s11947-019-02292-0.

Supplementary Material

Matlab script for RCA 30 kDa

```
%Plot function of flux over flux

t_min = [0:2:60];
t_sec = t_min * 60;

% J in L/m2.h
J_org = [38.59 36.82 30.56 29.48 27.88 27.88 25.65 26.34...
    25.73 25.65 26.11 25.81 25.58 25.04 24.89 24.73...
    24.66 24.58 24.43 24.43 24.12 23.97 23.81 23.66...
    23.28 23.13 22.90 22.74 22.51 22.67 22.51];

J_smth = smooth(J_org,7);
J_smth = smooth(J_smth,7);
J_smth = smooth(J_smth,7);
J_smth = smooth(J_smth,7);
J_smth = smooth(J_smth,7);
J_smth = smooth(J_smth,7);

subplot(2,2,1)
plot(t_sec, J_smth)
title('RCA 30')
xlabel ('t [s]');
ylabel ('J [L m-2 h]');
axis ([0 3600 20 40])

J_man = zeros(1,33);
J_man(1)= J_smth(1) + (J_smth(1) - J_smth(2));
J_man(2:32) = J_smth;
J_man(33) = J_smth(31);
```

```
l = length(J_man);

for n = 0:2
    for i = 2:l-1
    f_J(n+1,i-1) = -((J_man(i+1) - J_man(i-1))/120)*((J_man(i))^(n-2));
    end
end

    subplot(2,2,2)

    plot(J_smth(1:26),f_J(1,1:26),'o')
    hold
    plot([J_smth(26),J_smth(9)],[f_J(1,26),f_J(1,9)],'r')
    title('n=0')
    xlabel ('J [L m-2 h]');
    ylabel ('f(J) [m-1]');
    %axis ([20 40])

    subplot(2,2,3)
    plot(J_smth(1:26),f_J(2,1:26),'o')
    title('n=1')
    xlabel ('J [L m-2 h]');
    ylabel ('f(J) [s-1]');
    %axis ([20 40])

    subplot(2,2,4)
    plot(J_smth(1:26),f_J(3,1:26),'o')
    title('n=2')
    xlabel ('J [L m-2 h]');
    ylabel ('f(J) [m s-2]');
    %axis ([20 40])
```

Chapter 5: The influence of membrane charge and porosity upon the fouling and cleaning during the ultrafiltration of orange juice

Introductory text

The preceding chapter (Chapter 4) presented that fouling and cleaning during the ultrafiltration altered the membrane hydrophobicity and surface roughness. The pure water flux values and membrane surface roughness varied as a function of MWCO such that RCA30 > RCA100 > RCA10. These suggested that hydrophobicity and roughness were more important than molecular weight cut off in determining the performance of UF membranes for the separation of phytosterols from orange juice. Besides the hydrophobicity of the membrane, other important membrane characteristics are membrane surface charge and porosity. The zeta potential via the streaming potential method and Brunauer-Emmett-Teller (BET) analysis were carried out to observe the surface charge and porosity factors that affected the separation properties and membrane fouling tendencies. Both analyses were conducted using apparatus at Lappeenranta University of Technology (LUT), Finland. This chapter explains the changes in the surface charge and porosity of RCA membranes throughout the fouling and cleaning cycles during the filtration. This work was carried out as a continuation in the membrane characterisation study after fouling and cleaning processes. This paper also reported the presence of protein peaks on the fouled membranes via FTIR analysis. This confirmed that protein-based foulants were trapped on the membrane surfaces or in the membrane pores.

Statement of Authorship

This declaration concerns the article entitled:
The influence of membrane charge and porosity upon the fouling and cleaning during the ultrafiltration of orange juice

Publication status (tick one)				
Draft manuscript	**Submitted** ☐	**In review** ☐	**Accepted** ☐	**Published** ☑

Publication details (reference)	Abd-Razak, N.H., Pihlajamäki, A., Virtanen, T., John Chew, Y.M., Bird, M.R., 2021. The influence of membrane charge and porosity upon fouling and cleaning during the ultrafiltration of orange juice. *Food and Bioproducts Processing* 126, 184-194. https://doi.org/10.1016/j.fbp.2021.01.009
Candidate's contribution to the paper (provide details, and also indicate as a percentage)	**Formulation of ideas (70%):** Mike Bird proposed the idea of carrying out surface charge analysis in Lappeenranta University of Technology (LUT), Finland as LUT had expertise in that area. Arto Pihlajamäki suggested the porosity analysis using BET method. I contributed to the microscopy and spectroscopy analysis presented in the paper. **Design of methodology (80%):** I planned the design of experiments for the ultrafiltration and membrane characterisations. Tiina Virtanen designed the BET analysis. **Experimental work (80%):** I prepared the membrane samples, and carried out the surface charge and FTIR spectroscopy analysis. Tiina Virtanen performed the porosity analysis in LUT Finland. I carried out the data interpretation after discussions with my co-authors. **Presentation of data in journal format (80%):** I prepared the manuscript for the journal including the outlines, graphics in the journal format and incorporated feedback from co-authors. The co-authors contributed in revising individual sections by providing feedback which improved the overall quality of the paper.
Statement from Candidate	This paper reports on original research I conducted during the period of my Higher Degree by Research candidature.
Signed ███	**Date** 25 Feb 2021

The influence of membrane charge and porosity upon the fouling and cleaning during the ultrafiltration of orange juice

Nurul Hainiza Abd-Razak[a,c], Arto Pihlajamäki[b], Tiina Virtanen[b], Y.M. John Chew[a], Michael R. Bird[a*]

[a]Centre of Advanced Separations Engineering, Department of Chemical Engineering, University of Bath, Bath BA2 7AY, UK
[b]LUT School of Engineering Science, LUT University, P.O. Box 20, 53851 Lappeenranta, Finland
[c]Rubber Research Institute of Malaysia, Malaysian Rubber Board, P.O. Box 10150, 50908 Kuala Lumpur, Malaysia

Abstract

The ultrafiltration of orange juice has been performed to separate phytosterols from proteins. Commercial regenerated cellulose acetate (RCA) ultrafiltration membranes of different molecular weight cut offs (MWCOs) of 10 kDa, 30 kDa and 100 kDa were fouled with orange juice and cleaned with a cleaning agent, *Ultrasil 11* over two operational cycles. Fouling and cleaning mechanisms were investigated by using surface zeta potential, Brunauer-Emmet-Teller (BET) analysis and Fourier transform infrared (FTIR) analysis. The RCA conditioned membranes displayed zeta potential values of -0.2 to -31.5 mV. Fouling caused RCA membranes to have a greater magnitude of negative surface charge and cleaning restored the membrane surface charges close to its pristine state. Fouling increased both the total surface area and the total pore volume of all membranes. The total surface area and total pore volume for RCA 100 kDa after fouling increased by 102% and 185%, respectively. Pore area and volume distributions revealed that the porosities were returned close to the original level after cleaning. The recovery flux ratios of RCA 10, RCA 30 and RCA 100 decreased after fouling by 27%, 6% and 10% respectively; and changes were 25%, 9% and 1%, respectively after cleaning. The charge of membrane surfaces after two operational cycles and the IR intensity of RCA membrane deposits, varied with MWCO such that RCA 30 > RCA 100 > RCA 10. Ultrafiltration using RCA 10 kDa membrane displayed the best separation efficiency with 32 ± 4% rejection of phytosterols. Changes in membrane surface charge and porosity have been found to affect the RCA membrane performance due to fouling and cleaning during the isolation of phytosterols from orange juice.

1.   Introduction

Membrane fouling is the deposition of unwanted material on the membrane surface or inside its porous structure, leading to flux decline and a change (either an increase or a decrease) in separation performance (Jones *et al.*, 2011). Fouling phenomena depend upon the physical properties of the membrane such as molecular weight cut off (MWCO), pore size distribution and membrane material (Jeon *et al.*, 2016), and also membrane surface chemistry such as surface charge, hydrophobicity, roughness and chemical bonding interactions (Argyle *et al.*, 2015; Evans *et al.*, 2009). Fouling is also dependent on operating conditions such as transmembrane pressure, feed component concentrations and pH (Mulder, 1996). Fouling can be mitigated by pre-treatment of the feed solution, modifying the membrane properties, changing the module design or by membrane cleaning. Chemical cleaning is the most commonly used method of reducing fouling in membrane separations especially in practical operations, where industrially relevant feeds are filtered.

Membrane cleaning is required after every filtration process to prolong the lifespan of the filtration process and maintain the membrane performance. The choice of cleaning protocol depends on the module design, type of membrane, type of foulant and severity of fouling (Echavarría *et al.*, 2011; Mulder, 1996). The chemical cleaning method involves alkali treatment using sodium hydroxide, acid flush using nitric acid, enzymatic hydrolysis and surfactant flush or in combination of them (Ilame and V. Singh, 2015). Chemical cleaning is often carried out as cleaning-in-place by passing the cleaning solution through the membrane module for a fixed period of time at low pressure and moderate temperatures (Scott, 1998). Frequent membrane chemical cleaning can modify the membrane properties, reduce the membrane lifetime and increase the operational cost (Park *et al.*, 2018).

Membranes subjected to fouling and cleaning have been found to undergo surface modification including changes to the surface charge (Argyle *et al.*, 2015; Breite *et al.*, 2016) and membrane porosity (Virtanen *et al.*, 2020). The zeta potential at the solid-liquid interface can be measured via the electrokinetic method (Pihlajamaki and Nyström, 1995). The determination of zeta potential by streaming potential or current is applied in various fields such as characterization of membranes and filters, semiconductors, textiles, polymer and mineral processing (Anton-Paar, 2012). The influence of surface charge upon ultrafiltration of black tea (Evans *et al.*,

2008) and sulphite liquor (Weis *et al.*, 2005) using regenerated cellulose membrane has been reported by other researchers. Surface charge may affect the membrane tendency to foul and its subsequent cleanability. Fouling caused the regenerated cellulose membranes to have a greater negative charge and cleaning returned the surface charge to a pristine state (Evans *et al.*, 2008; Weis *et al.*, 2005). Changes in membrane porosities can be characterised by Brunauer-Emmett-Teller (BET) technique which has been used to analyse the effect of membrane fouling caused by wood originated compounds. The formation of a fouling layer was observed in the meso-pores region and resulted in an increase in accumulated pore volumes and pore areas (Virtanen *et al.*, 2020).

This paper builds on the foundation of the previous study (Abd-Razak *et al.*, 2019) where the ability of ultrafiltration in isolating phytosterols from orange juice by using synthetic membranes was reported. In the previous study, RCA membranes with a range of MWCO values were tested with the aim of removing the proteins and transmit more sterols. The 10 kDa membrane exhibited the largest permeate concentration of phytosterols. The mass concentration ratio of sterol to protein increased from 0.3 in the feed to 5.0 in the permeate when filtration was carried out using a RCA 10 kDa membrane. Contrastingly, 30 kDa and 100 kDa membranes resulted in a relatively higher rejection of phytosterols (Abd-Razak *et al.*, 2020). This study extends the previous work to understand that nature of the fouling layers.

Therefore, the objective of this work was to study the effect of membrane surface charge and porosity during the separation of phytosterols and proteins from orange juice using ultrafiltration. Changes to the surface charge and porosity of RCA membranes are examined throughout the fouling and cleaning cycle during filtration. Surface zeta potential measurements were carried out using streaming current method in order to understand the nature of the fouling and cleaning mechanisms occurring in this system. The changes to the surfaces of virgin, fouled and cleaned membranes at different MWCO values are reported.

2. Materials and methods

2.1. Pre-filtration of the feed solution

Orange juice (not from concentrate) was purchased from *Cobell*, UK. The juice was pre-filtered by using a pressurized feed vessel (*Amicon*, Danvers, USA) that consists of a *Memtech* stainless steel 25 µm cartridge filter (UK) to remove pulp prior to ultrafiltration. A feed volume of 3 L orange juice was used. Orange juice contains a polydisperse distribution of particle sizes from pulp trashes to small particles less than 2 µm in diameter (Corredig *et al.*, 2001; Stinco *et al.*, 2012). The particles in orange juice (feed and retentate) contain larger particle size which was more than 100 nm and the particle sizes of permeate after the ultrafiltration was around 1 nm at 90% composition. A pre-filtration step is needed in order to produce a sample with a standard particle size that can be passed through the ultrafiltration membrane. The content of total phytosterols in the orange juice (feed) was determined at 0.3 ± 0.1 mg/ml and this finding agrees with earlier studies (Jiménez-Escrig *et al.*, 2006; Piironen *et al.*, 2003). The amount of protein in the feed sample was 0.9 ± 0.1 mg/ml. Sugar content in feed was measured in term of °Brix which was 11 ± 0.1. Total suspended solid in the feed sample was $8.5 \pm 0.1\%$ (Abd-Razak *et al.*, 2020).

2.2. Preparation of the cleaning agent solution

The cleaning agent solution was prepared by dissolving 0.5 w/w% *P3-Ultrasil 11* (*Henkel Ecolab*, US) in reverse osmosis water. The pH of the cleaning solution was 10. The cleaning agent solution contained 44 wt% sodium hydroxide, >30 wt% tetrasodium salt of EDTA, < 5 wt% anionic surfactant and < 5 wt% non-ionic surfactant (Weis *et al.*, 2005).

2.3. Membranes

Three flat-sheet regenerated cellulose acetate (RCA) membranes with 10 kDa, 30 kDa and 100 kDa MWCO values, were supplied by *Alfa Laval*, Denmark. RCA 10 kDa is a commercial membrane with *Alfa Laval* code RC70PP. RCA 30 and 100 kDa are prototype membranes. The characteristics of the membranes (Alfa-Laval, 2017)

are summarised in Table 1. Membranes were cut to size with a membrane area of 336 cm^2 and placed in the membrane filtration system *LabStak M10* module. New membranes were initially conditioned by using hot wash method (Weis *et al.*, 2003) to remove glycerol coating from the surface of the virgin membrane. The membranes were conditioned by using filtering reverse osmosis water at 60 °C for 120 minutes with a TMP of 1.0 bar.

Table 1: The characteristics of the RCA membranes from *Alfa Laval* (Alfa-Laval, 2017)

Membrane	RCA 10	RCA 30	RCA 100
Material for selective layer	[RCA]	[RCA]	[RCA]
Membrane substrate (non-woven backing/ textile)	[PP]	[PET]	[PET]
MWCO (kDa)	10	30	100
pH operating range		1 – 10	
pH cleaning operating range		1 – 11.5	
Operating pressure (bar)		1 – 10	
Operating temperature (°C)		5 – 60	
Pure water permeance (L m^{-2} h^{-1} bar^{-1}) at 1.0 bar	100 ± 5	240 ± 5	210± 5

[RCA] = regenerated cellulose acetate, [PP] = polypropylene, [PET] = polyethylene terephthalate

2.4. *Fouling and cleaning experiments*

Ultrafiltration fouling and cleaning experiments were conducted by using a laboratory scale cross flow membrane filtration system *LabStak M10* manufactured by *DSS* (now *Alfa Laval*), Denmark. Two RCA membrane samples of each MWCO (10 kDa, 30 kDa and 100 kDa) were used in the experiments. The ultrafiltration

fouling and cleaning cycle for one run consists of membrane conditioning (120 minutes), pure water flux (PWF) for 10 minutes, filtration (60 minutes), rinsing (5 minutes), PWF (10 minutes), cleaning (10 minutes) and PWF (10 minutes) steps as described in detail by Abd-Razak et al. (2019). The temperature of the orange juice feed was maintained at 20 ± 2 °C throughout the experiments. Filtration was carried out at TMP value of 1.0 bar and the CFV was at 1.5 m s^{-1}. The PWF of the membrane was determined using reverse osmosis water before fouling, after fouling and after cleaning. The fouling experimental time was limited to 60 min, as this is sufficient to obtain a pseudo steady-state permeate flux. The recovery flux ratio can be calculated using Equation (1):

$$Recovery\ flux\ ratio = \frac{PWF_1 - PWF_2}{PWF_1} \tag{1}$$

where PWF_1 is the pure water flux before fouling and PWF_2 is the pure water flux after fouling. The separation efficiency was determined by calculating the rejection and separation factor. The rejection (R) towards of solutes (total phytosterols and proteins) was calculated using Equation (2):

$$R = (1 - \frac{C_p}{C_r}) \tag{2}$$

where C_p is the solute concentration in the permeate and C_r is the solute concentration in the retentate (Mulder, 1996). Separation factor (α) was calculated using Equation (3):

$$\alpha_{A/B} = \frac{y_A / y_B}{x_A / x_B} \tag{3}$$

where y_A and y_B are concentrations of components A and B in the permeate and; x_A and x_B are concentrations of components A and B in the feed.

2.5. Surface charge of membranes

The measurements of RCA membranes zeta potential were carried out by using an Electrokinetic Analyzer (*SurPASS, Anton Parr*, Graz, Austria). A potassium chloride (KCl) solution of concentration 0.001 M was prepared and used as the electrolyte solution. The pH range covered was 3 to 8. The solution pH was first shifted to about pH 8 by dilute KOH solution and then automatically titrated from pH 8 to 3 by using 0.05 M HCl solution during the analysis. The presence of a surface charge leads to ions in the solution of an opposite charge being attracted towards the membrane surface. This leads to a greater concentration of counter ions close to the surface rather than in the solution. Thus, a bound layer of counter ions at the surface and a diffusive layer at greater distance from the surface will be formed.

2.6. Brunauer-Emmet-Teller (BET) analysis

The regenerated cellulose membranes were cut into small pieces and degassed at 80 °C using the *Smart VacPrep 067* (*Micromeritics Instrument,* USA) degassing units. The analysis was then carried out using *Micromeritics 3Flex* surface characterisation analyser (*Micromeritics Instrument,* USA). The surface areas and pore volumes of the membrane samples were measured using the nitrogen gas adsorption and desorption method. *MicroActive* software was applied to calculate the results based on Barrett, Joyner and Halenda (BJH) method (Barrett *et al.*, 1951). Unfortunately, the layers of RCA 10 kDa were easily delaminated during the sample preparation, and therefore, the comparable porosities of the RCA 10 kDa samples could not be measured.

2.7. Statistical analysis

Two RCA membranes of each MWCO (10 kDa, 30 kDa and 100 kDa) were used in the experiments. All zeta potential measurements were done in two replicates. The standard deviation was calculated based on two membrane samples for each MWCO. Each membrane samples were prepared at four stages; conditioned, fouled, cleaned and cleaned-fouled. The measurements of RCA membranes zeta potential were carried out by using a SurPASS Electrokinetic Analyzer. The zeta potential graphs

show the averaged values obtained from two replicate measurements. Error bars represent the standard deviations of two replicate measurements.

In BET measurement, the total surface area of the sample should be preferably more than 1 m^2 when the adsorbate gas is nitrogen. Composite sampling was carried out because the surface areas available in individual membrane samples were below the above mentioned limit (*i.e.* membrane samples from the twice replicated fouling and cleaning experiments were composited into one). It should be noted that available surface areas of the RCA 100 CON and RCA 100 F1C1 samples were still only 0.71 m^2 and 0.57 m^2, respectively which may have reduced the accuracy of the results of the samples.

2.8. *Membrane fouling and cleaning evaluation by FTIR*

The FTIR spectra were recorded on a *FTIR Spectrum 100* spectrometer (*Perkin Elmer*, USA) with diamond attenuated total reflection (ATR) head and processed by *Perkin Elmer Spectrum* version 10.4.00 software. FTIR analysis was carried out to study the effect of fouling and cleaning towards the foulant on the membrane surfaces. Membrane samples were prepared at four stages; conditioned, fouled, cleaned and cleaned-fouled. The FTIR spectra in the range of 4000 – 650 cm^{-1} were used to analyse the membrane surfaces at different conditions. The identification of the functional groups presented on polymeric membranes was carried out using ATR-FTIR analysis. The spectra were normalised and processed with baseline correction. The membrane samples were dried at room temperature for 24 hours prior to analysis (Pihlajamäki *et al.*, 1998).

2.9. *Scanning electron microscope (SEM)*

Field emission scanning electron microscope (FESEM) model JEOL JSM-6301F (Japan) was used to observe the cross-sectional morphology of the membranes after fouling and cleaning. The samples were frozen in liquid nitrogen.

3. Results and discussion

3.1. *Surface zeta potential measurements*

Changes in membrane hydrophobicity and surface roughness have been found to affect the RCA membrane performance due to fouling and cleaning during the isolation of phytosterols from orange juice (Abd-Razak *et al.*, 2020). Surface charge has also been shown to be a key factor in determining membrane performance (Breite *et al.*, 2016; Sun *et al.*, 2018; Wu and Bird, 2007) and this may affect the transmission of phytosterols into permeate and rejection of proteins. In this study, the zeta potential of the RCA membranes was measured for membranes that were; conditioned, fouled-once, fouled-cleaned and cleaned once-fouled twice. The zeta potential was measured at different pH values between 3 and 8. Zeta potential measurements below pH 3 were not carried out because it may lead to inaccurate results (Wu and Bird, 2007). The AgCl coating of the electrodes may not be stable in too high pH or in basic solutions if pH values above 8 are applied. A potassium chloride (KCl) solution of concentration 0.001 M was used as the electrolyte solution in this study.

The zeta potentials for the virgin-conditioned RCA membranes are shown in Figure 1. The membranes were first conditioned using reverse osmosis water to remove the glycerol coating applied by the manufacturer from the surface. In general, the zeta potentials for the conditioned RCA membranes were below zero and decreased as the pH increased from 3 to 8. All conditioned membranes showed a similar declining trend of zeta potential with increasing pH, irrespective of the molecular weight cut off value. This suggests that the RCA membrane surfaces were negatively charged initially. This result is expected for clean cellulose surface as found by other study (Evans *et al.*, 2008).
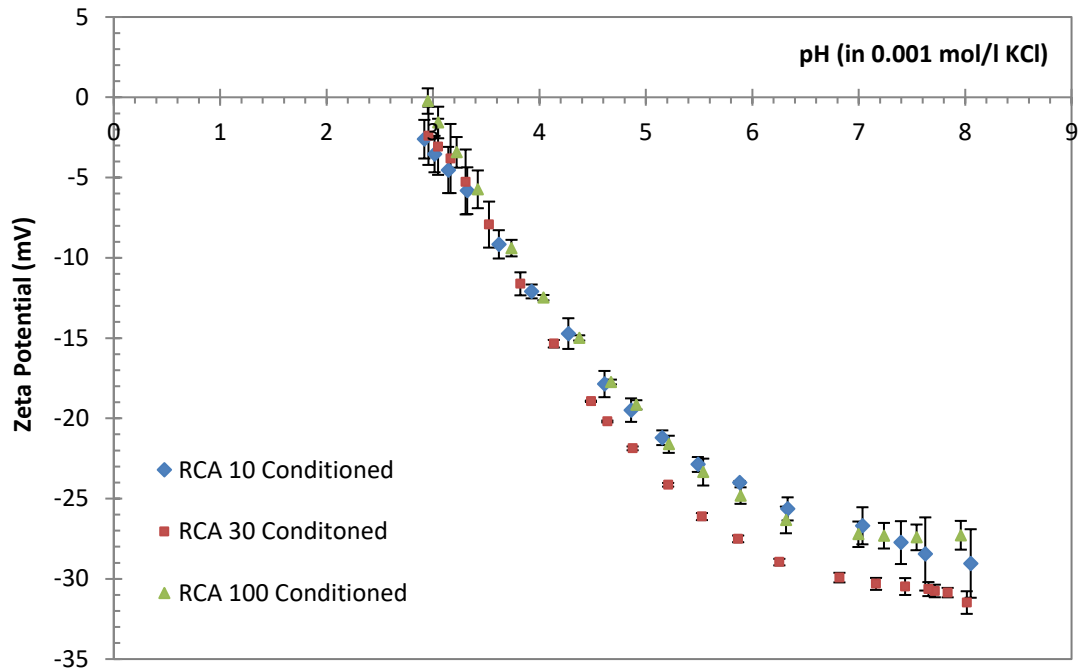
Figure 1: The zeta potential of RCA conditioned membranes as a function of pH in 0.001 M KCl. The graphs show the averaged values obtained from replicate measurements; the error bars indicate the correspondent standard deviations.

Figure 2 (a) to (c) show the zeta potential for each of the RCA membranes as a function of pH in 0.001 M KCl at four different points in the operational cycle; conditioned, fouled once, fouled once-cleaned and fouled twice-cleaned once. Over the pH range examined (3 to 8), the RCA 10 membranes showed negative surface charge. The RCA 30 and RCA 100 membranes tended to display a bigger range of zeta potential charge over the pH range from 3 to 8. RCA 30 fouled membranes showed isoelectric points (IEP) of pH 2.9 at Cycle I and pH 3.4 at Cycle II. RCA 100 fouled membranes showed isoelectric points of pH 3.1 at Cycle I and pH 3.4 at Cycle II. It can be seen in Figure 2, fouled once and fouled twice membranes showed higher values of negative charges. This may suggest that fouling caused all RCA membranes to have a greater magnitude of negative charge due to very highly negative molecules adsorbing onto the surfaces or more likely the foulants are exposing their negative parts towards solution (facing their uncharged or even positive sides towards cellulose surface.

As shown in Figure 2 (a), the RCA 10 conditioned membrane displayed zeta potential values of -2.6 to -28.5 mV, and the charges changed from -0.9 to -30.3 mV

for fouled once then cleaned membranes. There was very little difference in zeta potential profiles recorded for these two membranes, suggesting that they were easily cleaned or returned to initial charge values. When the membrane was cleaned once and fouled twice, the zeta potential decreased as the pH values increased. This may suggest that the RCA 10 kDa membrane did not fouled significantly during the first fouling cycle, but that multiple fouling cycles produced a large negative charge value due to fouling of the membrane surface. Figure 2 (b) shows the streaming potential for RCA 30 kDa membranes at all conditions across pH 3 to 8. Interestingly, the RCA 30 fouled membranes displayed a more negative charge compared to that of either the RCA 10 or the RCA 100 membrane. The RCA 30 membrane that was fouled once showed the zeta potential range of 0.1 to -56.2 mV. This value range was similar to that of the RCA 30 membrane; fouled twice and cleaned once. This may suggest that the cleaning was quite successful. The RCA 30 fouled once membrane displayed an isoelectric point of 3. The IEP increased to 3.4 when the membrane was cleaned once and fouled twice. This may suggest that more foulants with positive charges were fouled on the RCA 30 membrane surfaces.

Figure 2 (c) shows the zeta potential trends for the filtration using RCA 100 kDa membranes. The RCA 100 conditioned membrane displayed zeta potential values in the range of -0.2 to -27.3 mV. Once the membrane was fouled and cleaned once, the zeta potential values recorded are between those of the conditioned and the fouled once membrane. This suggests that the membrane was not totally restored after fouling and cleaning (Jones *et al.*, 2011). It can be postulated that the cleaning method used was not effective in completely removing the foulants. The RCA 100 kDa membrane which was fouled twice displayed higher magnitude of negative charge compared to RCA 100 cleaned once and fouled once membrane. This may suggest that the second fouling resulted in a more negative charge value due to more substances present on the membrane surfaces. It can be concluded that the cleaning makes the surface more suited to secondary fouling. Membranes displayed isoelectric point values of 3.1 for the RCA 100 fouled once membrane, and 3.4 for the RCA 100 cleaned once-fouled twice sample.

Fouling caused all membranes to have a greater negative charge regardless of the pore size, due to negatively charged species deposited on the membrane surfaces (Jones *et al.*, 2011). It can be seen that the magnitude of the negative charge on the membrane surface fouled-once membranes varied with MWCO such that RCA 30 >

RCA 100 > RCA 10. This corresponds to the order of the increased surface roughness (Abd-Razak *et al.*, 2020). When the RCA 10 membrane was cleaned using *Ultrasil 11*, the membrane surface charge was returned back to the original value. This implies that the cleaning procedure is removing the negatively charged foulants on the RCA 10 membrane. This also suggests that RCA 10 membrane was easily cleaned after first fouling. The membranes appeared to be even more negatively charged after cleaning. This means that the membranes were not totally restored after the first fouling and cleaning cycles. It is possible that the cleaning method was not completely effective under the conditions used (Jones *et al.*, 2011).

The RCA 30 and RCA 100 membranes that were fouled twice had isoelectric point of *ca.* 3. This may suggest that proteins foulants with positive charges were fouled on membrane surfaces, since proteins become positively charged at low pH and negatively charged at high pH. Potassium citrate was found on the RCA membrane surfaces, therefore it is possible that the potassium ions were retained on the membrane surfaces after fouling and cleaning. Thus, it was clear that surface charge controlled the performance of the membrane filtration, rather than the MWCO of the membrane. In general, it can be seen that fouling caused all membrane surfaces to be more negative and cleaning restored the membrane surfaces close to its pristine state (Figure 2). A big difference in surface charge was observed between conditioned and cleaned membranes. Interestingly, RCA 30 fouled once and fouled twice showed that the fouling was not worse in the second cycle. However, the fouling in the second cycle was stronger compared to first cycle for RCA 10 and 100 kDa.
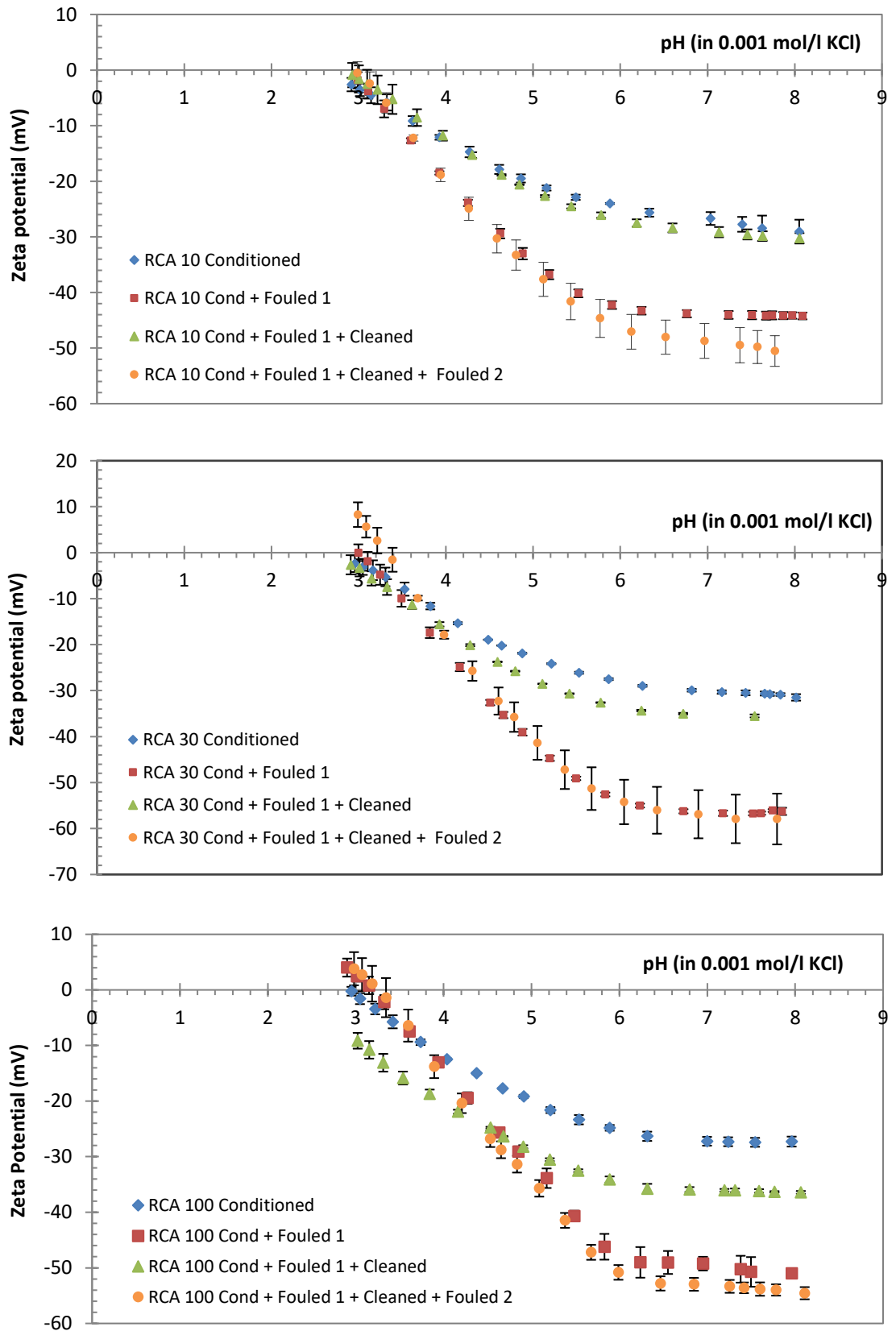
Figure 2: The zeta potential of RCA membranes as a function of pH in 0.001 M KCl, (a) RCA 10, (b) RCA 30 and (c) RCA 100. Data are shown as averages with error bars represent the standard deviation.

3.2. Porosity measurement by BET analysis

Table 2 shows the total surface area and total pore volume of conditioned, fouled and cleaned RCA 30 and 100 kDa membranes. It can be seen that the total pore volume of the conditioned RCA 30 membrane is more than two times higher than the total pore volume of conditioned RCA 100 membrane. The significant difference in the porosities of the membranes might explain the higher PWF of RCA 30 compared to RCA 100.

Table 2: Total surface area and total pore volume from the BET analysis

Sample	Total surface area (m^2/g)	Total pore volume (cm^3/g)
RCA 30 Conditioned	1.71	0.0051
RCA 30 Fouled 1	1.50	0.0033
RCA 30 Cleaned	1.48	0.0045
RCA 100 Conditioned	0.64	0.0020
RCA 100 Fouled 1	1.29	0.0057
RCA 100 Cleaned	0.55	0.0015

Membrane fouling had interestingly contrary effects on the total pore areas and volumes of the membranes. A decrease of 12% in total surface area and a decrease of 35% in total pore volume were found for the RCA 30 membrane after fouling, which might originate in smoothing of the membrane surface or in blocking of the pores. The total surface area and total pore volume for RCA 100 after fouling increased by 102% and 185%, respectively, which indicate the formation of a porous fouling layer. The cleaning process restored total surface area and total pore volume partly for both of the membranes. The total surface area and total pore volume for RCA 30 after fouling and subsequent cleaning decreased by 13% and 12%, respectively. A decrease of 14% in total surface area and a decrease of 25% in total pore volume were found for the RCA 100 membrane after cleaning. This could be explained by the modification effect of membrane by the fouling and cleaning cycle.

Another observation here is that the cleaning method established was effective in removing the fouling layer from the membrane surfaces.

The pore-specific alterations behind the cumulative changes of porosities of RCA 30 and RCA 100 membranes are revealed by pore area and pore volume distributions that are shown in Figure 3. Distributions of RCA 30 membrane show that fouling increased the porosity below pore sizes of 5 nm but decreased the porosity at larger pore diameters. This result could be explained by the adsorption of bigger molecules such as proteins onto the larger pores and voids on the membrane skin layer. Blocking and smoothing of the larger pores could explain formation of smaller pores with diameters below 5 nm. Pore area and pore volume distributions of cleaned RCA 30 in Figure 3 (a) and (c) show how cleaning restored the porosity of the membrane almost to the initial state.

Figure 3 (b) and (d) show that fouling increased the porosity of RCA 100 membrane at all pore diameters which most probably stems from the built-up of a highly porous cake or gel fouling layer. The possible profound difference in the fouling mechanism of the RCA 30 and RCA 100 membranes is a highly interesting finding. The results suggest that the RCA 100 kDa was less prone to blockage of the mesopores than RCA 30 kDa (which can be explained by the differences in the MWCOs), and for some reason favouring the formation of a porous fouling layer. This finding may suggest that a cake layer was formed on the surface of RCA 100 and is in agreement with the SEM images. Pore area and volume distributions also revealed that cleaning restored the porosity of the RCA 100 membrane near the initial state, similarly than in the case on RCA 30 membrane.

Figure 3 shows the pore size distribution based on the BJH calculation. The pore size distribution has uncertainties regarding small pores in the distribution. The pores should start at zero reading. However, Figure 3 shows open pores on the left-hand side of the graph. This result could be due to the low pressure used when measuring the adsorption isotherm was too high to explore the pores. The relative pressure (P/P_0) used was in the range of $0.01 - 0.99$ with the pressure (P) values in the range of $8 - 749$ mmHg and the saturation pressure (P_0) at 755 mmHg. In order to capture the small pores distribution, the relative pressures will need to go down to 10^{-9} (Micrometrics, 2013).
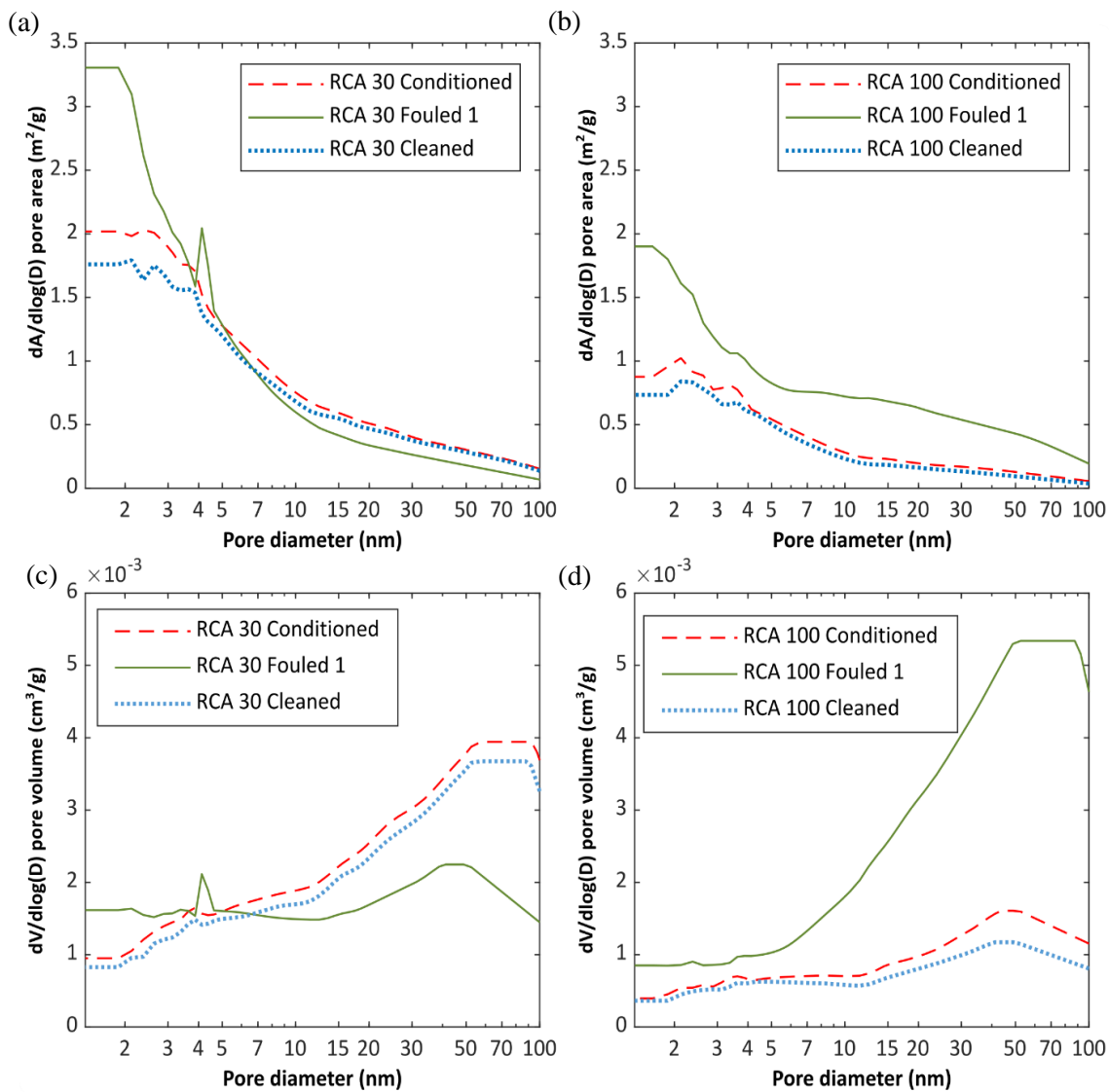
Figure 3: BJH pore area distributions of (a) RCA 30 kDa and (b) RCA 100 kDa and pore volume distributions of (c) RCA 30 kDa and (d) RCA 100 kDa membranes fouled with orange juice

3.3. *Flux analysis*

The cross-flow filtration cycle included (i) PWF measurement before fouling, (ii) filtration of orange juice, (iii) PWF measurement after fouling, (iv) chemical cleaning and rinsing and (v) PWF measurement after cleaning. Figure 4 shows the permeate flux profiles for the three membranes fouled at TMP of 1.0 bar and 20 °C. The operating conditions in Cycles **I** and **II** are maintained as close as possible. Initial permeate fluxes varied for RCA 10, RCA 30 and RCA 100 which were 29 L $m^{-2} h^{-1}$, 39 L $m^{-2} h^{-1}$ and 42 L $m^{-2} h^{-1}$, respectively. It is likely that the membrane with larger pore size resulted in a higher filtration flux. After approximately 2 min, permeate fluxes declined gradually until the filtration was stopped at 60 min. All membranes presented steady-state permeate flux at *ca*. 22 L $m^{-2} h^{-1}$.

Pure water flux was measured for membranes using reverse osmosis water under these conditions (i) before fouling, (ii) after fouling and (iii) after cleaning. The effectiveness of the membrane cleanability after fouling and cleaning cycle could be explained by the changes in PWF (Evans *et al.*, 2008). It can be seen in Figure 4, the RCA 10 kDa and RCA 100 kDa membranes showed lower pure water fluxes than the RCA 30 kDa membrane. The RCA 10 membrane with the smallest MWCO (10 kDa) exhibited the lowest water flux of 75 – 132 L $m^{-2} h^{-1}$. RCA 100 with the highest MWCO (100 kDa) displayed the PWF of 186 – 205 L $m^{-2} h^{-1}$. Meanwhile, RCA 30 membrane with the intermediate MWCO (30 kDa) showed the highest water flux of 230 – 288 L $m^{-2} h^{-1}$. It is possible that surface modification is occurring during the fouling and cleaning due to the adsorption of *Ultrasil 11* surfactant to the membrane surface (Weis *et al.*, 2003). Based on these results, the PWF decreased in the following order, RCA 30 > RCA 100 > RCA 10. This result is in agreement with the membrane surface charge measurements. These results showed that PWF were not correlated with the MWCO of the membranes and therefore, MWCO was a poor indicator of permeate flux.

The PWF reduced after fouling (PWF 2) for all membranes in both cycles, suggesting that the ultrafiltration process was affected by membrane fouling. Hence, an effective cleaning method is required to regenerate the membrane. The commercial cleaning formulation, *Ultrasil 11* was used in this study. This product is widely used for membrane cleaning in laboratory situations (Wu and Bird, 2007). Figure 4 demonstrates that the flux of pure water passing through the membrane after

cleaning was higher than that after fouling (*e.g.:* PWF 3 I was higher than PWF 2 I). The recovery flux ratios of RCA 10, RCA 30 and RCA 100 decreased after fouling (in Cycle I) by 27%, 6% and 10%, respectively. After cleaning, the recovery flux ratio for RCA 10, RCA 30 and RCA 100 increased by 25%, 9% and 1%, respectively. It is possible that surface modification is occurring due to the adsorption of *Ultrasil 11* surfactant to the membrane surface (Weis *et al.*, 2003). This shows the membranes were cleaned and regenerated after the cleaning technique is applied. According to fluxes measurements, all membranes performed consistently after two multiple filtration and cleaning cycles were completed. However, based on the surface charges data, the PWF was a poor indicator of permeate flux in this system. The reduction in the magnitude of surface charges indicated that membrane fouling increased, which is in agreement with the findings of Evans et al. (2008).
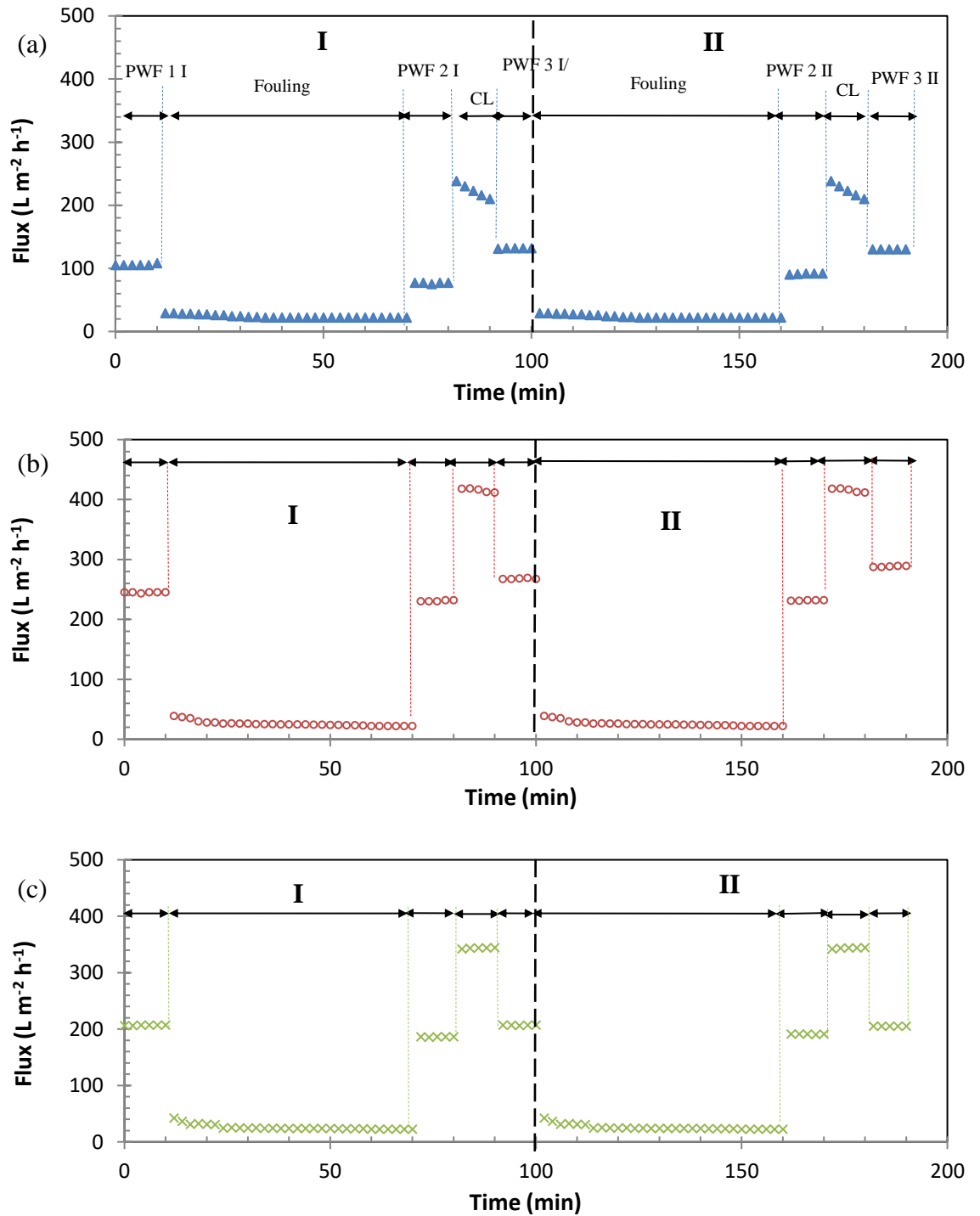
Figure 4: Ultrafiltration of three membranes tested; (a) RCA 10, (b) RCA 30 and (c) RCA 100 during three filtration cycles (60 min of fouling, 10 min of pure water flow (PWF), 10 min of cleaning (CL)) operated at TMP = 1 bar and CFV = 1.5 ms^{-1}. Regions identified by roman numerals represent the two filtration cycles. Average uncertainty of the pure water flux is ± 2 L m^{-2} h^{-1}.

3.4. *Spectral chemistry determination by ATR- FTIR*

The intensity of IR absorption bands was used qualitatively to identify changes in the composition of material present on membrane surfaces due to fouling and cleaning processes (Wu and Bird, 2007). Figure 5 illustrates the FTIR spectra of all tested RCA membranes at four conditions; conditioned, fouled, cleaned and cleaned-fouled. It was observed that all samples showed identical FTIR spectra with slightly shifted absorption bands. A strong and broad band observed around 3500 – 3000 cm^{-1} corresponds to O-H stretching vibration of hydroxyl group in the RCA membrane (Madaeni and Heidary, 2011). It can be seen in all spectra, the highest O-H peaks were observed in all conditioned membranes. The absorbance intensity of O-H peaks for fouled membranes were the lowest and the peaks intensity returned to original state for cleaned membranes. This could be due to the adsorption of *Ultrasil 11* surfactant to the membrane surface.

The absorption band for RCA membrane at 1020 cm^{-1} is assigned to C-O stretching. The CH$_2$ symmetric bending was characterised at 1420 cm^{-1} and the band at 1340 cm^{-1} is due to the C-H bending (Azuwa *et al.*, 2015). The infrared spectrum of PP was detected in RCA 10 kDa membrane as shown in Figure 5 (a). The absorption peak at 2950 cm^{-1} is attributed to CH$_3$ asymmetric stretching vibration and the band at 2850 cm^{-1} is due to the CH$_2$ symmetric stretching (Gopanna *et al.*, 2019). The RCA 10 kDa membrane displayed the spectrum of membrane substrate (PP), most probably due to the selective layer of this membrane was easily delaminated as shown in the SEM images. According to the spectra obtained in Figure 5 (b) and (c), there were peaks that correspond to infrared absorption bands of PET polymer as the membrane substrate used was PET. The bands were detected at 1710 cm^{-1} (stretching of C=O of carboxylic acid group, 1240 cm^{-1} (terephthalate group) and 1080 cm^{-1} (methylene group and vibrations of the ester C-O bond) (Pereira *et al.*, 2017). The membrane substrates of RCA 30 and 100 membranes might have been more visible in the spectra due to the thicknesses of their selective layers, which were thinner than RCA 10 kDa membrane as shown in the SEM images.

The higher intensity demonstrated that more foulant was deposited on the membrane surface (Evans *et al.*, 2008). Figure 5 showed that membrane surfaces which were fouled twice produced higher intensity compared to the membrane

surfaces which were fouled once. It can be seen in Figure 5, the intensity of RCA membrane deposits varied with MWCO such that RCA 30 > RCA 100 > RCA 10. These results correlate well with the membrane surface charges and pure water flux measurements. The protein peaks were identified in the area of $1400 - 1800$ cm^{-1} with two peaks called amide I peak at 1540 cm^{-1}and amide II peak near 1650 cm^{-1} (Metsamuuronen, 2003). The presence of proteins in orange juice has been studied by other researchers (Lerma-García *et al.*, 2016; Okino Delgado and Fleuri, 2016; Sass-Kiss and Sass, 2000). It is therefore likely that the foulants are largely proteinaceous in nature (Wu and Bird, 2007). The FTIR analysis showed the presence of protein peaks on the fouled membranes. Proteins are known to be amphoteric, with both positive and negative charges depending on surrounding solution pH. This led to a speculation that protein-based foulants were trapped on the membrane surfaces or in the membrane pores.
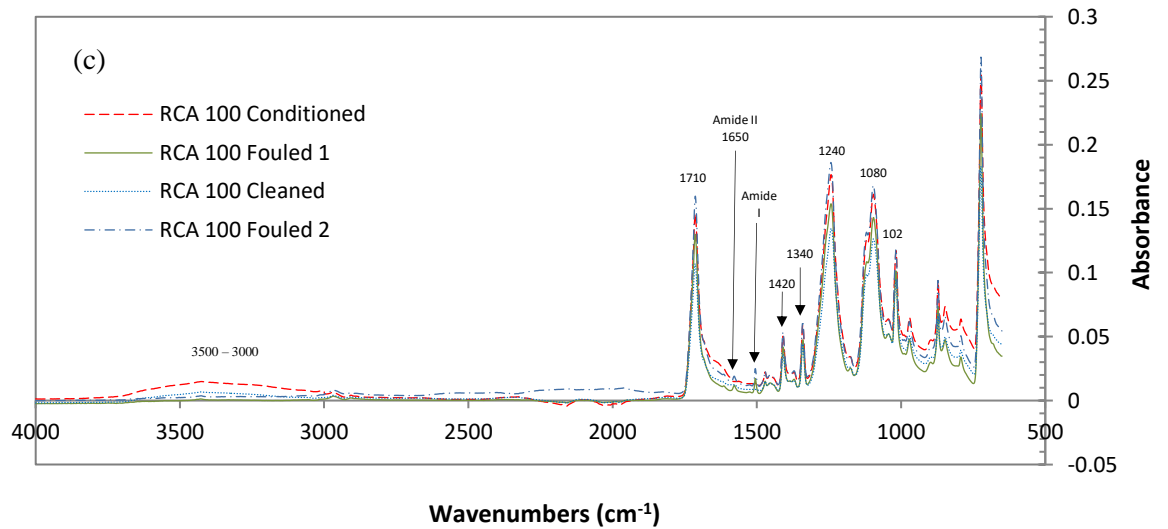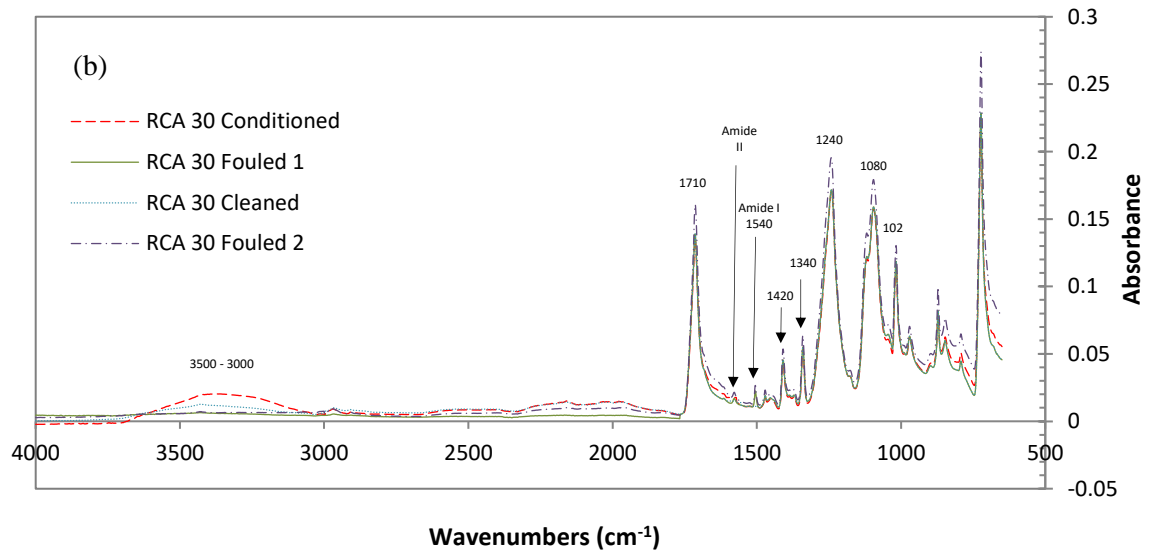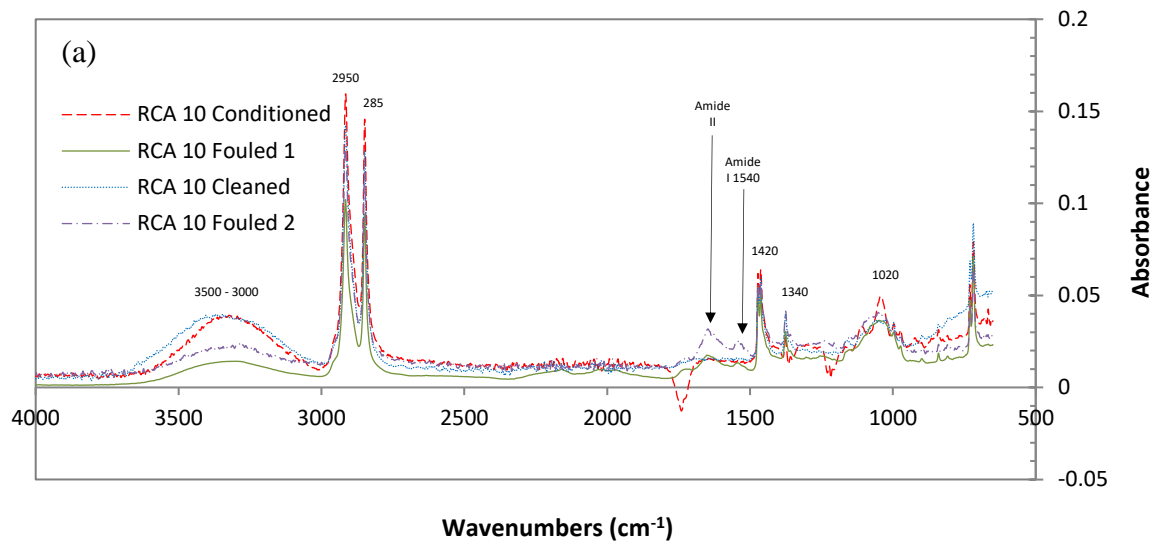
Figure 5: Infrared spectra of three membranes tested; (a) RCA 10, (b) RCA 30 and (c) RCA 100 for conditioned, fouled-once, fouled/cleaned and fouled twice membranes.

3.5. *Membrane morphology by SEM*

Field emission scanning electron microscope (FESEM) analysis was carried out to monitor the cross-sectional morphology of the membranes at different conditions; before fouling, after fouling and after cleaning. As shown in Figure 6, the membrane consists of a dense cellulosic top layer and a membrane substrate. In the cross-sectional images, it can be seen that the cellulosic top layers of the membranes were affected, and the membrane structures were deteriorated by the fouling and cleaning steps. The cellulosic top layer of the RC10 kDa membrane became detached from the membrane substrates in two of the three samples examined. The membrane substrate of RCA 10 was prepared from polypropylene (PP). Meanwhile, polyethylene terephthalate (PET) was used as the membrane substrate for RCA 30 and RCA 100 kDa membranes. This may suggest that the adhesion of RCA 10 kDa to PP support is weaker than that to the PET support for the RCA 30 and RCA 100 kDa membranes. The delamination was caused by the sample preparation protocol. The samples were frozen in liquid nitrogen to expose their cross-sectional area. However, the membrane was well performed during the ultrafiltration operation. It can be seen in Figure 6 (g) and (h), the cellulosic top layer of RCA 100 kDa fouled membrane is about twice thicker than RCA 100 kDa conditioned membrane. This may suggest that a cake layer was formed on the surface of RCA 100 and this result is supported by the porosity analysis.
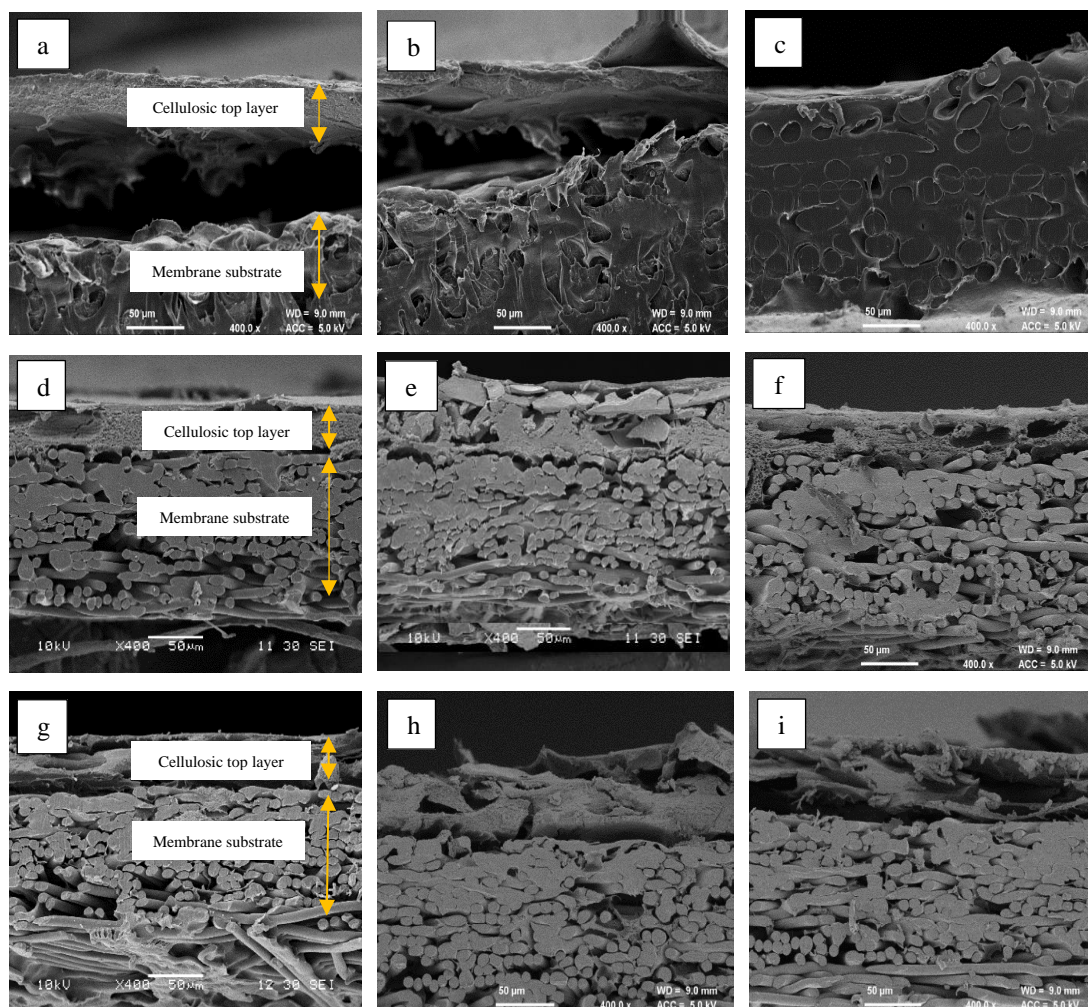
Figure 6: SEM images of cross sections of RCA membranes taken at 400x magnification: (a) RCA 10 kDa conditioned, (b) RCA 10 kDa fouled, (c) RCA 10 kDa cleaned, (d) RCA 30 kDa conditioned, (e) RCA 30 kDa fouled, (f) RCA 30 kDa cleaned, (g) RCA 100 kDa conditioned, (h) RCA 100 kDa fouled and (i) RCA 100 kDa cleaned.

3.6. *Separation efficiency*

The separation efficiency was measured in terms of rejection and separation factor. The solute is partly or completely rejected by the membrane. The goal of this work was to produce low rejection of phytosterols and high rejection of proteins in the permeate. Table 3 shows the separation efficiency of total phytosterols and protein from orange juice using three different membranes. It can be seen in Table 3, 30 kDa and 100 kDa membranes displayed a higher rejection of phytosterols of $74 \pm 6\%$ and

58 ± 4%, respectively. For proteins, 30 kDa and 100 kDa membranes gave lower rejection of proteins of 69 ± 3% and 67 ± 3%, respectively. The lowest separation factor which was 0.6 ± 0.1 can be seen in Table 3 (b) for the ultrafiltration using RCA 30 kDa. Therefore, it can be concluded that the 10 kDa RCA membrane produced good separation efficiency with 32 ± 4% rejection of phytosterols and 96 ± 1% rejection of proteins. Ultrafiltration using RCA 10 kDa membrane displayed the highest separation factor which was 17.0 ± 0.3 (Table 3). As reported previously (Abd-Razak *et al.*, 2020), the loss of phytosterols in the system for RCA 10 kDa membrane was 21%, 50% loss for RCA 30 kDa and 28% loss for RCA 100 kDa membranes. The rejection and loss of phytosterols and proteins were presumably due to the fouling effect during the filtration (Cassano *et al.*, 2008).

Table 3: Separation efficiency of total phytosterols and protein by UF process of orange juice with different membranes; (a) RCA 10, (b) RCA 30 and (c) RCA 100.

Membrane	Rejection towards phytosterols (%)	Rejection towards proteins (%)	Separation factor
(a) RCA 10	32 ± 4	96 ± 1	17.0 ± 0.3
(b) RCA 30	74 ± 6	69 ± 3	0.6 ± 0.1
(c) RCA 100	58 ± 4	67 ± 3	1.1 ± 0.1

4.   Conclusion

In this paper, streaming current measurements have been used to investigate the surface charges of RCA membranes used in the isolation of phytosterols from orange juice. The importance of membrane surface charge upon ultrafiltration performance due to variations in fouling and cleaning mechanisms has been demonstrated. The pure water flux of conditioned membranes was a poor separation performance indicator in this system. The RCA membrane surfaces were negatively charged

initially. The RCA conditioned membranes displayed zeta potential values of -0.2 to -31.5 mV. Fouling caused RCA membranes to have a greater magnitude of negative surface charge regardless of the pore size, due to negatively charged species deposited on the membrane surfaces. The magnitude of negative charge of membrane surfaces was observed such that RCA 30 > RCA 100 > RCA 10. This correlates with the rank order of the pure water flux steady state values of the three membranes. Fouling increased both the total surface area and total pore volume, and the porosities were restored very close the original level after cleaning. The total surface area and total pore volume for RCA 100 kDa after fouling increased by 102% and 185%, and decreased to 14% and 25% after cleaning. This suggests that the RCA 100 kDa was less prone to blockage of the mesopores than RCA 30 kDa. The recovery flux ratios of RCA 10, RCA 30 and RCA 100 decreased after fouling by 27%, 6% and 10% respectively; and changes were 25%, 9% and 1%, respectively after cleaning. The results demonstrate that flux and molecular weight cut off were not the main criteria in determining membrane performance during the filtration of phytosterols from orange juice. Surface charge and the porosity were important in determining the filtration properties and the resulting fouling and cleaning mechanisms of the RCA membranes tested. These results have important implications in the industrial processing of orange juice to produce sterol-based nutraceutical products.

Acknowledgements

References

Abd-Razak, N.H., Chew, Y.M.J., Bird, M.R., 2019. Membrane fouling during the fractionation of phytosterols isolated from orange juice. *Food and Bioproducts Processing* 113, 10-21.

Abd-Razak, N.H., Zairossani, M.N., Chew, Y.M.J., Bird, M.R., 2020. Fouling Analysis and the Recovery of Phytosterols from Orange Juice Using Regenerated Cellulose Ultrafiltration Membranes. *Food and Bioprocess Technology* 13, 2012-2028.

Alfa-Laval, 2017. Alfa Laval - UF flat sheet membrane, Denmark. https://www.alfalaval.co.uk/products/separation/membranes/flat-sheet-membranes/uf-flat-sheet/. Accessed 14 February 2020.

Anton-Paar, 2012. Instruction Manual SurPASS Electrokinetic Analyzer. Anto Paar, Graz, Austria.

Argyle, I.S., Pihlajamäki, A., Bird, M.R., 2015. Black tea liquor ultrafiltration: Effect of ethanol pre-treatment upon fouling and cleaning characteristics. *Food and Bioproducts Processing* 93, 289-297.

Azuwa, M.M., W., S.W.N., Juhana, J., F., I.A., Muhazri, A.M., Munira, J.S., 2015. Feasibility of recycled newspaper as cellulose source for regenerated cellulose membrane fabrication. *Journal of Applied Polymer Science* 132.

Barrett, E.P., Joyner, L.G., Halenda, P.P., 1951. The Determination of Pore Volume and Area Distributions in Porous Substances. I. Computations from Nitrogen Isotherms. *Journal of the American Chemical Society* 73, 373-380.

Breite, D., Went, M., Prager, A., Schulze, A., 2016. The critical zeta potential of polymer membranes: how electrolytes impact membrane fouling. *RSC Advances* 6, 98180-98189.

Cassano, A., Donato, L., Conidi, C., Drioli, E., 2008. Recovery of bioactive compounds in kiwifruit juice by ultrafiltration. *Innovative Food Science & Emerging Technologies* 9, 556-562.

Corredig, M., Kerr, W., Wicker, L., 2001. Particle size distribution of orange juice cloud after addition of sensitized pectin. *J Agric Food Chem* 49, 2523-2526.

Echavarría, A.P., Torras, C., Pagán, J., Ibarz, A., 2011. Fruit Juice Processing and Membrane Technology Application. *Food Engineering Reviews* 3, 136-158.

Evans, P.J., Bird, M.R., Pihlajamäki, A., Nyström, M., 2008. The influence of hydrophobicity, roughness and charge upon ultrafiltration membranes for black tea liquor clarification. *Journal of Membrane Science* 313, 250-262.

Evans, P.J., Bird, M.R., Rogers, D., Wright, C.J., 2009. Measurement of polyphenol–membrane interaction forces during the ultrafiltration of black tea liquor. *Colloids and Surfaces A: Physicochemical and Engineering Aspects* 335, 148-153.

Gopanna, A., Mandapati, R.N., Thomas, S.P., Rajan, K., Chavali, M., 2019. Fourier transform infrared spectroscopy (FTIR), Raman spectroscopy and wide-angle X-ray scattering (WAXS) of polypropylene (PP)/cyclic olefin copolymer (COC) blends for qualitative and quantitative analysis. *Polymer Bulletin* 76, 4259-4274.

151

Ilame, S.A., V. Singh, S., 2015. Application of Membrane Separation in Fruit and Vegetable Juice Processing: A Review. *Critical Reviews in Food Science and Nutrition* 55, 964-987.

Jeon, S., Rajabzadeh, S., Okamura, R., Ishigami, T., Hasegawa, S., Kato, N., Matsuyama, H., 2016. The Effect of Membrane Material and Surface Pore Size on the Fouling Properties of Submerged Membranes. *Water* 8, 602.

Jiménez-Escrig, A., Santos-Hidalgo, A.B., Saura-Calixto, F., 2006. Common Sources and Estimated Intake of Plant Sterols in the Spanish Diet. *Journal of Agricultural and Food Chemistry* 54, 3462-3471.

Jones, S.A., Bird, M.R., Pihlajamäki, A., 2011. An experimental investigation into the pre-treatment of synthetic membranes using sodium hydroxide solutions. *Journal of Food Engineering* 105, 128-137.

Lerma-García, M.J., D'Amato, A., Simó-Alfonso, E.F., Righetti, P.G., Fasoli, E., 2016. Orange proteomic fingerprinting: From fruit to commercial juices. *Food Chemistry* 196, 739-749.

Madaeni, S.S., Heidary, F., 2011. Improving separation capability of regenerated cellulose ultrafiltration membrane by surface modification. *Applied Surface Science* 257, 4870-4876.

Metsamuuronen, S., 2003. Critical flux and fouling in ultrafiltration of proteins. Lappeenrannan : Lappeenrannan teknillinen yliopisto, Lappeenrannan.

Micromeritics, 2013. Mesopore and Micropore Surface Characterization Analysis. Micromeritics Instrument Corporation. https://https://www.azom.com/article.aspx?ArticleID=8303. Accessed 7 May 2021.

Mulder, M., 1996. Basic Principles of Membrane Technology, Second ed. Kluwer Academic Publishers, The Netherlands.

Okino Delgado, C.H., Fleuri, L.F., 2016. Orange and mango by-products: Agro-industrial waste as source of bioactive compounds and botanical versus commercial description—A review. *Food Reviews International* 32, 1-14.

Park, K.-B., Choi, C., Yu, H.-W., Chae, S.-R., Kim, I.S., 2018. Optimization of chemical cleaning for reverse osmosis membranes with organic fouling using statistical design tools. *Environmental Engineering Research* 23, 474-484.

Pereira, A.P.d.S., Silva, M.H.P.d., Lima Júnior, É.P., Paula, A.d.S., Tommasini, F.J., 2017. Processing and Characterization of PET Composites Reinforced With Geopolymer Concrete Waste. *Materials Research* 20, 411-420.

Pihlajamaki, A., Nyström, M., 1995. Streaming potential methods in characterization of membranes, in: Bowen, W.R., Field, R.W., Howell, J.A. (Eds.), Proceedings of EuroMembrane 95. European Membrane Society, Bath, UK, pp. 521-524.

Pihlajamäki, A., Väisänen, P., Nyström, M., 1998. Characterization of clean and fouled polymeric ultrafiltration membranes by Fourier transform IR spectroscopy–attenuated total reflection. *Colloids and surfaces. A, Physicochemical and engineering aspects* 138, 323-333.

Piironen, V., Toivo, J., Puupponen-Pimiä, R., Lampi, A.-M., 2003. Plant sterols in vegetables, fruits and berries. *Journal of the Science of Food and Agriculture* 83, 330-337.

Sass-Kiss, A., Sass, M., 2000. Immunoanalytical method for quality control of orange juice products. *J Agric Food Chem* 48, 4027-4031.

Scott, K., 1998. Handbook of Industrial Membranes. Elsevier Science.

Stinco, C.M., Fernández-Vázquez, R., Escudero-Gilete, M.L., Heredia, F.J., Meléndez-Martínez, A.J., Vicario, I.M., 2012. Effect of Orange Juice's Processing on the Color, Particle Size, and Bioaccessibility of Carotenoids. *Journal of Agricultural and Food Chemistry* 60, 1447-1455.

Sun, C., Zhang, N., Li, F., Ke, G., Song, L., Liu, X., Liang, S., 2018. Quantitative Analysis of Membrane Fouling Mechanisms Involved in Microfiltration of Humic Acid–Protein Mixtures at Different Solution Conditions. *Water 2018* 10, 1306.

Virtanen, T., Rudolph, G., Lopatina, A., Al-Rudainy, B., Schagerlöf, H., Puro, L., Kallioinen, M., Lipnizki, F., 2020. Analysis of membrane fouling by Brunauer-Emmet-Teller nitrogen adsorption/desorption technique. *Scientific Reports* 10, 3427.

Weis, A., Bird, M.R., Nyström, M., 2003. The chemical cleaning of polymeric UF membranes fouled with spent sulphite liquor over multiple operational cycles. *Journal of Membrane Science* 216, 67-79.

Weis, A., Bird, M.R., Nyström, M., Wright, C., 2005. The influence of morphology, hydrophobicity and charge upon the long-term performance of ultrafiltration membranes fouled with spent sulphite liquor. *Desalination* 175, 73-85.

Wu, D., Bird, M.R., 2007. The Fouling and Cleaning of Ultrafiltration Membranes During The Filtration of Model Tea Component Solutions. *Journal of Food Process Engineering* 30, 293-323.

Supplementary Information

Suface area, pore volume and pore distribution analysis

The Brunauer, Emmet, and Teller (BET) method was applied to determine the surface area using the nitrogen gas adsorption and desorption method which incorporates multilayer coverage (Bardestani *et al.*, 2019). The process begins with the adsorption of gas molecule on the sample surface at low pressure. Further increasing gas pressure created a multilayer coverage. Smaller pores in the sample were filled first. The sample surface area was calculated when the area was covered by adsorbed gas molecules. The classification of pore sizes is divided into micropores (< 2 nm), mesopores (2 - 50 nm) and macropores (> 50 nm). BET equation was used to calculate the surface area using Equation (4); where *W* is the weight of gas adsorbed, *P / P0* is the relative pressure, *Wm* is the weight of adsorbate as monolayer and *C* is the BET constant.

$$\frac{1}{W\left((P_0/P)-1\right)} = \frac{1}{W_m\,C} + \frac{C-1}{W_m C}\left(\frac{P}{P_0}\right) \tag{4}$$

Nitrogen gas adsorption and desorption isotherms are categorised into six types (Sing, 1985). Type I or Langmuir isotherm shows the pores fill at very low relative pressure with a steep uptake. Non-porous and macropores materials refers to isotherm of type II (reversible isotherm), where gas molecules are absorbed into mono/ multi-layers without restriction. Type III isotherm is when the adsorbate interaction with an adsorbed layer is greater than the interaction with the adsorbent surface. Type IV isotherm occur on porous adsorbents with pores in the range of 1.5 – 100 nm, the slope shows increased uptake of adsorbate as pores become filled at higher pressures. Type V is associated with pores in the 1.5 - 100 nm range observed for small adsorbate-absorbent interaction potentials. Type VI corresponds to a multilayer adsorption on a uniform non-porous surface. The Barrett, Joyner, and Halenda (BJH) calculation was employed to calculate the pore diameter, pore volume and pore distribution from the nitrogen adsorption and desorption isotherms (Bardestani *et al.*, 2019). The BJH method applies only to the mesopore and small macropore size range. Total pore volume is derived from the amount of vapour

adsorbed at a relative temperature close to unity with the assumption that pores are filled with liquid adsorbate.

Nitrogen adsorption/desorption isotherms of RCA membranes

Figure 7 shows the nitrogen adsorption/ desorption isotherms of conditioned and fouled membranes for RCA 30 kDa and RCA 100 kDa. The isotherms in Figure 7 seem to be closest to the type II isotherms, indicated that the samples were mainly non-porous or contain relatively large pores. However, the absence of the hysteresis loop (characteristic of type II isotherms) was not conclusive evidence on non-porosity because certain pore geometries can yield isotherms without hysteresis loop even if the sample has some meso-sized pores (Webb and Orr, 1997). Moreover, there were very narrow hysteresis loops between the adsorption and desorption branches (characteristic of type IV isotherms), which indicates that there was also some mesoporosity pores (Bardestani *et al.*, 2019). A clear hysteresis loop can be seen in Figure 7 (d). The occurrence of wider and distinct hysteresis loop in the isotherm of sample RCA100 fouled membranes demonstrated that formation of fouling layer has increased the mesoporosity with the amount of pores sizes between 2 - 50 nm. This result is in agreement with the findings in the pore size distribution plot.

References

Bardestani, R., Patience, G.S., Kaliaguine, S., 2019. Experimental methods in chemical engineering: specific surface area and pore size distribution measurements—BET, BJH, and DFT. *The Canadian Journal of Chemical Engineering* 97, 2781-2791.

Sing, K.S.W., 1985. Reporting physisorption data for gas/solid systems with special reference to the determination of surface area and porosity (Recommendations 1984). *Pure and Applied Chemistry* 57, 603-619.

Webb, P.A., Orr, C., 1997. Analytical Methods in Fine Particle Technology. Micromeritics Instrument, Georgia, USA.
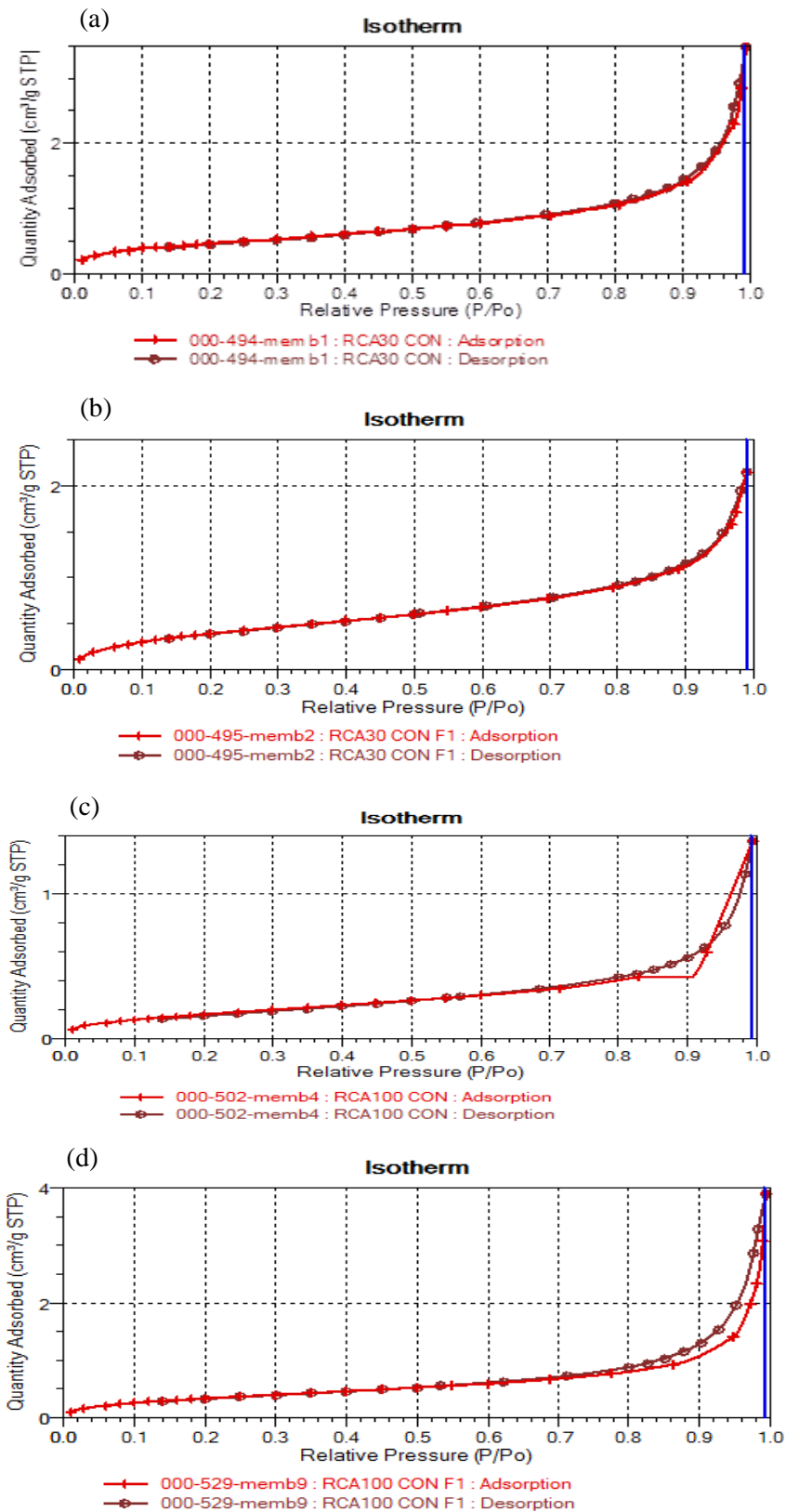
Figure 7: Nitrogen adsorption/desorption isotherms of RCA membranes; (a) RCA 30 kDa conditioned, (b) RCA 30 kDa fouled, (c) RCA 100 kDa conditioned and (d) RCA 100 kDa fouled.

Chapter 6: Orange juice ultrafiltration: Characterisation of deposit layers and membrane surfaces after fouling and cleaning
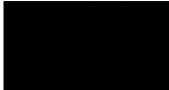
Introductory text

The previous chapters (Chapter 3 to 5) reported ultrafiltration process of orange juice with the use of chemical cleaning agent (*P3-Ultrasil 11*) for the membrane cleaning. The results show that the chemical cleaning has modified the membrane surface properties such as hydrophobicity, surface roughness, surface charge and porosity. This paper reports the novel application of the fluid dynamic gauging (FDG) technique to assess the cleaning behaviours of RCA membranes by mechanical cleaning, without affecting the membrane surface modification caused by chemical cleaning. In the FDG method, the shear stress is required to remove the fouling layers. Mechanical cleaning using FDG technique has been studied in this work and compared to the chemical cleaning that has been applied in Chapter 3 to 5.

In the previous chapters (Chapter 3 and 4), the ultrafiltration process at 20 °C using 3 L feed volume has shown potential for separation of phytosterols from orange juice. However, the phytosterols compounds obtained by using 10 kDa RCA membrane was relatively low (43 ± 2 mg L^{-1}). Based on the literature review, fouling is also dependent on operating conditions such as temperature and concentration of feed components. This chapter also presents the optimisation of ultrafiltration processes at different operating conditions such as temperature (10 – 40 °C) and feed volumes (3 - 9 L) for better separation of phytosterols from proteins in orange juice.

This chapter also describes the particle size analysis and the development of total phytosterols analysis for orange juice, which have not been discussed before. Both experiments were carried out at the beginning of this Phd project.

Statement of Authorship

This declaration concerns the article entitled:

Orange juice ultrafiltration: Characterisation of deposit layers and membrane surfaces after fouling and cleaning

Publication status (tick one)

Draft manuscript	☐	**Submitted**	✓	**In review**	☐	**Accepted**	☐	**Published**	☐

Publication details (reference)	Abd-Razak, N.H., John Chew, Y.M., Bird, M.R., 2021. Orange juice ultrafiltration: Characterisation of deposit layers and membrane surfaces after fouling and cleaning.
Candidate's contribution to the paper (provide details, and also indicate as a percentage)	**Formulation of ideas (80%):** The fluid dynamic gauging (FDG) was developed by John Chew. The application of FDG in membrane cleaning was suggested by John Chew. I proposed ideas for membrane characterisations and ultrafiltration process optimisation. **Design of methodology (80%):** John Chew proposed the experimental plan for FDG experiments. I designed the experimental set-up for the detailed characterisation of the membranes after fouling and cleaning to justify the findings from FDG analysis. **Experimental work (90%):** I carried out the experimental works in this paper including data analysis. AFM analysis of the samples was carried out by the technical staff. **Presentation of data in journal format (90%):** I prepared the manuscript for the journal including the outlines, graphics in the journal format and incorporated feedback from co-authors. The co-authors contributed in revising the draft manuscript.
Statement from Candidate	This paper reports on original research I conducted during the period of my Higher Degree by Research candidature.
Signed	▮	**Date**	25 Feb 2021

Orange juice ultrafiltration: Characterisation of deposit layers and membrane surfaces after fouling and cleaning

Nurul Hainiza Abd-Razak[1,2], Y.M. John Chew[1], Michael R. Bird[1*]

[1]Centre of Advanced Separations Engineering, Department of Chemical Engineering, University of Bath, Bath BA2 7AY, UK

[2]Rubber Research Institute of Malaysia, Malaysian Rubber Board, PO Box 10150, 50908 Kuala Lumpur, Malaysia

*Corresponding author. Email address: M.R.Bird@bath.ac.uk

Abstract

The influence of feed condition and membrane cleaning during the ultrafiltration (UF) of orange juice for phytosterol separation was investigated. To study the effect of feed conditions, the UF was performed using regenerated cellulose acetate (RCA) membranes at different molecular weight cut-off (MWCO) with a total filtration area of 336 cm^2 at different temperatures (10 – 40°C) and different feed volumes (3 - 9 L). Fluid Dynamic Gauging (FDG) was applied to assess the fouling and cleaning behaviours of RCA membranes fouled by orange juice and cleaned using *P3 Ultrasil 11* over two complete cycles. During the FDG testing, fouling layers were removed by fluid shear stress caused by suction flow. The cleanability was characterised by using *ImageJ* software analysis. The phytosterol content was quantified using a Liebermann-Buchard-based method. The results show that of the membranes tested, RCA 10 kDa filters exhibited the best separation of phytosterols from protein in orange juice at 20 °C using 3 L feed with a selectivity factor of 17. Membranes that were fouled after two cycles showed higher surface coverage compared to one fouling cycle. The surface coverage decreased with increasing fluid shear stress from 0 to 3.9 Pa. FDG achieved 80 to 95% removal at 3.9 Pa for all RCA membranes. Chemical cleaning using *P3-Ultrasil 11* altered both the membrane surface hydrophobicity and roughness. These results show that the fouling layer on RCA membranes can be removed by fluid shear stress without affecting the membrane surface modification caused by chemical cleaning.

Keywords: Ultrafiltration; Fouling; Chemical cleaning; Fluid dynamic gauging; Shear Stress

1.   Introduction

In the recent decades, ultrafiltration (UF) has grown to be an important process for industrial applications such as wastewater treatment (Lafi et al., 2018), food processing (Gulec et al., 2017) and recovery of bioactive compounds (Cassano et al., 2018). Membrane processes are of great interest in reducing the number of unit operations, recycling the process water and reducing the operation cost (Guo et al., 2012). However, the separation efficiency of membrane filtration can be limited by membrane fouling. Fouling refers to the accumulation of unwanted material on the membrane surface and/ or inside the membrane pores during the filtration. Membrane fouling will result in low permeate flux, reduced productivity, increase feed pressure, alter membrane properties and shortened membrane life (Meng et al., 2019). Fouling depends on membrane surface chemistry such as hydrophobicity, surface roughness and surface charge (Argyle et al., 2015; Evans et al., 2009). Fouling is also dependent on operating conditions such as transmembrane pressure, flow rates and concentration of feed components (Mulder, 1996). Temperature is an important parameter in membrane filtration for juice processing such as UF to separate anthocyanins, naritunin and hesperidin from orange juice (Cassano et al., 2007) and to recover anthocyanin from black currant juice (Pap et al., 2012). Therefore, the influence of temperature and feed concentration are essential to study in order to maintain the separation performance.

Study of membrane cleaning has been a complement to developing knowledge of membrane fouling. While fouling in membrane filtration is an unavoidable challenge, membrane cleaning has been developed to ensure that membrane technology is competitive with other technologies. Cleaning techniques such as chemical cleaning, mechanical cleaning, electric and hydraulic cleaning have been used to regenerate membranes. The cleaning method selected depends upon the configuration of the membrane module, the type of the membrane, the nature of the fouling layer and the degree of fouling present (Echavarría et al., 2011). Cleaning-in-place is applied by using cleaning agents such as acids, alkalis, oxidants, surfactants, enzymes or a combination thereof. The cleaning agent typically restores the membrane by dissolving, displacing or chemically modifying the fouling layer (Shi et al., 2014). The chemical agents can easily modify the membrane properties, thereby altering the filtration selectivity, reduce the membrane lifespan and increase

operational cost (Park et al., 2018). Mechanical cleaning has been applied to tubular membrane modules using sponge balls (Mulder, 1996), but this cleaning method was not able to remove organic foulants formed inside the membrane pores. The use of mechanical cleaning in membrane bioreactors by using scouring agents was developed as a novel approach to controlling membrane fouling (Aslam et al., 2017). The efficiency of mechanical cleaning is highly dependent on the types of foulants present. Small particles such as proteins may not be removed easily from the membrane surface using scouring agents.

Fluid dynamic gauging (FDG) is a technique developed to measure the thickness of soft fouling layers deposited on a non-porous (Tuladhar et al., 2000) and porous (Chew et al., 2007) substrates. Fluid dynamic gauging (FDG) has been applied to estimate the thickness of fouling layers of molasses solution deposited on microfiltration membranes (Jones et al., 2010) and to measure the strength of a softwood Kraft lignin on RCA membrane during the cross-flow microfiltration (Mattsson et al., 2015). Interestingly, FDG was also used to monitor the removal of cake layers in membrane cleaning through thickness measurement with controlled application of fluid shear to the surface of the cake layer (Lewis et al., 2012). Mechanical cleaning using FDG technique will be studied in this work and will be compared to the chemical cleaning that has been used in our previous study (Abd-Razak et al., 2020). The cleaned membranes after chemical cleaning was found to cause surface modification such as hydrophobicity, roughness (Abd-Razak et al., 2020) and surface charge (Abd-Razak et al., 2021).

The aims of this study are to assess the effects of operating conditions such as temperature and feed volume on the recovery of phytosterols from orange juice and to evaluate the cleanability of the membranes by chemical and/ or hydraulic cleaning. The novelty of this work is the application of FDG to study cleaning of fruit juice foulants formed on UF membranes. The purpose of using FDG is both in the quantification of the shear stress required to remove the fouling layers, and in the determination of the need for chemical cleaning to achieve an effective restoration of filtration performance.

2. Materials and Methods

2.1 Orange juice, solvents and standards

Processed orange juice (not from concentrate) was obtained from the local juice's manufacturer where the juice was prepared by using extraction and centrifugation (*Cobell*, UK). It was then stored in a cold room at 4 °C up to 2 months. The juice was first pre-filtered through a stainless steel 25 μm cartridge filter (*Memtech*, UK) to remove pulp prior to UF. Chloroform, methanol, acetic anhydride and sulphuric acid were purchased from *Merck*, UK. Stigmasterol from *Sigma Aldrich*, UK was used as characterisation standard. Protein assay kit was purchased from *Bio-Rad*, UK. The chemical cleaning after fouling was carried out using 0.5% *P3-Ultrasil 11* (*Henkel Ecolab*, USA) which contains sodium hydroxide, tetrasodium salt of EDTA, anionic surfactant and non-ionic surfactant (Weis et al., 2005).

2.2 Particle size analysis

The particle size distributions are characterised by the light scattering techniques such as laser diffraction and dynamic light scattering (Williams et al., 2017). In this study, the particle size distribution was analysed by laser diffraction using a Malvern Mastersizer X (*Malvern*, UK) at 20 °C. Five to 10 mL of orange juice was dispersed in RO water and introduced into the Mastersizer and circulated at 2000 rpm. The reading was recorded by the computer that equipped with Malvern Mastersizer software.

2.3 Membrane and ultrafiltration experiment

UF experiments were carried out using a cross flow filtration apparatus *LabStak M10*, developed by *Alfa Laval* (previously *DSS*) (Denmark). The regenerated cellulose acetate (RCA) flat-sheet membranes were supplied by *Alfa Laval* (Denmark). With a membrane area of 336 cm^2, the membranes were cut to size and positioned inside the membrane module. The membranes were initially conditioned using reverse osmosis (RO) water at 60 °C and at transmembrane pressure (TMP) of 1 bar for 120 minutes, to remove glycerol coating from the membrane surface. The

UF cycle comprises of membrane conditioning, pure water flux (PWF), filtration, rinsing and cleaning steps as described previously (Abd-Razak et al., 2019). The UF of orange juice was run for 60 minutes at TMP of 1 bar and the cross-flow velocity (CFV) of 1.5 m s^{-1}. There are two parts of experiments in this study. All UF experiments were done in triplicates.

The first part was focused on the investigation of feed conditions i.e. temperature and feed volume during the UF of orange juice using 10 kDa membrane with a commercial code RC70PP (*Alfa Laval,* Denmark). The operating temperature range for RCA membranes suggested by *Alfa Laval* is 5 to 60 °C. To study the effect of different feed conditions, the temperature of the feedstock during the UF using 10 kDa RCA membrane was adjusted from 10 to 40 °C and the orange juice feed volume used was 3L, 6L and 9L.

In the second part of this study, RCA membranes at three different MWCO (10 kDa, 30 kDa and 100 kDa) were used for the investigation of membrane cleaning. The membrane characteristics have been summarised previously in Abd Razak *et al.,* (2020). In order to study the effect of different membrane cleaning, the UF using RCA membranes were performed at 20°C using 3L orange juice. The membranes were cleaned by using chemical cleaning agent *P3-Ultrasil 11* at 60 °C for 10 minutes with a TMP of 1.0 bar. Mechanical cleaning was performed using fluid dynamic gauging (FDG) at 20 °C. These experiments are summarised in Figure 1.

Different Temperature		Different Feed Volume	
3 L Orange juice		3 L/ 6 L/ 9 L Orange juice	
10 °C/ 20 °C/ 40 °C		20 °C	

Conditioning	PWF 1	Ultrafiltration (UF)	Rinsing 1
RO water	RO water	Orange juice	RO water
60 °C	20 °C	60 minutes	20 °C
120 minutes	10 minutes	CFV 1.5 ms^{-1}	5 minutes
CFV 1.0 ms^{-1}	CFV 1.0 ms^{-1}	*For FDG, UF was run at 20°C using 3L orange juice	CFV 1.0 ms^{-1}

PWF 3	Rinsing 2	Chemical cleaning	PWF 2
RO water	RO water	*P3 Ultrasil-11*	RO water
20 °C	20 °C	60 °C	20 °C
10 minutes	5 minutes	10 minutes	10 minutes
CFV 1.0 ms^{-1}	CFV 1.0 ms^{-1}	CFV 1.0 ms^{-1}	CFV 1.0 ms^{-1}

Figure 1: Summary of ultrafiltration experiments. All steps were run at TMP 1.0 bar. 10 kDa membrane was used to study the effect of feed conditions. The UF step was run at 20 °C using 10 kDa, 30 kDa and 100 kDa RCA membranes to study the effect of membrane cleaning.

2.4 Fluid dynamic gauging (FDG)

Fluid dynamic gauging (FDG) has been shown to be a non-contact technique to measure the thickness and strength of deposits on surfaces (Chew et al., 2004; Lewis et al., 2012; Mattsson et al., 2015). Figure 2 and Figure 3 illustrate the apparatus used in this FDG study. This technique works by inducing a constant flow rate of fluid into the FDG nozzle. The suction flow into the gauge imposes a fluid shear stress (τ) on the fouling layers, to remove the foulant from the membrane surface. The fluid shear stress can be estimated by using Equation (1):

$$\tau = \frac{3\mu m}{\rho \pi h^2 r} \tag{1}$$

where μ is the dynamic viscosity of fluid, m is the gauging mass flow rate, ρ is the fluid density, h is the gap between the gauge and fouling sample and r is the inner radius of the FDG nozzle. Peck *et. al* (2015) who studied the removal of biofilms

deposit suggested that the shear stress imposed by the gauging flow is related to the mean pipe flow velocity (μ_{min}) as shown in Equation (2):

$$\mu_{min} = \sqrt{\frac{2\,\tau_{wall}}{\rho\,C_f}} \tag{2}$$

Where τ_{wall} is the wall shear stress, C_f is the friction factor, and ρ is the fluid density. For turbulent flow regimes, the friction factor (C_f) is equal to 0.005.

The shear stress on the surface due to gauging flow depends on the dimensionless value of h/d_t and flow conditions (Peck et al., 2015). The dimensionless value of h/d_t is the ratio of nozzle clearance distance to the nozzle inner diameter. Figure 2(a) shows the schematic of a FDG nozzle. Figure 2(b) shows an example of a fouled RCA membrane. The dashed line shows a dimension and footprint of the FDG nozzle inner diameter, $d_t = 5$ mm and nozzle outer diameter = 10 mm. The FDG nozzle was installed in a custom-made test rig as described in Figure 3. The process fluid used for FDG tests was RO water that is drawn through a nozzle at a constant flow rate of 25 ml min^{-1}. The suction flow was controlled by a digital mass flow meter (*mini CORI-FLOW*, Bronkhorst, UK). A fouled membrane was cut and mounted on the stainless-steel plate at the bottom of the FDG nozzle. The gauging nozzle was positioned at the centre of the membrane sample that installed on the stage as shown in Figure 3. Measurements were performed for a set of known values of h/d_t at difference nozzle clearance heights to impose a range of shear stress. All h/d_t measurements were done in triplicate. A micrometer (*Mitutoyo*, Japan) was used to adjust the vertical movements of the gauge and to measure the clearance height from the membrane. A traversing screw was installed to the rig to allow the horizontal movements of the gauge. The system was controlled and monitored by using a *LabView* visual interface. All images of fouled and cleaned membranes were captured using the *Samsung A3* camera. The removal of fouling layers on the membrane surfaces were analysed using *ImageJ* analysis by measuring the percentage area of the membrane that covered with the foulants, with a known scale bar to convert the actual pixels on the images.
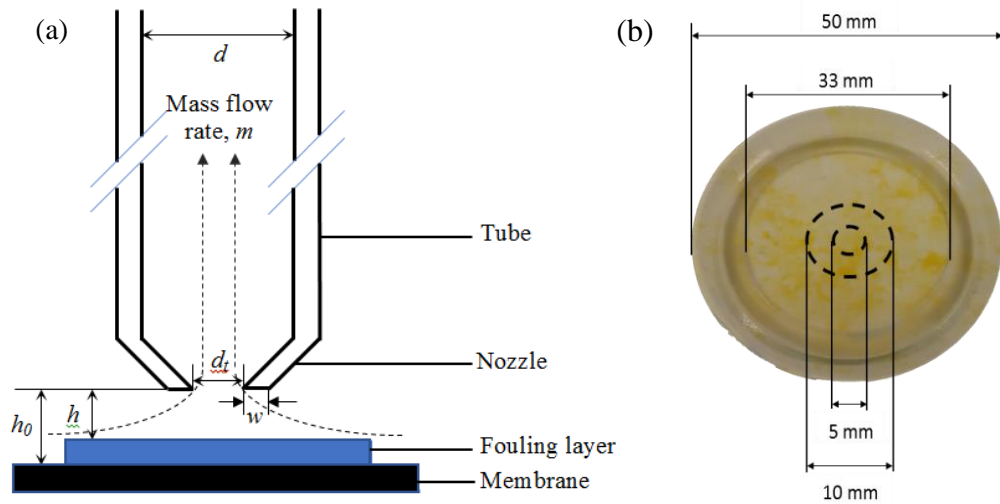
Figure 2: (a) Schematic of a FDG nozzle showing dimensions, where the nozzle inner diameter, d_t = 5 mm, tube inner diameter, d = 25 mm and nozzle thickness, w = 2 mm; (b) example of a membrane fouled by orange juice, where dashed line shows a dimension of the nozzle inner diameter, d_t = 5 mm and nozzle outer diameter = 10 mm.
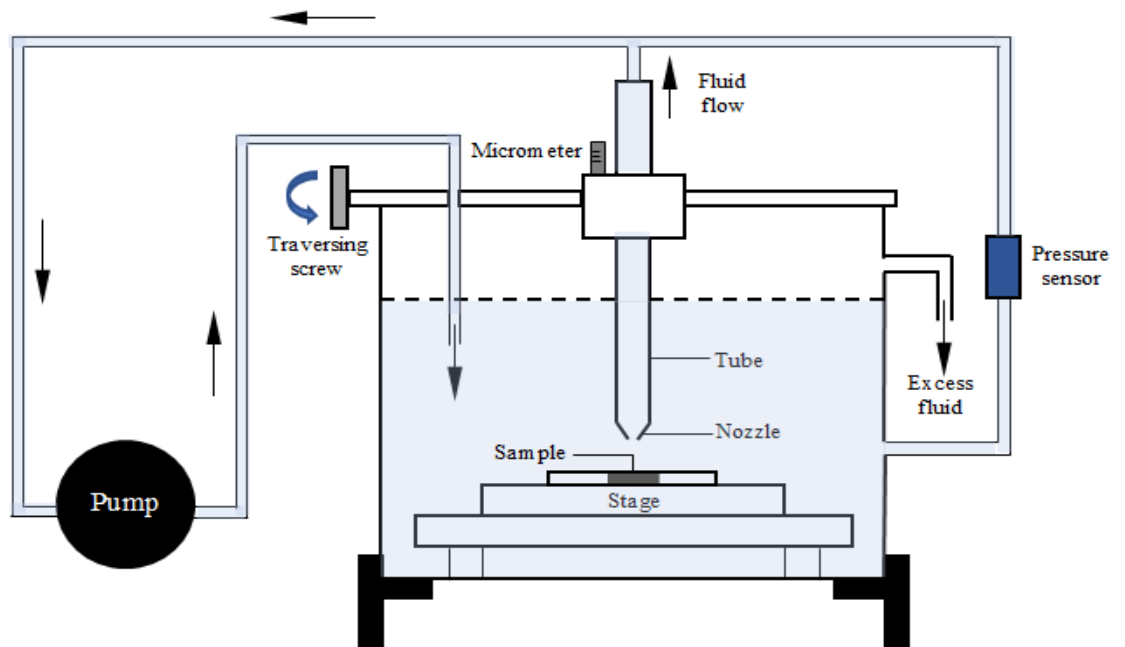
Figure 3: Schematic of the FDG test rig used in this study. The fluid used was RO water.

2.5   Fouling and cleaning experiment

RCA membranes at different molecular weight cut-off were fouled with orange juice over two fouling-cleaning cycles and cleaned using two different cleaning methods. Chemical cleaning was applied using 0.5% *P3-Ultrasil 11*, as mentioned in Section 2.1. Mechanical cleaning was carried out using fluid dynamic gauging (FDG) as described in Section 2.4. The fouling and cleaning cycles were performed as summarised and labelled below:

i.   **Fouled 1 (F1)** – to understand the fouling characteristics of orange juice.

ii.   **Fouled 1 (F1) → Chemical cleaning (CC)** – to investigate the effect of chemical cleaning on surface properties of membrane.

iii.   **Fouled 1 (F1) → Fluid dynamic gauging (FDG)** – to investigate the effect of mechanical cleaning imposed by FDG on surface properties of membrane.

iv.   **Fouled 1 (F1) → Chemical cleaning (CC) → Fouled 2 (F2)** – to investigate the effect of chemical cleaning on fouling behaviour.

v.   **Fouled 1 (F1) → Chemical cleaning (CC) → Fouled 2 (F2) → Fluid dynamic gauging (FDG)** – to investigate the effect of chemical cleaning on fouling removal.

2.6   Membrane performance

The permeate flux is defined as the volumetric flow rate of the fluid through the membrane (Mulder, 1996). The permeate flux can be calculated according to Equation (3):

$$J = \frac{\Delta P}{\mu R_{tot}} \tag{3}$$

where J is the flux through the membrane (L m^{-2} h^{-1}), ΔP (Pa) is the transmembrane pressure (TMP), μ is the dynamic viscosity (kg m^{-1} s^{-1}) and R_{tot} is the total resistance (m^{-1}). The resistance in series model is represented in Equation (4) (Jiraratananon and Chanachai, 1996):

$$J = \frac{\Delta P}{\mu \left(R_m + R_f + R_{cp} \right)} \tag{4}$$

167

where R_m is the membrane resistance, $R_{f\,is}$ the total fouling resistance and R_{cp} is the resistance due to concentration polarisation. The rejection ratio, R, was calculated by using Equation (5):

$$R = (1 - \frac{C_p}{C_r})$$ (5)

where C_p is the solute concentration in the permeate and C_r is the solute concentration in the retentate (Mulder, 1996). The separation factor, $\alpha_{A/B}$, was calculated using Equation (6):

$$\alpha_{A/B} = \frac{y_A / y_B}{x_A / x_B}$$ (6)

where y_A and y_B are concentrations of phytosterols and proteins in the permeate, and x_A and x_B are concentrations of phytosterols and proteins in the feed.

2.7 Quantitative determination of compounds

2.7.1 Total phytosterols analysis

Total phytosterols content was determined spectrophotometrically by using Liebermann-Buchard (LB) based method (Mbaebie et al., 2012; Sathishkumar and Baskar, 2014). The absorbance was measured at 420 nm using an Ultraviolet-visible (UV-Vis) Spectrophotometer (Cary 100, *Agilent,* USA). The LB reagent was prepared by dissolving sulphuric acid in acetic anhydride in the ratio 1:10. 5 ml chloroform was added to 1 ml sample in a test tube, followed by vortex mixed for 1 minute. A portion of 2 ml extract was taken from the solution and mixed with 2 ml LB reagent. The tubes were incubated for 5 to 20 minutes under dark condition at 20°C. The colour of the solution was found to change from yellow to green colour after the addition of LB reagent indicated the presence of phytosterol. Standard solutions of stigmasterol were used for calibration. Chloroform was used as the blank. The total phytosterol content (TPC) was calculated using the standard photometric correlation Equation (7) (Araújo et al., 2013; Kim and Goldberg, 1969):

$$\text{TPC} = C_s \times \frac{A_u}{A_s} \tag{7}$$

where C_s is the concentration of stigmasterol in standard solution, A_u is the absorbance of the sample, A_s is the absorbance of the standard solution. All measurements were done in triplicate and the results were averaged.

2.7.2 Protein analysis

Protein concentration was quantified by the Bradford method (Cassano et al., 2008; Kruger, 1994). The assay is based on the binding of acidic dye solution Coomassie Brilliant Blue G-250 to protein at maximum absorbance from 465 to 595 nm (Bradford, 1976). The dye reagent was prepared by diluting one part of protein assay dye reagent concentrate (*Bio-Rad Laboratories*, Hercules, USA) with 4 parts of deionized water. A calibration curve was constructed by a serial dilution of bovine serum albumin (BSA) from 0.2 to 1.0 mg ml^{-1}. 5 ml of diluted dye reagent was added to 100 μl of standard and sample solutions. The mixed solutions were mixed vigorously and incubated at room temperature for 10 minutes. Absorbance for the protein concentration was measured at 595 nm using UV-Vis Spectrophotometer (*Cary 100, Agilent*, USA). All measurements were done in triplicate and the results were averaged.

2.8 Membrane surface analysis techniques

2.8.1 Contact angle measurement
The hydrophobicity of the membrane surface before and after fouling and cleaning was determined by measuring the contact angle via sessile drop method. Contact angle measurements were conducted at 20°C using *DataPhysics Optical Contact Angle System OCA 25* (Filderstadt, Germany) equipped with image processing software *DataPhysics Instruments SCA 22*. A deionised water was used to form the drop for the contact angle measurement.

2.8.2 Surface roughness measurement

The surface roughness of fouled and cleaned membranes were determined by atomic force microscopy (AFM) analysis. The instrument used was a Multimode AFM (*Veeco Metrology*, USA) with a *Nanoscope Analysis 1.7* software. The cantilever was used in contact mode with silicon soft tapping mode tips (*Tap150AI-G, Budget Sensors*, Bulgaria). Images were scanned at 1 μm × 1 μm scan size at a rate of 1 Hz.

2.8.3 Scanning electron microscope (SEM) analysis

Scanning electron microscope (SEM) images of membranes surfaces were taken at 10,000 or 15,000× magnification. The samples were viewed with a *JEOL SEM* model *JSM 6480LV* (Japan).

3. Results and Discussion

3.1 Particle size distribution

Orange juice contains a polydisperse distribution of particle size from pulp trashes to small particles which are less than 2 μm in diameter (Corredig et al., 2001). The pre-filtration step was carried out using a 25 μm cartridge filter. A pre-filtration step is required to remove pulp and particles with diameter > 25 microns prior to UF. The UF process was conducted using RCA membranes with 10 kDa MWCO (RCA 10 kDa). To assess the efficiency of the pre-filtration and UF process, particle size distribution of orange juice was investigated.

Figure 4 shows the particle size distribution in four orange juice samples namely, Pre-filtration-Feed, Pre-filtration-Permeate, UF-Feed and UF-Permeate. Sample named Pre-filtration-Feed is fresh orange juice before the pre-filtration process and Pre-filtration-Permeate is orange juice collected after pre-filtration using the 25 μm cartridge. Sample labelled as Pre-filtration-Permeate was kept for 24 hrs and used as the feed for the UF (UF-Feed). Meanwhile, UF-Permeate refer to orange juice that was collected after the UF in the permeate. The analysis clearly shows that Pre-filtration-Feed contain particle size more than 100 μm. The particle sizes for Pre-filtration-Permeate and UF-Feed were less than 25 μm. However, the particle size distribution differs between both samples. This confirmed the stability of the feed

sample for the UF after 24 hrs storage, but the samples might be coagulated after 24 hrs storage. The particle sizes of UF-permeate after the ultrafiltration was around 1 nm at 95% composition. To conclude, the UF produces smaller particle size than the pre-filtration and the pre-filtration using 25 μm cartridge filter was efficient in this system.
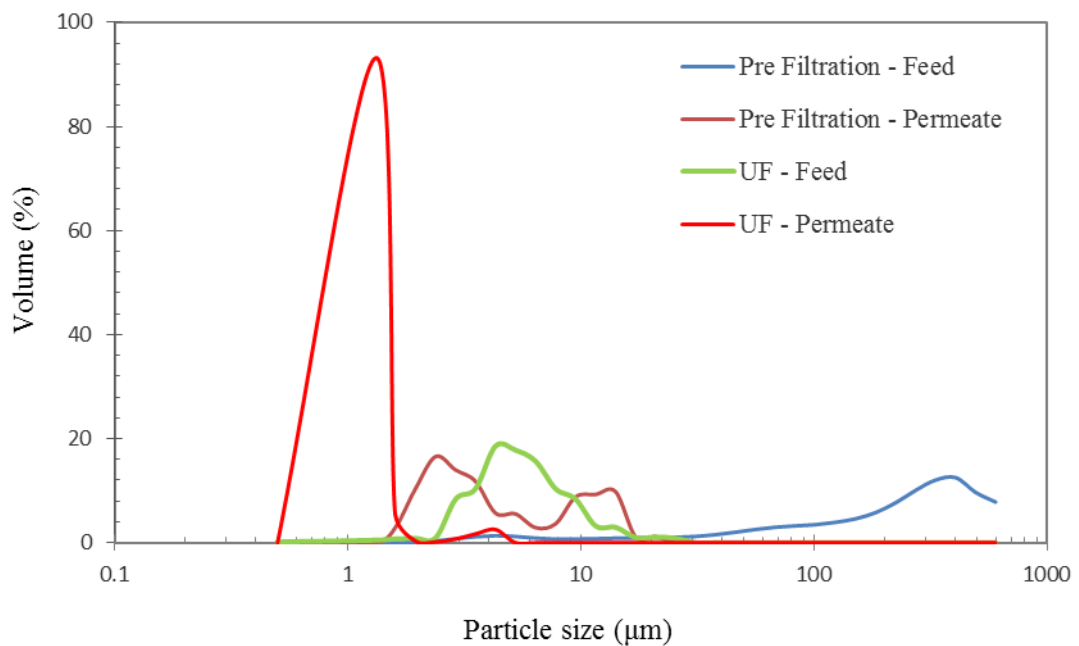
Figure 4: Particle size distribution in the different orange juice samples.

3.2 Modification of total phytosterol analysis

Total phytosterols analysis was carried out after UF using UV-spectrophotometer by Liebermann-Buchard (LB) method. The LB method have been widely used for the qualitative and quantitative determination of steroids especially cholesterols (Kenny, 1952; Kim and Goldberg, 1969). Phytosterols are cholesterol-like molecules that are present in plants and therefore LB method has been applied in this work (Araújo et al., 2013; Mbaebie et al., 2012; Sathishkumar and Baskar, 2014). The analysis method was modified for the total phytosterols content in orange juice since there is no study reported using this sample. The incubation time for the reaction to take place was modified because other studies used different incubation times between 5 to 30 minutes before the UV analysis. The LB reagent reacts with the chloroform extract to produce a greenish solution that indicates the presence of phytosterol, and

the absorbance was measured via UV spectrophotometer. In the existence of the LB reagent, the phytosterols are protonated and dehydrated with loss of H_2O, which produces carbonium ion of 3,5-cholestadiene (Burke et al., 1974). The absorbance for phytosterols detection was observed at two wavelengths i.e. 420 nm (Kenny, 1952; Mbaebie et al., 2012) and/ or 625 nm (Araújo et al., 2013; Kim and Goldberg, 1969) after wavelength scanning from 400 nm to 900 nm.

Figures 5 (a) and (b) show the UV spectrums for the LB reaction of standard stigmasterol at concentration 1.0 mg ml^{-1} and 0.5 mg ml^{-1}, respectively. The suitable wavelength for this analysis was at 420 nm, as shown in Figure 5 (c), because the orange juice samples produced the absorbance signal only at wavelength 420 nm. Similar findings have been observed in other studies (Kenny, 1952; Mbaebie et al., 2012). The chemical reaction produced final compound called cholestahexaene sulfonic acid which can be detected at 420 nm. The reaction produced an intermediate compound called pentaenylic cation which detected at 625 nm. The behaviour of the reaction is possibly due to conversion of acetate derivatives of the steroids after the reaction with LB reagent as discussed by Burke *et al.* (1974). According to the incubation time for the reaction, for both concentrations of standard stigmasterol, maximum absorbance was achieved at 15 min after the addition of LB reagent (Figure 5 (a) and (b)). The absorbance increased from 5 min to 15 min and then decreased after 15 min. Therefore, the incubation time during the analysis of orange juice was carried out for 15 minutes.
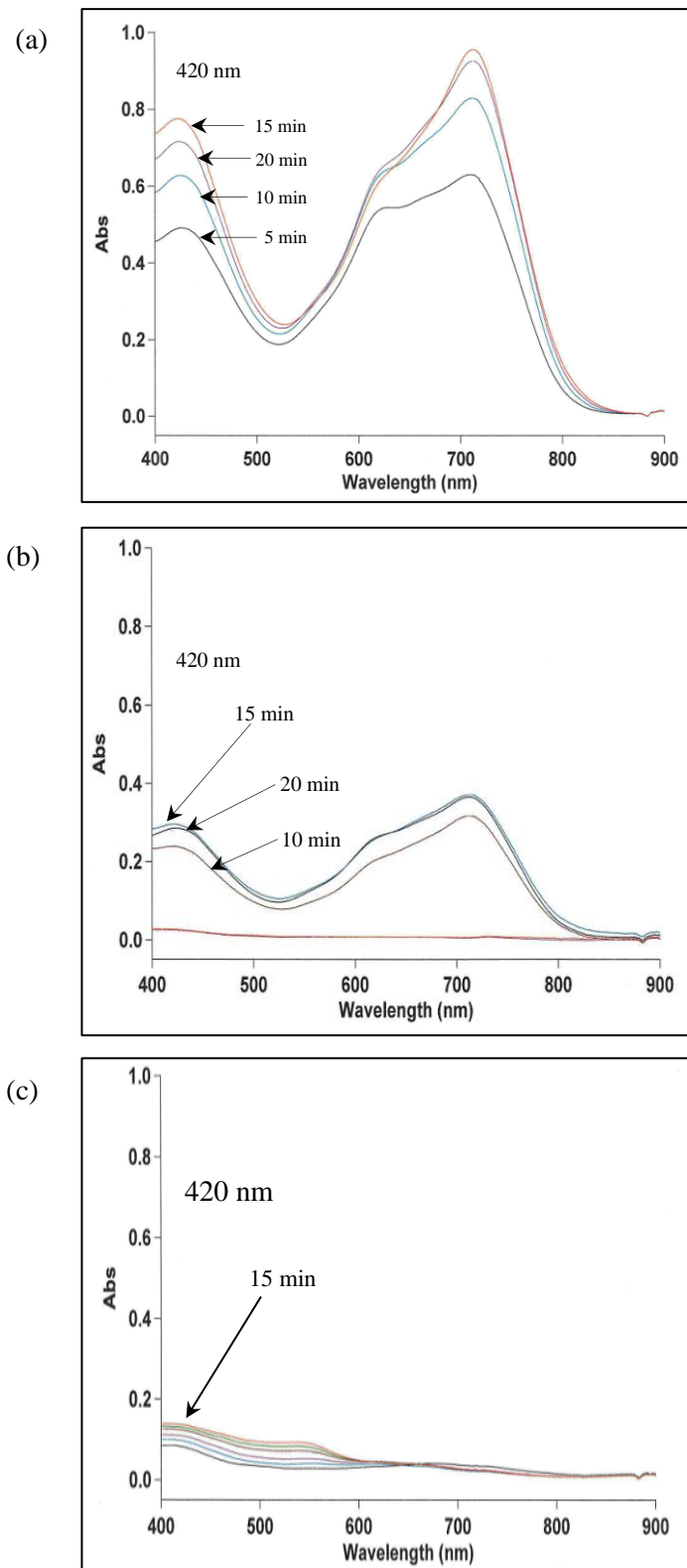
Figure 5: UV spectrums for the LB reaction of (a) standard stigmasterol at 1.0 mg ml^{-1}, (b) standard stigmasterol at 0.5 mg ml^{-1} and (c) orange juice samples at different concentrations.

3.3   Effect of feed conditions

3.3.1 Effect of temperature

The permeate flux in a UF unit with a total recycle mode increased by 60 % as the feed temperature increased from 25 °C to 45 °C for the black current juice processing (Pap et al., 2012). Based on the recommended operating temperature of RCA membranes by *Alfa Laval*, which is in the range of 5 °C to 60 °C, the temperature of the permeate fluxes were investigated from 10 °C to 40 °C. The changes of membrane permeate flux and total fouling resistances (R_f) with operating time at different temperature are presented in Figure 6. The highest initial flux at 46 L m^{-2} h^{-1} was obtained at a temperature value of 40 °C. The initial permeate fluxes at 10 °C and 20 °C were 25 L m^{-2} h^{-1} and 29 L m^{-2} h^{-1}, respectively. This result is in agreement with the studies conducted by Pap *et al.* (2012) and Qaid et al., (2017) which could be attributed to the reduction in solute viscosity and higher solute permeability at higher temperature. The diffusion coefficient of macromolecules increases when the temperature increase in the UF for clarification of *Valencia* orange juice (Qaid et al., 2017). The initial flux declined gradually in the first 10 min for all three conditions. This suggests that some particles were blocking the membrane pores and larger particles were accumulating on the membrane surface which led to a reduction in filtration area. After 10 min, the permeate flux approached pseudo steady state value until the filtration stopped at 60 min. The highest steady state permeate flux of RCA membrane was achieved at 40 °C with flux value 25 L m^{-2} h^{-1} indicating a flux decline of 46 %. The lowest steady state permeate flux of was achieved at 10 °C with flux value 17 L m^{-2} h^{-1} indicating a flux decline of 32 %. The decreasing in permeate flux can be explained by the effect of membrane fouling (Cassano et al., 2007). The fouling mechanism during the UF of blood orange juice was changed from a partial to a complete pore blocking as reported by Cassano et al., (2007). Even though 40 °C gave higher overall flux but the degree of decrease is more severe due to fouling.

The total fouling resistances (R_f) against filtration time for RCA membranes tested at different temperature were calculated from flux data by rearrangement of Equation (3). The graph was plotted with membrane resistance, $R_m = 3 \times 10^{12}$ m^{-1} as shown in Abd Razak *et al.,* (2020). In this work, the concentration polarisation

resistance (R_{cp}) is negligible. The resistance graph shows that there was a difference in fouling resistance at 40 °C. UF at 40 °C gave higher fouling resistance compared to UF at 10 °C and 20 °C. This may suggest that orange juice at higher temperature with lower viscosity produced high fouling resistance that led to membrane fouling. Black currant juice filtration at low temperature was suggested by Pap *et al.* (2012) to avoid precipitation of protein particles and to reduce membrane fouling. This result suggests that the operating temperature at 40 °C is not optimal for orange juice filtration.
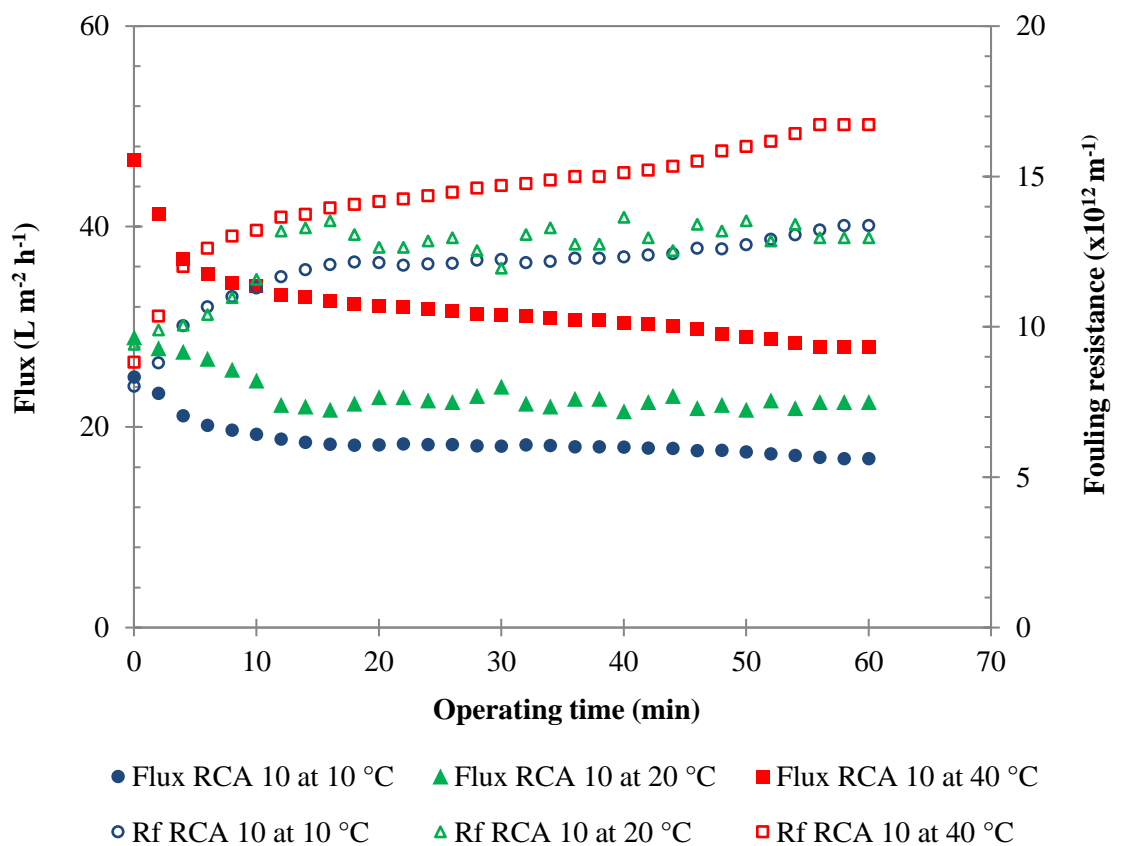
Figure 6: Time course of permeate flux decline and total fouling resistance for RCA membranes tested at different temperatures. The largest error for this set of data is ± 1.5 L m^{-2} h^{-1}. Closed symbols in Figure 6 represent the permeate fluxes, and open symbols represent the total fouling resistances.

Figure 7 shows the rejection of key compounds i.e. total phytosterols and proteins by RCA 10 kDa membranes at three different temperatures. The best separation should present a low rejection of phytosterols and a high rejection towards

proteins. Previously, Abd Razak *et al.* (2020) reported that UF at 20 °C using RCA 10 kDa membrane displayed good separation efficiency with 32 ± 4 % rejection of phytosterols and 96 ± 1 % rejection of protein. Figure 7 shows that UF at lower temperature (10 °C) using RCA 10 kDa membrane exhibited different separation efficiency with 56 ± 1 % rejection of phytosterols and 95 ± 2 % rejection of protein. The results also show that more phytosterols were collected in the permeate at higher temperatures. Therefore, an attempt has been made to run the filtration at higher temperature which was at 40 °C. As expected, lower rejection of phytosterols (35 ± 5 %) was achieved during the UF at 40 °C using RCA 10 kDa membrane. In general, proteins were highly rejected by RCA 10 kDa membrane at 10 °C and 20 °C. However, only 72 ± 2 % rejection of proteins was observed at 40 °C. Soy bean processing at high temperature (40 – 50 °C) changed the conformation of the protein structure that leads to protein precipitation (Zayas, 1997). Aghajanzadeh et al., (2017) studied the effect of thermal processing on proteins stability in orange juice. Temperature above 40 °C caused denaturation of proteins called pectin methylesterase (PME) in orange juice. The proteins structure changed due to the breaking up of the hydrogen bonds and unfolding of the tertiary protein structure at 40 °C (Aghajanzadeh et al., 2017). Therefore, more proteins have been passed through the RCA 10 kDa membrane and collected in the permeate at 40 °C.
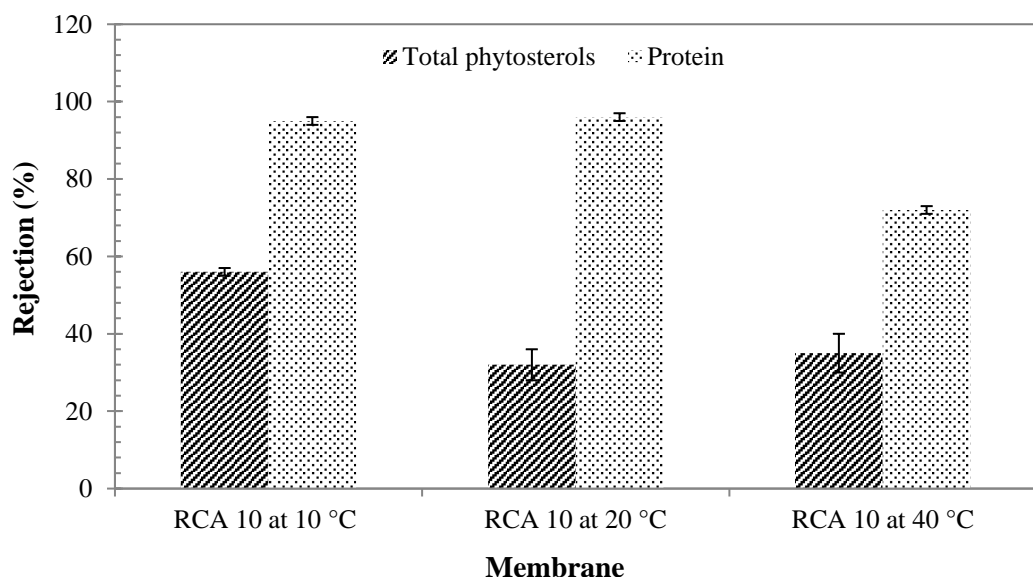
Figure 7: Rejection of total phytosterols and proteins by RCA 10 kDa membranes at different temperatures.

The mass balance for the total phytosterols and proteins following UF using 10 kDa membranes at 10 °C, 20 °C and 40 °C is presented in Table 1. In order to study the effect of temperatures, the initial feed volume of orange juice was 3 L with 830 ± 70 mg total phytosterols present in the feed solution. The yields of total phytosterols in the permeate for filtrations at 10 °C, 20 °C and 40 °C were 78 mg, 135 mg and 190 mg respectively. The mass concentration ratio of phytosterol to protein was increased from feed to permeate streams at all conditions (Table 1). The quality of separation is expressed by the separation factor of the membrane which was calculated from the mass concentration ratio. The lowest separation factor which was 2.0 can be seen in Table 1 (c) for the UF at 40 °C. This result is consistent with the rejection data (Figure 7) that showed more proteins were collected in the permeate probably due to the changes in membrane pore size at high temperature (Goosen et al., 2002). UF using RCA 10 kDa membrane at 20 °C gave the highest separation factor which was 17.3. The mass concentration ratio of phytosterol to protein increased from 0.3 in the feed to 5.2 in the permeate (Table 1 (b)). The losses of phytosterols and proteins at all three conditions were presumably due to the fouling effect during the filtration (Cassano et al., 2008). The phytosterols were trapped by the fouling layer and not passed through the membrane. This finding revealed that proteins can be separated from the phytosterols by UF at 20 °C.

Table 1: Mass balance and separation factor for total phytosterols and protein by UF process of orange juice with 10 kDa RCA membranes at; (a) 10 °C, (b) 20 °C and (c) 40 °C.

(a) At 10 °C	Feed	Permeate (% of feed)	Retentate (% of feed)	Total (%)
Volume (ml)	3000	600 (20%)	2400 (80%)	100
Total phytosterols (mg)	913	78 (9%)	707 (78%)	87
Protein (mg)	2911	25 (1%)	2235 (77%)	78
Concentration ratio (phytosterols to protein)	0.3	3.1		
Separation factor	10.3			

(b) At 20 °C	Feed	Permeate (% of feed)	Retentate (% of feed)	Total (%)
Volume (ml)	3000	850 (28%)	2150 (72%)	100
Total phytosterols (mg)	810	135 (17%)	504 (62%)	79
Protein (mg)	2910	26 (1%)	2408 (83%)	84
Concentration ratio (phytosterols to protein)	0.3	5.2		
Separation factor	17.3			

(c) At 40 °C	Feed	Permeate (% of feed)	Retentate (% of feed)	Total (%)
Volume (ml)	3000	1200 (40%)	1800 (60%)	100
Total phytosterols (mg)	755	190 (25%)	441 (58%)	83
Protein (mg)	2807	317 (13%)	1721 (61%)	74
Concentration ratio (phytosterols to protein)	0.3	0.6		
Separation factor	2.0			

3.3.2   Effect of feed volume

In this study, the loss of phytosterols to the foulant layers was addressed by increasing the total volume of feed filtered, whilst maintaining the membrane area at the same value. As a hypothesis, the filtration with larger feed volume can be used to increase the total amount of sterol present in the system. The UF was carried out at 20 °C based on the results from previous experiment. In Figure 8 there is a clear trend of decreasing permeate flux with operating time at three different feed volumes. Figure 8 shows that the initial permeate fluxes for all membranes were almost similar (26 ± 1 L m^{-2} h^{-1}). The initial permeate fluxes using 3 L, 6 L and 9 L orange juices decreased with filtration time until it reached steady-state values of 23 L m^{-2} h^{-1}, 19 L m^{-2} h^{-1} and 18 L m^{-2} h^{-1} at approximately 12 minutes. The initial fluxes declined gradually within the first 10 min for all three conditions. It is likely that the membranes were fouled which led to a reduction of filtration area. After the 60 min filtration, UF using 6 L and 9 L orange juices showed lower permeate flux compared to 3 L feed volume. This is likely due to the higher concentration of proteins in high volume of feed solution which caused the membrane fouling. The losses of proteins in feed solution were presumably due to the solute-membrane interaction and adsorption of solute on the membrane surface or inside the pores (Cassano et al., 2008).
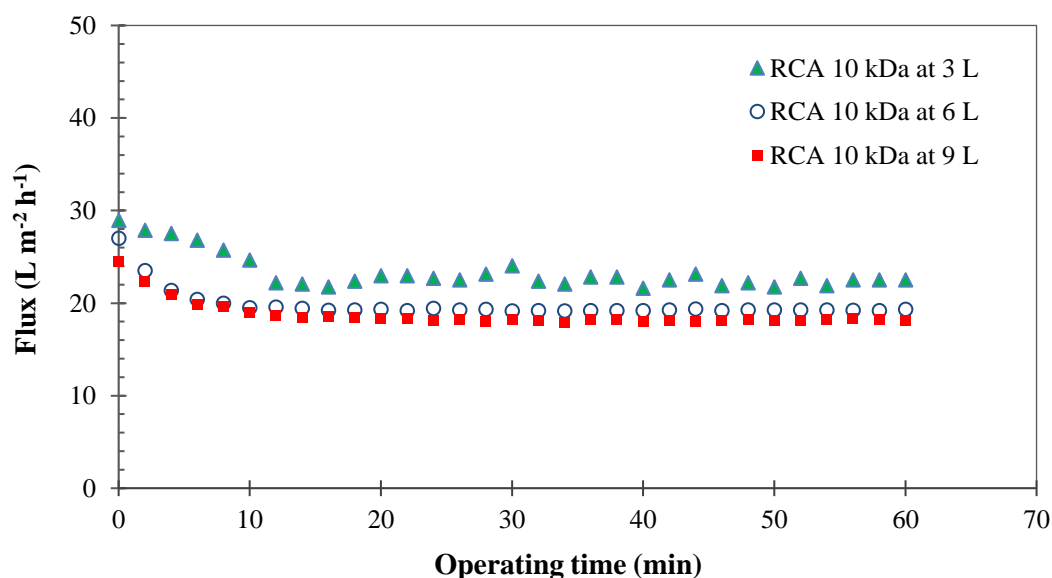
Figure 8: Time course of permeate flux decline for RCA membranes tested at different feed volume at 20 °C. The largest error for this set of data is ± 1.5 L m^{-2} h^{-1}.

Table 2 presents a mass balance and separation factor for total phytosterols and proteins by UF with 10 kDa RCA membranes using three different feed volumes; 3 L, 6 L and 9L orange juices. In this experiment, the initial total phytosterols present in feed solution were varied from 810 mg in 3 L orange juice to 2430 mg in 9 L orange juice. Meanwhile the initial proteins in feed solution were of 2910 mg and 8640 mg for 3 L and 9 L orange juice. This is in agreement with the hypothesis that larger feed volume offered larger amount of phytosterol in the system. The mass concentration ratio of sterol to protein was increased from feed to permeate streams at all conditions (Table 2). The mass concentration ratio of sterol to protein increased from 0.3 in the feed to 5.2 in the permeate for the UF using 3 L orange juice. The mass concentration ratio of sterol to protein changed from 0.3 in the feed to 4.6 in the permeate for the UF using 9 L orange juice. The separation factor (Equation 4) for the UF using 3 L, 6 L and 9L orange juices were 17.3, 13.0 and 15.3 respectively. To conclude, increasing feed volume could not improve the separation efficiency in this system.

Table 2 also shows that there was insignificant difference in volume of permeate after 60 min filtration for all three conditions. UF using 3 L orange juice produced 850 ml permeate. Interestingly, 800 ml permeate was collected from the filtration using larger feed volume which was 6 L and 9 L orange juice. This means that less total phytosterols can be collected in the permeate. The lower separation factor seen in Table 2 for 6 L and 9 L orange juice are possibly linked to a greater loss of proteins into the cake layer. The 22 % loss of proteins in the system at 6 L feed volume and 23 % loss for 9 L feed volume were most probably due to the fouling during the filtration (Cassano et al., 2008). It is possible that the phytosterols were trapped by the fouling layer which is proteins and not passed through the membrane. This study discovered that the best separation of phytosterols from proteins in orange juice by UF using RCA membranes at cross flow velocity (CFV) of 1.5 m s^{-1} can be achieved by using 3 L feed volume. In the future, this process can be improved by increasing the CFV to increase the permeate flux in order to achieve higher permeate volume.

Table 2: Mass balance and separation factor for total phytosterols and protein by UF process of orange juice with 10 kDa RCA membranes at different feed volume; (a) 3 L, (b) 6 L and (c) 9L.

(a) 3 L	Feed	Permeate (% of feed)	Retentate (% of feed)	Total (%)
Volume (ml)	3000	850 (28%)	2150 (72%)	100
Total phytosterols (mg)	810	135 (17%)	504 (62%)	79
Protein (mg)	2910	26 (1%)	2408 (83%)	84
Concentration ratio (phytosterols to protein)	0.3	5.2		
Separation factor	17.3			

(b) 6 L	Feed	Permeate (% of feed)	Retentate (% of feed)	Total (%)
Volume (ml)	6000	800 (13%)	5200 (87%)	100
Total phytosterols (mg)	1620	137 (9%)	1155 (71%)	80
Protein (mg)	5760	35 (1%)	4420 (77%)	78
Concentration ratio (phytosterols to protein)	0.3	3.9		
Separation factor	13.0			

(c) 9 L	Feed	Permeate (% of feed)	Retentate (% of feed)	Total (%)
Volume (ml)	9000	800 (9%)	8200 (91%)	100
Total phytosterols (mg)	2430	147 (6%)	1885 (78%)	84
Protein (mg)	8640	32 (1%)	6560 (76%)	77
Concentration ratio (phytosterols to protein)	0.3	4.6		
Separation factor	15.3			

3.4 Membrane fouling and cleaning

3.4.1 Fluid dynamic gauging (FDG)
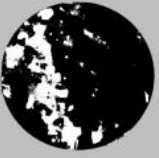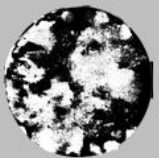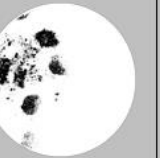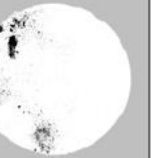
The cleaning of regenerated cellulose membranes using FDG was carried out in order to compare with chemical cleaning method. The purpose of using FDG is to measure the shear stress required to remove the fouling layers and to determine if chemical cleaning is sufficient to achieve effective cleaning. FDG has previously been demonstrated as a method for the estimation of fouling layer thickness and strength during membrane filtration (Jones et al., 2010; Mattsson et al., 2015). However, the fouling layers obtained in this work were too thin and the thickness of the fouling layers could not be measured reliably. Therefore, the surface coverage of the membranes was analysed using *ImageJ* analysis to characterise removal of fouling deposits by using FDG.

Figure 9 (a) shows the images of FDG cleaning for RCA 10 kDa after first fouling-cleaning cycle (**(F1)** → **(FDG)**). The images of FDG cleaning for RCA 10 kDa after second fouling-cleaning cycle (**(F1)** → **(CC)** → **(F2)** → **(FDG)**) are presented in the Supporting Information. For RCA 10 kDa (**(F1)** → **(FDG)**), the surface coverage decreased from 84 ± 2 % to 4 ± 2 % at shear stress from 0 Pa to 3.9 Pa. The same trend was observed in RCA 10 kDa (**(F1)** → **(CC)** → **(F2)** → **(FDG)**) with surface coverage decreased from 87 ± 4 % to 8 ± 2 % at shear stress from 0 Pa to 3.9 Pa. These results indicate that RCA 10 kDa membranes which were fouled twice gave a bit higher surface coverage compared to one time fouling. According to Abd Razak *et. al* (2020), it was postulated that the RCA 10 kDa membrane was fouled with a cake of proteins, as proteins were highly rejected by the 10 kDa membrane. Hydrophilic membranes like RCA 10 kDa were found to have more reversible than irreversible fouling.

The FDG cleaning for RCA 30 kDa (**(F1)** → **(CC)** → **(F2)** → **(FDG)**) is shown in Figure 9 (b). Figure 12 in the Supporting Information presents the images of FDG cleaning for RCA 100 kDa membrane. At shear stresses from 0 Pa to 3.9 Pa, the surface coverage of RCA 30 kDa (**(F1)** → **(FDG)**) and RCA 30 kDa (**(F1)** → **(CC)** → **(F2)** → **(FDG)**) were 88 ± 3 % to 9 ± 3 % and 94 ± 2 % to 13 ± 2 % respectively. These results suggest that the surface coverage after two-times fouling was higher than that for one-time fouling. Abd Razak *et. al* (2020) reported that

intermediate pore blocking was the dominant fouling mechanism for both RCA 30 kDa and RCA 100 kDa membranes. The larger pore membranes enabled protein-based foulants to enter the structure more deeply. Thus, a higher shear stress is needed to achieve a greater removal of fouling from these two membranes. In general, Figure 9 shows that the surface coverage decreased with increasing shear stress from 0 to 3.9 Pa for all membranes. The RCA 10 kDa membrane was cleaned more easily using FDG than either theRCA 30 kDa or the RCA 100 kDa membranes, as the RCA 10 kDa membrane showed the lowest surface coverage. This result indicates that mechanical cleaning using fluid shear stress did not alter the fouling behaviour of the membrane.

(a) RCA 10 kDa ((**F1**) → (**FDG**))

h/dt	No gauging	0.15	0.10	0.06	0.04
Shear stress [Pa]	0	0.28	0.62	1.73	3.90
Before					
Image J					
% Surface coverage (ImageJ)	84 ± 2	57 ± 2	35 ± 3	11 ± 3	4 ± 2
Area/ $Area_0$	1.00	0.68 ± 0.02	0.42 ± 0.03	0.13 ± 0.03	0.05 ± 0.01

(b) RCA 30 kDa ((**F1**) → (**CC**) → (**F2**) → (**FDG**))

h/dt	No gauging	0.15	0.10	0.06	0.04
Shear stress [Pa]	0	0.28	0.62	1.73	3.90
Before					
Image J					
% Surface coverage (ImageJ)	94 ± 2	74 ± 3	62 ± 2	36 ± 2	13 ± 2
Area/ $Area_0$	1.00	0.79 ± 0.02	0.66 ± 0.01	0.39 ± 0.01	0.14 ± 0.02

Figure 9: Surface coverage of the RCA membranes after FDG cleaning analysed by *ImageJ*; (a) RCA 10 kDa ((**F1**) → (**FDG**)), and (b) RCA 30 kDa ((**F1**) → (**CC**) → (**F2**) → (**FDG**)).

Figure 10 shows the surface coverage of RCA membranes after FDG cleaning at four different shear stress values, from 0.28 to 3.9 Pa. Open symbols in Figure 10 represent the first fouling-cleaning cycle ((**F1**) → (**FDG**)) and close symbols represent second fouling-cleaning cycle ((**F1**) → (**CC**) → (**F2**) → (**FDG**)). The surface coverage for all membranes decreased with increasing shear stress from 0.28 to 3.9 Pa (Figure 10). Membranes that were fouled twice gave higher surface coverage compared to one-time fouling for all samples examined. This is consistent

with findings from the *ImageJ* analysis. RCA 30 kDa membranes showed the highest surface coverage at shear stress values of 0.62 and 1.73 Pa. RCA 100 kDa showed the highest surface coverage at shear stress values of 0.28 and 3.90 Pa. Figure 10 also shows that mechanical cleaning using FDG achieved 82 - 95% removal at 3.9 Pa. The RCA 10 kDa was the membrane that most easily cleaned using FDG, as RCA 10 kDa showed the lowest surface coverage for shear stress values of 0.28 to 3.9 Pa. The fluid velocity can be calculated from the shear stress values using Equation (2). For a turbulent flow at 3.9 Pa, the fluid velocity (water was used in this case) was 1.3 m s^{-1}. This result shows that the FDG can be used to optimise the cross-flow velocity (CFV) used during PWF and rinsing in the cleaning process. Currently, PWF and rinsing were carried out using reverse osmosis water at CFV of 1.0 m s^{-1}. This finding indicates that a higher CFV is needed to remove the majority of reversible fouling during PWF and rinsing.
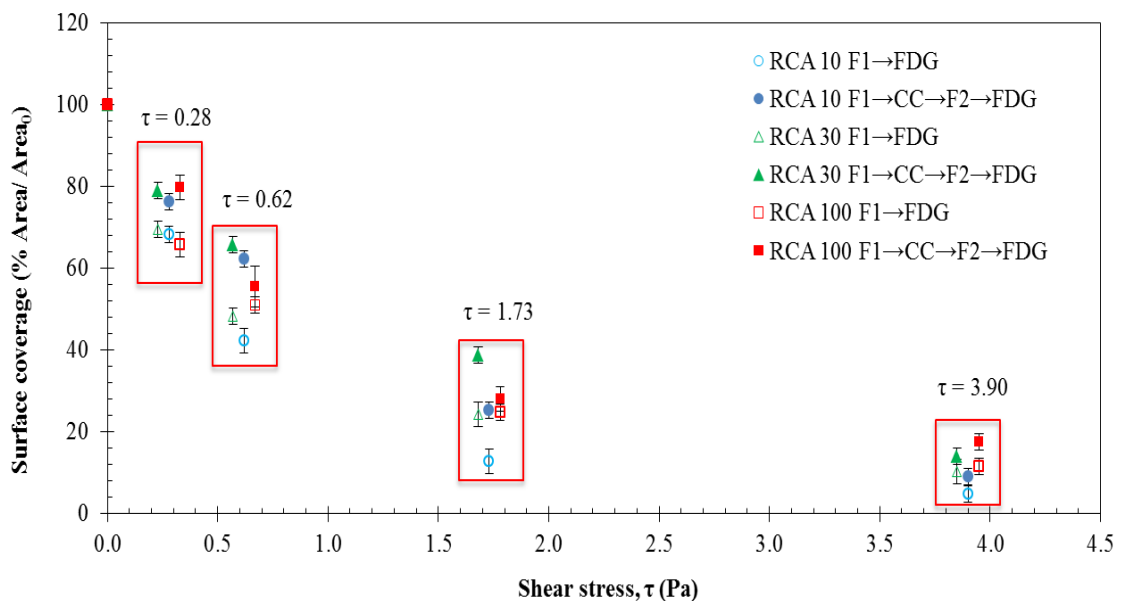
Figure 10: Surface coverage of RCA membranes after FDG cleaning at four different shear stress values.

3.4.2   *Membrane hydrophobicity*

Contact angle measurements were conducted to determine the surface hydrophobicity of RCA membrane to investigate the effect of fouling and cleaning upon the membrane properties. Membrane hydrophobicity was measured using the

sessile drop method. As the water drop contact angles measured were much less than 90° (Table 3), all membranes tested were considered to be highly hydrophilic. The contact angles of conditioned RCA 10, RCA 30 and RCA 100 membranes were $11 \pm 2°$, $13 \pm 2°$ and $18 \pm 2°$, respectively. The RCA membrane hydrophobicity results recorded in this study were in good agreement with those reported in the literature (Amy, 2001; Mohammad et al., 2011; Nguyen et al., 2015). Table 3 shows that the hydrophobicity of conditioned and cleaned RCA membranes varied with MWCO such that RCA100 > RCA30 > RCA10. All fouled membranes displayed contact angle of $10 \pm 2°$ after first fouling cycle. The membranes became more hydrophilic after fouling and the hydrophobicity increased after cleaning (Table 3). The contact angle measurements for membranes after FDG cleaning (labelled as **F1→FDG**) were returned back to the pristine condition (conditioned membrane). In contrast, after first cleaning using chemical cleaning (labelled as **F1→CC**), the contact angle was lower than the conditioned membrane. For membranes which were fouled twice, first cleaned using chemical cleaning and second cleaned using FDG (labelled as **F1→CC→F2→FDG**), the contact angles were returned close to cleaned membranes after first cycle of chemical cleaning. It is postulated that chemical cleaning changed the membrane hydrophobicity due to the adsorption of *P3-Ultrasil 11* surfactant to the membrane surface (Weis et al., 2003). This may suggest that mechanical cleaning using FDG is effective in cleaning the membrane without modifying the membrane hydrophobicity.

Table 3   Contact angles measured using the sessile drop method.

Membrane	Hydrophobicity (° contact angle)					
	Conditioned	**F1**	**F1→CC**	**F1→FDG**	**F1→CC →F2**	**F1→CC →F2→ FDG**
RCA 10 kDa	11 ± 2	10 ± 2	8 ± 2	11 ± 2	10 ± 2	8 ± 2
RCA 30 kDa	13 ± 2	10 ± 2	12 ± 2	13 ± 2	10 ± 3	11 ± 2
RCA 100 kDa	18 ± 2	10 ± 2	15 ± 2	17 ± 2	11 ± 3	14 ± 2

3.4.3   Membrane surface roughness

Atomic force microscopy (AFM) was used to investigate the surface roughness of membranes before and after fouling and cleaning. Table 4 shows that the roughness of RCA membranes varied with MWCO such that RCA30 > RCA100 > RCA10. The surface roughness values of conditioned RCA 10, RCA 30 and RCA 100 membranes were $3 \pm 1°$, $17 \pm 1°$ and $10 \pm 2°$ respectively. Evans *et al.*, (2008) also reported similar roughness value for the virgin conditioned RCA 10 membranes. After the first FDG cleaning, surface roughnesses for membranes were returned to their original values (labelled as **F1→FDG**). However, after first treatment using chemical cleaning (labelled as **F1→CC**), the surface roughness values reduced, but did not return to the initial roughness values. This indicates that the surfaces have not been returned to a pristine condition after chemical cleaning due to the membrane surface modification. Membranes labelled **F1→CC→F2→FDG** which were fouled twice and cleaned twice (first using chemical and second using FDG) showed surface roughness close to those seen for membranes treated by chemical cleaning alone (**F1→CC**). Thus, from this analysis, the FDG cleaning did not change the membrane surface roughness.

Table 4   Surface roughness values measured using AFM.

Membrane	Surface Roughness (nm)					
	Conditioned	**F1**	**F1→CC**	**F1→FDG**	**F1→CC →F2**	**F1→CC →F2→ FDG**
RCA 10 kDa	3 ± 1	31 ± 2	10 ± 2	8 ± 2	33 ± 2	12 ± 2
RCA 30 kDa	17 ± 1	42 ± 3	20 ± 2	18 ± 2	40 ± 2	21 ± 2
RCA 100 kDa	10 ± 2	39 ± 2	15 ± 1	11 ± 2	38 ± 2	15 ± 3

3.4.4   Visualisation of membrane after fouling and cleaning by SEM

Scanning electron microscope (SEM) analysis was performed to monitor the morphology of the membranes at different conditions; after fouling and cleaning. Membrane surface images of RCA membranes tested are presented in Figure 11. Deposition is clearly seen on the fouled membrane surfaces as shown in Figure 11 (a), (e) and (i). SEM images show that all membranes could be cleaned using chemicals and FDG after the first fouling. After the second fouling, cleaning was not as effective. This is in agreement with the surface coverage data using *Image J* analysis which shows the membranes that were fouled twice (labelled as (4)) gave higher surface coverage values compared to one-time fouling (labelled as (3)) for all membranes. After cleaning, the membrane surfaces changed from a rough surface on fouled membranes to a smooth surface. Cleaned membrane surfaces in Figure 11 (c, g, k) demonstrate that the FDG cleaning regime used is effective in removing the foulants.

(1) Fouled 1 (F1)	(2) Fouled 1 (F1) → Chemical cleaning (CC)	(3) Fouled 1 (F1) → Fluid dynamic gauging (FDG)	(4) Fouled 1 (F1) →(CC) → Fouled 2 (F2) → (FDG)
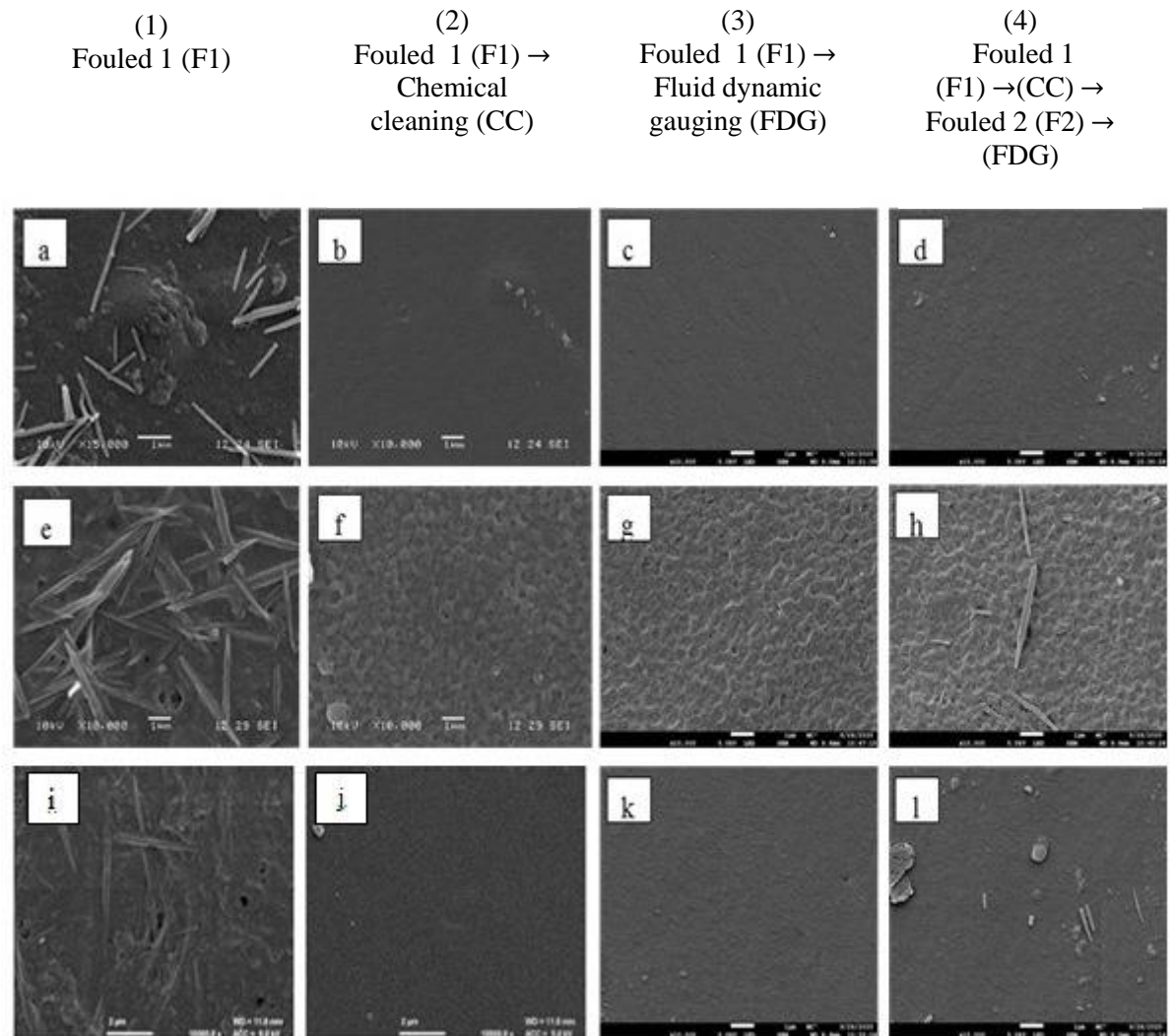
Figure 11: Scanning electron microscope (SEM) images of RCA membranes after fouling and cleaning; (a) to (d) RCA 10 kDa, (e) to (h) RCA 30 kDa and (i) to (l) RCA 100 kDa membranes.

4.   Conclusions

The optimisation of operating conditions in the membrane separation of phytosterols from orange juice has been investigated. Permeates generated using RCA 10 kDa membranes were relatively high in phytosterols, and low in protein. RCA 10 kDa membranes displayed an acceptable flux, and an effective separation of sterol from orange juice. From the conditions investigated, the most effective separation of phytosterols from protein in orange juice (with a selectivity factor of 17), was seen at a temperature of 20 °C using a 3 L feed volume. However, fouling adversely affected the performance of the membrane. Therefore, membrane cleaning is needed after

every filtration process, both to prolong the lifespan of the membrane and maintain the membrane performance. For the mechanical cleaning, removal of fouling layers was facilitated using suction flow from an FDG, and the cleanliness of the membrane was characterised using *ImageJ* analysis. For all RCA membranes tested, FDG achieved 80% to 95% removal at shear stress values of 3.9 Pa, corresponding to a water velocity of 1.3 m s^{-1}. In comparison to chemical cleaning, FDG did not change the surface property of membrane after application. Chemical cleaning using *P3-Ultrasil 11* altered both the membrane surface hydrophobicity and the roughness. These results show that the fouling layer on RCA membranes can be removed by applying the FDG technique, without affecting the membrane surface modification previously caused by chemical cleaning.

Acknowledgements

Conflict of Interest

The authors declare that they have no conflicts of interest.

Nomenclature

Abbreviations

CFV	cross-flow velocity (m s^{-1})
FDG	fluid dynamic gauging
LB	Liebermann-Buchard
MWCO	molecular weight cut-off
PME	pectin methylesterase
PWF	pure water flux

R	rejection ratio
RCA	regenerated cellulose acetate
RO	reverse osmosis
TPC	total phytosterol content
UF	ultrafiltration

Symbols

A_u	absorbance of the sample
C_f	friction factor
C_p	solute concentration in the permeate (mg ml^{-1})
C_r	solute concentration in the retentate (mg ml^{-1})
C_s	concentration of stigmasterol in standard solution (mg ml^{-1})
d	tube inner diameter (m)
d_t	nozzle inner diameter (m)
h	distance between the gauge and fouling layer (m)
h_0	distance between the gauge and membrane (m)
J	flux through the membrane (L m^{-2} h^{-1})
m	gauging mass flow rate (kg s^{-1})
r	inner radius of the FDG nozzle (m)
R_{tot}	total resistance (m^{-1})
TMP	transmembrane pressure (Pa)
w	nozzle thickness (m)

Greek symbols

α	separation factor
ρ	fluid density (kg m^{-3})
τ	fluid shear stress (Pa)
τ_{wall}	wall shear stress (Pa)
μ	dynamic viscosity of fluid (Pa s)
μ_m	mean pipe flow velocity (m s^{-1})

References

Abd-Razak, N.H., Chew, Y.M.J., Bird, M.R., 2019. Membrane fouling during the fractionation of phytosterols isolated from orange juice. *Food and Bioproducts Processing* 113, 10-21.

Abd-Razak, N.H., Pihlajamäki, A., Virtanen, T., John Chew, Y.M., Bird, M.R., 2021. The influence of membrane charge and porosity upon fouling and cleaning during the ultrafiltration of orange juice. *Food and Bioproducts Processing* 126, 184-194.

Abd-Razak, N.H., Zairossani, M.N., Chew, Y.M.J., Bird, M.R., 2020. Fouling Analysis and the Recovery of Phytosterols from Orange Juice Using Regenerated Cellulose Ultrafiltration Membranes. *Food and Bioprocess Technology* 13, 2012-2028.

Aghajanzadeh, S., Kashaninejad, M., Ziaiifar, A.M., 2017. Cloud stability of sour orange juice as affected by pectin methylesterase during come up time: Approached through fractal dimension. *International Journal of Food Properties* 20, S2508-S2519.

Amy, G.L., 2001. NOM Rejection By, and Fouling Of, NF and UF Membranes. American Water Works Association.

Araújo, L.B.D.C., Silva, S.L., Galvão, M.A.M., Ferreira, M.R.A., Araújo, E.L., Randau, K.P., Soares, L.A.L., 2013. Total phytosterol content in drug materials and extracts from roots of Acanthospermum hispidum by UV-VIS spectrophotometry. *Revista Brasileira de Farmacognosia* 23, 736-742.

Argyle, I.S., Pihlajamäki, A., Bird, M.R., 2015. Black tea liquor ultrafiltration: Effect of ethanol pre-treatment upon fouling and cleaning characteristics. *Food and Bioproducts Processing* 93, 289-297.

Aslam, M., Charfi, A., Lesage, G., Heran, M., Kim, J., 2017. Membrane bioreactors for wastewater treatment: A review of mechanical cleaning by scouring agents to control membrane fouling. *Chemical Engineering Journal* 307, 897-913.

Bradford, M.M., 1976. A rapid and sensitive method for the quantitation of microgram quantities of protein utilizing the principle of protein-dye binding. *Anal Biochem* 72, 248-254.

Burke, R.W., Diamondstone, B.I., Velapoldi, R.A., Menis, O., 1974. Mechanisms of the Liebermann-Burchard and Zak color reactions for cholesterol. *Clinical chemistry* 20, 794-781.

Cassano, A., Conidi, C., Ruby-Figueroa, R., Castro-Muñoz, R., 2018. Nanofiltration and Tight Ultrafiltration Membranes for the Recovery of Polyphenols from Agro-Food By-Products. *Int. J. Mol. Sci.* 19, 351.

Cassano, A., Donato, L., Conidi, C., Drioli, E., 2008. Recovery of bioactive compounds in kiwifruit juice by ultrafiltration. *Innovative Food Science & Emerging Technologies* 9, 556-562.

Cassano, A., Marchio, M., Drioli, E., 2007. Clarification of blood orange juice by ultrafiltration: analyses of operating parameters, membrane fouling and juice quality. *Desalination* 212, 15-27.

Chew, J.Y.M., Paterson, W.R., Wilson, D.I., 2004. Fluid dynamic gauging for measuring the strength of soft deposits. *Journal of Food Engineering* 65, 175-187.

Chew, Y.M.J., Paterson, W.R., Wilson, D.I., 2007. Fluid dynamic gauging: A new tool to study deposition on porous surfaces. *Journal of Membrane Science* 296, 29-41.

Corredig, M., Kerr, W., Wicker, L., 2001. Particle size distribution of orange juice cloud after addition of sensitized pectin. *J Agric Food Chem* 49, 2523-2526.

Echavarría, A.P., Torras, C., Pagán, J., Ibarz, A., 2011. Fruit Juice Processing and Membrane Technology Application. *Food Engineering Reviews* 3, 136-158.

Evans, P.J., Bird, M.R., Rogers, D., Wright, C.J., 2009. Measurement of polyphenol–membrane interaction forces during the ultrafiltration of black tea liquor. *Colloids and Surfaces A: Physicochemical and Engineering Aspects* 335, 148-153.

Goosen, M.F.A., Sablani, S.S., Al-Maskari, S.S., Al-Belushi, R.H., Wilf, M., 2002. Effect of feed temperature on permeate flux and mass transfer coefficient in spiral-wound reverse osmosis systems. *Desalination* 144, 367-372.

Gulec, H.A., Bagci, P.O., Bagci, U., 2017. Clarification of Apple Juice Using Polymeric Ultrafiltration Membranes: a Comparative Evaluation of Membrane Fouling and Juice Quality. *Food and Bioprocess Technology* 10, 875-885.

Guo, W., Ngo, H.-H., Li, J., 2012. A mini-review on membrane fouling. *Bioresource Technology* 122, 27-34.

Jiraratananon, R., Chanachai, A., 1996. A study of fouling in the ultrafiltration of passion fruit juice. *Journal of Membrane Science* 111, 39-48.

Jones, S.A., Chew, Y.M.J., Bird, M.R., Wilson, D.I., 2010. The application of fluid dynamic gauging in the investigation of synthetic membrane fouling phenomena. *Food and Bioproducts Processing* 88, 409-418.

Kenny, A.P., 1952. The determination of cholesterol by the Liebermann-Burchard reaction. *Biochemical Journal* 52, 611-619.

Kim, E., Goldberg, M., 1969. Serum cholesterol assay using a stable Liebermann-Burchard reagent. *Clinical chemistry* 15, 1171-1179.

Kruger, N.J., 1994. The Bradford method for protein quantitation. *Methods in molecular biology (Clifton, N.J.)* 32, 9-15.

Lafi, R., Gzara, L., Lajimi, R.H., Hafiane, A., 2018. Treatment of textile wastewater by a hybrid ultrafiltration/electrodialysis process. *Chemical Engineering and Processing - Process Intensification* 132, 105-113.

Lewis, W.J.T., Chew, Y.M.J., Bird, M.R., 2012. The application of fluid dynamic gauging in characterising cake deposition during the cross-flow microfiltration of a yeast suspension. *Journal of Membrane Science* 405-406, 113-122.

Mattsson, T., Lewis, W.J.T., Chew, Y.M.J., Bird, M.R., 2015. In situ investigation of soft cake fouling layers using fluid dynamic gauging. *Food and Bioproducts Processing* 93, 205-210.

Mbaebie, B.O., Edeoga, H.O., Afolayan, A.J., 2012. Phytochemical analysis and antioxidants activities of aqueous stem bark extract of Schotia latifolia Jacq. *Asian Pacific Journal of Tropical Biomedicine* 2, 118-124.

Meng, S., Zhang, M., Yao, M., Qiu, Z., Hong, Y., Lan, W., Xia, H., Jin, X., 2019. Membrane Fouling and Performance of Flat Ceramic Membranes in the Application of Drinking Water Purification. *Water* 11, 2606.

Mohammad, A., Hilal, N., Ying Pei, L., Nurul Hasyimah Mohd Amin, I., Raslan, R., 2011. Atomic Force Microscopy as a Tool for Asymmetric Polymeric Membrane Characterization. *Sains Malaysiana* 40, 237-244.

Mulder, M., 1996. Basic Principles of Membrane Technology, Second ed. Kluwer Academic Publishers, The Netherlands.

Nguyen, L.A.T., Schwarze, M., Schomäcker, R., 2015. Adsorption of non-ionic surfactant from aqueous solution onto various ultrafiltration membranes. *Journal of Membrane Science* 493, 120-133.

Pap, N., Mahosenaho, M., Pongrácz, E., Mikkonen, H., Jaakkola, M., Virtanen, V., Myllykoski, L., Horváth-Hovorka, Z., Hodúr, C., Vatai, G., Keiski, R.L., 2012.

Effect of Ultrafiltration on Anthocyanin and Flavonol Content of Black Currant Juice (Ribes nigrum L.). *Food and Bioprocess Technology* 5, 921-928.

Park, K.-B., Choi, C., Yu, H.-W., Chae, S.-R., Kim, I.S., 2018. Optimization of chemical cleaning for reverse osmosis membranes with organic fouling using statistical design tools. *Environmental Engineering Research* 23, 474-484.

Peck, O.P.W., John Chew, Y.M., Bird, M.R., Bolhuis, A., 2015. Application of Fluid Dynamic Gauging in the Characterization and Removal of Biofouling Deposits. *Heat Transfer Engineering* 36, 685-694.

Qaid, S., Zait, M., El Kacemi, K., Midaoui, A., el Hajji, H., Taky, M., 2017. Ultrafiltration for clarification of Valencia orange juice: Comparison of two flat sheet membranes on quality of juice production. 8, 1186-1194.

Sathishkumar, T., Baskar, R., 2014. Screening and quantification of phytochemicals in the leaves and flowers in the leaves and flowers of Tabernaemontana heyneana Wall. *Indian Journal of Natural Products and Resources* 5, 237-243.

Shi, X., Tal, G., Hankins, N.P., Gitis, V., 2014. Fouling and cleaning of ultrafiltration membranes: A review. *Journal of Water Process Engineering* 1, 121-138.

Tuladhar, T.R., Paterson, W.R., Macleod, N., Wilson, D.I., 2000. Development of a novel non-contact proximity gauge for thickness measurement of soft deposits and its application in fouling studies. *The Canadian Journal of Chemical Engineering* 78, 935-947.

Weis, A., Bird, M.R., Nyström, M., 2003. The chemical cleaning of polymeric UF membranes fouled with spent sulphite liquor over multiple operational cycles. *Journal of Membrane Science* 216, 67-79.

Weis, A., Bird, M.R., Nyström, M., Wright, C., 2005. The influence of morphology, hydrophobicity and charge upon the long-term performance of ultrafiltration membranes fouled with spent sulphite liquor. *Desalination* 175, 73-85.

Williams, P.M., Oatley-Radcliffe, D.L., Hilal, N., 2017. Chapter 17 - Feed Solution Characterization, in: Hilal, N., Ismail, A.F., Matsuura, T., Oatley-Radcliffe, D. (Eds.), Membrane Characterization. Elsevier, pp. 379-404.

Zayas, J.F., 1997. Solubility of Proteins, Functionality of Proteins in Food. Springer Berlin Heidelberg, Berlin, Heidelberg, pp. 6-75.

Supporting Information

(a) RCA 10 kDa ((**F1**) → (**CC**) → (**F2**) → (**FDG**))

h/dt	No gauging	0.15	0.10	0.06	0.04
Shear stress [Pa]	0	0.28	0.62	1.73	3.90
Before					
Image J					
% Surface coverage (ImageJ)	87 ± 4	66 ± 3	54 ± 2	22 ± 2	8 ± 2
Area/ Area$_0$	1.00	0.76 ± 0.02	0.62 ± 0.01	0.25 ± 0.01	0.09 ± 0.02

(b) RCA 30 kDa ((**F1**) → (**FDG**))

h/dt	No gauging	0.15	0.10	0.06	0.04
Shear stress [Pa]	0	0.28	0.62	1.73	3.90
Before					
Image J					
% Surface coverage (ImageJ)	88 ± 3	61 ± 2	43 ± 2	22 ± 2	9 ± 3
Area/ Area$_0$	1.00	0.69 ± 0.02	0.48 ± 0.02	0.24 ± 0.02	0.10 ± 0.03

(c) RCA 100 kDa ((**F1**) → (**FDG**))

h/dt	No gauging	0.15	0.10	0.06	0.04
Shear stress [Pa]	0	0.28	0.62	1.73	3.90
Before					
Image J					
% Surface coverage (ImageJ)	89 ± 2	59 ± 2	46 ± 2	22 ± 2	10 ± 2
Area/ $Area_0$	1.00	0.65 ± 0.02	0.51 ± 0.02	0.25 ± 0.01	0.12 ± 0.02

(d) RCA 100 kDa ((**F1**) → (**CC**) → (**F2**) → (**FDG**))
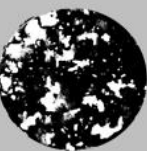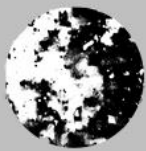
h/dt	No gauging	0.15	0.10	0.06	0.04
Shear stress [Pa]	0	0.28	0.62	1.73	3.90
Before					
Image J					
% Surface coverage (ImageJ)	95 ± 2	76 ± 3	53 ± 4	27 ± 3	17 ± 2
Area/ $Area_0$	1.00	0.80 ± 0.03	0.56 ± 0.05	0.28 ± 0.03	0.18 ± 0.02

Figure 12: Surface coverage of the RCA membranes after FDG cleaning analysed by *ImageJ*; (a) RCA 10 kDa ((**F1**) → (**CC**) → (**F2**) → (**FDG**)), (b) RCA 30 kDa ((**F1**) → (**FDG**)), (c) RCA 100 kDa ((**F1**) → (**FDG**)) and (d) RCA 100 kDa ((**F1**) → (**CC**) → (**F2**) → (**FDG**)).

Calculation of the velocity from the shear stress

For turbulent flow regimes, the friction factor (C_f) is equal to 0.005. Water was used in this study. Based on this study, the maximum shear stress at the wall (τ_{wall}) from the FDG experiment was 3.9 Pa. Thus, the water velocity (μ_{water}) was calculated as below according to Equation (2);

$$\mu_{min} = \sqrt{\frac{2\,\tau_{wall}}{\rho\,C_f}}$$

$$\mu^2{}_{water} = \frac{2\,\tau_{wall}}{\rho_{water}\,C_f}$$

$$\mu^2{}_{water} = \frac{2\,x\,3.9}{1000\,x\,0.005}$$

$$\text{Velocity}, \mu_{water} = 1.3\,m\,s^{-1}$$

Chapter 7: Conclusions and recommendations

This chapter summarises the key findings from the preceding chapters reported in this thesis based on the objectives in Chapter 1. The recommendations for future work are also presented in this chapter.

7.1 Conclusions

The membrane ultrafiltration process has been developed using a cross-flow membrane filtration bench unit *LabStak M10* with a total filtration area of 336 cm^2 at 20 ^{o}C and a TMP value of 1 bar. To conclude, the novel use of ultrafiltration method in separating phytosterols from orange juice has been established. Model feedstock which is orange juice was used in this work due to similar total phytosterols (0.2 – 0.3 mg ml^{-1}) to those present in natural rubber serum (NRS). The pH of orange juice (pH 3.45) was found to be almost similar with pH of NRS (pH 3.56). Thus, the same process is thought to be applicable and transferable to natural rubber industry. The viscosities of orange juice and NRS at 20 °C were 9.24 mPa.s and 3.5 mPa.s, respectively. The NRS showed 3 times lower in viscosity compared to the orange juice and the NRS might produce higher flux that lead to fouling. Thus, the NRS need to be pre-treated in order to reduce the fouling effect during the ultrafiltration. The ultrafiltration membranes have shown the potential to separate phytosterols from proteins in orange juice.

Of the membranes tested at 10 kDa MWCO, RCA membrane demonstrated the highest transmission of phytosterols into the permeate compared to PS and FP membranes (32% rejection towards phytosterols). PES and FP (more hydrophobic membranes) revealed higher rejections towards phytosterol compounds (76% and 75% respectively). Proteins were 100% rejected by the 10 kDa membranes and sugar was 100% recovered in the permeate. Therefore, RCA membrane with higher MWCO was then used in order to transmit more sterols and to remove proteins. The ultrafiltration was carried out using different RCA membranes with 10 kDa, 30 kDa and 100 kDa MWCO. Contrastingly, RCA 30 kDa and 100 kDa membranes resulted in a higher rejection of phytosterols compared to 10 kDa membrane. The RCA 10 kDa membranes showed the best separation performance with the lowest rejection of

phytosterols ($32 \pm 4\%$) and the highest rejection of proteins ($96 \pm 1\%$). Permeate fluxes for all three RCA membranes decreased gradually with filtration time to similar steady-state values (22 L m^{-2} h^{-1}). The pure water flux (PWF) was a poor indicator of permeate flux in this system because PWF values varied with MWCO such that RCA 30 > RCA 100 > RCA 10. Reversible fouling was found to play an important effect in the flux decline. Hermia flux decline analysis showed that intermediate pore blocking was the dominant mechanism for RCA 30 and RCA 100 membranes because larger pores enabled the accumulation of protein-based foulants or other hydrophilic compounds such as potassium citrate on the membrane surfaces or in the membrane pores. Membrane surface roughness and surface charge varied as a function of MWCO such that RCA30 > RCA100 > RCA10. Fouling increased the membrane porosity and surface roughness, and decreased the membrane hydrophobicity. As a conclusion, the membranes characteristics were more important than molecular weight cut off in determining the performance of ultrafiltration membranes in this system.

The use of chemical cleaning agent (*P3-Ultrasil 11*) for the membrane cleaning has modified the membrane surface properties such as hydrophobicity, surface roughness, surface charge and porosity. Thus, the novel application of the fluid dynamic gauging (FDG) technique has been established to monitor the removal of orange juice fouling layers in membrane cleaning with controlled of fluid shear to the surface of the fouling layer. To conclude, the FDG achieved 80 - 95% removal at shear stress values of 3.9 Pa, corresponding to a water velocity of 1.3 ms^{-1} without affecting the membrane surface modification caused by chemical cleaning. Different operating conditions such as temperature and concentration of feed components were also introduced to optimise the separation of phytosterols from orange juice. The best separation of phytosterols ($32 \pm 4\%$) from orange juice using this system was achieved using RCA 10 kDa membrane operated at 20 °C using 3 L feed with a selectivity factor of 17. The operating temperature at 40 °C is not optimal for orange juice filtration. Ultrafiltration at low temperature was found to be more effective in separating phytosterols in orange juice to avoid precipitation of proteins and to reduce membrane fouling. These findings have important implications for the industrial application of membrane technology to process orange juice and other sterol-rich feeds.

7.2 Recommendation for future works

In term of future work, an interesting area of study came to light through literature review and experimental data. Therefore, further experiments can be carried out and listed as below:

7.2.1 Validation of the ultrafiltration process using natural rubber serum

The ultrafiltration protocol for the separation process of phytosterols from orange juice can be applied to other feedstock such as NRS. The compounds analyses and membranes characterisations can be used to validate the feasibility of using ultrafiltration technology to separate the phytosterols from NRS.

7.2.2 Pre-treatment of NRS before the ultrafiltration

The difference in viscosity between the orange juice and the actual NRS will give difference impact in fouling potential. The NRS need to be pre-treated before the ultrafiltration in order to increase the viscosity. The NRS can be concentrated via centrifugation or by rotary evaporation.

7.2.3 Pre-filtration of orange juice

In order to produce smaller particle size of feed solution before the ultrafiltration, a pre-filtration at 0.2 microns can be carried out. Pre-filtration is needed to remove pulp in the orange juice and thereby, the fouling effect can be reduced.

7.2.4 Separation and purification of phytosterols by gas chromatography

Further investigation would be required for a detailed characterisation and purification of the phytosterols compounds. The separation of phytosterols in orange juice extract into different isomers can be developed and tested using gas chromatography (GC) with flame ionization detection. Solid phase extraction (SPE) method can be applied for the sample preparation for GC analysis.

7.2.5 Introduction of second step filtration

Since the yield of total phytosterols compounds that are fractionated by using 10 kDa ultrafiltration membranes was relatively low, there is a potential to modify the processing procedure to produce higher amount of phytosterols. Thus, an attempt can be made to introduce the second step filtration such as nanofiltration or diafiltration.

7.2.6 Modification of the ultrafiltration rig

The feed tank can be modified to include the stirrer and to install the heat jacketed tank. The stirrer can be used to homogenise the feed stock during the ultrafiltration and the heat jacketed tank is useful in maintaining the operating temperature. This may lead to beneficial improvements of phytosterols separation using ultrafiltration technology.
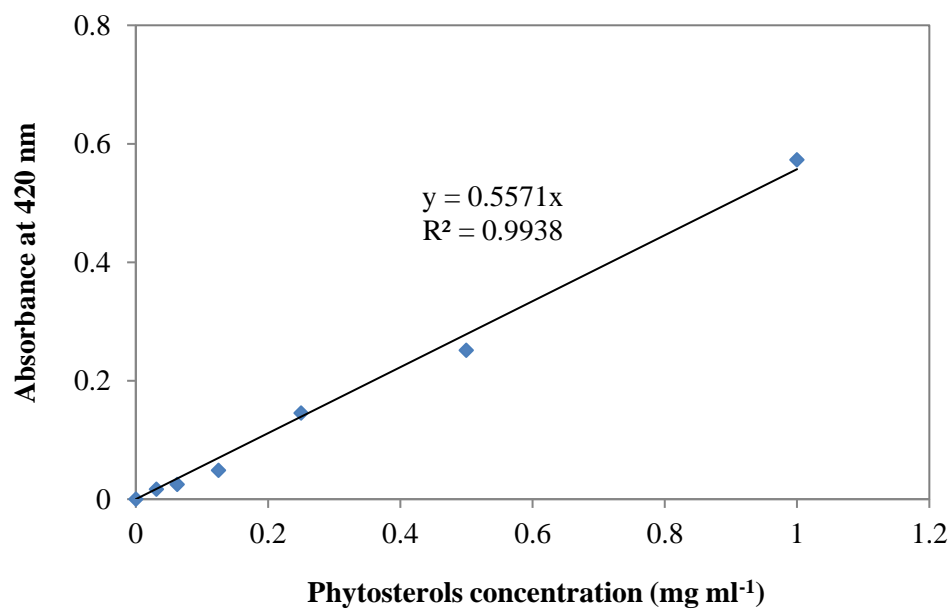
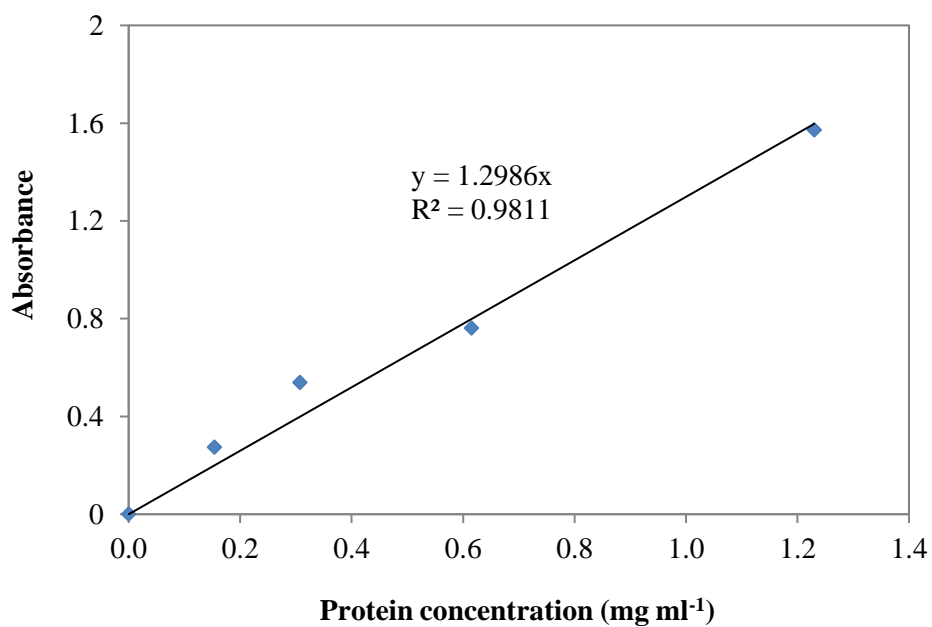# Appendix

Figure A.1: Calibration curve of phytosterol standard

Figure A.2: Calibration curve of proteins standard